5-2-2016

Stable Isotopic Evidence for Landscape Environmental Reconstructions, Kapthurin Formation, Kenya

David E. Leslie
University of Connecticut - Storrs, daveleslietvc@gmail.com

Stable Isotopic Evidence for Landscape Environmental Reconstructions, Kapthurin Formation, Kenya

David E. Leslie, PhD

University of Connecticut, 2016

Global, regional, and local changes in environments are critically important to understanding the selective pressures that affected the hominin lineage. Shifts in regional environments of East Africa, driven by solar insolation, have been associated with adaptive niches of hominins during the Pleistocene epoch, a time period that spans the inception of the genus *Homo* and the emergence of own species, *Homo sapiens*. Several hypotheses link the influence of changing environments and the evolution of the genus *Homo*, based on global drying trends during the Pleistocene, but also the increased variability of dry and wet cycles near the equator, driven by Milankovitch cycles. These hypotheses are buttressed by continental and global environmental data from ice and ocean cores, but lack high-resolution, regional environmental data for support.

The distribution of archaeological material across a paleolandscape is best understood, in the context of modern foragers' daily activities, as a continuum of large, highly concentrated to small, highly diffuse archaeological sites. Landscape archaeology offers researchers a way to address this larger foraging context by reconstructing regional paleolandscapes and collecting representative samples of archaeological material. The Middle Pleistocene (781 – 126 ka) of East Africa records many significant events in human evolution; it encompasses the emergence of our own species, *Homo sapiens*, the development of technologies that are "modern", and a shift to resource extraction from a diverse range of environments. Paleoanthropologists regularly

use stable isotope ratios of several proxies (paleosols, pedogenic carbonates, mammalian teeth, tufa composition) to reconstruct environments associated with hominin evolution, but these are rarely applied to the Middle Pleistocene of East Africa. The application of stable isotope analyses to Middle Pleistocene sedimentary sequences may be useful for discerning the local environments associated with hominins who used Acheulean and Middle Stone Age technologies.

In this dissertation, I combine a landscape perspective with paleoenvironmental reconstructions, primarily using stable isotope analyses of paleosols, mammalian tooth enamel, and pedogenic carbonates. This technique is applied to two paleolandscapes preserved in the Kapthurin Formation, a well-documented Middle Pleistocene sedimentary sequence containing Acheulean and Middle Stone Age technology, hominin remains identified to *Homo erectus* and *Homo sp.*, and chimpanzee fossils. I also develop a novel technique for correlating modern primary biomass productivity with stable carbon isotope values of bulk soil organic matter, and provide a method for extrapolating primary biomass productivity from well preserved paleosols. The high-resolution landscape environmental reconstructions presented in this dissertation provide the first evidence for hominin site choice in two well-documented landscapes of the Middle Pleistocene, indicating that both Terminal Acheulean and MSA foragers regularly occupied wooded grassland ecosystems.

Stable Isotopic Evidence for Landscape Environmental Reconstructions, Kapthurin Formation, Kenya

David Edward Leslie

B.A., West Virginia University, 2006

M.A., Florida Atlantic University, 2008

A Dissertation

Submitted in Partial Fulfillment of the

Requirements for the Degree of

Doctor of Philosophy

at the

University of Connecticut

2016

APPROVAL PAGE

Doctor of Philosophy Dissertation

Stable Isotopic Evidence for Landscape Environmental Reconstructions,

Kapthurin Formation, Kenya

Presented by

David E. Leslie, B.A., M.A.

Major Advisor _____

Sally McBrearty

Associate Advisor _____

Gideon Hartman

Associate Advisor _____

Daniel S. Adler

University of Connecticut

2016

ACKNOWLEDGEMENTS

There are many people to thank for this dissertation. First, I would like to thank my wife, Sarah Sportman, for continuing to support me while I completed my studies. She has also read and edited many versions of this dissertation, although her academic interests lie within the archaeology of northeastern North America. I would like to dedicate this dissertation, such as it is, to our son, Charlie, who is a never-ending source of continuing inspiration to me; through his two-year old's eyes I have begun to find a new appreciation for all aspects of nature and the world. I would also like to thank my parents, who have supported me over many years, and instilled in me an early appreciation for nature.

My advisor, Sally McBrearty, has provided me with a wealth of knowledge and support throughout my graduate career, and facilitated much of this research through her own grant funding. Gideon Hartman provided lab space for much of these analyses, but more importantly, his door was always open to me from the very beginning of this project, providing endless feedback on ideas, manuscript drafts, and grant proposals. Dan Adler dedicated much of his time to reading and editing previous versions of this dissertation; without his careful attention to the theoretical underpinnings of these manuscripts, my work would have surely suffered. I count myself luck to have had three such advisors who dedicated much of their time and resources to my dissertation and career.

There are many financial institutions to thank for this project. The National Science Foundation facilitated this research with a Doctoral Dissertation Improvement Grant (BCS 1343214). The Anthropology Department at UConn has been very supportive of my graduate career and research, providing Summer Research Fellowships, graduate support in the form of several teaching and research assistantships, and a dissertation writing fellowship. Sigma Xi

provided a Grant-in-Aid of research for a component of this dissertation research. The Center for Environmental Science and Engineering provided a fellowship that supported some of the early data collection for this research. Finally, the College of Liberal Arts and Sciences, the Graduate School, and the Humanities Institute, all at UConn, funded portions of this research through fellowships.

I also have many colleagues, advisors, and friends to thank for various support and feedback during this eight (!) year period of my life. In no particular order, and this list is by no means complete, I would like to thank the following people for support over the years: Bonface Kimeu, Nick Blegen, Cara Johnson, Breanne Clifton, Ali Mant, Andrew Hill, Bernard Muende, Mathew Macharwas, Simeon Chelal, Julius Marti, Alison Brooks, John Yellen, Rick Potts, Cliff Brown, Rob McCarthy, Natalie Munro, Alexia Smith, Zach Singer, Gabe Hrynick, Bill Farley, Lucas Proctor, Siavash Samei, and Jackie Meier. This dissertation research would also not have been possible without support from the National Museums of Kenya and their dedicated staff. Finally, I would like to thank the following individuals and organizations for facilitating stable isotope analyses: Bob Michener and the Stable Isotope Laboratory, Boston University; Marie Balasse, Joël Ughetto, and the Centre National de la Recherche Scientifique, Museum National d'Histoire Naturelle; and David Dettman and the Environmental Isotope Lab at the University of Arizona.

TABLE OF CONTENTS

Page

Chapter 4: Stable Isotopic Evidence for Paleoenvironments from the Kapthurin Formation, Kenya: Evidence from Pedogenic Carbonates and Paleosols

Page

Chapter 5: Environmental and Behavioral Variability Traces in the Kapthurin Formation, Kenya

Chapter 6: Conclusions

Page

Appendices & References Cited

LIST OF FIGURES

LIST OF TABLES

Chapter 1: Introduction

Global, regional, and local changes in environments are critically important to understanding the selective pressures that affected the hominin lineage. Shifts in regional environments of East Africa, driven by solar insolation, have been associated with adaptive niches of hominins during the Pleistocene epoch, dated to between 2.58 million years ago (Ma) and 11.7 thousand years ago (ka) (International Commission on Stratigraphy 2014), a time period that nearly spans the inception of the genus *Homo* (see Villmoare, et al. (2015)) and the emergence of own species, *Homo sapiens* (McDougall, et al. 2008). The influence of changing environments on the evolution of the genus *Homo* are thought to be substantial, based on global drying trends during the Pleistocene, but also the increased variability of dry and wet cycles near the equator, driven by Milankovitch cycles (Ambrose 1998; Bräuer 2008; deMenocal 2011; Kingston, et al. 2007; Potts 1998; Potts and Faith 2015; Vrba 1993). These hypotheses are buttressed by continental and global environmental data (deMenocal, et al. 2000; Lüthi, et al. 2008; Petit, et al. 1999; Schmieder, et al. 2000) from ice and ocean cores, and lack high-resolution, regional environmental data for support, although recent drilling investigations of rift-lakes in East Africa may provide a wealth of information about regional shifts in environments during the Pleistocene (Cohen, et al. 2016).

Highly-visible, high density archaeological sites are well studied during the Pleistocene and have a wealth of information about the material culture, environmental context of site choice, and habitats of Pleistocene hominins, but they limit the information about the use of larger landscapes for foraging activities such as food and raw material procurement (Dunnell and Dancey 1983; Ebert 1992; Foley 1981). Instead, the distribution of archaeological material

across a paleolandscape is best understood, in the context of modern foragers' daily activities, as a continuum of large, highly concentrated to small, highly diffuse archaeological sites. Landscape archaeology offers researchers a way to address this larger foraging context by reconstructing regional paleolandscapes and collecting representative samples of archaeological material associated with these landscapes. The Middle Pleistocene (781 – 126 ka), formerly the Ionian, of East Africa records many significant events in human evolution; it encompasses the emergence of our own species, *Homo sapiens*, the development of technologies that are "modern", and a shift to resource extraction from a diverse range of environments (Clark 1988; Christopher S. Henshilwood and Curtis W. Marean 2003; McBrearty and Brooks 2000). Paleoanthropologists regularly use stable isotope ratios of several proxies (paleosols, pedogenic carbonates, mammalian teeth, tufa composition) to reconstruct environments associated with hominin evolution, but these are rarely applied to the Middle Pleistocene of East Africa (Ashley, et al. 2010; Cerling, Andanje, et al. 2015; Cerling, Wynn, et al. 2011; Kingston and Harrison 2007; Kingston, et al. 1994; Levin, et al. 2011; Levin, et al. 2004; Quinn, et al. 2013), but see Leslie, et al. (2016) and Robinson, et al. (2016). The application of stable isotope analyses to Middle Pleistocene sedimentary sequences may be useful for discerning the local environments associated with hominins who used Acheulean and Middle Stone Age technologies.

In this dissertation, I combine a landscape perspective with paleoenvironmental reconstructions, primarily using stable isotope analyses of paleosols, mammalian tooth enamel, and pedogenic carbonates, of two paleolandscapes preserved in the Kapthurin Formation, a well-documented Middle Pleistocene sedimentary sequence containing Acheulean and Middle Stone Age technology, hominin remains identified to *Homo erectus* and *Homo sp.*, and chimpanzee fossils (Blegen 2015; Deino and McBrearty 2002; Johnson and McBrearty 2010, 2012; Leakey,

et al. 1969; McBrearty 1999; Tallon 1976; C. A. Tryon and S. McBrearty 2002; Christian A. Tryon and Sally McBrearty 2002; Wood and Van Noten 1986). These environmental reconstructions are useful as a backdrop to understanding hominin site choice, particularly when using an optimal foraging perspective (Winterhalder 1981).

1.1 Kapthurin Formation

The Kapthurin Formation is geographically located to the west of Lake Baringo and is a part of the Middle Pleistocene sedimentary sequence of the Tugen Hills succession in the Kenyan Rift Valley. The formation consists of interstratified alluvial, lacustrine, and volcanic sediments, is roughly exposed over an area of 150 km^2, and has an observed thickness of approximately 125 meters (Deino and McBrearty 2002; Martyn 1969; Tallon 1976). The formation has been dated using the $^{40}Ar/^{39}Ar$ method (Blegen 2015; Deino and McBrearty 2002; Dunkley, et al. 1993), and has been subdivided by Martyn (1969) into five formal members. Members K1, K3, and K5 are informally referred to as the Lower, Middle, and Upper Silts and Gravels members, and are composed of terrigenous sediments derived from the Tugen Hills. Members K2 and K4 are pyroclastic sediments that intercalate the Silts and Gravels members; K2, the Pumice Tuff, is dated to 543 ± 3 ka; K4, the Bedded Tuff, has several eruptive facies, three of which have been dated to 380 ± 7 ka, 284 ± 12 ka, and 235 ± 2 ka; The Grey Tuff also subdivides K3, and is dated to 509 ± 9 ka (Deino and McBrearty 2002). The basal date of K4 was recently developed through tephrostratigraphic correlation to the Korosi Airfall Pumiceous Tuff (Blegen 2015) and dated by Dunkley, et al. (1993), also using the $^{40}Ar/^{39}Ar$ method. The Kapthurin Formation also lies unconformably above the Chemeron Formation, the contact between these two formations is represented by the Ndau Trachymugearite, which is dated to

1.57 Ma, using the K-Ar method (Hill, et al. 1986). All of the sediments in the Kapthurin Formation are normally magnetized (Dagley, et al. 1978) and postdate the Matuyama-Brunhes Boundary, currently estimated at 775 ka using the $^{40}Ar/^{39}Ar$ method, and providing a more accurate estimate for the maximum age of the Kapthurin Formation.

K3 sediments preserve the archaeological material and paleolandscapes discussed in this dissertation and is subdivided by the Grey Tuff, by alluvial facies (referred to hereafter as K3) to the west of the formation, and by lacustrine facies (referred to hereafter as K3') to the east of the formation. The sediments of K3 are composed of unstratified silt and pebble beds, which are marked by massive conglomerates in the western and southern portions of the formation, and occasional soil formation, mainly below K4 and the Grey Tuff (Tallon 1976). The sediments of K3' consist of red, black, and green claystones and siltstones; the sedimentary and geochemical structures of K3' sediments indicate they were deposited in a shallow lake that alternated between freshwater and saline-alkaline (Johnson and McBrearty 2012; Renaut, et al. 1999; Tallon 1976). The research presented here focuses on two main time intervals preserved within K3: Time Interval 1 (543 – 509 ka) is represented by archaeological and paleontological sites deposited above K2 and below the Grey Tuff, but most of the sites are stratigraphically closer to the Grey Tuff; Time Interval 2 (509 – 380 ka) is represented by archaeological and paleontological sites deposited above the Grey Tuff and below K4, but most of the sites are stratigraphically closer to K4.

1.2 Middle Pleistocene Archaeology

One of the most important features of the African Middle Pleistocene archaeological record is the transition from the use of the Acheulean techno-complex to the more

technologically diverse toolkit of the Middle Stone Age, a transition that occurred between 500 and 300 ka (Blegen 2015; Johnson and McBrearty 2010; McBrearty and Brooks 2000; Christian A. Tryon and Sally McBrearty 2002; Tryon, et al. 2005; Wilkins and Chazan 2012; Wilkins, et al. 2012). Handaxes, cleavers, and knives are trademarks of the Acheulean industry, and are generally referred to as large cutting tools (Clark 1994; Clark and Kleindienst 1974). The Acheulean industry was first developed during the Early Pleistocene, a time period formally referred to as the Calabrian and Gelasian (International Commission on Stratigraphy 2014), in East Africa at approximately 1.76 Ma (Lepre, et al. 2011), and remains relatively uniform in production methods and tool forms throughout its use into the later Middle Pleistocene (Clark 1977; J D Clark 2001; Isaac 1972; Leakey 1971). The use of Acheulean tools spans over one million years, and occurred in Africa, Europe, and Asia, clearly marking it as a successful behavioral adaptation useful for foraging activities. The end of this tradition, the Terminal Acheulean, is marked by a shift in technological production to smaller, flaked handaxes, and the introduction of new flaking techniques, such as the Levallois method and blade production (Adler, et al. 2014; Johnson and McBrearty 2010; Tryon, et al. 2005; Wilkins and Chazan 2012).

Middle Stone Age archaeological sites are characterized by the presence of stone points that were hafted as hunting armatures, replacing the popular cutting tools associated with Acheulean sites (Brooks, et al. 2006; Clark 1988; John J. Shea 1993). MSA sites contrast the near global uniformity of the Acheulean tradition, displaying regional patterning in point production, which has been interpreted as early evidence for regionally bounded cultural identity (Clark 1999; McBrearty and Brooks 2000). Middle Stone Age sites are also commonly associated with hominin expansions into new habitats, increased foraging ranges, and the use of diverse lithic raw materials from distant sources (Ambrose 2001a, 2012; Clark 1988; McBrearty

and Brooks 2000; Tryon and Faith 2013). Analyses of Middle Stone Age faunal and lithic assemblages suggest the use of new hunting techniques (Faith 2008; Klein 1982; Marean 1997; Milo 1998) and increased breadth of diet (Brooks, et al. 1995; Henry, et al. 2014; McBrearty and Brooks 2000; Yellen, et al. 1995) were common behaviors by the later Middle Pleistocene of Africa. The Middle Stone Age also coincides with the earliest evidence for well-established symbolic representation (Henshilwood, et al. 2002; McBrearty and Brooks 2000).

The behavioral complex associated with the Middle Stone Age is often termed "modern", and although it is difficult to define behavioral modernity, most archaeologists accept that the earliest evidence for behavioral modernity lies in the African Middle Stone Age (Christopher S. Henshilwood and Curtis W. Marean 2003; McBrearty and Brooks 2000). Hominin phylogenies during the Middle Pleistocene complicate our understanding of behavioral modernity, due in part to the older age associated with the origins of the Middle Stone Age (~500 – 300 ka) than the earliest representatives of *Homo sapiens* (McDougall, et al. 2008). All of the early fossils of *Homo sapiens* are associated with Middle Stone Age technology (Basell 2008; Bräuer 2008; McDougall, et al. 2008), but other archaic hominins (*Homo heidelbergensis*, *Homo erectus*) are intermittently associated with earlier MSA technology (Johnson and McBrearty 2010; Morgan and Renne 2008; Sahle, et al. 2013; Wilkins, et al. 2012). Direct association between hominins and the Middle Stone Age is thus beyond the resolution of archaeological data, and in all likelihood impossible, particularly if an archaic species, such as *Homo heidelbergensis*, is associated with both Terminal Acheulean and Middle Stone Age technology. Due to this temporal and behavioral uncertainty, I will refer to Middle Stone Age and Terminal Acheulean industries, not particular hominin species which may or may not be associated with these industries. The Kapthurin Formation provides the best stratigraphic sequence of the transition

from Terminal Acheulean to Middle Stone Age technology (Blegen 2015; Tryon 2006; Tryon and Faith 2013; Tryon and McBrearty 2006), providing an ideal location to reconstruct paleolandscapes and local environments of the Middle Pleistocene.

1.3 Landscape Archaeology

Hominins during the Middle Pleistocene did not live and forage at a single occupation site, but instead, ranged across landscapes, probably in relatively small social groups, similar to modern foraging behavior (Kelly 1995). A central goal of landscape archaeology is to identify the behavioral patterns, particularly how these patterns relate to resource extraction and mobility, and how these behaviors changed through time. Younger archaeological sites and assemblages lend themselves to landscape perspectives, including the spatial analyses of site choice, resource distribution and extraction, and ethnographic and ethnohistoric behaviors of foraging societies (Binford 1980; Jarman, et al. 1972; Mehrer and Wescott 2005; Wescott and Brandon 2003). The application of these approaches to the Middle Pleistocene are difficult, given that the modern landscapes, environmental resources, and distribution of animal communities often bear little resemblance to the paleolandscapes and resources (Cerling, Andanje, et al. 2015). There are several Early Stone Age site complexes where landscape archaeology investigations are common, including Gona (Braun, et al. 2008), Turkana (Rogers, et al. 1994), Olorgesailie (Potts, et al. 1999), and Olduvai Gorge (Blumenschine, et al. 2012; Peters and Blumenschine 1995). Similar landscape scale investigations at Middle Stone Age sites are less common, although newer projects have been developed at Omo Kibish (Assefa, et al. 2008; Brown, et al. 2012), Aduma (Yellen, et al. 2005), Rusinga Island (Tryon, et al. 2014; Tryon, et al. 2010), and the Kapthurin Formation (Johnson and McBrearty 2012; C. A. Tryon and S. McBrearty 2002).

Most Pleistocene archaeological sites occur near ephemeral or perennial water sources such as streams, rivers, and lakes (Basell 2008; Peters and Blumenschine 1995; Potts, et al. 1999; Rogers, et al. 1994), probably due to the presence of higher primary (plants) and secondary (animals) biomass available for exploitation near these water sources. Site formation processes associated with sites close to water sources might be over-representing hominin activity, due to the low topographic position of lakes and streams, as well as the increased sediment input from water sources, while sites that are upland of water sources continuously lose sediment (Gifford and Behrensmeyer 1977; Schick 1997; Waters and Kuehn 1996). As others have noted, proximity to water sources is not the only factor when considering hominin ranging patterns: hominins were probably active in upland areas (Potts, et al. 1999), at sources of raw material for technological exploitation (Blumenschine, et al. 2007; Potts 1991), or selected woodland sites for cover from the sun, escape from predators, and proximity to important food sources (Peters and Blumenschine 1995). Environmental reconstructions that utilize fine-grained data, such as pedogenic carbonates, paleosols, and mammalian teeth, and are sampled with respect to paleolandscape markers (dateable, mappable geologic boundaries such as tephra) offer archaeologists a window into the microhabitats associated with the paleolandscapes understudy.

1.4 Stable Isotope Ecology

Stable isotope analyses provide unique methods for assessing past environments and have been a useful tool for paleoanthropologists over the past four decades (Loftus, et al. 2016). Traditional methods include sampling components of fossil soils, teeth, and bone. When studying isotopic composition of plants, animals, and soils, normalized ratios of the heavy and light isotopes are used, such as:

Equation 1.1: $\delta^X = \left(\frac{R_{sample}}{R_{standard}} - 1\right) \times 1000 \quad X = {}^{13}C, {}^{18}O; R = {}^{13}C/{}^{12}C, {}^{18}O/{}^{16}O$

Vienna Pee Dee Belemnite (VPDB) is the reference standard for $\delta^{13}C$ and Vienna Standard Mean Ocean Water (VSMOW) is the reference standard for $\delta^{18}O$.

Equation 1.1 allows researchers to track two quantities of heavy and light isotopes with a single notation. The stable carbon isotope values of bulk soil organic matter (SOM), pedogenic carbonates, and mammalian teeth reflect the three main photosynthetic pathways available to C_3, C_4, and Crassulacean Acid Metabolism (CAM) plants prevailing in East Africa. Plants that use each of these pathways fix carbon dioxide (CO_2) from the atmosphere for photosynthesis in different ways: C_3 plants utilize a 3-carbon compound, C_4 plants use a 4-carbon compound intermediate phase, and CAM plants store carbon dioxide in an acid before using it for photosynthesis (Ehleringer, et al. 1997; Farquhar, et al. 1989; Osmond, et al. 1982). The CAM photosynthetic pathway represents a small portion of plants (cacti and epiphytes) and is not particularly useful for reconstructing the environment of landscapes in East Africa. The C_3 biome represents the most common adaptation, and is comprised of trees and most shrubs, aquatic plants, herbs, as well as high latitude grasses (Kohn 2010; Osmond, et al. 1982). C_3 plants are depleted in their $\delta^{13}C$ values when compared to the standard (VPDB); values commonly range between -20 per mil (‰) to -37‰ (Bender 1971; Kohn 2010). In tropical forests, the canopy effect traps ^{13}C depleted CO_2 produced during soil respiration, resulting in the most negative values of the C_3 biome. The "canopy effect" produces a gradient of negative $\delta^{13}C$ values; the most negative values are produced in the forest floor, while the most positive values are produced in the upper story of the forest. The C_4 pathway is commonly represented by mid-latitude grasses and flowering plants (Ehleringer, et al. 1997). C_4 plants are comparatively

enriched in $\delta^{13}C$ values; values commonly range between -10‰ and -14‰ (Ehleringer, et al. 1997; Farquhar, et al. 1989). Mixed C_3/C_4 environments lie intermediately between these two ranges.

Soil carbonates undergo many diffusion and mixture events where the isotopic composition of the carbonates is enriched on average 14‰ to 16‰, relative to bulk SOM carbon values (Cerling, et al. 1989). Carbon isotope ratios of SOM are particularly useful because the values are directly determined by the fraction of litter derived from C_3 and C_4 plants (Wynn and Bird 2007) and the soil development processes that are associated with decomposition of above ground vegetation (Baisden, et al. 2002; Ladd, et al. 2014). This is contrary to pedogenic carbonate formation, which although still a useful environmental proxy, can be inhibited by densely forested environments, which are associated with acidic soils and high precipitation (Tucker and Wright 1990). Pedogenic carbonates also have a seasonal bias in formation, and are associated with warm, dry season precipitation conditions, rather than the mean plant growing season (Breecker, et al. 2009). Paleosols, fossil soils that have undergone relatively minor burial alteration, preserve the SOM and pedogenic carbonates of past soils and can be used as reliable indicators of past environments (Retallack 1991). For paleo reconstructions of carbon values, a 2‰ correction is needed to compensate for the differences between pre-industrial and modern atmospheric values of CO_2 (Indermuhle, et al. 1999).

Stable oxygen isotope values of fossil carbonates and teeth reflect water availability in local environments. The $\delta^{18}O$ composition of soil water can be derived from pedogenic carbonates and calculated if temperatures during formation are assumed (Breecker, et al. 2009; Friedman and O'Neil 1977). The $\delta^{18}O$ values of converted soil water during carbonate formation can be used as a proxy for the $\delta^{18}O$ value of precipitation, meteoric water, and the degree of

evaporation (Dansgaard 1964). These estimates of precipitation and evaporation values are useful for reconstructing the state of aridity in an environment, using isotope values derived from pedogenic carbonates (Koch 1998).

The stable carbon isotope composition of herbivorous tooth enamel is directly related to the isotopic composition of the plants an animal ingests during enamel formation (DeNiro and Epstein 1978b; Benjamin H. Passey, et al. 2005). The plant diet and water consumed by the animal is recorded during the tooth mineralization processes early in life (Balasse 2002; Koch, et al. 1989). Studies of extant ruminant ungulate mammals from different habitats suggests an average enrichment factor ($\varepsilon_{enamel\text{-}diet}$) associated with the incorporation of carbon into tooth enamel during formation of approximately $14.1 \pm 0.5‰$ (Cerling and Harris 1999). This known enrichment factor provides a simple equation to calculate the C_3 and C_4 contributions to diet. The $\delta^{18}O$ values of large herbivores' tooth enamel carbonate is derived from drinking water and diet (Bryant and Froelich 1995; Kohn, et al. 1996). Tooth enamel oxygen isotope values can reflect meteoric water composition and the degree of environmental aridity, depending on the species studied (Leslie, et al. 2016; Levin, et al. 2006). Tooth enamel is highly mineralized and less susceptible to diagenetic alteration than pedogenic carbonate, providing a relatively secure signature for oxygen isotope values (Koch, et al. 1997; Quade, et al. 1992; Wang and Cerling 1994).

While bulk SOM and pedogenic carbonates offer a local environmental signature, the teeth of medium to large herbivores can offer a much broader environmental signature, documenting regional scale environments, depending on the species' ranging patterns. Despite potential taphonomic biases (Behrensmeyer and Hill 1988), recent work by Western and Behrensmeyer (2009) suggests that modern bone assemblages accurately represent the relative

proportions of different taxonomic groups of living animals, implying that fossils of animals are good indicators for past habitats. Unfortunately, not all habitats are represented in the fossil record equally (Behrensmeyer and Hill 1988; Hill 1979) and individual habitats differentially fossilize (Gifford and Behrensmeyer 1977). Isotope analyses of tooth enamel can be used to verify or falsify reconstructions based on the habitat preferences of modern analogs, and can be contrasted with SOM and pedogenic carbonate values to produce holistic, fine-grained environmental reconstructions on a landscape scale.

1.5 Biomass Productivity

While $\delta^{13}C$ and $\delta^{18}O$ values from fossil teeth, SOM, and pedogenic carbonates provide baseline information about past environments, the primary biomass productivity of paleoenvironments is of interest to paleoanthropologists as well. Primary biomass productivity measures go far beyond usual environmental measures (Box, et al. 1989); by deriving biomass productivity values, the carrying capacity and stress level of an environment can be investigated, in conjunction with the types of plants that dominate an environment. To derive the biomass productivity of modern environments, high-resolution satellite imagery (Rapid Eye Imagery 0.8 meter resolution per pixel) was sampled for Normalized Difference Vegetation Index (NDVI) values, using an algorithmic-based technique after correcting for haze inducing problems, such as atmospheric conditions, cloud cover, and location of the Sun relative to the satellite (Tan, et al. 2012). NDVI values are derived on a scale of -1 to 1, but values pertaining to vegetation reflectance are comprised of values from 0 to 1. Values that approximate 1 indicate vegetation (and primary biomass) that is productive and has a high carrying capacity (wet, dense forests),

while values that approximate 0 indicate sparse vegetation with a low carrying capacity (arid deserts).

Recent work by Cerling et al. (2011) has shown a correlation between the fraction of wooded cover and $\delta^{13}C$ values derived from modern SOM. These correlations suggest that other links may exist among stable isotope values of SOM and measures of primary biomass. The relationship between NDVI and primary biomass productivity is well established, and has more recently been linked with accurate habitat predictions of modern animal communities (Box, et al. 1989; Cerling, et al. 2009; Hunt 1994; Pettorelli, et al. 2006; Pettorelli, et al. 2011; Tucker, et al. 1986). By establishing a paleo-proxy for biomass productivity, and contrasting this with the woody cover index developed by Cerling et al. (2011), I believe paleoanthropologists may be able to avoid arguments based on possible time averaged reconstructions, and instead focus on more ecologically centered reconstructions. Similar to the woody cover calibration developed by Cerling et al. (2011), the correlation between primary plant biomass productivity and carbon isotope ratios of bulk SOM provides a calibration for estimating paleo-biomass productivity; this technique offers paleoanthropologists another proxy for reconstructing environments.

1.6 Research Questions

In this dissertation, I address the following research questions by applying a landscape archaeology approach with fine-grained, paleoenvironmental reconstructions, to reconstruct hominin site choice and thus foraging behavior in the Lake Baringo Basin, during the Middle Pleistocene.

1. What is the relationship between modern SOM and NDVI assessed through high resolution satellite imagery, and can these NDVI values be used as proxies for paleo-biomass productivity?
2. What are the environmental conditions and resources available to hominins during Time Intervals 1 and 2, based on the following proxies: $\delta^{13}C$ values of SOM, pedogenic carbonates, and mammalian tooth enamel; $\delta^{18}O$ values of pedogenic carbonates and mammalian tooth enamel; paleo-NDVI values; fraction woody cover values?
3. Based on these environmental reconstructions, what are the differences, if any, in Acheulean and Middle Stone Age hominin site choice and landscape use during Time Intervals 1 and 2.

Chapter 2: A Middle Pleistocene intense monsoonal episode from the Kapthurin Formation, Kenya: Stable isotopic evidence from bovid teeth and pedogenic carbonates

2.1 Introduction

Changes in environments have long been associated with the evolution and technological choices of hominins (Ambrose 1998; Bräuer 2008; Darwin 1871; deMenocal 1995; Potts 1996; Reed 1997; Vrba 1993). Stable carbon and oxygen ($\delta^{13}C$; $\delta^{18}O$) values derived from herbivorous mammal biogenic carbonated apatite (tooth enamel) and pedogenic carbonates provide valuable data for environmental reconstructions (Cerling 1984; DeNiro and Epstein 1978a; Kingston, et al. 1994; Koch, et al. 1989; Levin, et al. 2011; Quade, et al. 1992). The stable isotope values of tooth enamel are independent of taxonomic identification of fossil specimens, and provide a useful way to confirm or falsify environmental reconstructions based on the habitat preferences of modern analogs. Despite potential taphonomic biases, Western and Behrensmeyer (2009) suggest that modern bone assemblages accurately represent the relative proportions of different taxonomic groups of living animals, implying that fossils of animals are good indicators for past habitats. Unfortunately, not all habitats are equally represented in the fossil record (Behrensmeyer and Hill 1988; Hill 1979) and habitats differentially "fossilize". Isotope analysis of tooth enamel can be used to verify reconstructions based on habitat preferences of modern analogs and relative taxonomic abundance, because the preferences of modern taxonomic groups may have differed in the past.

Pedogenic carbonates form at depth (>40cm) in equatorial soils at negative water balance conditions through the combined contribution of plant decay and diffusion (CO_2) at equilibrium

with soil water (Cerling and Quade 1993). Pedogenic carbonate carbon isotope values reflect soil CO_2 carbon isotope values and = oxygen isotope values of pedogenic carbonates reflect soil water oxygen isotope values (Cerling 1984). Thus, the isotopic composition of pedogenic carbonates can serve as a usefulproxy for local vegetation and hydrological habitats (Kingston 2007; Levin, et al. 2011; Quinn, et al. 2013).

Here, I use stable isotopes of carbon and oxygen from tooth enamel to reconstruct the dietary habits of fossil bovids collected at paleontological and archaeological sites from the Middle Pleistocene sediments of the Kapthurin Formation, Kenya. These dietary data, associated with taxonomic uniformitarian behavior of bovids (Bibi, et al. 2009), are used to reconstruct a landscape exploited by Acheulian hominins and chimpanzees between 543 ± 3 ka and 509 ± 9 ka (Leakey, et al. 1969; McBrearty, et al. 1996; McBrearty and Jablonski 2005). I also use stable isotopes of carbon and oxygen derived from pedogenic carbonates to augment these paleoecological reconstructions. Finally, I use stable isotopes from both pedogenic carbonates and tooth enamel to test the regional paleoclimatic predictions (Rossignol-Strick, et al. 1998; Schefuß, et al. 2003) of an intense monsoonal system affecting East Africa at ~528 ka. This research is directly relevant to comprehending the paleoenvironmental context of the terminal Acheulian and the beginnings of the Middle Stone Age technocomplexes, and the foraging behavior of hominins.

The Middle Pleistocene, 781 – 126 ka, formerly the Ionian (International Commission on Stratigraphy 2014), of Africa records a significant time period in human evolution; it marks the appearance of *Homo sapiens*, the development of new technologies often referred to as "modern", and the Middle Stone Age shift to the occupation of diverse habitats (Clark 1988; C. S. Henshilwood and C. W. Marean 2003; McBrearty and Brooks 2000). Acheulian technology

has long been assumed to be relatively uniform from its inception during the early Pleistocene, 2.58 Ma – 781 ka, formally the Calabrian and Gelasian (International Commission on Stratigraphy, 2014) through its eventual disuse during the later Middle Pleistocene (Clark 1977; Isaac 1972; Leakey 1971). Researchers have documented the variability in lithic manufacture, including the production of flakes via the Levallois method and the systematic production of blades during the terminal Acheulian (Adler, et al. 2014; Johnson and McBrearty 2012; McBrearty 2001; Tryon, et al. 2005). Some of these technological innovations occur prior to the appearance of the Middle Stone Age technocomplex, and could indicate a period of technological experimentation and innovation, focused around perennial freshwater springs and biomass rich habitats (Johnson, et al. 2009; Johnson and McBrearty 2012), similar to foraging behavior associated with some later Middle Stone Age hominins (Curnoe, et al. 2006; McCarthy, et al. 2010). The Kapthurin Formation preserves evidence of late Acheulian behavior and the only documented fossil *Pan* remains (McBrearty and Jablonski 2005). Detailed environmental reconstructions will help elucidate this period of innovation that precedes the Middle Stone Age, the habitat range of hominins, and the habitat range of chimpanzees during the Middle Pleistocene.

2.2 Background

2.2.1 Kapthurin Formation

Lying to the west of Lake Baringo, the Kapthurin Formation is part of the Middle Pleistocene sedimentary sequence of the Tugen Hills succession in the Kenyan Rift Valley (Figures 2.1 and 2.2). The formation consists of interstratified alluvial, lacustrine, and volcanic sediments, is exposed over an area of 150 km^2, and has an observed thickness of approximately

125m (Martyn 1969; Tallon 1978; Christian A. Tryon and Sally McBrearty 2002). All ages quoted are direct dates generated with the $^{40}Ar/^{39}Ar$ method (Deino and McBrearty 2002) (Figure 2.1). Martyn (1969) subdivided the formation into 5 members; K1, K3, and K5 are informally named the Lower, Middle, and Upper Silts and Gravels and are largely composed of terrigenous sediments from the Tugen Hills; K2, the Pumice Tuff Member, dated to 543 ± 3 ka, and K4, the Bedded Tuff Member, with successive eruptive facies dated to 284 ± 12 ka and 235 ± 2 ka separate the Silts and Gravel Members; K3 is also subdivided by the Grey Tuff, dated to 509 ± 9 ka, and by fluviolacustrine facies to the west (K3) and lacustrine facies to the east (K3'); K3' sediments consist of red, black, and green claystones and siltstones (Tallon 1978), and the sedimentary and geochemical structures of the clays and silts indicate deposition in a shallow lake that alternated between freshwater and saline-alakaline (Johnson and McBrearty 2012; McBrearty, et al. 1996; Renaut, et al. 1999).

The Kapthurin Formation lies unconformably above the Chemeron Formation, and is underlain by the Ndau Trachymugearite, which is dated to 1.57 Ma (Deino, et al. 2002; Hill, et al. 1986) using the K/Ar technique, and provides a maximum age for the Kapthurin Formation. All of the Kapthurin Formation's sediments are normally magnetized (Dagley, et al. 1978), and thus postdate the Matuyama-Brunhes Boundary, which is currently estimated at 775 ka using the $^{40}Ar/^{39}Ar$ method (Coe, et al. 2004), providing a maximum age for the Kapthurin Formation.

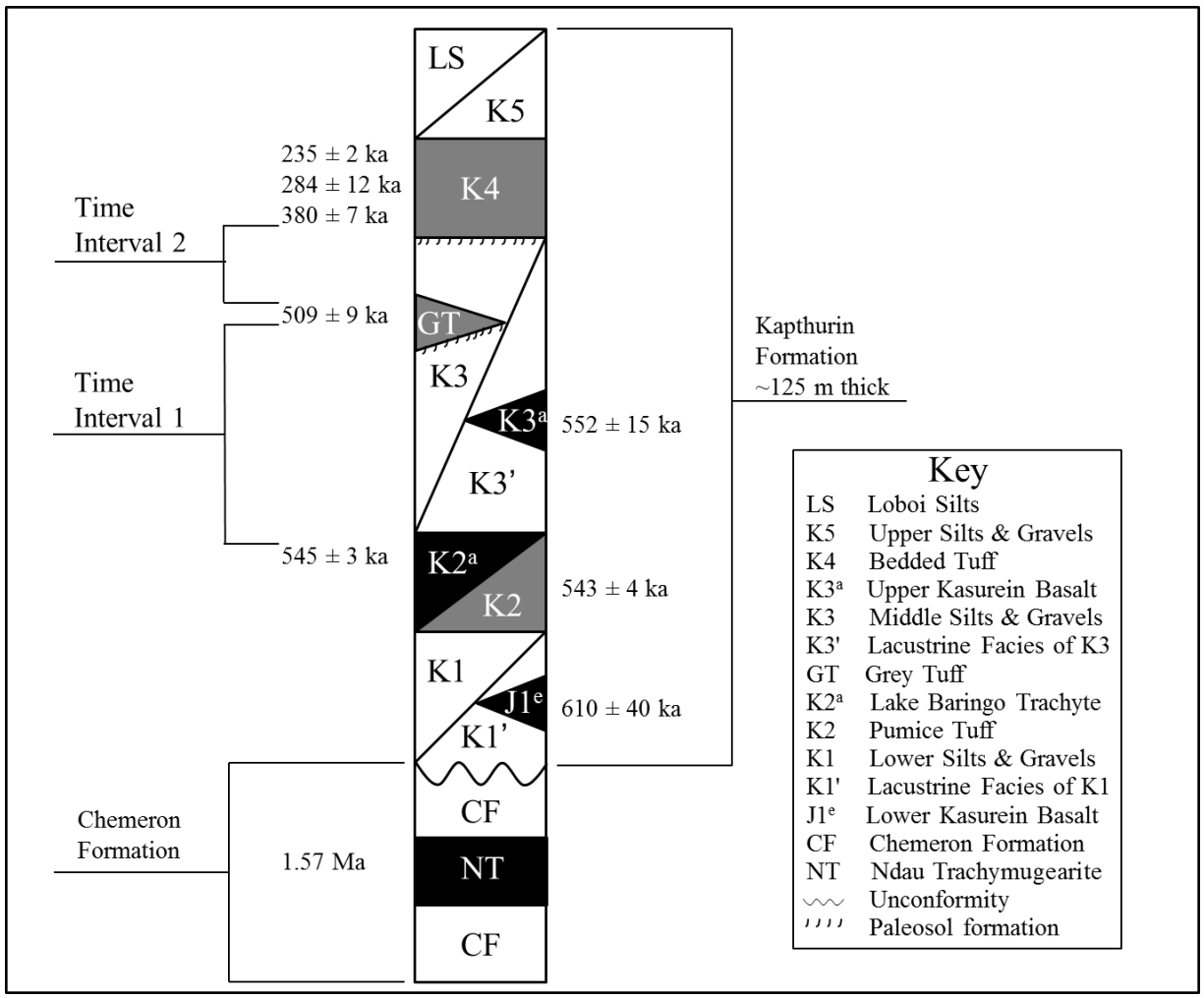

Figure 2.1: Generalized stratigraphic section of the Kapthurin Formation. Section is after Deino and McBrearty (2002). All dates are derived from the $^{40}Ar/^{39}Ar$ method, except the Ndau Trachymugearite, reported by Hill *et al.* (1986) using the K-Ar method. Shaded areas represent volcanic layers, light areas represent fluviolacustrine sediments.

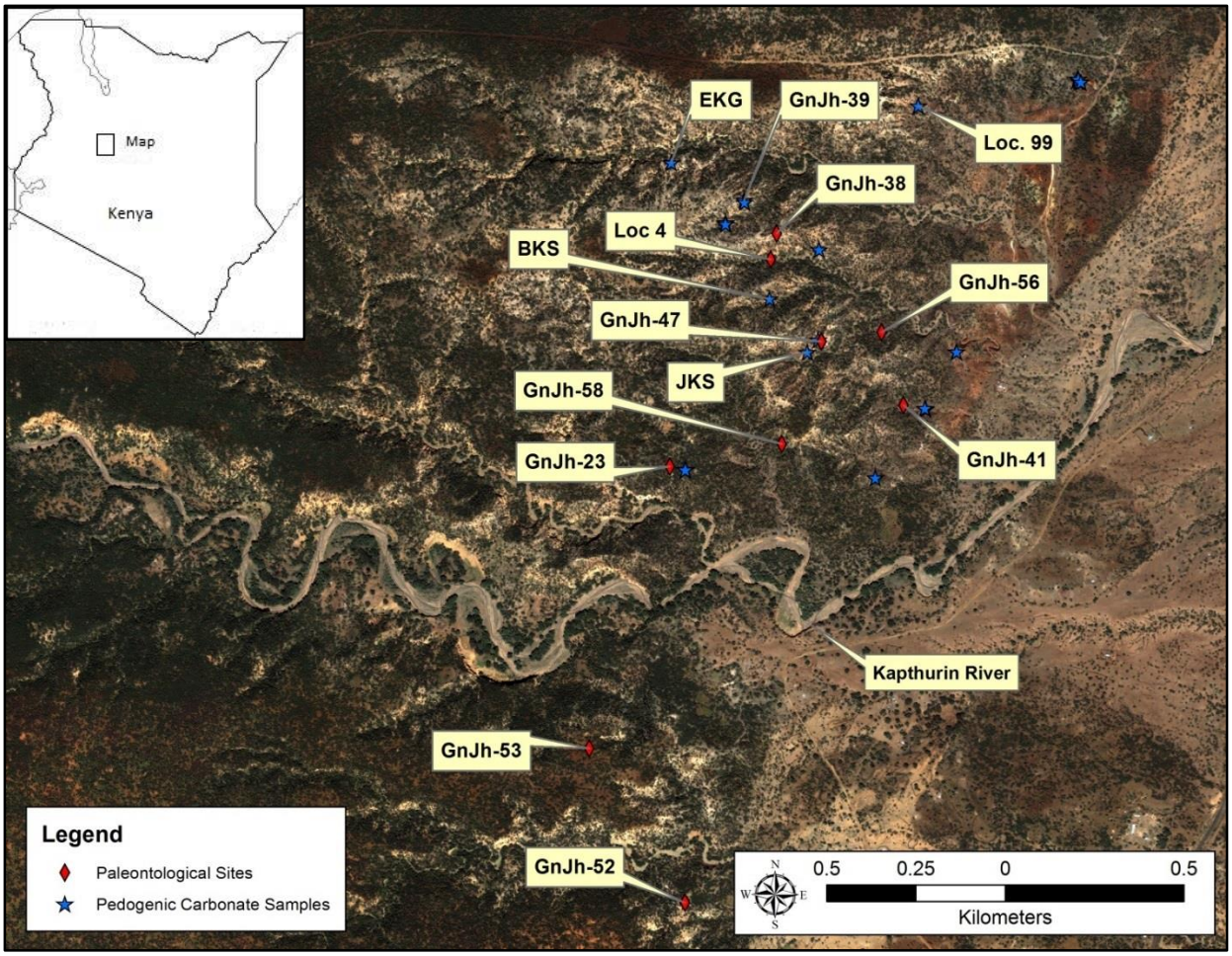

Figure 2.2: Satellite image (IKONOS 1.8 m resolution) with relevant archaeological and paleontological sites containing fossil bovid teeth and pedogenic carbonates sampled for stable isotope values ($\delta^{13}C$ and $\delta^{18}O$). Inset map is not to scale.

The focus of this research is the time interval represented by fossils recovered from deposits that lie above K2, the Pumice Tuff Member (543 ± 3 ka), and below the Grey Tuff (509 ± 9 ka). McBrearty (1999) noted the excellent faunal preservation below the Grey Tuff, and reconstructed the ancient environments from taxonomic identification of fauna, suggesting dense vegetation and marsh depositional conditions, possibly near a braided river system, with grasslands farther from the rivers. Tallon (1978) also interpreted paleochannels found above and below the Grey Tuff as a product of a braided river system. Johnson, et al. (2009) documented a

fossiliferous tufa in the southern exposure of the lacustrine facies (K3'), stratigraphically below the Grey Tuff. The presence of this tufa demonstrates a rich wetland environment in an otherwise semi-arid environment, confirming earlier predictions. McBrearty and Jablonski (2005) document the presence of *Pan* fossils at Loc. 99, which together with other fauna at the site (hippopotamus, crocodile, catfish, colobine monkey, and bushpig), indicates a locally wooded habitat near the shore of an alternating fresh and alkaline lake, with marshy patches. Hominin fossils identified as *Homo sp.* and *Homo erectus* (Leakey, et al. 1969; Wood and Van Noten 1986) have also been found in this interval, in the K3 fluvial facies, close in time and space (<1km) to the fossil *Pan* locality, indicating that chimpanzees and hominins occupied habitats in near proximity to one another *ca* 500 ka (McBrearty and Jablonski 2005).

The archaeology of the deposits from K3 and K3' in the Kapthurin Formation has been described by several researchers (Cornelissen 1992; Johnson and McBrearty 2010, 2012; McBrearty 1999; McBrearty, et al. 1996; Tryon 2003). This previous work has documented that Middle Pleistocene toolkits from the Kapthurin Formation were highly diverse, and include handaxe assemblages (LHA, GnJh-17), assemblages lacking *fossiles directeures* that are dominated by flakes and cores (GnJh-42, 50), the early presence of prepared core technology (LHA, GnJh-17), and systematic blade production (GnJh-42, 50). Tryon, et al. (2005) suggested that regional variability in Acheulian methods of flake production, including the Levallois method, present in the Kapthurin Formation, demonstrate variability in artifact manufacturing techniques before the Middle Stone Age transition, not regionalization of Acheulean lithic manufacture (McBrearty 2001; McBrearty, et al. 1996). These technological innovations could be related to methods of adaptive niche construction and exploitation of patchy, resource rich environments (Johnson and McBrearty 2012), although higher resolution environmental

reconstructions are necessary to test these assumptions, and are currently in progress (Leslie, et al. 2014).

2.2.2 Stable Carbon Isotopes

Throughout this paper, results are reported and discussed in the standard per mil (‰) notation:

Equation 2.1: $\delta^X = (R_{sample}/R_{standard} - 1) \times 1000$; $X = {}^{13}C, {}^{18}O$; $R = {}^{13}C/{}^{12}C, {}^{18}O/{}^{16}O$

The isotope standard is Vienna Pee Dee Belemnite (VPDB). The stable carbon isotopic composition of herbivorous tooth enamel ($\delta^{13}C_{enamel}$) directly reflects the isotopic composition of plants consumed by the animal during periods of enamel formation and mineralization (Ambrose and DeNiro 1986; Cerling and Harris 1999; DeNiro and Epstein 1978a). There are three main photosynthetic pathways available to plants prevailing in East Africa, C_3, C_4, and CAM (Crassulacean Acid Metabolism), of which only the first two serve as primary dietary sources for mammalian herbivores. C_3 plants use a 3-carbon compound and C_4 plants utilize a 4-carbon compound intermediate phase to fix CO_2 from the atmosphere during photosynthesis (Ehleringer, et al. 1997; Farquhar, et al. 1989; Osmond, et al. 1982). C_3 plants, which represent the most common photosynthetic adaptation, are generally trees and closed habitat vegetation, as well as high latitude grasses (Osmond, et al. 1982). The C_4 pathway is most commonly represented by mid-latitude grasses, wetland sages, and arid landscape chenopods (Ehleringer, et al. 1997). $\delta^{13}C$ values of C_3 plants in closed canopy environments in sub-Saharan Africa are highly negative relative to the standard (VPDB), averaging -31.4‰, while open canopy C_3 plants average -27.8‰, and savanna and bushland C_3 plants average -27.0‰; Conversely, the $\delta^{13}C$ values of sub-Saharan African C_4 plants are elevated relative to VPDB, mesic C_4 plants average -11.8‰

and xeric C_4 plants average -13.1‰ (Cerling, et al. 2003).. Studies of extant ruminant ungulate mammals from differing habitats display an average enrichment factor ($\varepsilon_{enamel\text{-}diet}$) associated with carbon incorporation into tooth enamel during formation of 14.1 ± 0.5‰ (Cerling and Harris 1999). More recent work by Benjamin H. Passey, et al. (2005) has shown that the enrichment factor varied over 4‰ when comparing the $\delta^{13}C$ values of both diet and enamel of voles, rabbits, pigs, and cattle. However, given the conclusions by Benjamin H. Passey, et al. (2005) that these differences in enrichment are mainly a result of diet, and the assumption that the fossil bovids under study are ruminant herbivores, I apply the enrichment factor from Cerling and Harris (1999). With this known enrichment factor, $\delta^{13}C_{enamel}$ values can be used to reconstruct diets, following Cerling, Andanje, et al. (2015), as C_4 hypergrazers ($\delta^{13}C_{enamel} \geq$-2‰), C_4 grazers ($\delta^{13}C_{enamel} \geq$-1‰), C_3 closed canopy browsers ($\delta^{13}C_{enamel} \leq$ -14‰), C_3 hyper-browsers ($\delta^{13}C_{enamel} \leq$ -12‰), C_3 browsers ($\delta^{13}C_{enamel} \leq$ -8‰), and C_3/ C_4 mixed feeders –(1‰$\leq \delta^{13}C_{enamel} \geq$-8‰). Following Cerling, et al. (2003), the diets of bovids must be considered as part of a grazing to browsing spectrum, where hypergrazers consume over 95% C_4 grasses, grazers consume between 70-95% C_4 grasses, hyperbrowsers or frugivores consume over 95% C_3 browse, browsers consume between 70-95% C_3 browse, and mixed feeders consume more than 30% C_4 grasses and more than 30% C_3 browse.

Pedogenic carbonates are calcite nodules, clast coverings, and cemented horizons that are formed in soils found in sub-humid to arid regions of the world. Birkeland (1999) suggests that the dissolution of Calcium bearing minerals from dust and soil, release Calcium ions, which are transported downward with soil water and are eventually re-precipitated as pedogenic carbonates at depth in soils (>40cm). Pedogenic carbonates formation can be inhibited by a few factors, including seasonal bias in formation, mainly forming during warm, dry seasons, not during the

mean growing season (Breecker, et al. 2009). The formation of pedogenic carbonates is also inhibited by densely forested environments, because high precipitation and acid leaching repress carbonate precipitation, indicating a possible C_4 bias when using pedogenic carbonates for environmental reconstructions (Tucker and Wright 1990). The formation time of pedogenic carbonates, as individual nodules or horizons, varies between 10^2 and 10^5 years (Jenny 1980). Equatorial pedogenic carbonates at depths greater than 30 cm below surface vegetation in soils with high respiration rates incorporate soil CO_2 associated with decaying organic matter derived directly from surface vegetation during soil development (Cerling 1984; Cerling and Quade 1993). Assuming minimal fluctuations in atmospheric CO_2 during the Pleistocene (Cerling 1991), the main source of variation in carbon isotope values of pedogenic carbonates ($\delta^{13}C_{pc}$) from the Kapthurin Formation should bederived from local decay products of surface vegetation (Levin, et al. 2011; Wynn 2004). Positive fractionation of carbon isotopes between soil CO_2 and pedogenic carbonates is determined by both kinetic (Cerling, et al. 1991) and temperature dependent equilibrium (Romanek, et al. 1992) processes, resulting in a combined ^{13}C enrichment between plants and pedogenic carbonates of 12-14‰ under high respiration and 14-17‰ under low respiration (Levin, et al. 2011). More recently, Cerling et al. (2011) developed a regression equation to calculate the fraction of woody canopy cover from $\delta^{13}C_{pc}$ values, using the following isotope values to discriminate differences in vegetation cover: Forests, a landscape with continuous stands of trees at least 10 m tall ($\delta^{13}C_{pc}$ <-11.5‰); Woodland/Bushland/Shrubland, where woodlands are an open stand of trees at least 8 m tall and a field layer dominated by grass and woody cover over 40%, bushlands are an open stand of bushes between 3 and 8 m tall and woody cover over 40%, and shrublands are an open or closed stand of bushes up to 2 m tall ($\delta^{13}C_{pc}$ between -11.5 and -6.5‰); Wooded Grasslands, land covered with grassland and

between 10 and 40% tree and shrub coverage ($\delta^{13}C_{pc}$ between -6.5 and -2.3‰); Grasslands, land covered with grasses and less than 10% is covered with trees and shrubs ($\delta^{13}C_{pc}$ >-2.3‰).

2.2.3 Stable Oxygen Isotopes

The $\delta^{18}O$ values measured in medium and large-sized herbivore tooth enamel carbonate ($\delta^{18}O_{enamel}$) is derived from drinking water and diet, mediated by physiology (Bryant and Froelich 1995; Kohn 1996). Tooth enamel can reflect meteoric water composition and thus the degree of environmental aridity, depending upon the species studied (Levin, et al. 2006). In obligate drinkers the $\delta^{18}O_{enamel}$ values directly track the $\delta^{18}O$ value of drinking water ($\delta^{18}O_{drinking\ water}$), which is associated with local temperature, precipitation, latitude, altitude, aridity, and evaporative processes, and are a good proxy for changes in drinking water composition, local rainfall, or moisture source (Dansgaard 1964). Other animals obtain most of their ingested water from the food they consume and are termed non-obligate drinkers. Non-obligate drinkers' water sources range from roots and stems to fruit and leaves. The $\delta^{18}O_{enamel}$ values of leaf eating non-obligate drinkers are often elevated when compared with meteoric water due to preferential transpiration of isotopically light water ($H_2{}^{16}O$) from the leaf surface, while the water content of roots, stems, and fruit usually tracks the isotopic composition of the drinking water source (Ehleringer and Dawson 1992; Sternberg 1989). Leaf water $\delta^{18}O$ enrichment (relative to stem water $\delta^{18}O$ values) is most expressed under hot and arid conditions, thus further elevating the $\delta^{18}O_{enamel}$ measured in arid-adapted animals that obtain their water from leaves (Ayliffe and Chivas 1990; Dongmann, et al. 1974). Levin, et al. (2006) suggest tracking fluctuations in meteoric water availability using an aridity index by separating mammals as Evaporative Insensitive (EI), obligate drinkers, and Evaporative Sensitive (ES), or non-obligate drinkers

whose $\delta^{18}O$ values track the isotopic enrichment associated with leaf water. As environmental aridity increases, the disparity between EI and ES $\delta^{18}O_{enamel}$ values should increase, providing an independent measure of aridity from meteoric water isotopic composition. Thus, $\delta^{18}O_{enamel}$ values from both obligate and non-obligate drinkers can be useful in reconstructing the isotopic composition of local meteoric water, paleoenvironmental conditions, and paleoaridity.

The $\delta^{18}O$ values of pedogenic carbonates ($\delta^{18}Opc$) are controlled by the oxygen isotopic composition of soil water and temperature. The $\delta^{18}O$ value of soil water is determined by the $\delta^{18}O$ value of rainfall water and the degree of soil water evaporation. Soil water is recharged through infiltration and surface run-off, and accumulations of rainfall over the course of a season (Breecker, et al. 2009). The $\delta^{18}O$ values of rainfall vary with climate, elevation, and distance from humidity source (Dansgaard 1964). In East Africa, the main determinants of rainfall $\delta^{18}O$ values are rainfall amounts, elevation, and distance from humidity sources (Levin, et al. 2009; Rozanski, et al. 1996). Because surface water is subject to increased evaporation, due to increased time available for evaporation, $\delta^{18}O_{pc}$ values are often elevated in near surface samples, where there is increased potential for soil water evaporation (Breecker, et al. 2009; Quade, et al. 1989). Finally, $\delta^{18}O_{pc}$ values are a function of soil temperature, because the fractionation between soil water and pedogenic carbonates is temperature dependent (-0.2‰/°C) (Kim and O'Neil 1997). Passey, et al. (2010) demonstrated that soil temperatures during the last 4 million years of the Turkana Basin exceed those of Mean Annual Temperatures (MAT) today. More recently, Cerling, Mace, et al. (2015) have shown that soil temperatures, taken over 25 cm below surface in open environments in East Africa, are elevated by as much as 7°C when compared with MAT, while soil temperature in forest soils are similar to MAT estimates.

2.2.4 Paleoclimate Predictions

Deep sea formation of organic-rich layers (sapropel) in the eastern Mediterranean Sea indicate periods of increased fresh water discharge from the Nile River and have been explained by intensified monsoonal activity in East Africa during periods of Northern Hemisphere insolation maxima (Rossignol-Strick, et al. 1982; Rossignol-Strick and Paterne 1999). The formation of sapropels in the Mediterranean has also been previously linked with hominin activity in East Africa (McDougall, et al. 2008). Others (Deino, et al. 2006; Kingston, et al. 2007) have demonstrated orbital forcing of cooling and heating events are well grounded in East African field data. Sapropel A has been identified by Rossignol-Strick, et al. (1998) and correlated to an insolation maximum at ~525–528 ka using astronomic calibration (Hilgen 1991). Sapropel A formation exhibits a relatively low monsoon index (30) and exceptionally negative $\delta^{18}O$ values, measured in foraminifera (*Globigerinoides ruber*) from the sapropel, which indicate marked decrease in salinity and/or an increase in the water input from the Nile. The intensity of African monsoonal activity and sea surface temperature in the tropical Atlantic Ocean has been linked with turnover events of equatorial African C_3 and C_4 vegetation that are largely controlled by aridity (Schefuß, et al. 2003). Schmieder, et al. (2000) document the presence of thick interstratified layers of the giant diatom *Ethmodiscus rex* in deep ocean cores from the South Atlantic Ocean at the onset of Marine Isotope Stage (MIS) 13, approximately 533 ka (Lisiecki and Raymo 2005). These diatoms are commonly found today in warm equatorial oceans (Mikkelsen 1977) and Schmieder, et al. (2000) suggest that the presence of these laminated layers indicate a period of extreme paleooceanographic variability in temperature and circulation in the South Atlantic Ocean throughout MIS 13 (~533–478 ka) (Lisiecki and Raymo 2005). Kukla and Cílek (1996) report a peak in the magnetic susceptibility stack from the Chinese Loess plateau that suggests soil formation in a warm and humid climate during MIS 13. Clark, et al.

(2006) interpret this peak in the magnetic susceptibility stack as evidence for increased monsoonal activity over Asia and Africa. Hillenbrand, et al. (2009) also note the probable collapse of the Western Antarctic Ice Sheet during MIS 15–13 (~621–478 ka), suggesting it is most likely caused by a prolonged interglacial period that is marked by increased biological productivity and lithogenic sediment supply. These proxies provide good evidence for a period of intense precipitation in equatorial Africa during MIS 13, which is largely controlled by an intensified African monsoonal system, and indicate an increase in C_3 vegetation in East Africa (Figure 2.3). I will test these climatic predictions with African paleoecological data relevant to MIS 13.

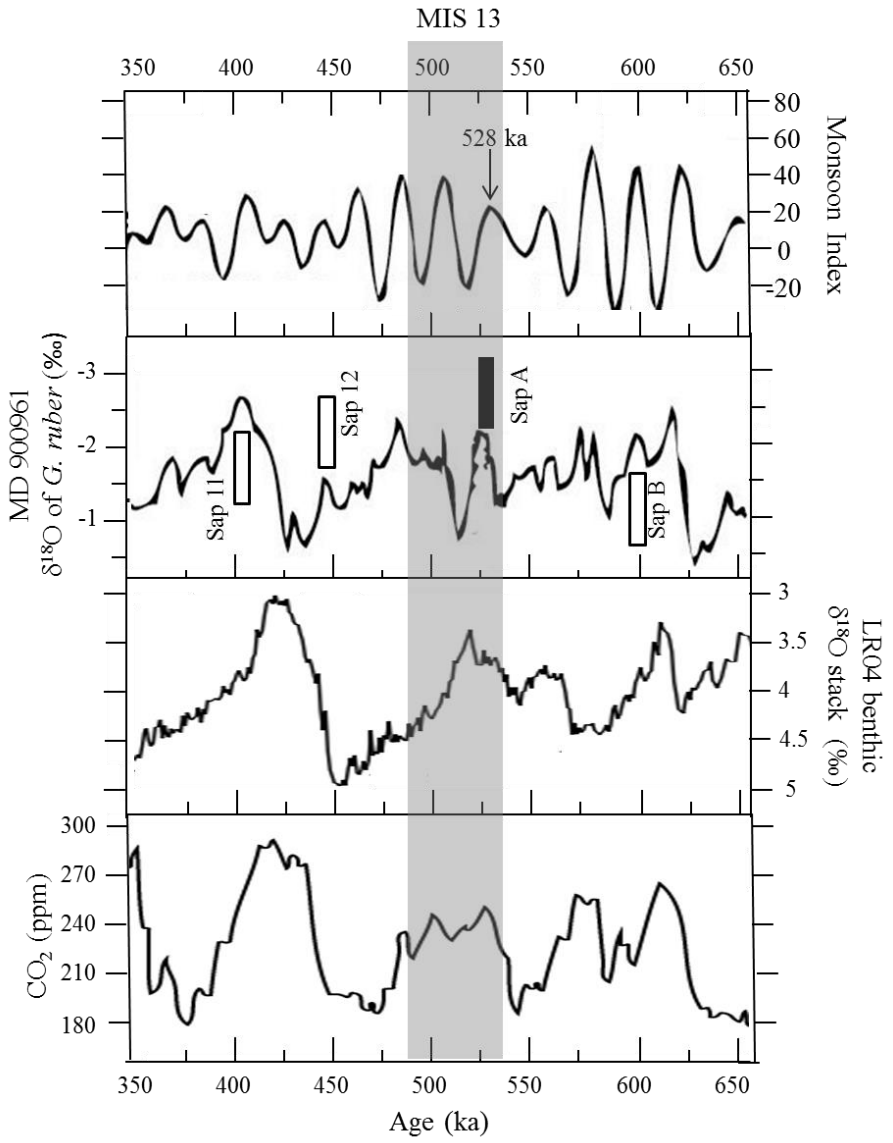

Figure 2.3: Composite paleoclimate data indicating an intensified African monsoonal system during MIS 13 (highlighted). CO_2 atmospheric composition measurements are from Allan Hills BIA (Site 27), Antarctica, from data in John A Higgins, et al. (2015). LR04 benthic $\delta^{18}O$ stack from 57 globally distributed records reported in Lisiecki and Raymo (2005). Core MD 900961 from Rossignol-Strick, et al. (1998) displays periods of sapropel formation in the Mediterranean Sea, generally correlated with intensified monsoonal systems. Monsoon index is controlled by insolation variations, and display variations in the intensity of the African monsoonal system over time, after Rossignol-Strick (1983). During MIS 13, CO^2 atmospheric pressure is high, indicating warmer global temperatures, and precipitation in equatorial Africa increases dramatically, indicated in the monsoon index.

2.3 Methods

Fossil bovid teeth (n=20) were collected from paleontological sites stratigraphically below the Grey Tuff (~509 ka). Sample sizes are small due to the nature of fossil preservation in the Kapthurin Formation, paleontological specimens are relatively rare, and generally only preserved during the time interval under study. Other paleontological specimens were discarded if they were not identified to tribe, or had incisions or breaks in surface enamel, which could be indicative of diagenetic alteration, or were currently under study by other researchers. The specimens are housed in the Department of Paleontology, National Museums of Kenya, Nairobi, not all specimens are accessioned; field identification numbers are used in place of accession numbers. Sites from the Kapthurin Formation sampled include GnJh-23, GnJh-38, GnJh-41, GnJh-47, GnJh-52, GnJh-53, GnJh-56, GnJh-58, and Locality 4 (Figure 2.2). Sampled teeth were identified to bovid tribe according to Gentry (1978) criteria. Bovid tribes sampled include: Neotragini, Reduncini, Tragelaphini, Alcelaphini, Cephalophini, and Bovini. Bovids were chosen for analysis because extant bovids inhabit diverse environments and should provide evidence for variation in past habitats, if it exists (Bibi, et al. 2009).

Coupled samples of $\delta^{13}C_{enamel}$ and $\delta^{18}O_{enamel}$ derived from serial samples of complete teeth, display dietary choices and changes in aridity during enamel formation, and thus offer a longer span of time to reconstruct habitats (Fricke and O'Neil 1996; Koch, et al. 1989; B. H. Passey, et al. 2005). Tooth formation can occur over periods of months or years depending upon the taxon (Hoppe, et al. 2004; Stevens, et al. 2011; Zazzo, et al. 2005; Zazzo, et al. 2002). Drilling samples perpendicular to the growth axis, samples derived near the occlusal surface of the tooth (apex) represent early periods of tooth formation, while samples near the tooth cervix represent late periods of tooth formation (B. H. Passey, et al. 2005). Balasse (2003) reports that

even though some isotopic mixing may occur given a simple sampling strategy perpendicular to the growth of the tooth, starting at the cervix and ending at the apex, the chronological order of enamel formation is preserved. Thus, sampling intra-tooth isotopic variation has become an important tool for reconstructing seasonal variability in climate, ecology, and behavior (Balasse, et al. 2003; Fricke, et al. 1998; Kohn, et al. 1998; Zazzo, et al. 2002).

Kenyan cultural heritage laws do not permit the export of fossil teeth, so all sampling was performed at the National Museums of Kenya. A dental drill (Vogue 6000) with a 1 mm diamond drill bit was used to sample the teeth serially, following the protocols of Balasse (2003). Fossil teeth were sampled incrementally, with individual samples drilled perpendicular to the growth axis of the tooth. Each tooth was drilled at an interval of approximately 1.5 mm, with initial samples taken at the cervix (late formation) and final samples taken at the apex (early formation) to reflect the animal's diet and water availability during enamel formation. Fossil teeth were chosen on the basis of site, taxon, tooth type, and preservation quality. I primarily sampled molar teeth to avoid early juvenile dietary signatures (Bedaso, et al. 2013). EI and ES fauna were identified following the criteria of Levin, et al. (2006) as well as modern physiological and behavioral adaptations (Kingdon 1988). Diagenesis of fossil enamel is a possibility, but Wang and Cerling (1994) have demonstrated that tooth enamel is consistently resistant to diagenetic alteration, and generally preserves the original isotopic signature. The $\delta^{13}C$ signatures of the fossil bovids sampled in this study are not outside the known ranges of extant faunal isotopic signals (Cerling, et al. 2003). Browser representatives, such as individual tragelaphini teeth, average -10.4‰ (Field ID 80), -7.9‰ (Field ID 5, not an average, only one sample is represented), -11.2‰ (Field ID 232), and -8.8‰ (Field ID 25), similar to modern ranges of -8.5‰ and -10.0‰ (Cerling, Andanje, et al. 2015). Hyper-grazer representatives, such

as individual alcelaphini teeth, average 1.2‰ (Field ID 99), 1.8‰ (Field ID 245), and 1.0‰ (Field ID 304) and are very close to the modern ranges of > 2‰ (Cerling, Andanje, et al. 2015). These results suggest that these fossils have not undergone significant diagenesis, and are within modern ranges once the 1.5‰ shift in modern carbon values is considered (Leuenberger, et al. 1992) (Table 2.1).

Each serial sample was composed of approximately 10 mg of powdered tooth enamel and was prepared following Balasse (2003). Samples were treated with 3% sodium hypochlorite (0.1 M NaOCl solution per mg of sample) for 24 hours to remove organic matter, and were neutralized with deionized water (dH_2O). Dried enamel samples were then reacted with acetic acid (0.1 M $C_2H_40_2$) for four hours to remove any diagenetic carbonates. Samples were submitted to the *Centre National de la Recherche Scientifique, Museum National d'Histoire Naturelle* (CNRS/MNHN) for stable isotope ratio analysis. The isotope analyses were performed using a Thermo-Finnigan Kiel IV carbonate analyzer coupled to a DeltaV mass spectrometer. Analytical precision was obtained using internal standards (MarbreLM) calibrated against NBS-19. These internal standards were run intermittently with the tooth enamel samples, with standard deviations for $\delta^{13}C$ of 0.016‰ and for $\delta^{18}O$ of 0.05‰. To estimate $\delta^{18}O_{drinking\ water}$ values, I converted the $\delta^{18}O_{enamel}$ from the VPDB to the VSMOW scale using the following approximation from Sharp (2007):

Equation 2.2: $\delta^{18}O_{VSMOW} = 1.03091 \times (\delta^{18}O_{enamel}) + 30.91$

Next, I calculate $\delta^{18}O_{drinking\ water}$ values of obligate drinkers (EI) using the conversion equation provided by Chenery, et al. (2012), who converted human carbonate (VSMOW) into phosphate oxygen ($\delta^{18}O_P$) values (VSMOW), combining their regression equations with the drinking water equation from Daux, et al. (2008), creating the following equation:

Equation 2.3: $\delta^{18}O_{drinking\ water\ (phosphate)} = 1.590 \times \delta^{18}O_{VSMOW(carbonate)} - 48.634$

I chose Equation 2.3, due to the low uncertainty for calculating $\delta^{18}O_{drinking\ water}$ values (±1‰, 2σ), when compared with larger errors (between ±1‰ and ±3‰) associated with drinking water conversion (Pollard, et al. 2011). Following Bedaso, et al. (2013), I calculate $\delta^{18}O_{drinking\ water}$ values using the most negative value of each obligate drinker's tooth sampled, to minimize evapotranspiration effects that would contribute to higher $\delta^{18}O$ values. These equations were developed for human phosphate and carbonate values, so I calibrate these equations by testing them on data provided in Levin, et al. (2006), reconstructing $\delta^{18}O_{drinking\ water}$ values from modern fauna and measured water values from the following sites: Arabuko-Sokoke (-3.9‰ vs. reported -2.3‰), Athi (-2.1‰ vs. reported -4.0‰), Mpala (+0.25‰, vs. reported -3.3‰), and Tsavo (-2.1‰, vs. reported -4.0‰). These estimates are within the error ranges reported by Pollard, et al. (2011) when reconstructing drinking water values. To reconstruct aridity, I calculated the enrichment between ES and EI taxa (after Levin, et al. 2006):

Equation 2.4: $\varepsilon_{ES\text{-}EI} = ((R_{ES}/R_{EI}) - 1) \times 1000$

The Anderson-Darling test for normality was used to determine if $\delta^{13}C_{enamel}$ and $\delta^{18}O_{enamel}$ values were normally distributed. *P*-values demonstrate that neither distribution is normal, and thus non parametric tests for significance are appropriate. Pairwise Mann-Whitney U tests (two-tailed) were applied to sample localities, as long as three teeth were sampled from each location. Mann-Whitney U tests were also applied to bovid tribes and to ES and EI identified specimens. Isoscapes of predicted carbon and oxygen isotope ratios were produced with ArcView 10.2. These data were interpolated between data points using inverse distance weighting, an interpolation technique appropriate for ecological data (Johnston 1998). Statistics were calculated using Microsoft Excel and *R* software.

Pedogenic carbonates nodules (n=24) were collected during 2011 and 2012 field seasons, from 20 different paleontological, archaeological, and geological settings. All samples were collected from well-developed paleosols, stratigraphically sampled below the Grey Tuff or individual paleontological and archaeological sites within the time interval under study (543 – 509 ka). Given these constraints, some time-averaging must be expected. Pedogenic carbonates were examined microscopically for cracks, infilling, and other diagenetic reworking by detrital carbonate; any with such alterations were discarded from analyses. Nodules were embedded in an epoxy-resin (EpoFix) and then cross-sectioned using a precision saw (Buehler Isomet 1000). Cross-sections of nodules were sampled using a high precision micromill (New Wave) with a 0.5 mm diamond drill bit. Nodules were serially sampled at 1 mm intervals to determine any internal nodular variability during formation (n=254), the serial samples have been averaged and are provided with individual standard deviations (Table 2.2). Powdered samples were submitted to the *Centre National de la Recherche Scientifique, Museum National d'Histoire Naturelle* (CNRS/MNHN) for stable isotope ratio analysis. The isotope analyses were performed using a Thermo-Finnigan Kiel IV carbonate analyzer coupled to a DeltaV mass spectrometer.

Analytical precision was obtained using internal standards (MarbreLM) calibrated against NBS-19. These internal standards were run intermittently with the carbonate samples, with standard deviations for $\delta^{13}C$ of 0.03‰ and for $\delta^{18}O$ of 0.05‰. Fraction woody cover (f_{wc}) was estimated following Cerling et al. (2011), by first converting the values of $\delta^{13}C_{pc}$ to the isotopic equivalent of organic carbon ($\delta^{13}C_{om}$), subtracting 14‰. I also applied the regression equation below (Equation 2.5) to estimate fraction woody cover during this time interval.

Equation 2.5: $f_{wc} = \{\sin[-1.06688 - 0.08538(\delta^{13}C_{SOM})]\}^2$

2.4 Results and Discussion

2.4.1 Carbon isotopic composition of tooth enamel by tribe

The results of stable isotope inquiry are displayed in Table 2.1. The range of $\delta^{13}C_{enamel}$ values measured for fossils from the 543 – 509 ka time interval of the Kapthurin Formation (-11.5 to +2.3 ‰) spans extant bovid adaptations to C_3 and C_4 diets (Cerling, Andanje, et al. 2015). The $\delta^{13}C_{enamel}$ values indicate consistent consumption of both C_3 and C_4 vegetation, with a few specimens falling within the expected range of mixed feeders. Generally the dietary preferences of individuals sampled did not show variation through serial sampling, with the notable exception of Field ID 25, a lower third molar of a tragelephine whose diet shifted seasonally to a mixed C_3/C_4 diet from a strict C_3 browsing diet during tooth formation (Figure 2.4). When teeth data are compared by tribe using pairwise Mann-Whitney U tests, alcelaphini, bovini, reduncini, and tragelaphini are all significantly different from one another ($P < 0.05$) in $\delta^{13}C_{enamel}$ values. Neotragini and cephalophini were not included in statistical comparisons due to sample sizes of n=1 for each tribe.

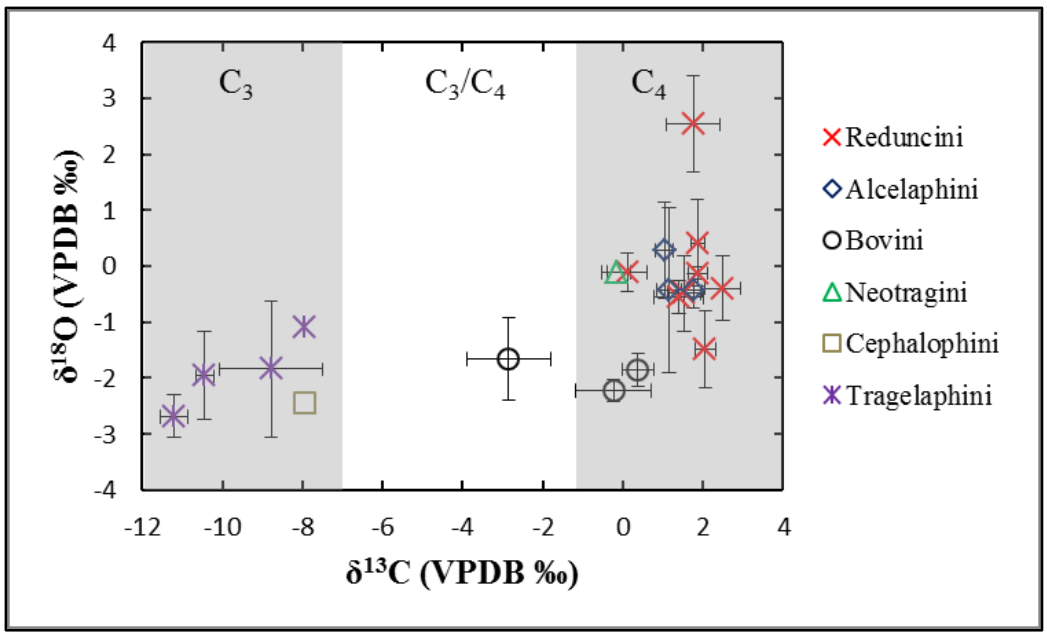

Figure 2.4: Average stable isotope values +1σ of serial bovid tooth enamel samples, displayed against x-axis ($\delta^{13}C$) and y-axis ($\delta^{18}O$). Samples are shown with respect to assumed diet type. Shaded and light areas reference C_3, Mixed C_3/C_4, and C_4 diets.

Alcelaphini- The diet of alcelaphines is dominated by C_4 vegetation, and does not appear to show any dietary shifts during tooth formation, although sample sizes are too small to permit statistical analyses (Table 2.1). The $\delta^{13}C_{enamel}$ values of sampled molars average 1.2‰ (Field ID 99), 1.8‰ (Field ID 245), and 1.0‰ (Field ID 304), indicating that the alcelaphines were grazers, feeding on C_4 grasses for the majority of their diet in open savanna environments (Table 2.1). These fossil data represent the second highest $\delta^{13}C_{enamel}$ values of the bovid taxa sampled, averaging between 1.0 and 1.8‰, and are very close to the modern ranges associated with alcelaphines (>2‰) indicating a similarly selective diet of C_4 grasses (Cerling, Andanje, et al. 2015). As in other studies, these data suggest that fossil alcelaphines had a slightly more plastic diet that was at least 1‰ lower than modern analogs, indicating a slight percentage of C_3 dietary sources and

must be considered grazers, not hyper-grazers (Cerling, Andanje, et al. 2015; Kingston and Harrison 2007). The presence of alcelaphines during this time interval indicates the existence of the grassland ecosystems that they commonly inhabit today.

Bovini- The diet of two of the bovines appear to be dominated by C_4 vegetation with average $\delta^{13}C_{enamel}$ values of 0.4‰ (Field ID 266) and -0.2‰ (Field ID254), while Field ID 228 has an average value of -2.9‰, indicating a C_3 dietary component (Table 2.1). Both Field ID 228 and 254 have sequential $\delta^{13}C_{enamel}$ values that trend more positive during tooth formation (-3.7 to -0.8‰, and -1.5 to 1.0‰ respectively), possibly indicating a shift in diet during tooth formation. The other tooth (Field ID 266) has relatively stable $\delta^{13}C$ values throughout tooth formation (between 0.7 and -0.5‰). Field IDs 254 and 266 average $\delta^{13}C_{enamel}$ values are indicative of a grazing adaptation, similar to extant bovines whose $\delta^{13}C_{enamel}$ values average 0.9 ±3.3‰ (Cerling, Andanje, et al. 2015). Field ID 228 $\delta^{13}C_{enamel}$ values average -2.9‰, and while indicating a C_3-C_4 mixed feeder dietary adaptation, are still within the range of extant bovine carbon enamel values (Cerling, Andanje, et al. 2015). Taken together, these enamel values indicate that during this time interval bovines in the Baringo Basin incorporated a large, yet not exclusive, portion of C_4 vegetation into their diet. While extant bovines diet can range from pure grazing to pure browsing depending on the habitat, the contribution of C_3 vegetation to the diet of Field ID 228 could presumably be from C_3 browse, grass, shrub, or aquatic sources (Cerling, Andanje, et al. 2015). Here, I interpret the presence of bovines to indicate the existence of open C_4 grasslands and C_3 browse, shrub, or aquatic plants given the low $\delta^{18}O_{enamel}$ average values associated with Field IDs 266 (-1.9‰), 228 (-1.7‰), and 254 (-2.2‰) (Table 2.1) (See section 4.2).

Cephalophini- The $\delta^{13}C_{enamel}$ values of the single Cephalophini specimen average -8.0‰, suggesting a browser dietary adaptation, although one that is quite different from modern analogs whose $\delta^{13}C_{enamel}$ values range between -10.6 and -14.3‰ (Cerling, Andanje, et al. 2015). Due to the small size of the molar, only two serial samples were manually drilled for $\delta^{13}C_{enamel}$ analysis resulting in values of -7.7 and -8.2‰. These $\delta^{13}C$ values are between 2 and 6‰ more positive than extant values for cephalophini and would suggest an open woodland habitat, with contributions from C_4 grasses, or a mixture of C_3 browse, shrub, herb, or grass plants whose $\delta^{13}C$ values range between -20 and -37‰ (Kohn 2010). This data is important despite the small sample size, because specimens of Cephalophini generally do not preserve well in the fossil record and due to the divergence of fossil $\delta^{13}C_{enamel}$ values from extant values (Bibi 2013; Cerling, Andanje, et al. 2015; Gentry, et al. 2010; Kingdon 1988).

Field ID	Serial #	Tribe	Genus	Tooth	Site	$\delta^{13}C$	$\delta^{18}O$	$\bar{x}\ \delta^{13}C$	$\bar{x}\ \delta^{18}O$
58	1	Reduncini +	*Redunca*	LM3	GnJh-23	1.2	-1.6	1.5	-0.5
	2					1.3	0.0		
	3					1.4	-0.3		
	4					2.2	0.0		
70	1	Reduncini +	*Redunca*	LM3	GnJh-23	1.9	-0.1	1.9	-0.1
	2					1.5	0.0		
	3					2.1	-0.3		
80	1	Tragelaphini ++	*Tragelephus*	LM	GnJh-23	-10.7	-2.8	-10.4	-2.0
	2					-10.2	-1.2		
99	1	Alcelaphini +	*Damaliscus*	UM3	GnJh-23	0.8	1.7	1.2	-0.4
	2					0.9	0.7		
	3					1.6	-0.6		
	4					1.3	-2.0		
	5					1.2	-1.9		
48	1	Neotragini ++	*Ourebia*	UM3	GnJh-23	-0.6	-0.9	-0.2	-0.1
	2					0.3	-0.5		
	3					-0.2	1.0		
57	1	Reduncini +	*Redunca*	UM3	GnJh-23	0.2	0.3	0.1	-0.1
	2					0.6	-0.2		
	3					-0.6	-0.5		
35	1	Reduncini +	*Reduncini*	UM	GnJh-38	0.6	1.1	1.8	2.5
	2					2.2	2.6		
	3					2.2	3.3		
	4					2.0	3.1		
5*	2	Tragelaphini ++	*Tragelephus*	UP3	GnJh-38	-7.9	-1.1	-7.9	-1.1
31	1	Reduncini +		UM	GnJh-38	2.2	0.3	2.5	-0.4
	2					2.2	-0.5		
	3					3.1	-1.1		
237	1	Cephalophini ++	*Sylvicapra*	LM3	GnJh-41	-8.2	-2.1	-8.0	-2.4
	2					-7.7	-2.8		
92	1	Reduncini +	*Redunca*	LM3	GnJh-41	1.8	-0.6	1.9	0.4
	2					2.1	0.4		
	3					1.7	1.3		
244	1	Reduncini +	*Kobus*	UM	GnJh47	0.6	-0.8	1.4	-0.6
	2					2.0	-0.1		
	3					1.6	-0.8		

Table 2.1: Serial and average stable isotope values of fossil bovid teeth sampled. Samples were collected serially and have been averaged from serial samples. $\bar{x}$=averages, *=averages are not possible, n=1. + Evaporative Insensitive, ++ Evaporative Sensitive, LM=Lower Molar, UM=Upper Molar, UP=Upper Premolar.

Field ID	Serial #	Tribe	Genus	Tooth	Site	$\delta^{13}C$	$\delta^{18}O$	$\bar{x}\ \delta^{13}C$	$\bar{x}\ \delta^{18}O$
266	1	Bovini ++	*Syncerus*	LM3	GnJh-47	-0.5	-1.8	0.4	-1.9
	2					0.5	-1.6		
	3					0.5	-1.8		
	4					0.8	-1.3		
	5					0.1	-2.1		
	6					0.3	-2.3		
	7					0.6	-2.1		
	8					0.7	-1.7		
245	2	Alcelaphini +	*Damaliscus*	UM	GnJh-47	1.7	-0.1	1.8	-0.4
	3					2.0	-0.4		
	4					1.5	-0.8		
228	1	Bovini ++	*Syncerus*	UM	GnJh-52	-0.8	-0.3	-2.9	-1.7
	2					-3.1	-1.7		
	3					-3.1	-1.6		
	4					-3.5	-2.3		
	5					-3.7	-2.4		
232	1	Tragelaphini ++	*Scriptus*	UM	GnJh-53	-10.9	-2.3	-11.2	-2.7
	2					-11.5	-3.1		
254	1	Bovini ++	*Syncerus*	UM	GnJh-56	1.0	-2.5	-0.2	-2.2
	2					0.7	-2.3		
	3					-0.4	-1.9		
	4					-1.0	-2.1		
	5					-1.5	-2.3		
255	1	Reduncini +	*Redunca*	LM	GnJh-56	1.7	-0.6	2.1	-1.5
	2					2.2	-1.6		
	3					2.3	-2.3		
304	1	Alcelaphini +	*Damaliscus*	UM	GnJh-58	1.1	0.8	1.0	0.3
	2					0.8	1.4		
	3					0.8	0.7		
	4					1.4	-0.7		
	5					1.1	-0.8		
25	1	Tragelaphini ++	*Tragelaphus*	LM3	Loc. 4	-7.6	-3.0	-8.8	-1.8
	2					-7.7	-2.8		
	3					-8.2	-3.0		
	4					-8.7	-1.8		
	5					-8.1	-2.2		
	6					-8.1	-2.2		
	7					-10.5	-0.1		
	8					-11.3	0.4		

Table 2.1 (continued): Serial and average stable isotope values of fossil bovid teeth sampled. Samples were collected serially and have been averaged from serial samples. $\bar{x}$= averages, *=averages are not possible, + Evaporative Insensitive, ++ Evaporative Sensitive, LM=Lower Molar, UM= Upper Molar, UP=Upper Premolar,

Neotragini- The average $\delta^{13}C_{enamel}$ values (-0.2‰) of the single Neotragini specimen are consistent with a C_4 grazing adaptation (Table 2.1). These values mirror the extant counterpart, *Ourebia ourebi*, the only true grazer in the Neotragini family (extant $\delta^{13}C_{enamel}$ values average -1.2‰) when compared with other neotragines that rely on C_3 vegetation as the major component of their diet (extant $\delta^{13}C_{enamel}$ values average between -10.4 and -24.1‰) (Cerling, Andanje, et al. 2015; Sponheimer, et al. 2003). Here, I interpret the Neotragini specimen to indicate of an open, C_4 grassland habitat.

Reduncini- The $\delta^{13}C_{enamel}$ values for reduncines are consistent with hyper grazing and grazing dietary adaptations, averaging 1.5‰ (Field ID 58), 1.9‰ (Field ID 70), 0.1‰ (Field ID 57), 1.8‰ (Field ID 35), 2.5‰ (Field ID 31), 1.9‰ (Field ID 92), 1.4‰ (Field ID 244), and 2.1‰ (Field Id 255) (Table 2.1). These results suggest that the fossil reduncines' diets were focused exclusively on C_4 vegetation and thus would have no seasonal $\delta^{13}C_{enamel}$ variability. These results are consistent with extant dietary choices of reduncines, whose $\delta^{13}C_{enamel}$ values average 0.7 to 2.3‰ (Cerling, Andanje, et al. 2015). I interpret these fossil reduncine $\delta^{13}C_{enamel}$ values to indicate the presence of grasslands, but also mesic, marshy environments dominated by C_4 grasses, perhaps in a sumpland environment fed by seasonal rains or a perennially active river (See section 4.2).

Tragelaphini- The $\delta^{13}C_{enamel}$ values of tragelaphines are largely consistent with browser dietary adaptations although there is evidence for one C_3-C_4 mixed feeder, averaging -10.4‰ (Field ID 80), -7.9‰ (Field ID 5, not an average, only one value sampled), -11.2‰ (Field ID 232), and -8.8‰ (Field ID 25) (Table 2.1). These results suggest that the fossil tragelaphines relied on C_3

vegetation for the majority of their diets, and on C_4 vegetation for smaller components of their diets. There are many possible explanations for the C_3 components of the tragelaphines diets, including browse, shrubs, herbs, or fruits, although given the associated negative $\delta^{18}O_{enamel}$ values (averaging between -1.1 and -2.7‰) shrubs or browse associated with perennial water sources, such as riparian woodlands, are the most likely explanations. One tooth (Field ID 25) shows marked variation in $\delta^{13}C_{enamel}$ values, and these values trend more positive during tooth formation (-7.6 to -11.3‰), indicating a possible seasonal shift away from a C_4 diet component to a greater reliance on C_3 browse material. These fossil $\delta^{13}C_{enamel}$ values are similar to those of extant tragelaphines values that average between -8.5 and -14.9‰ and usually indicate closed forested environments (Cerling, Andanje, et al. 2015; Kingdon 1988; Sponheimer and Lee-Thorp 2003; Sponheimer, et al. 2003). Here, I interpret the $\delta^{13}C_{enamel}$ values of tragelaphines to generally indicate open and closed woodland environments, possibly in riparian habitats given the associated negative $\delta^{18}O_{enamel}$ values (See section 4.2).

2.4.2 Oxygen isotopic composition of tooth enamel and aridity

The total range of $\delta^{18}O_{enamel}$ values sampled spans -3.1 and +3.3‰, providing the seasonal contribution of meteoric and leaf water sources, food, thermos-physiological adaptations, and possibly migration (Figure 2.4 and Table 2.1) The largest intra-tooth range in $\delta^{18}O_{enamel}$ values occurs in samples from an alcelaphine tooth (Field ID 99) with 3.8‰, and in a tragelaphine tooth (Field ID 25) with 3.5‰. The smallest intra-tooth range in $\delta^{18}O$ values come from a reduncine tooth (Field ID 70) at 0.3‰ and a bovine tooth (Field ID 254) at 0.6‰. Generally, these specimens do not show directional shifts in the $\delta^{18}O_{enamel}$ values sampled. However, a single tragelaphine tooth (Field ID 25), does show a seasonal trend towards more

negative oxygen isotope values (0.4 to -3.0‰) during enamel formation that coincide with a shift away from a C_3 dominated diet to one with increased C_4 components (-11.3 to -7.6‰). , This trend is consistent with early formation of C_3 dominated browse associated with ^{18}O enriched water due to leaf water transpiration. As C_4 vegetation contribution in the diet increases during late tooth formation, the oxygen isotope values begin to track meteoric water values more faithfully (Table 2.1) (Kohn, et al. 1996, 1998). Conversely, an alcelaphine tooth (Field ID 99), shows a directional trend toward positive $\delta^{18}O_{enamel}$ values, but without an alteration in a C_4 grazing diet (Table 2.1). This pattern could indicate the contribution of ephemeral water sources as a supplement to the alcelaphines water intake during the dry season. When tribes are compared using Mann-Whitney U pairwise tests, both reduncini and alcelaphini are significantly different from bovini and tragelephini, but not from each other in $\delta^{18}O_{enamel}$ values ($P = 0.737$). Likewise, bovini and tragelephini are not significantly different in their $\delta^{18}O_{enamel}$ values ($P = 0.441$). Finally, when all teeth are compared on the basis of ES or EI status, their $\delta^{18}O_{enamel}$ values are significantly different ($P < 0.01$).

The stable oxygen and carbon values of fossil fauna, in conjunction with dietary habits of their modern counterparts, were useful when classifying each bovid tribe as obligate drinkers (EI), who derive the majority of their $\delta^{18}O_{enamel}$ values from meteoric water, or non-obligate drinkers (ES), who derive large components of their $\delta^{18}O_{enamel}$ values from dietary water sources (after Levin, et al. 2006). Within the Kapthurin fauna sampled here, I classify tragelaphines, neotragines, bovines (*Syncerus* sp.), and cephalophines as ES specimens, and reduncines andalcelaphines (*Damaliscus* sp.) as EI specimens. I chose to classify *Syncerus* sp. as ES contra to Levin, et al. (2006), who suggest that the stable oxygen isotope values of bovines are similar to ES specimens but not at the $P < 0.05$ level, but had a P value 0.074 (Levin, et al. 2006). I also

classify *alcelaphines (Damaliscus* sp.) as EI species based on the criteria set forth in Levin, et al. (2006), their modern counterparts are hyper-grazers (Cerling, Andanje, et al. 2015; Cerling, et al. 2003), have medium to large body sizes, are obligate drinkers, and as a tribe are sometimes found in proximity to water sources (Kingdon 1988). The classification of alcelaphines follows data from Levin, et al. (2006) which showed no relationship between alcelaphines (impala) and water deficit (*P* value 0.311), and is contra Bedaso, et al. (2010) and Bedaso, et al. (2013), who classify alcelaphines as ES, but do not provide a justification for this classification. Surprisingly, EI classified taxa have $\delta^{18}O_{enamel}$ values that are overall more positive on average (-0.02‰) than ES specimens (1.8‰), contra to expectations that EI specimens should have lower $\delta^{18}O_{enamel}$ values than ES specimens. I attribute this to the overall wet conditions during this time interval, which suggest that the preferential evapotranspiration of $\delta^{18}O_{enamel}$ values is not exacerbated by arid conditions (Figure 2.3). This is similar to data reported by Levin, et al. (2006), where in the Ituri Rainforest, EI specimens have more positive $\delta^{18}O_{enamel}$ values than ES specimens.

Figure 2.5 shows the calculated paleoaridity using $\delta^{18}O_{enamel}$ values, and the relationship of $\varepsilon_{ES\text{-}EI}$ to the associated water deficit (a measure of mean annual precipitation and potential evapotranspiration), calibrated and modified from Levin, et al. (2006). Due to the small sample sizes from the Kapthurin Formation, I rely on the robust sample sizes from many taxa in Levin, et al. (2006) not included in our analysis (giraffidae, rhinocerotidae, proboscidea, hippopotamidae, equidae, and suidae). Again, due to the small sample sizes, I did not calculate the aridity index for any individual paleontological sites, but instead calculate it for the time interval under study, assuming that the fauna was deposited before the deposition of the Grey Tuff (509 ± 9 ka), although some time averaging must be expected. This method of correlation, following widespread, mappable temporal markers of paleolandscapes is common, and at best

provides a paleo-average of a landscape (Bedaso, et al. 2010). Our sample sizes for EI specimens is n=11 individual teeth, and for ES specimens is n=9 individual teeth. In Levin, et al. (2006), the authors note that for the aridity index to provide robust significance, 10 samples of both ES and EI taxa are necessary from individual sites. Following Levin, et al. (2006), I have calculated a power analysis (significance (α) = 0.05, power level (1-ß) = 0.2, two-tailed test), indicating that 10 samples are necessary from each population to determine a difference of 1.5‰ between populations of ES and EI $\delta^{18}O_{enamel}$ values with a standard deviation of 1.4‰. When a significance level of (α) = 0.10 is used, sample sizes of 8 are acceptable, although again, our samples represent pooled data from several sites. Although the sample sizes of specimens are not large enough to satisfy the statistical demands of Levin, et al. (2006), they are comparable to sample sizes of some datasets used in calculating their original aridity index.

I calculate the water deficit for the Kapthurin Formation during this time interval as 143 mm by rewriting the equation in Figure 2.5 as:

Equation 2.6: $WD = (\varepsilon_{ES\text{-}EI} + 2.348)/0.004$

This indicates a water deficit most similar to the modern Ituri Rainforest (-90 mm), based on the oxygen isotope enrichment among Kapthurin ES and EI taxa, $\varepsilon_{ES\text{-}EI} = -1.77$. When questionable taxa, such as alcelaphines and bovines (Bedaso, et al. 2013; Levin, et al. 2006) are removed from the EI calculations, a similar oxygen isotope enrichment between ES and EI taxa is found, $\varepsilon_{ES\text{-}EI} = -1.73$, suggesting water surplus of 154 mm. The similar $\varepsilon_{ES\text{-}EI}$ values of questionable and strict ES and EI taxa indicate that this was a very mesic period, quite different from the conditions predicted by overall drying trends inferred from other Pleistocene fossil localities (deMenocal 2004), and more similar to a variable period of increased rainfall (Potts 1996). The resemblance of deficit values for this time interval to the modern Ituri Rainforest's water deficit,

does not necessarily indicate a dense closed rainforest, but may instead suggest a period of increased precipitation from monsoonal activity, as suggested by Rossignol-Strick, et al. (1998) and Clark, et al. (2006), or a period of greatly reduced potential evapotranspiration. Given the elevated greenhouse gasses during this time period (John A Higgins, et al. 2015), I expect that temperature conditions were warm and were coupled with increased potential evapotranspiration in Equatorial Africa (Lüthi, et al. 2008), however these warm conditions would also be offset by the increased precipitation from the intensified African monsoon hypothesis for MIS 13 (Rossignol-Strick, et al. 1998),. If this interpretation is correct, I may infer a more precise age of ~533 ka (Lisiecki and Raymo 2005) for the fauna under consideration here.

The average $\delta^{18}O_{drinking\ water}$ values, as estimated by applying Equations 2 and 3 to obligate drinker taxa, is projected at -0.9 ± 1.5‰. This estimate is more positive than the average $\delta^{18}O_{drinking\ water}$ value (-2.5 ± 2.4‰) of several modern sources in Kenya provided in Levin, et al. (2009), but within the standard deviation. This estimate is somewhat higher than other Pleistocene $\delta^{18}O_{drinking\ water}$ values. Bedaso, et al. (2010) estimate the average drinking water values at -1.9‰ for the Middle Pleistocene of the Afar region of Ethiopia. The higher estimates from the Kapthurin Formation may be due to evaporation during dry seasons, and possibly the effects of Lake Baringo as a source for water; modern Lake Baringo has a $\delta^{18}O_{drinking\ water}$ value of 6.6‰ (Levin, et al. 2009), and thus represent the most positive estimate for Kapthurin $\delta^{18}O_{drinking\ water}$ values during this time interval. This discordant relationship between $\delta^{18}O_{drinking\ water}$ values and the aridity index merits further exploration. Our sample sizes may not be robust enough for calculation of the aridity index and could be indicating a much wetter environment than is merited. To determine the effects of small sample sizes, I have contrasted the aridity index results with oxygen values from pedogenic carbonates below (see section 4.4). Taxonomic

diversity is another possible issue, although the family Bovidae should be consistent enough to provide a relative indicator of different habitats (Bibi, et al. 2009). However, the lack of very positive $\delta^{18}O_{enamel}$ values in C_3 browsing taxa is a faithful indicator of mesic environments, due to the exacerbated ^{18}O enrichment associated with leaf water in more xeric environments (Dongmann, et al. 1974). The negative $\delta^{18}O_{enamel}$ values of browsing taxa are accurate indicators of these mesic conditions. The lack of C_3 dominated environments and the presence of C_4 habitats during this time interval indicates that a monsoonal system that fed riparian woodland environments and significant grassland ecosystem components is the most likely explanation for the low water deficit based on the Kapthurin Formation aridity index.

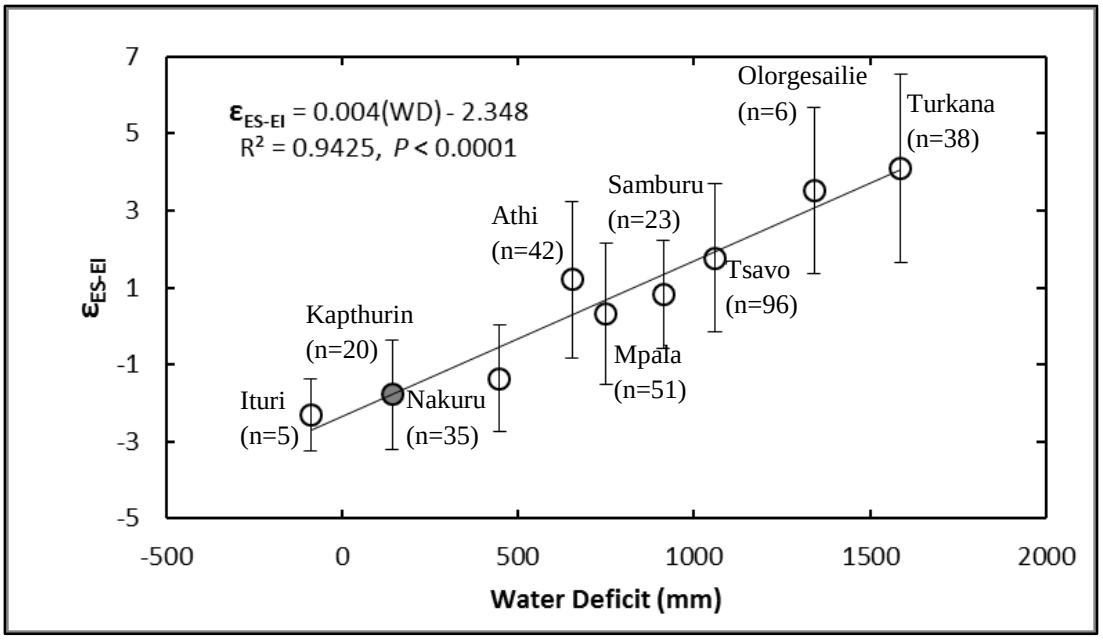

Figure 2.5: Relationship between the enrichment of oxygen isotopes in tooth enamel of modern and fossil ES and EI taxa, ε_{ES-EI}, and aridity (Water Deficit), based on calibration data from Levin, et al. (2006). All modern environments provided in Levin, et al. (2006) with both ES and EI taxa are displayed. Site location and sample sizes are listed next to plotted values. Only taxa that were positively identified as ES or EI in Levin, et al. (2006) are included. Kapthurin data are shaded. Error bars represent standard deviations of oxygen isotope values of both ES and EI taxa.

2.4.3 Paleoenvironmental interpretations from tooth enamel

Sample sizes are generally not large enough at individual paleontological sites for statistical comparisons among sites. In light of this, I present environmental indications based on pooled stable isotope values for the time interval under study. With this procedure, some time averaging among sites that are overlain by the Grey Tuff (509 ± 9 ka) must be assumed. The variety of habitats and paleosurfaces may well represent individual short time intervals within the larger time interval (543 ± 3 ka to 509 ± 9 ka) under study. This is likely, due to the sedimentology of the deposit, tectonic and erosional history of the Lake Baringo Basin, and modern geomorphology found in the area today (Martyn 1969; Tallon 1978). However, the preservation of the teeth within this large time interval appears to coincide with increased monsoonal activity during MIS 13 (~533–478 ka) (Lisiecki and Raymo 2005), and may have caused an increased sedimentation rate, creating ideal conditions for the rapid burial of fossils. I also assume that fossilized animal remains are faithful indicators of past habitats, based on the work of Western and Behrensmeyer (2009) and Behrensmeyer, et al. (2007). Within these limitations, I assume that the average carbon and oxygen isotopic values of bovid tooth enamel represent the general paleoenvironmental setting of the Lake Baringo Basin, allowing for the selective feeding preferences of some species, during the time interval under study (543 ± 3 ka to 509 ± 9 ka).

Average stable isotope values from serial tooth enamel data indicate a diverse environment between 543 and 509 ka, although oxygen isotope values suggest that the fauna was deposited during a monsoonal episode ~533 ka (Lisiecki and Raymo 2005; Rossignol-Strick, et al. 1998). Individual serial enamel values from Table 2.1 show that both wooded and open habitats were available to hominins during this time interval, but overall the stable isotope values

from Figures 2.5 and 2.6 indicate that the habitats were very mesic. There is little evidence for mixed C_3 and C_4 foragers, possibly due to sampling bias. The aridity indices calculated for this time interval (after Levin, et al. 2006), suggest a small water deficit and are most comparable to values for environments in the modern Ituri Rainforest (Figure 2.5). While these results suffer from small sample sizes of EI and ES for individual taxa, there are not any apparent elevated $\delta^{18}O_{enamel}$ values associated with C_3 browsing taxa, a faithful indicator of mesic conditions (Dongmann, et al. 1974). These results are somewhat consistent with other researchers' paleoenvironmental interpretations based on faunal taxonomic identification and geologic observations, although these hyper-mesic conditions suggest a wetter interval than previously predicted (Johnson, et al. 2009; McBrearty 1999; Renaut, et al. 2000; Tallon 1978). Our data indicate that the average paleoenvironmental conditions during this time period were characterized by wooded and marsh conditions near perennially active rivers and lake-shores, with semi-arid grassland components of the landscape at some distance from these water sources. These results are consistent with a strengthened monsoonal system affecting East Africa during MIS 13, as has been suggested elsewhere (Clark, et al. 2006; Rossignol-Strick, et al. 1998). Substantial precipitation is suggested by the paleochannels observed in the fluvial facies (K3) of the formation (Figure 2.1) (Tallon 1978), and suggest a more precise date for the fossil fauna at the onset of MIS 13 (~533 ka) (Lisiecki and Raymo 2005).

Archaeological remains of hominins from this interval seem to indicate exploitation of several different habitats (Figures 2.4 and 2.6), although higher resolution environmental reconstructions are necessary to test this hypothesis. Hominin fossil remains have been found at the site of EKG (Leakey, et al. 1969; Wood and Van Noten 1986), near the sites of GnJh-38 and Loc. 4. The combined isotope data from these locations indicates a riparian woodland, with a

drier grassland environment at some distance from the water source (closest to the site of EKG). I suggest that based on the average paleoenvironmental reconstructions for this time period, hominins would have had the opportunity to exploit many rich local habitats, ranging from wet, densely vegetated marsh and forests, to drier grassland landscapes. Higher resolution environmental reconstructions are necessary before I can begin to test the relationship of hominin technological choices to explicit and site microecology.

2.4.4 Carbon and oxygen composition of pedogenic carbonates

Pedogenic carbonates $\delta^{13}C_{pc}$ values average -3.5 ± 2.3‰ and range from -9.6 to 0.2‰, indicating that wooded grassland (n=12) was the dominant form of vegetation cover recorded by pedogenic carbonates, indicated by the average $f_{wc} = 0.19$ (Table 2.2 and Figure 2.6). Notably, the grassland category is also prevalent (n=9). Finally, there is some evidence for the woodland/bushland/shrubland category (n=3). There is no evidence for densely forested environments preserved in the pedogenic carbonate record. These reconstructions augment the dietary reconstructions of fossil bovids, and provide evidence for all of the habitats reconstructed in section 4.1. Interestingly, the area with the most wooded cover (66%) is Loc. 99, the fossil chimpanzee locality (McBrearty and Jablonski 2005).

Sample	$\bar{x}\ \delta^{13}C$	$\sigma_{\delta 13C}$	$\bar{x}\ \delta^{18}O$	$\sigma_{\delta 18O}$	n	$\bar{x}\ f_{wc}$	Site
DL-1-2011	-2.1	0.57	-2.9	0.28	8	0.09	Below GT
DL-2-2011	-2.2	1.37	-4.8	0.98	20	0.11	Below GT
DL-3-2011	-2.1	0.27	-5.7	0.52	16	0.09	Below GT
DL-4-2011	-2.7	0.79	-5.6	0.59	12	0.13	Below GT
DL-5-2011	-2.7	0.32	-6.8	0.60	10	0.12	Below GT
DL-6-2011	-1.1	0.46	-4.5	0.45	10	0.05	Below GT
DL-7-2011	-0.3	0.94	-4.6	0.65	10	0.03	Below GT
DL-7-1-2011	-1.7	1.28	-5.6	2.08	10	0.08	Below GT
DL-8-2011	-3.7	0.89	-3.8	0.40	10	0.19	Below GT
DL-9-2011	-3.1	0.90	-4.5	1.65	10	0.15	Below GT
DL-9-1-2011	-2.6	0.48	-5.2	1.07	10	0.12	Below GT
DL-10-2011	-1.5	0.48	-7.8	0.84	10	0.06	Below GT
DL-10-1-2011	-1.6	0.12	-8.6	0.38	10	0.07	Below GT
DL-1-2012	-6.5	0.29	-3.7	0.41	10	0.40	GnJh-39
DL-2-2012	0.2	0.41	-0.4	0.93	6	0.01	GnJh-39
DL-3-2012	-4.4	0.89	-3.4	0.39	15	0.24	Below GT
DL-4-2012	-4.8	0.99	-3.5	0.54	15	0.27	GnJh-39
DL-5-2012	-4.8	0.50	-2.5	0.57	10	0.26	Below GT
DL-7-2012	-5.6	0.21	-2.9	1.49	9	0.32	EKG
DL-9-2012	-6.8	0.24	-3.5	0.54	10	0.42	BKS
DL-10-2012	-6.0	0.27	-4.1	0.27	10	0.35	JKS
DL-11-2012	-5.3	0.22	-5.4	0.28	10	0.30	GnJh-23
DL-15-2012	-9.6	0.15	-3.8	0.29	3	0.66	Loc. 99
DL-20-2012	-2.3	1.39	-4.1	0.42	10	0.11	GnJh-27

Table 2.2: Average stable isotope values and standard deviations of serially sampled fossil pedogenic carbonates. Fraction Woody cover estimates and standard deviations are also displayed. Below GT refers to pedogenic carbonates collected from paleosols stratigraphically below the Grey Tuff (543 ka). n=number of samples, $\bar{x}$=average, σ=standard deviation, and f_{wc}=fraction woody cover estimate.

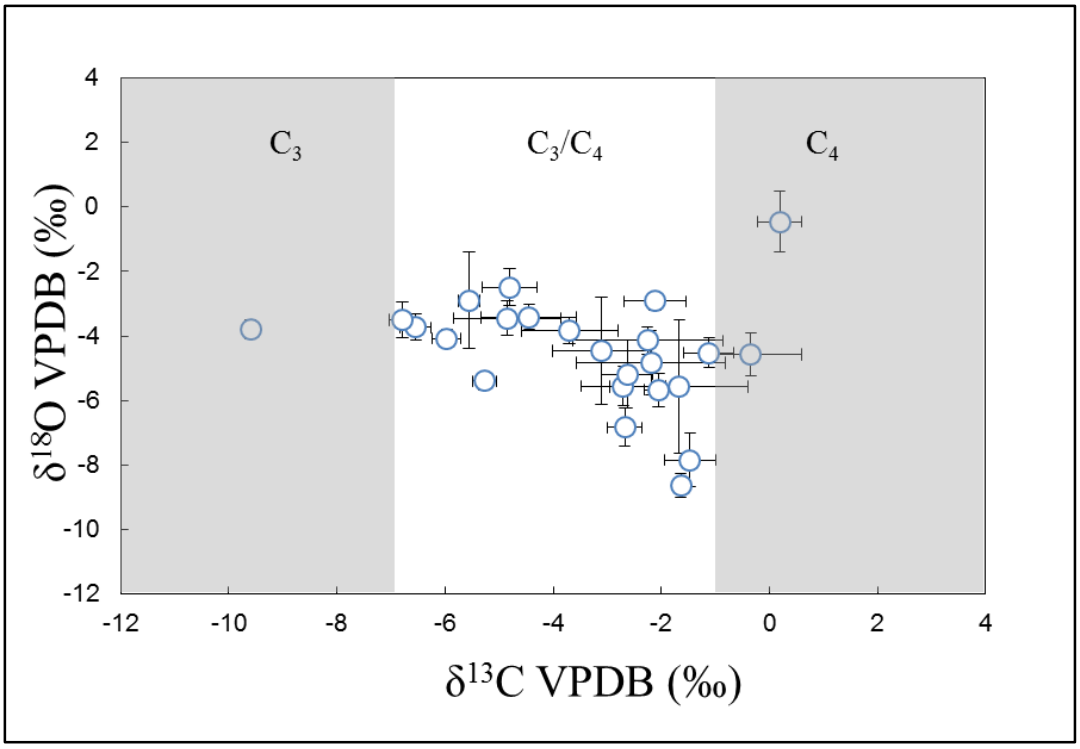

Figure 2.6: Average stable isotope values +1σ of serial pedogenic carbonate samples, displayed against x-axis ($\delta^{13}C$) and y-axis ($\delta^{18}O$). Samples are shown with respect to assumed vegetation type. Shaded and light areas reference C_3, Mixed C_3/C_4, and C_4 environments.

Pedogenic carbonate $\delta^{18}O_{pc}$ average -4.5 ± 1.7‰ and range from -8.6 to -0.4‰, indicating a diverse range of oxygen values (Figure 2.6 and Table 2.2). The lowest $\delta^{18}O_{pc}$ values are the best estimates for meteoric water $\delta^{18}O$ values, because they represent carbonate formation that records the least amount of evaporation. Samples DL-10-2011, and DL-10-1-2012, represent the lowest oxygen isotope values (-7.8 and -8.6‰ respectively), and were sampled from a paleosols adjacent to the Chemichemi Tufa (Johnson, et al. 2009), a record of a perennially active stream that was situated near lake margins and was fed by increased ground water inputs during this time interval (543 – 509 ka). These minimum values are also lower than minimum values of $\delta^{18}O_{pc}$ provided in Levin, et al. (2011) from the Turkana Basin (Nachukui

Formation, ~750 ka, ~-3‰). The minimum $\delta^{18}O_{pc}$ values from the Kapthurin Formation can also be juxtaposed by the average $\delta^{18}O$ (VSMOW) values of bodies of water in the Lake Baringo Basin today, the lake has an average value of 6.6‰ and the Molo River has a an average value of -2.9‰ (Levin, et al. 2009). These results suggest a maximum difference of -5.7‰ in oxygen isotope values of meteoric water during this time interval and the present, which may indicate lower meteoric water values from rainfall, a shift in aridity, or a difference in soil temperature. The latter possibility can be fully excluded as greenhouse gas concentration (CO_2 and CH_4) in the atmosphere is elevated during this time interval (John A. Higgins, et al. 2015). The average $\delta^{18}O_{pc}$ value (-4.5‰) from this time interval is also lower than the average $\delta^{18}O$ (VSMOW) value of meteoric water in Kenya today (-2.9‰). Interestingly, the average $\delta^{18}O_{pc}$ value is over 3‰ lower than the projected drinking water value from ES taxa (-0.9‰), indicating that the ES taxa probably incorporated significant components of standing or other evaporated water into their drinking water. Taken together with the evidence from the fossil bovid record, I suggest that these values indicate a period of increased rainfall, that are not obliterated by high evaporative climate conditions associated with insolation maximum and overall warmer global conditions during MIS 13.

2.5 Conclusions

I have described here isotopic analyses of bovid fossil teeth and pedogenic carbonates from the Kapthurin Formation, collected from localities within the Middle Silts and Gravels (K3) member of the Kapthurin Formation, stratigraphically above the Pumice Tuff (K2) (543 ± 3 ka) and below the Grey Tuff (509 ± 9 ka). The teeth represent taxa from six tribes; they were sampled serially to reconstruct dietary vegetation and ancient habitats. These fauna represent the

full range of dietary adaptations, ranging from pure C_3 to pure C_4, although there is little evidence for mixed (C_3/C_4) foraging behavior. The stable oxygen isotope data suggests that most bovid taxa were EI, tracking meteoric water faithfully, while a few were ES, their values tracking the oxygen isotope composition of the C_3 vegetation they consumed. Applying the modified aridity index of Levin, et al. (2006), I estimate the oxygen enrichment between these two groups as $\varepsilon_{ES\text{-}EI} = -1.77$, approximating a paleowater deficit of 143 mm. The $\delta^{13}C_{pc}$ values suggest a landscape dominated by wooded grassland vegetation, with open grassland and woodland influences, and the $\delta^{18}O_{pc}$ values suggest a wetter environment than the modern basin, and confirm the presence of a perennially active stream during this time interval. These values suggest a paleohabitat that was perforated with very mesic and mildly xeric components, with riparian woodlands, sumplands, and fringe grasslands ecosystems.

These general paleoenvironmental indicators suggest a habitat that was rich in biodiversity, and accords well with faunal identifications that have portrayed the environment as closed, wet, and marshy habitats near an alternating alkaline and freshwater lake with arid components farther afield (McBrearty 1999). A Middle Pleistocene African monsoonal system that dominated this time interval is the most likely explanation for the rapid sedimentation rates, numerous paleochannels, good fossil preservation and burial, and modified paleoaridity index of -1.77 during this time interval (~543 – 509 ka). This research represents the first confirmation of this Middle Pleistocene African monsoonal event with African paleoecological data (Clark, et al. 2003; Rossignol-Strick, et al. 1998). This paleolandscape would have shown exceptional ecological diversity, providing hominins with a number of different local habitats and a broad range of resources. From the archaeological evidence, it seems that hominins exploited both wet and dry locales with wooded, marshy, and grassland vegetation. Hominins during this time

period also began to experiment with the systematic production of blades (Johnson and McBrearty 2010), a new technology which may have been developed as a response to the ecological diversity of the Lake Baringo Basin, although higher resolution environmental reconstructions are necessary to verify this suggestion.

Shifts in environments have been cited as stimuli for evolutionary and technological change among hominins (Ambrose 1998; Bräuer 2008; Darwin 1871; deMenocal 1995; Potts 1996; Reed 1997; Vrba 1993). Researchers have noted a general cooling trend during the Pliocene that continues into the Pleistocene, resulting in more xeric and open grassland conditions in East Africa (Bobe and Behrensmeyer 2004; Coppens 1975; deMenocal 1995, 2004; Vrba 1985). Isotopic data from the Kapthurin Formation suggests, contrary to expectations (deMenocal 1995), that during this time interval (543 – 509 ka) the Lake Baringo region provided hominins and chimpanzees with hyper mesic, wooded refugium, in addition to nearby grasslands, both sources of valuable resources. Increased monsoonal activity at the onset of MIS 13 (~533 ka) may have driven the appearance of this hyper mesic environment, which may have stimulated the production and use of new technologies, although further exploration and additional examples are necessary to test this hypothesis. This correlation allows for more precision when dating the Kapthurin Formation sediments deposited during K3 and K3', and suggests a time interval of ~533 – 509 ka. This reconstruction accords with those of Kingston, et al. (1994) who noted that the Tugen Hills succession does not provide evidence for a shift to C_4 dominated environments throughout the Neogene and Pliocene, and that a range of local habitats existed at any given point in time. These results highlight the need to ground global or regional climate reconstructions in local paleoecological data from individual archaeological and paleontological sites.

Chapter 3: A New Proxy for Paleo-Biomass Productivity: Incorporating Stable Isotopes and the Satellite-derived Normalized Differential Vegetation Index

3.1 Introduction

The role of hominin landscape use and ranging patterns, and grassland and forest ecosystems in human evolution has been hotly debated by paleoanthropologists for quite some time (Cerling, Wynn, et al. 2011; Coppens 1975; Klein 2009; Potts 1998; Vrba 1993). The expansion of grasslands during the Neogene buttresses many environmental hypotheses of human evolution; it has been linked with the origins of the genus *Homo* and a burgeoning reliance on animal protein in the diet that is scavenged or hunted from the available animal biomass in savannah ecosystems (Aiello and Wheeler 1995; deMenocal 2004, 2011; Domínguez-Rodrigo, et al. 2014; Ungar, et al. 2006; Ungar and Sponheimer 2011). Paleoenvironmental reconstructions have thus focused on savannah versus forest contrasts, with varying degrees of success.

Paleoanthropologists regularly use stable isotopes derived from pedogenic carbonates, mammalian teeth, soil organic matter, and tufa composition to reconstruct terrestrial environments associated with human evolution (Ashley, et al. 2010; Cerling, Andanje, et al. 2015; Cerling, Wynn, et al. 2011; Kingston and Harrison 2007; Kingston, et al. 1994; Levin, et al. 2004; Loftus, et al. 2016; Quinn, et al. 2013). Recently, Cerling et al. (2011) offered a more precise method for estimating the fraction of woody cover in past environments, based on the modern relationships of carbon isotope ratios in soils and the degree of woody coverage in a given environment. Similarly, I develop a newer method for estimating above ground biomass

productivity of plants in paleoenvironments, by contrasting the modern (actively developing) carbon isotope ratios of tropical soils with an independent measure of biomass productivity, namely a satellite-derived Normalized Differential Vegetation Index (NDVI). The relationship between NDVI and plant biomass is well established, and has more recently been linked with predicting habitats of modern animal communities (Box, et al. 1989; Cerling, et al. 2009; Hunt 1994; Pettorelli, et al. 2006; Pettorelli, et al. 2011; Tucker, et al. 1986).

By establishing a paleo-proxy for biomass productivity, and contrasting this with the woody cover index developed by Cerling et al. (2011), I believe paleoanthropologists may be able to avoid arguments based on possible time averaged reconstructions, and instead focus on more ecologically centered reconstructions. Similar to the woody cover calibrations developed by Cerling et al. (2011), the correlation between primary plant biomass productivity and carbon isotope ratios of soils provides a calibration for estimating paleo-biomass productivity; this novel paleo-NDVI technique offers paleoanthropologists another proxy for reconstructing environments. Paleo-NDVI values are calculated based on this correlation for paleontological and archaeological sites within the Kapthurin Formation, Kenya, a Middle Pleistocene sedimentary sequence, although I believe this method could be applied elsewhere as well. Two time intervals relevant to Middle Pleistocene archaeology are preserved in the Kapthurin Formation (Time Interval 1: 543 – 509 thousand years ago (ka); Time Interval 2: 509 – 380 ka) and were sampled for landscape environmental reconstructions.

3.2 Materials and Methods

3.2.1 Bulk Soil Organic Matter

Stable isotope analyses of paleosols offer researchers an important means for reconstructing past environments. Wooded plants and high latitude grasses, almost exclusively use the C_3 photosynthetic pathway during plant photorespiration, while mid-latitude and tropical grasses use the C_4 photosynthetic pathway during photorespiration (Ehleringer 1978; Ehleringer and Monson 1993). The C_3 biome is quite diverse, with plant types such as herbs, trees, aquatic plants, and grasses with carbon isotope values ($\delta^{13}C_{plant}$) ranging between -20 and -37‰. In tropical forests, the canopy effect traps ^{13}C depleted CO_2 produced during soil respiration and recycled during photosynthesis, resulting in the most negative carbon values from the C_3 biome (Ehleringer, et al. 1987; van der Merwe and Medina 1991). The canopy effect results in a gradient of negative $\delta^{13}C$ values, with the most negative carbon values produced in the forest floor and the highest values in the upper story (Medina and Minchin 1980). The range of C_3 values are contrasted by C_4 plants, generally grasses and flowering plants, with $\delta^{13}C_{plant}$ values ranging between -10 and -14‰ (Farquhar, et al. 1989; Kohn 2010). Due to these differences in the discrimination of CO_2 by wooded (C_3) and grassy (C_4) plants in the tropics, the stable carbon values of bulk soil organic matter ($\delta^{13}C_{SOM}$) are useful measures of modern and past environments. Studies of $\delta^{13}C_{SOM}$ values are particularly useful because the values are directly determined by the fraction of litter derived from C_3 and C_4 plants (Wynn and Bird 2007) and soil development processes that are associated with decomposition of above ground vegetation (Baisden, et al. 2002; Ladd, et al. 2014). This is contrary to pedogenic carbonate formation, which although still a useful environmental proxy, can be inhibited by densely forested environments associated with acidic soils and high precipitation (Tucker and Wright 1990). Pedogenic carbonates also have a seasonal bias in formation, associated with warm, dry season precipitation conditions, rather than the mean plant growing season (Breecker, et al. 2009).

Paleosols, fossil soils that have undergone relatively minor burial alteration, preserve the soil organic matter of past soils and can be used as reliable indicators of past environments (Retallack 1991).

3.2.2 Study Area

All modern soil (actively developing) samples were collected from the Baringo District, Kenya, an area that has undergone relatively little modern agricultural disturbance (Ngugi and Conant 2008; Oindo and Skidmore 2002; Wasonga, et al. 2011). Situated in the Kenyan Rift Valley, the Baringo District is dominated by semi-arid bushlands in the valleys and higher altitude ridges with more moderate moisture and climatic conditions that range from semiarid lowlands to humid subtropical highlands (Thom and Martin 1983). Subsistence farming and pastoral grazing are practiced in the district, with larger homesteads in the Tugen Hills, were water is more readily available. The Baringo District, one of nine districts in Kenya, is a key resource area that provides wild and domesticated animals with water and plant availability during droughts, including dry season grazing and foraging reserves (Ngugi and Conant 2008; Vetter 2005). The Baringo District is thus well suited as a possible modern analog to Pleistocene and Pliocene environments, even with the modern subsistence agricultural disturbances.

Paleosols were sampled from the Kapthurin Formation, a Middle Pleistocene sedimentary sequence of the Tugen Hills succession that lies to the west of Lake Baringo in the Kenyan Rift Valley (Figures 3.1 and 3.2). The formation is composed of interstratified volcanic, lacustrine, and alluvial sediments, is exposed over an area of 150 km^2, and has an observed thickness of approximately 125 meters (Martyn 1969; Christian A. Tryon and Sally McBrearty 2002). The formation has been dated using the $^{40}Ar/^{39}Ar$ method (Deino and McBrearty 2002). Martyn

(1969) partitioned the formation into 5 members. K1, K3, and K5 are members largely composed of terrigenous sediments from the Tugen Hills, and are informally named the Lower, Middle and Upper Silts and Gravels. K2 and K4 members separate the Silts and Gravel members; K2, referred to as the Pumice Tuff Member, is dated to 543 ± 3 thousand years (ka), and K4, referred to as the Bedded Tuff Member, has successive eruptive facies that are dated to 380 ± 7 ka, 284 ± 12 ka, and 235 ± 2 ka. The Grey Tuff also subdivides K3, and is dated to 509 ± 9 ka (Deino and McBrearty 2002). Recently the basal date of K4 has been refined by Blegen (2015) through tephrastratigraphic correlation to the Korosi Airfall Pumiceous Tuff (Dunkley, et al. 1993), also dated with the $^{40}Ar/^{39}Ar$ method.

Paleosols were sampled at archaeological and paleontological sites within the Kapthurin Formation from two main time intervals, below the Grey Tuff (509 ± 9 ka) and above the Pumice Tuff (543 ± 3 ka), and below the Bedded Tuff (380 ± 7 ka) and above the Grey Tuff (509 ± 9 ka). Where possible, paleosols were sampled below either the Grey Tuff or Bedded Tuff, to reduce problems of time averaging. This procedure was followed to provide the most accurate representation of paleo-surfaces for each time interval. Given this method, some time-averaging must still be assumed. The variety of paleo-surfaces and habitats that are represented in our reconstructions may very well represent individual, short time intervals within the two larger time intervals under study. This is likely, given the sedimentology of the deposits, tectonic and erosional history of the Lake Baringo Basin, and modern geomorphology in the area today (Martyn 1969; Tallon 1978). Given these limitations, the landscape approach I employ still offers a valuable perspective into basin-wide habitat reconstructions.

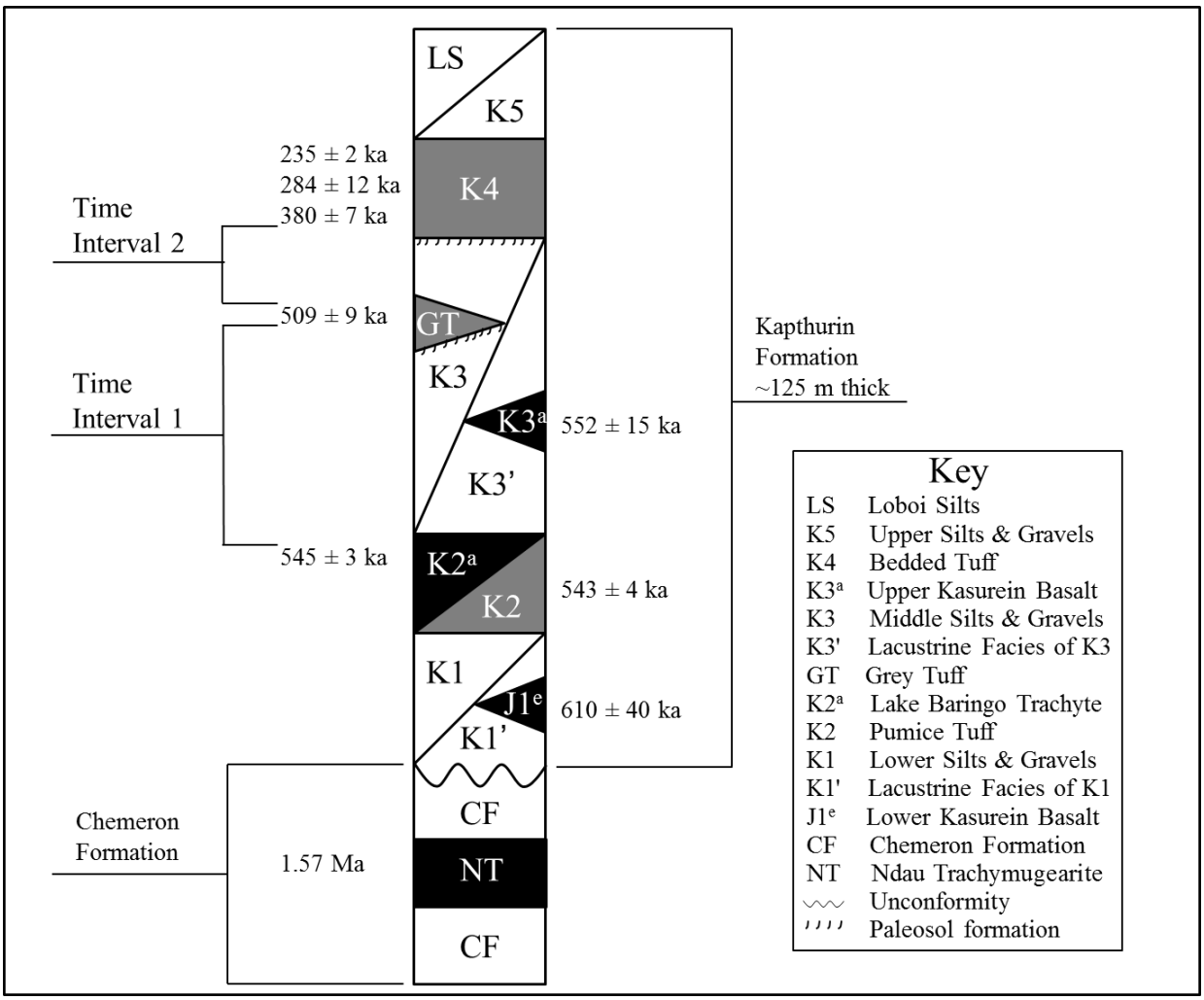

Figure 3.1: Generalized stratigraphic section of the Kapthurin Formation. Section is after Deino and McBrearty (2002). All dates are derived from the $^{40}Ar/^{39}Ar$ method, except the Ndau Trachymugearite, reported by Hill *et al.* (1986) using the K-Ar method.

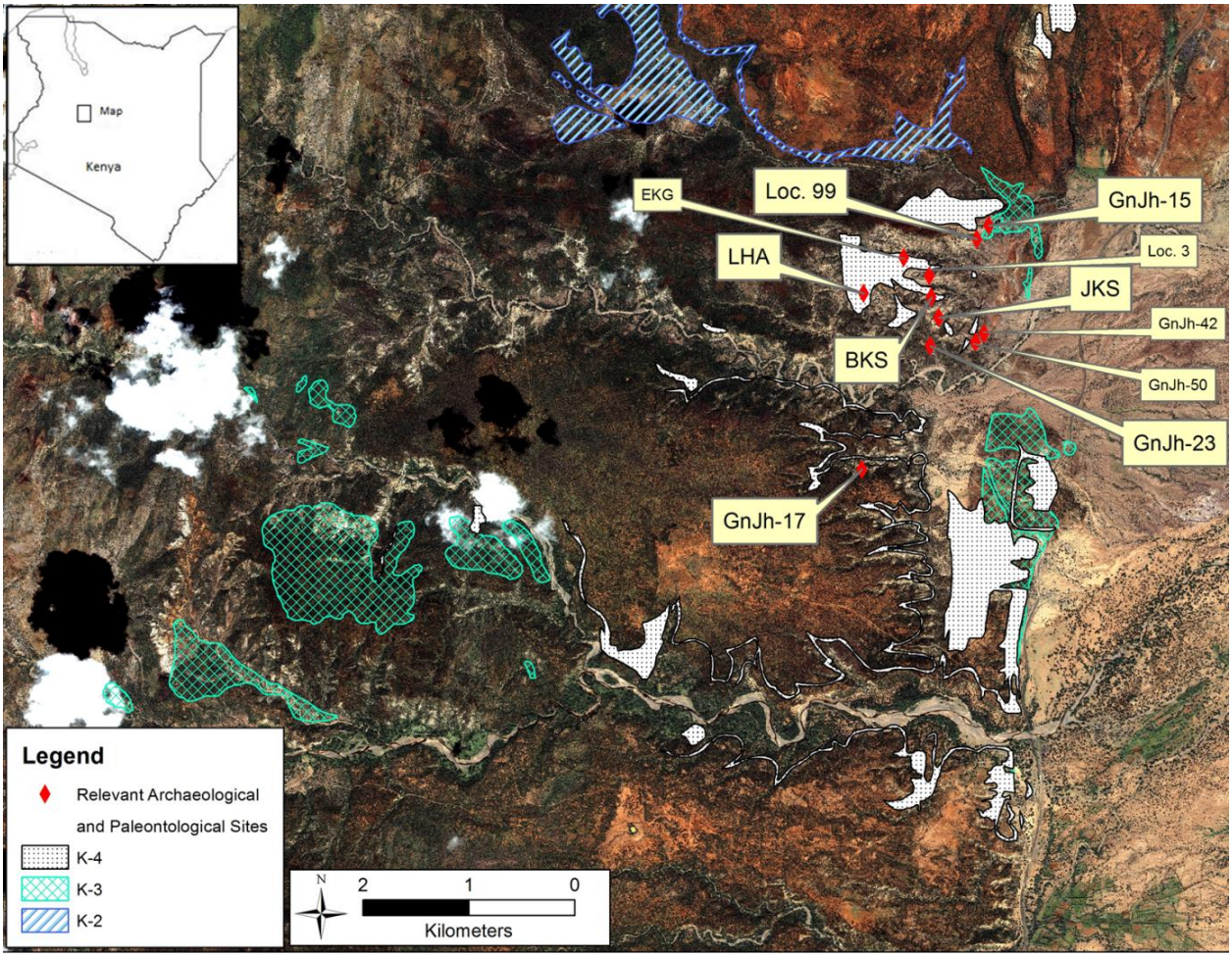

Figure 3.2: Satellite image (IKONOS, 1.8 m resolution) showing relevant geologic exposures and archaeological and paleontological sites of the Kapthurin Formation. Inset not to scale.

Environmental reconstructions for Time Interval 1 (543 – 509 ka) of the Kapthurin Formation by McBrearty (1999) focused on taxonomic identification of fauna, reconstructing dense vegetation and marsh environments, near a braided river system, with grasslands farther from rivers. Tallon (1978) reconstructed paleochannels throughout the deposits of K3 and suggested they were derived from an active braided river system draining the Tugen Hills. Johnson, et al. (2009) documented a fossiliferous tufa in the southern exposure of the Kapthurin Formation, demonstrating a rich wetland habitat during Time Interval 1. McBrearty and

Jablonski (2005) documented the presence of *Pan* fossils at Locality (Loc.) 99, and with other fauna collected from the site (hippopotamus, crocodile, catfish, colobine monkey, and bushpig), indicate a locally wooded environment near an alternating fresh and alkaline paleolake, with marshy patches. Hominin fossils identified as *Homo sp.* and *Homo erectus* have also been described from Time Interval 1, found at the site of MAS and EKG, less than 1 km from Loc. 99, indicating that chimpanzees and hominins occupied habitats in near proximity (Leakey, et al. 1969; McBrearty and Jablonski 2005; Wood and Van Noten 1986). More recently, Leslie, et al. (2016) reconstructed environments from Time Interval 1 using carbon and oxygen stable isotopes derived from pedogenic carbonates and herbivorous tooth enamel, suggesting this landscape was dominated by hyper mesic conditions, probably driven by an intense monsoonal episode, resulting in woodland areas, perennially active streams, marsh and sumpland environments, and a surrounding grassland ecosystem.

Environmental reconstructions for Time Interval 2 (509 – 380 ka) are more difficult, due largely to the poor fossil preservation conditions. The deposition of K4 and K3 sediments during Time Interval 2 was similar to deposition during Time Interval 1, seasonal streams drained upland areas, resulting in alluvial fan deposition on the margin of a paleo-lake (Tryon 2003). Scott (2005) reconstructed the environment at Rorop Lingop, a footprint site found in K4 deposits, suggesting the site was situated on an alluvial plain on the shores of a freshwater lake, with high vertebrate trace diversity, indicating a species rich environment. The deposition of Rorop Lingop postdates Time Interval 2, but it provides context for the diversity of species interacting with previous iterations of the paleo Lake Baringo. Previous studies (Cornelissen, et al. 1990; Kingston, et al. 1994) have used stable carbon and oxygen isotopes from pedogenic carbonates to reconstruct paleoenvironments from Time Interval 2, but have only included two

sites, GnJh-15 and GnJh-17, for analysis. Cornelissen, et al. (1990) report $\delta^{13}C$ and $\delta^{18}O$ values that indicate a grassland dominated environment with arid influences, similar to modern environments in the region, while Kingston, et al. (1994) report $\delta^{13}C$ values that suggest a mixed grassland and forested environment at GnJh-15.

Many researchers have documented the variability in Middle Pleistocene toolkits from the Kapthurin Formation, which include handaxe assemblages (Leakey Handaxe Area or LHA, GnJh-17), assemblages lacking *fossils directeures* dominated by flakes and cores (GnJh-42, GnJh-50), the early presence of prepared core technology (LHA, GnJh-17), and the systematic production of blades (GnJh-42, GnJh-50) (Cornelissen 1992; Johnson and McBrearty 2010, 2012; McBrearty 1999; McBrearty, et al. 1996; Tryon 2003). Tryon, et al. (2005) suggest that the regional variability in methods of Acheulean flake production, which include the Levallois method and are found in the Kapthurin Formation, demonstrate that variability in artifact manufacturing techniques predate the MSA transition. These innovations in artifact manufacture could be related to the exploitation of patchy, resource-rich environments and adaptive niche construction by hominins (Johnson and McBrearty 2012), a hypothesis that can be tested through the environmental reconstructions presented here. Clark (1988) and Ambrose (2001a) have suggested that MSA foragers began to occupy the ecotone between grasslands and woodlands because it afforded them efficient resource extraction from both environments. The occupation of environment with reliable access to water and tree cover may have been important hunting blinds for MSA hominins ambushing large herbivorous prey (Johnson, et al. 2009; Johnson and McBrearty 2012). Basell (2008) also suggests that MSA sites were concentrated at the margins of woodland and grassland environments with access to water due to climate variability, which lead to increasing resource fragmentation and refugia. High-resolution landscape environmental

reconstructions of Time Intervals 1 and 2 from the Kapthurin Formation will be used to test the hypothesis that MSA foragers began to occupy the wooded grassland ecotone for resource extraction.

3.2.3 Satellite-Derived Biomass Productivity

To derive the biomass productivity values from modern environments, high resolution satellite imagery (5 m per pixel, Rapid Eye-1, captured in February of 2012) was used to produce NDVI values, using ERDAS Imagine software. Atmospheric Correction and Haze Reduction software (ATCOR) was used to correct for haze inducing problems on the day of satellite acquisition, including atmospheric conditions, cloud cover, and the location of the Sun relative to the satellite (Tan, et al. 2012). NDVI values are derived on a scale from -1 to 1, but values pertaining to vegetation reflectance range from 0 to 1. High NDVI values are indicative of vegetation that is very productive with a high carrying capacity (wet, dense forests), while low NDVI values are indicative of sparse vegetation and bare soils with a low carrying capacity (Box, et al. 1989; Hunt 1994).

NDVI values were extracted for the study area with two low-resolution (30 m per pixel) Landsat images that were captured in January of 1986 and 2000. Using these NDVI values as a baseline for vegetation over the past 30 years, these images were contrasted to determine areas that experienced minimal change in biomass productivity over this 14 year period, and to standardize the season of collection of NDVI values (dry season) (Figure 3.3). Mean annual rainfall during this 14 year period for the Baringo District was 654 ± 58 mm, and did not vary dramatically (Kipkorir 2002). Using areas of little to no environmental change based on the net difference in NDVI values between 1986 and 2000, higher resolution imagery captured in

February of 2012 (5 m per pixel Rapid Eye-1) was sampled for current NDVI values. This procedure ensures that relict soil organic matter in modern soils from the past 30 years will not offset the biomass productivity measures from satellite imagery. NDVI values were derived from 32 individual locations that span the range of relevant biomass productivity values (0.01 to 1) (Figure 3.4).

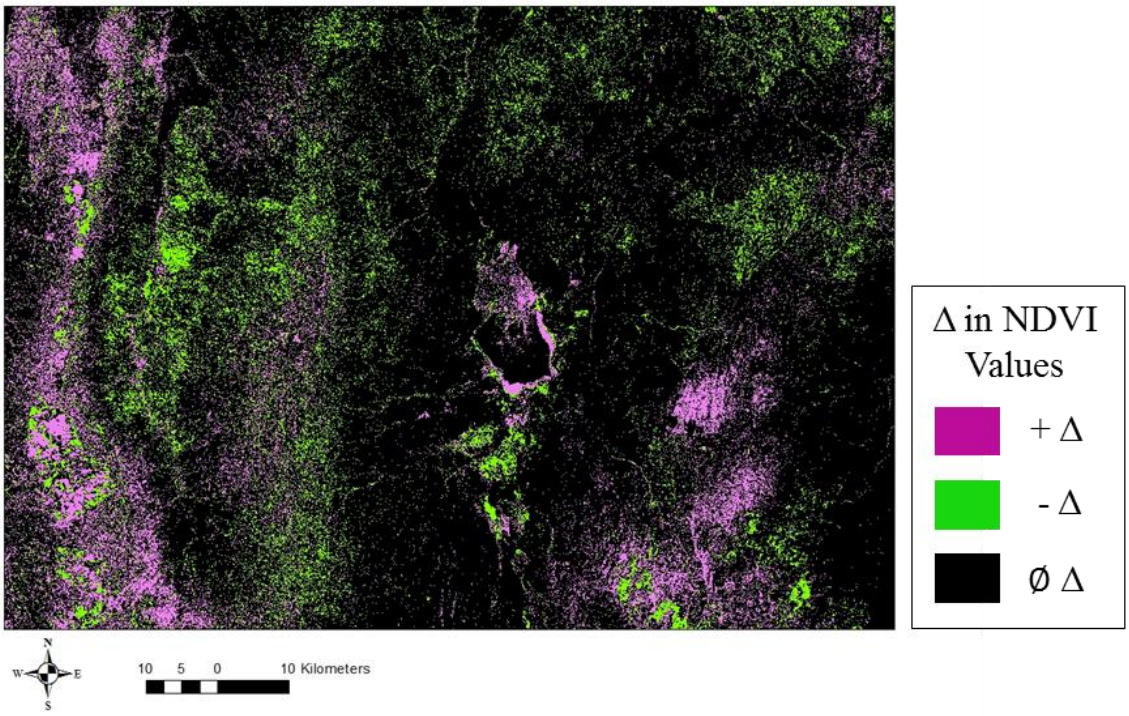

Figure 3.3: Map of differences in Baringo District NDVI values between 1986 and 2000. Δ = Change, Ø = No change

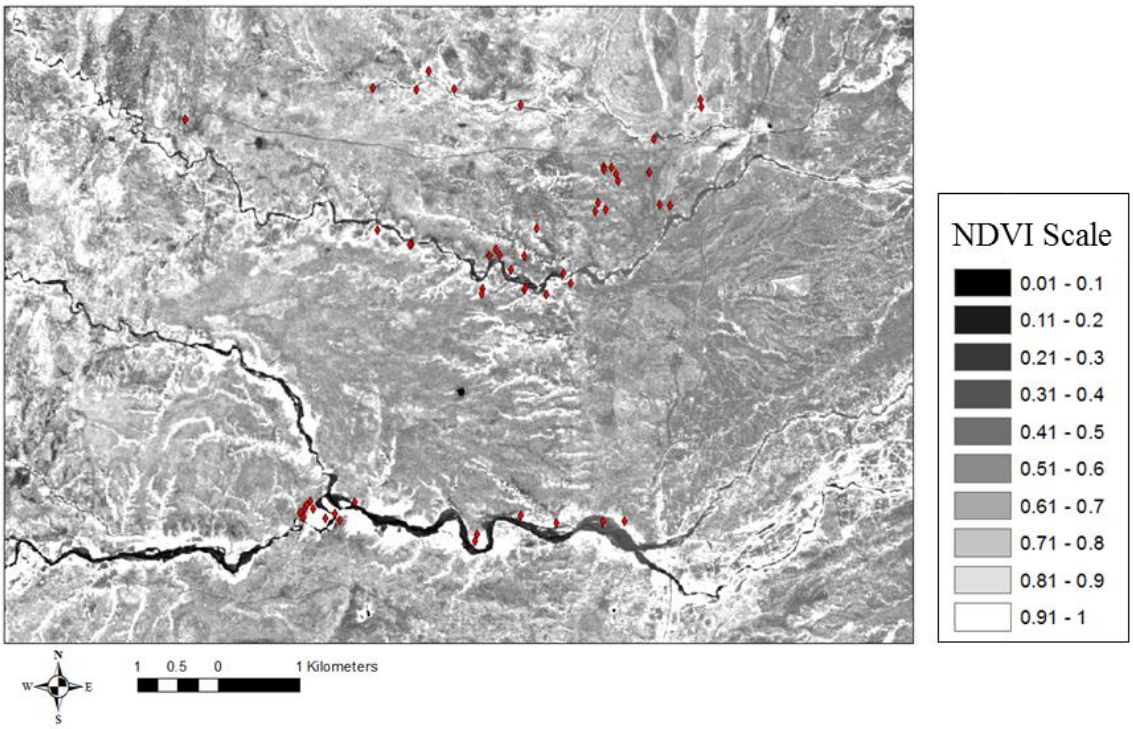

Figure 3.4: Map of Baringo District NDVI values, acquired in February of 2012. White values indicate high NDVI values, while black values indicate low NDVI values. Red stars indicate modern $\delta^{13}C_{SOM}$ sampling locations.

3.2.4 Soil Samples

To test the relationship between biomass productivity of above ground vegetation and $\delta^{13}C_{SOM}$ values, modern soil samples were collected during January of 2012 from the corresponding 32 NDVI sampled locations. These 32 loci were located using a differential global positioning system (GPS). The differential GPS device (Magellan MobileMapper Pro with Stakemill Survey software) provided decimeter accuracy in both X and Y coordinates. Local environmental conditions at each sampling location were documented to provide a record of the above ground biomass, while soils were described by order, morphologically, and

according to Munsell color categories (Retallack 1991). Soils were sampled between 0 and 10 cm below the surface of the modern topography. For each corresponding NDVI pixel and sample location, soil samples were collected in triplicates from a 1x1 meter tape measured square. A total of 32 environments were sampled, for a total of 89 modern soil samples (Figure 3.4).

During 2012 field season, a total of 21 archaeological and paleontological locations were sampled, 11 were sampled from Time Interval 1 (543 – 509 ka) and 10 were sampled from the Time Interval 2 (509 – 380 ka). To reduce issues of time-averaging, samples were collected below dated horizons where possible, samples from Time Interval 1 are close in age to 509 ka and samples from Time Interval 2 are close in age to 380 ka. Some samples were also collected from non-archaeological or paleontological locations and serve as controls to provide environmental data for locations not used by hominins. Paleosols were sampled at least 50 cm below surface exposure of outcrops to minimize remodeling from extant environments (Retallack 1991). These sampling locations were also recorded using a differential GPS device and are stored in a geographic information system (GIS) database.

Modern and paleosol samples were dried and prepared for isotopic analysis following conventional protocols (Hartman 2011). Soil samples were dried in an oven at 60°C, disaggregated, and screened through 2 mm sieves to remove any large gravel or visible plant remains. Samples were then immersed in hyper-saturated sodium chloride (NaCl) solutions and agitated to float and remove the remaining organic detritus material. Soil samples were then washed with Milli-Q© purified water (EMD Millipore, Billerica MA) and dried. Next, soil carbonates were removed by reacting 10 grams of soil samples with 1 M Hydrochloric Acid

(HCl) in uncovered 50 ml tubes and agitated until the release of CO_2 terminated. Samples were finally neutralized with Milli-Q© purified water and dried at 60°C.

Bulk $\delta^{13}C_{SOM}$ samples were measured at Boston University's Stable Isotope Laboratory after combustion in a Vector Euro elemental analyzer. The combustion gas (CO_2) was separated on a GC column, passed through a GVI diluter (GV Instruments) and reference gas box, and introduced into the GVIIsoPrime isotope ratio mass spectrometer. Water was removed using a magnesium perchlorate water trap. Ratios of $^{13}C/^{12}C$ were expressed as the relative per mil (‰) difference between these samples and the international standard, Vienna Pee Dee Belemnite (V-PDB), where,

Equation 3.1: $\delta^X = \left(\frac{R_{sample}}{R_{standard}} - 1\right) \times 1000 \qquad X = {}^{13}C;\ R = {}^{13}C/{}^{12}C$

The sample isotope ratio was also compared to a secondary gas standard with an isotope ratio that was calibrated to international standards, NBS 20 (Solnhofen limestone -1.05 ± 0.02‰). All international standards were obtained from the National Bureau of Standards in Gaithersburg, Maryland. Continuous flow also reported mass percent C and were calibrated against known quantities of the peptone and glycine standards (± 0.2‰). It was assumed that any variation of $\delta^{13}C$ of atmospheric CO_2 would be incorporated into the $\delta^{13}C_{SOM}$ at all sites, and thus not affect the results (Tans, et al. 1979).

3.2.5 Data Analysis

Stable isotope and NDVI data were analyzed using Microsoft Excel and R statistics. Isotopic values of modern $\delta^{13}C_{SOM}$ were contrasted with current NDVI measurements for individual sampling locations using both linear and multiple regressions. Correlations were

tested for significance using the F statistic within ANOVA calculations. I also applied the woody cover proxy developed by Cerling et al. (2011) using the fossil $\delta^{13}C_{SOM}$ values, and compared these results to paleo-NDVI estimates. Finally, I calculated a normalized probability curve for each time interval, when applying either the paleo-NDVI or woody cover calculation. Isoscapes of predicted carbon isotope ratios, paleo-NDVI and woody cover values were produced using ArcView 10.2. These data were interpolated using inverse distance weighting, a data interpolation technique appropriate for ecological data (Johnston 1998).

3.3 Results and Discussion

When the modern $\delta^{13}C_{SOM}$ values were compared with the high resolution NDVI values for each sampling location, I found a strong correlation coefficient ($R^2 = 0.79$, Mann-Whitney U test, $P<0.001$)) between these two variables (Figure 3.5 and Appendix 1). The correlation between these two variables is best explained using a logarithmic regression, explaining 79% of the variance in NDVI values. These results show that NDVI values that approach 0, or ecological areas with little biomass productivity, are correlated with $\delta^{13}C_{SOM}$ values that approach 0‰, while NDVI values that approach 1, or ecological areas with high biomass productivity, are correlated with $\delta^{13}C_{SOM}$ values that approach -30‰.

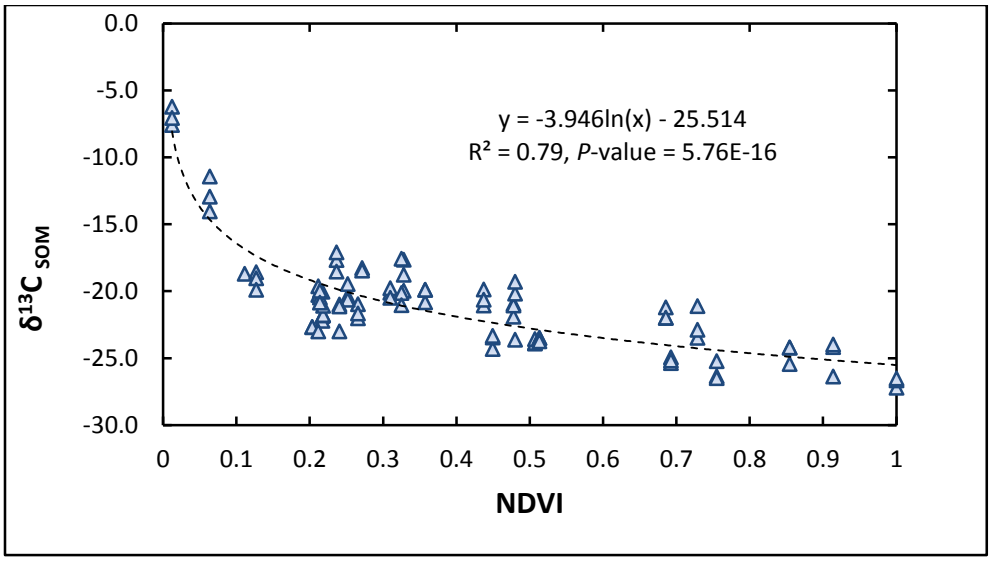

Figure 3.5: The relationship between modern $\delta^{13}C_{SOM}$ and NDVI values sampled from the same geographical location, shown across a broad range of ecosystems.

3.3.1 Modern Biomass Productivity

These results (Figure 3.5 and Appendices 1 and 2) confirm the hypothesis that $\delta^{13}C_{SOM}$ values are well correlated with primary biomass productivity, as measured by NDVI values in East Africa. NDVI values are useful for predicting 79% of the $\delta^{13}C_{SOM}$ values of individual sampling locations within the Lake Baringo District. The remaining 21% of the variance may be explained by the low representation of dense forested environments in the Baringo Basin today, or by the resolution (0.8 m per pixel) of the imagery, future work will focus on resolving this discrepancy. This high correlation could be due to the relatively higher contribution of C_4 plants associated with lower latitude environments, as Ladd, et al. (2014) note when they correlate $\delta^{13}C_{SOM}$ values from tropical and temperate ecosystems with measures of leaf area index. The correlation with biomass productivity should be unsurprising, given that soil organic matter is formed directly from the decay of plant biomass, recording the photosynthetic pathways of plants

(Cerling, et al. 1989; Smith and Epstein 1971). Instead, what is surprising is that satellite imagery is now readily available at a high enough resolution to approximate biomass productivity effectively. NDVI values extracted from high resolution imagery (5 m per pixel) provide researchers with the opportunity to asses ecological productivity, without traditional definitions of habitats (savannah, woodland, riparian woodland, etc.). Our results conflict with previous research (Ladd, et al. 2014) that suggested satellite-derived measures of leaf area index do not correlate with $\delta^{13}C_{SOM}$ values, but were instead only correlated with on-the-ground measurements of leaf area index. The differences in these results can best be explained by the coarse satellite resolution used by Ladd, et al. (2014) (1 km per pixel), compared with the high resolution imagery (5 m per pixel) used here to derive NDVI values. When higher resolution imagery becomes available, it may be possible to show a higher correlation between primary biomass productivity and SOM carbon values. Approximating paleo-NDVI values from fossil $\delta^{13}C_{SOM}$ values provides paleoanthropologists another proxy for environmental reconstructions, and can be compared to modern ecological data about animal communities and biomass productivity (Pettorelli, et al. 2011; Pettorelli, et al. 2005).

3.3.2 Paleo Biomass Productivity

For these results to be useful, the logarithmic regression equation must be rewritten to predict paleo-NDVI values, if values of fossil $\delta^{13}C_{SOM}$ are known, and offset for the 1.5‰ shift in modern $\delta^{13}C$ values of atmospheric CO^2 when compared with pre-industrial values (Leuenberger, et al. 1992). To this end, I have redefined the relationship between $\delta^{13}C_{SOM}$ and NDVI values as,

Equation 3.2: $NDVI = e^{\frac{\delta^{13}C_{SOM}+24.014}{-3.946}}$

Using equation 3.2, known fossil $\delta^{13}C_{SOM}$ values can be used to produce estimates for paleo-NDVI values, and can be contrasted with the woody cover proxy developed by Cerling et al. (2011). For paleosol samples that include $\delta^{13}C$ values from pedogenic carbonates, a -14‰ offset may be applied to convert the carbonate to the equivalent organic carbon (Cerling 1984). Figures 3.6 and 3.7 display the fossil $\delta^{13}C_{SOM}$ values from Time Interval 1 of the Kapthurin Formation (543 – 509 ka), as well as a normalized probability curve of the most common NDVI and woody cover values, indicating many mixed C_3/C_4 microenvironments. Isoscapes displayed in Figure 3.8 similarly present the fossil $\delta^{13}C_{SOM}$ data and predicted paleo-NDVI values (see Appendix 2). These isoscapes also display the environmental reconstructions geographically, and are labeled with important archaeological and paleontological information.

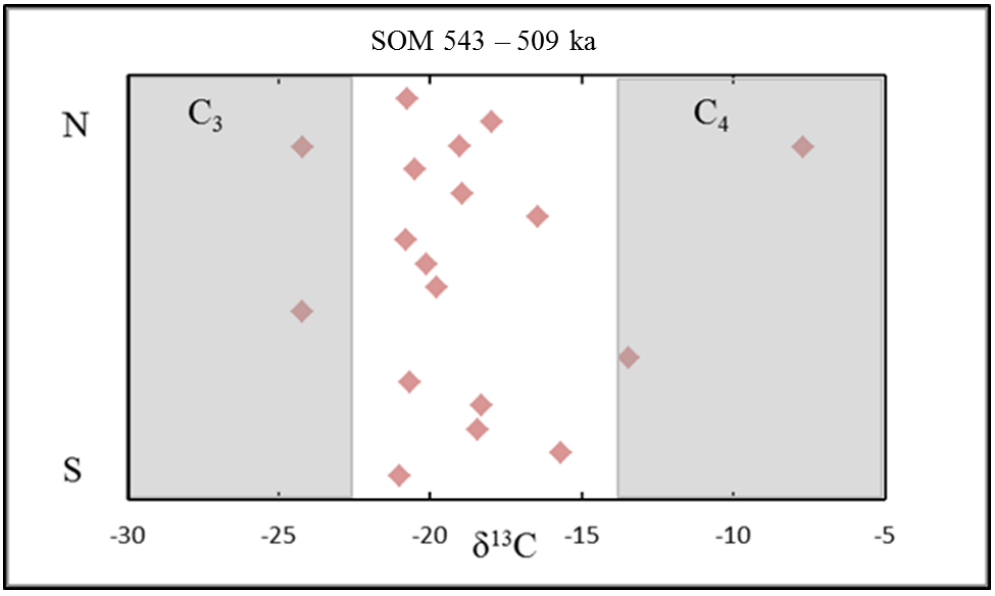

Figure 3.6: Fossil $\delta^{13}C_{SOM}$ (VPDB ‰) values from 543 – 509 ka, displayed on the y-axis as geographically North to South of the Kapthurin Formation. Mixed C_3/C_4 sources of plant material dominate. Shaded areas indicate C_3 and C_4 ranges.

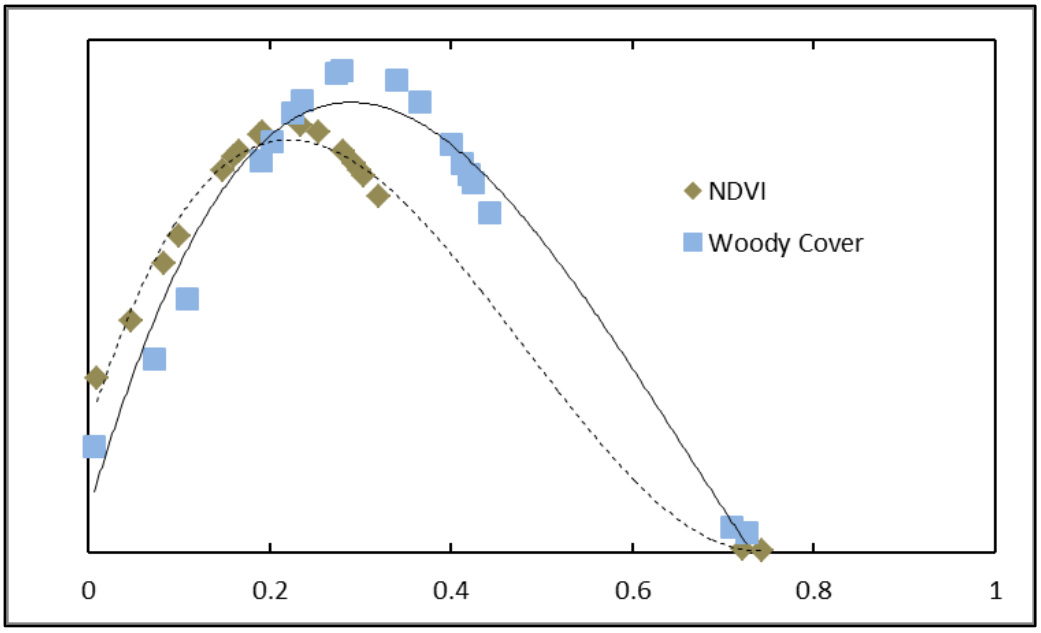

Figure 3.7: Normalized probability of paleo-NDVI and woody cover values for the landscape under study. Both probability curves indicate similar measures of paleo-habitats. The average paleo-NDVI value is 0.25, and the average paleo woody cover value is 0.32, indicating a mixed habitat of shrub and grassland environments.

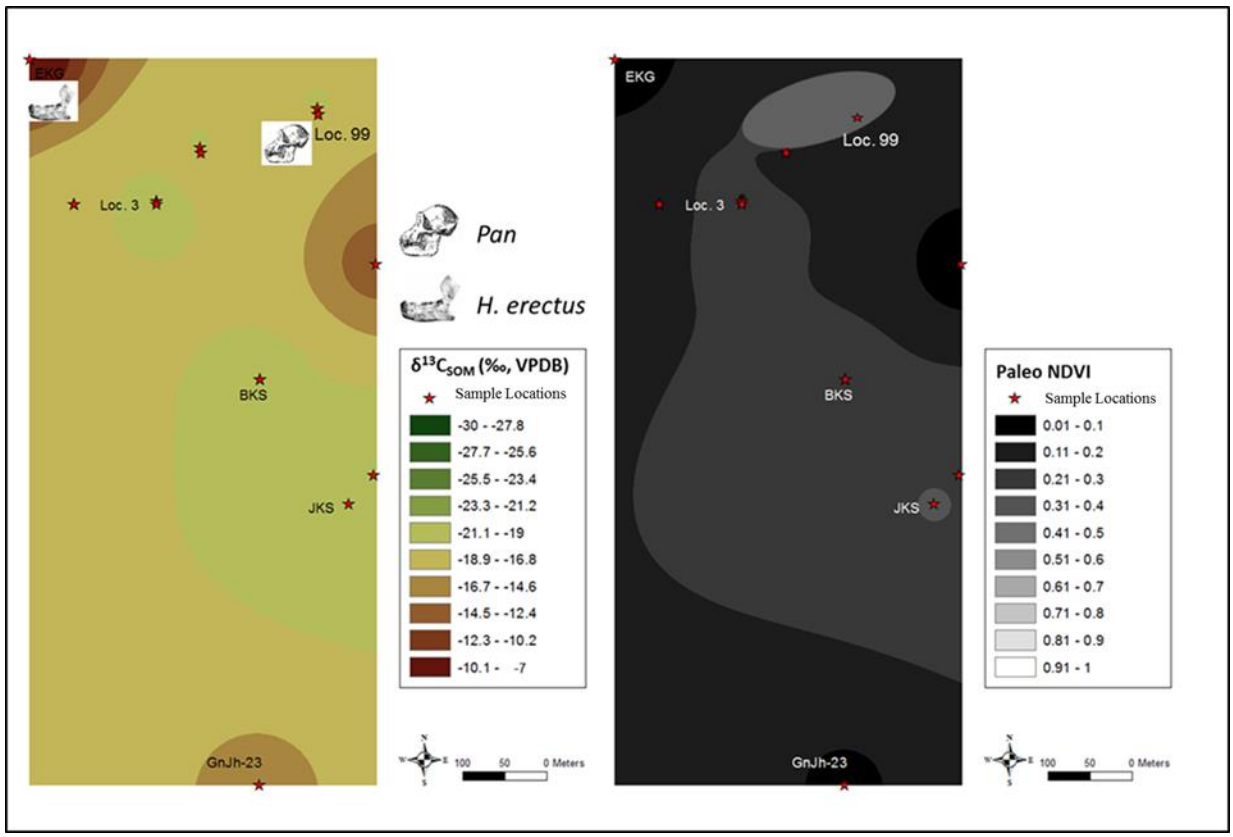

Figure 3.8: Isoscape of fossil $\delta^{13}C_{SOM}$ values from 543 – 509 ka, with relevant archaeological and paleontological sites (left). Isoscape of paleo-NDVI predicted values from 543 – 509 ka, with relevant archaeological and paleontological sites (right).

The data from Time Interval 1 (543 – 509 ka) suggests that the ecology ranged between grasslands and forests, although most of the environments sampled would indicate a mixed C_3/C_4 signature. Interestingly at the site of EKG, where hominin fossils have been identified to *Homo erectus* (Leakey, et al. 1969; Wood and Van Noten 1986), we have the clearest signature of an open grassland habitat, with a $\delta^{13}C_{SOM}$ value of -7.2‰ and a paleo-NDVI value of 0.01, indicating very low plant biomass productivity. Although very close geographically, Loc. 99, where chimpanzee fossils were excavated (McBrearty and Jablonski 2005), reveals a more forested signature (although not completely forested), with a $\delta^{13}C_{SOM}$ value of -23.8‰ and a paleo-NDVI value of 0.96. These results may indicate that chimpanzee populations during this

Time Interval 1 were utilizing a forested microhabitat, in an otherwise wooded grassland and open grassland landscape.

Fossil $\delta^{13}C_{SOM}$ values from Time Interval 2 (509 – 380 ka), displayed in Figure 3.9, indicates an overall shift to a more wooded landscape (see Appendix 2). This shift is also demonstrated in the normalized probability curves of both paleo-NDVI and woody cover estimates in Figure 3.10. Isoscapes displayed in Figure 3.11 depict the estimated ecological variation geographically, with both fossil $\delta^{13}C_{SOM}$ data and predicted paleo-NDVI values. Relevant archaeological and paleontological sites are labeled on Figure 3.11. Hominins during this Time Interval 2 (509 – 380 ka) appear to have been presented with a range of habitats, but mostly focused on intermediate C_3/C_4 habitat exploitation, including mixed habitats at GnJh-15 ($\delta^{13}C_{SOM}$ value of -21.73‰ and a paleo-NDVI value of 0.56), at LHA ($\delta^{13}C_{SOM}$ value of -16.1‰ and a paleo-NDVI value of 0.14), and at GnJh-17 ($\delta^{13}C_{SOM}$ value of -17.1‰ and a paleo-NDVI value of 0.17).

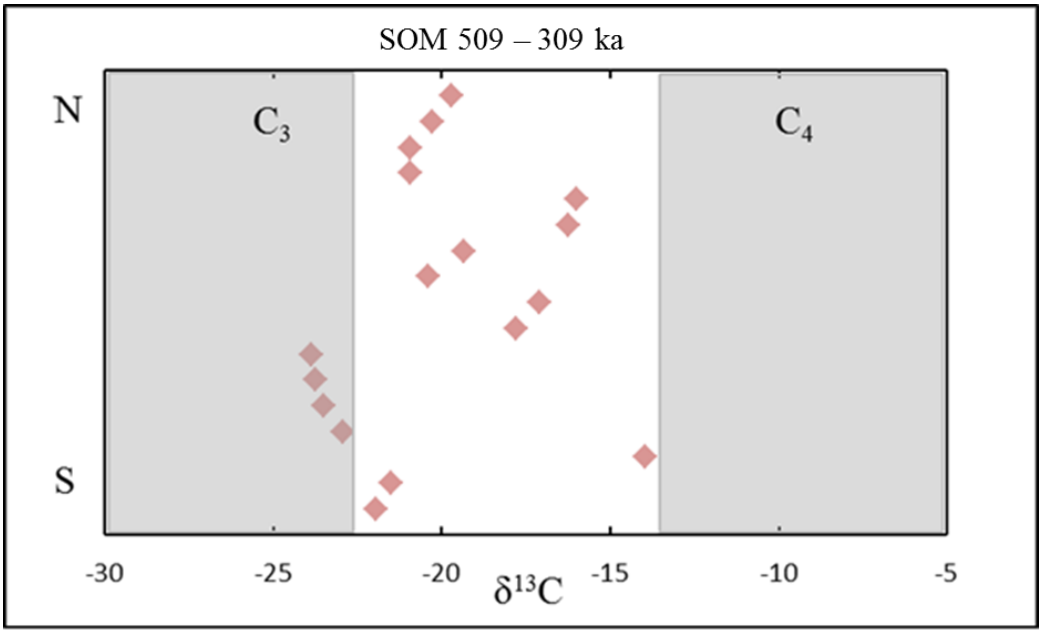

Figure 3.9: Fossil $\delta^{13}C_{SOM}$ (VPDB ‰) values from 509 – 380 ka, displayed on the y-axis as geographically North to South in the Kapthurin Formation. Mixed C_3/C_4 sources still dominate, with a slight shift to C_3 sources of vegetation in the Southern part of the formation. Shaded areas indicate C_3 and C_4 ranges.

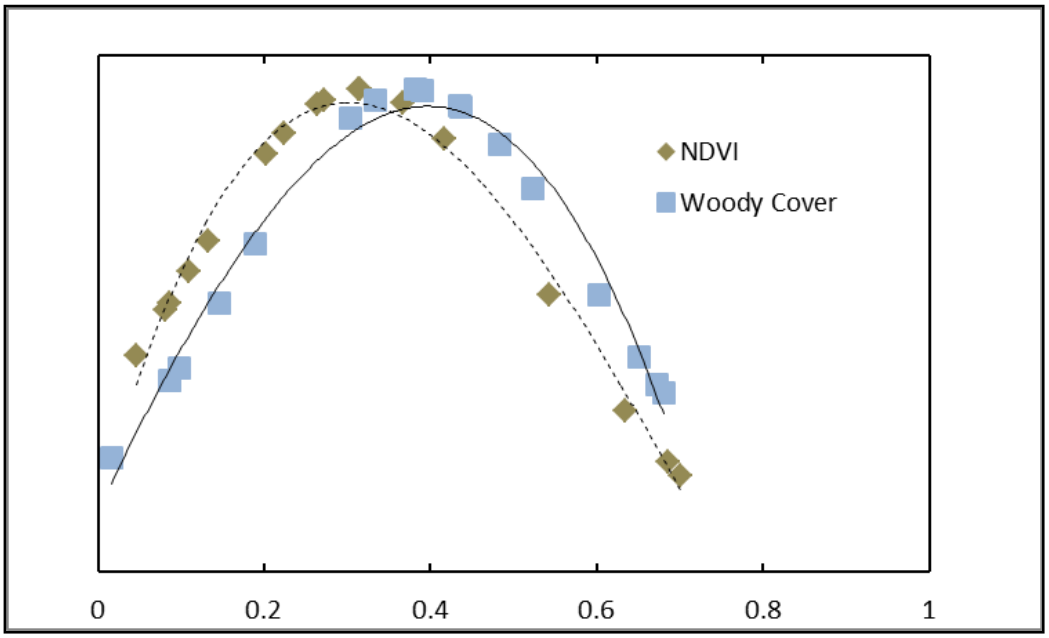

Figure 3.10: Normalized probability of paleo-NDVI and woody cover values for the landscape during the Time Interval 2. The average paleo-NDVI value is 0.31 and the average woody cover value is 0.38, indicating a mixed habitat of shrub, grassland, and forested environments.

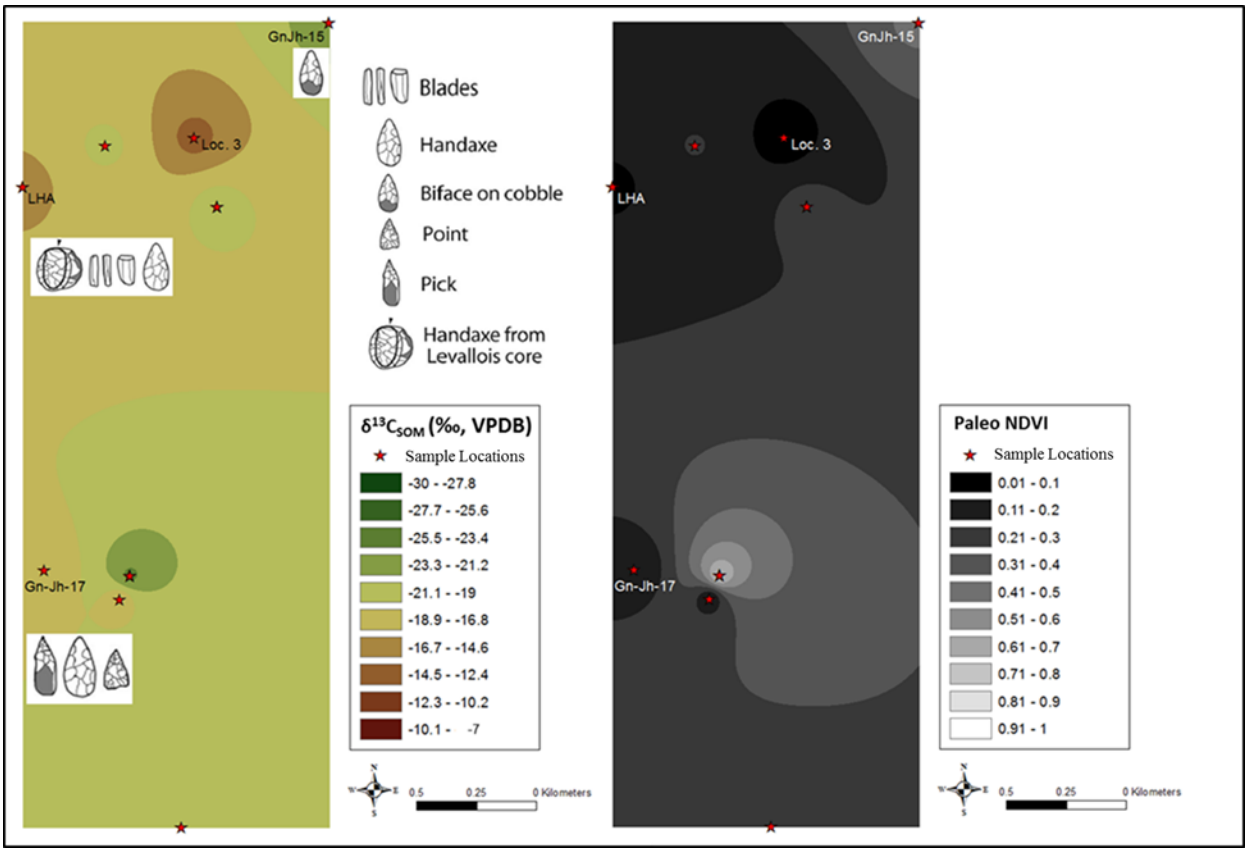

Figure 3.11: Isoscape of fossil $\delta^{13}C_{SOM}$ values from 509 – 380 ka, with relevant archaeological and paleontological sites (left). Isoscape of paleo-NDVI predicted values from 509 – 380 ka, with relevant archaeological and paleontological sites (right).

Paleo-NDVI and $\delta^{13}C_{SOM}$ values from both intervals indicate diverse habitats available to hominins. NDVI values have been used recently to assess the distribution of large herbivores by ecologists in Africa, including elephants (Cerling, et al. 2009; Wittemyer, et al. 2009), buffalo (Ryan, et al. 2006), wildebeest (Boone, et al. 2006), and other ungulates (Pettorelli, et al. 2009). However, as modern ecologists have noted, NDVI values peak during the wettest months, when biomass productivity is maximized (Pettorelli, et al. 2005). In Kenya, higher NDVI values have actually been correlated with lower species richness, while habitats with more heterogeneous NDVI values were correlated positively with species richness (Oindo and Skidmore 2002).

Higher NDVI values indicate biomass that is derived from ligneous vegetation and stored in cellulose and lignin, most of which is not available as food sources to herbivores. Non-woody vegetation is more readily available as renewable food sources and support higher secondary biomass productivity associated with herbivores. Given these constraints intermniediate NDVI values, those that encompass grasslands, shrublands, and patches of forests, would provide hominins with the most resource rich habitats to exploit. The paleo-NDVI values presented here at best represent the time-averaged NDVI values over several years of soil formation, as soil carbon is often remodeled on the scale of decades, although this varies with different soil types (Brovkin, et al. 2008; Retallack 1991).

Also, by pooling NDVI and $\delta^{13}C_{SOM}$ values from both time intervals, some additional time averaging among sites must be assumed. The variety of habitats and paleosurfaces at each site may represent individual, shorter time intervals within the larger two time intervals under study. This scenario is likely, given the sedimentology of the deposits, tectonic and erosional history of the Lake Baringo Basin, and modern geomorphology of the East African Rift Valley today (Martyn 1969; Tallon 1978). Given these limitations, we assume that the paleo-NDVI and $\delta^{13}C_{SOM}$ values represent the general paleoenvironmental setting of the Lake Baringo Basin, during the two time intervals under study.

3.4 Conclusions

Remote sensing techniques, such as NDVI, provide landscape ecologists with an accurate means of predicting modern biomass productivity of above-ground plants, and also the distribution of many modern animals (Oindo and Skidmore 2002; Pettorelli, et al. 2009;

Pettorelli, et al. 2011). NDVI values extracted from high resolution satellite imagery captured in February of 2012 from the Lake Baringo Basin (Figures 3.3 and 3.4) are well correlated with modern $\delta^{13}C_{SOM}$ values (R^2=0.79 Figure 3.5) collected in January of 2012 from the same geographic locations. NDVI values were chosen from the spectrum of relevant values (0.01 – 1.00) and should represent a range of different environments from the Lake Baringo Basin, an area with relatively little modern agricultural disturbance. Using this correlation, it is possible to devise an equation to estimate the paleo-NDVI values, if fossil $\delta^{13}C_{SOM}$ values are known (Equation 3.2), $\delta^{13}C$ values of pedogenic carbonates must be converted to $\delta^{13}C_{SOM}$ values for use with Equation 3.2, following Cerling (1984).

Paleo-NDVI calculations provide a new method for reconstructing past biomass productivity, an exciting new avenue of paleoenvironmental reconstructions. However, we must be cautious in our interpretation of these NDVI values to predict past animal behavior. As Cerling, Andanje, et al. (2015) have shown, many animals in East Africa between 1 and 4 million years ago had diets that differed substantially from their modern counterparts, as assessed through $\delta^{13}C$ values derived from tooth enamel, suggesting differences in habitat preference as well. With this caveat in mind, we have reconstructed paleo-NDVI values from Time Intervals 1 and 2 in the Kapthurin Formation (543 – 509 ka) and (509 – 543 ka), using fossil $\delta^{13}C_{SOM}$ values, and compared these results with woody cover values (Cerling et al. 2011). In both time intervals, it is clear that a range of different habitats are available to hominins, yet they are exploiting areas with moderate NDVI values. During Time Interval 1 (543 – 509 ka) the landscape is exceptionally diverse ecologically and non-continuous; chimpanzee fossils were found in a fragmented woody habitat, while hominin fossils were found in an open grassy habitat (Figure 3.8) (McBrearty and Jablonski 2005). During Time Interval 2 (509 – 380 ka) hominins

appear to be extracting resources mainly from mixed C_3/C_4 environments with moderate NDVI values, although other environments are present (Figure 3.11).

Traces of hominin activity during Time Interval 2 are associated exclusively with wooded grassland ecosystems, although other environments are present. Previous researchers have suggested that the exploitation of wooded grasslands is a feature of the MSA (Ambrose 2001a; Basell 2008; Clark 1988), although this is the first time that several MSA sites within a centralized landscape have been associated with wooded grassland environments, verifying previous hypotheses. What could be the catalyst for this shift to wooded grassland environments? Modern foragers in tropical and sub-tropical regions regularly utilize the wooded grassland ecosystem for numerous foraging activities, including: access to vegetable and fruit resources, water, shade from the mid-day sun, cover for hunting large animals, honey, and wood for the production of tools (Kelly 1995; Marlowe 2010; Murray, et al. 2001; Vincent 1985). During the MSA, many of the foraging behaviors associated with modern humans become established (Christopher S. Henshilwood and Curtis W. Marean 2003; McBrearty and Brooks 2000); MSA foragers would have needed to access both woodlands and grasslands for many of their foraging activities as well, making the wooded grassland ecotone an adaptive environment to exploit. Given the association of MSA activity with wooded grasslands during Time Interval 2, it would seem that the preference for the wooded grassland ecosystem for resource extraction activities was also established during the Middle Pleistocene.

Widespread application of this innovative method, using a landscape perspective, to a variety of time intervals and geographic locations, in conjunction with the application of Cerling et al. (2011) woody cover index will revolutionize our understanding of hominin evolution in Africa and finally allow the direct testing of environment-based hypotheses that have dominated

recent debates. In the future, we plan to expand the sample size of modern $\delta^{13}C_{SOM}$ values and contrast these with additional NDVI values from other East African environments, to arrive at a more accurate paleo-NDVI index. In the interim, these calculations can serve as estimations of past biomass productivity, and may help archaeologists reconstruct environments that hominins exploited in the past. In the Kapthurin Formation, a complicated record of micro-environments is beginning to emerge from both time intervals, indicating that hominins had multiple types of environments available for exploitation (Leslie, et al. 2016), but largely chose areas of intermediate to low primary biomass productivity for resource extraction. This may be due to the higher correlation with species richness associated with lower NDVI values (Oindo and Skidmore 2002). Paleo-NDVI values provide another ecological proxy that will be useful in reconstructing paleohabitats of hominins and other animal communities. The direct association of MSA technology with wooded grassland ecosystems verifies assumptions (Ambrose 2001a; Basell 2008; Clark 1988) about site choice by MSA foragers, and is in keeping with many resource extraction activities of modern foraging societies (Kelly 1995; Marlowe 2010; Murray, et al. 2001; Vincent 1985).

Chapter 4: Stable isotopic evidence for paleoenvironments from the Kapthurin Formation, Kenya: Evidence from pedogenic carbonates and paleosols

4.1 Introduction

The reconstruction of Middle Pleistocene paleoenvironments using a landscape perspective in East Africa is essential for understanding the diversity of resources available to hominins and the site and technological choices that led to the transition from Acheulean to Middle Stone Age technology. The Kapthurin Formation, Kenya, preserves evidence of Acheulean and Middle Stone Age technology that is interstratified, dating between 543 and 235 thousand years (ka) (Deino and McBrearty 2002; Christian A. Tryon and Sally McBrearty 2002). Regional and global changes in environments and climates have been hypothesized to affect the evolution and technological choices of hominins (Bräuer 2008; Cohen, et al. 2016; Darwin 1871; deMenocal 2011; Potts 1996; Potts and Faith 2015; Reed 1997; Vrba 1993). These hypotheses largely remain untested, and our understanding of this critical time period in human evolution may benefit from environmental reconstructions that utilize a landscape perspective and fine-grained data. Here, I apply this perspective to two separate time intervals within the Kapthurin Formation (543 – 509 ka and 509 – 380 ka), to determine what influence, if any, the local environments had on hominin technological or foraging choices, based on site choices by hominins for resource extraction.

The Middle Pleistocene (781-126 ka), formerly the Ionian (International Commission on Stratigraphy 2014), of Africa encompasses many significant events in human evolution; it records the first appearance of *Homo sapiens*, the development of technologies referred to as "modern," and a shift to regular resource extraction from a diverse range of habitats (Clark 1988;

Christopher S. Henshilwood and Curtis W. Marean 2003; McBrearty and Brooks 2000). Acheulean lithic technology was first developed during the early Pleistocene (2.58 Ma – 781 ka), formally referred to as the Calabrian and Gelasian (International Commission on Stratigraphy 2014), in East Africa (~1.76 Ma) (Lepre, et al. 2011); it has been assumed to be relatively uniform in production methods and tool forms throughout its use into the later Middle Pleistocene (Clark 1977; J D Clark 2001; Isaac 1972; Leakey 1971). More recently, researchers have begun documenting the variability in lithic manufacture during the terminal Acheulean, including the production of flakes via the Levallois method and the systematic production of blades (Adler, et al. 2014; Johnson and McBrearty 2010; McBrearty, et al. 2001; Tryon, et al. 2005). These technological innovations occur prior to the first appearance of Middle Stone Age technology, possibly indicating a period of technological innovation focused around perennial freshwater springs and biomass rich habitats (Johnson, et al. 2009; Johnson and McBrearty 2012; Leslie, et al. 2016), similar to the foraging behavior that is associated with later Middle Stone Age hominins (Curnoe, et al. 2006; McCarthy, et al. 2010). The Kapthurin Formation preserves evidence of late Acheulean and early Middle Stone Age behavior, providing an ideal location to reconstruct environments and landscapes from the Middle Pleistocene (Tryon 2003).

Paleoanthropologists regularly utilize stable isotopes from mammalian teeth, pedogenic carbonates, tufa composition to reconstruct terrestrial environments associated with human evolution, however these have rarely been applied to the Middle Pleistocene of East Africa (Ashley, et al. 2010; Cerling, Andanje, et al. 2015; Cerling, Wynn, et al. 2011; Kingston and Harrison 2007; Kingston, et al. 1994; Levin, et al. 2004; Loftus, et al. 2016; Quinn, et al. 2013). The application of these techniques to Middle Pleistocene sediments will be useful for distinguishing the local environments associated with hominins that utilized Acheulean and

Middle Stone Age technologies. Here, I test assumptions about environmental influences on site choices of hominins by combining a landscape perspective with paleoenvironmental reconstructions of the Kapthurin Formation, using stable isotope analyses of paleosols, including sedimentary carbonates, bulk soil organic matter (SOM), paleo-NDVI values, and fraction woody cover values (f_{wc}) (Cerling, Wynn, et al. 2011).

4.2 Research Questions

1. What are the environmental conditions and resources available to hominins during Time Intervals 1 and 2 projected from $\delta^{13}C$ values derived from pedogenic carbonates and bulk SOM, $\delta^{18}O$ values derived from pedogenic carbonates, paleo-NDVI values, and f_{wc} values?
2. Based on these environmental reconstructions, what are the differences or similarities in Acheulean and Middle Stone Age site choice and landscape use during Time Intervals 1 and 2?

4.3 Background

4.3.1 Kapthurin Formation

The Kapthurin Formation is preserved to the west of Lake Baringo and is part of the Middle Pleistocene sedimentary sequence of the Tugen Hills succession in the Kenyan Rift Valley (Figure 4.1). The formation is composed of interstratified alluvial, lacustrine, and volcanic sediments, it has an observed thickness of approximately 125 meters, and it is exposed over an estimated 150 km^2 (Figure 4.2) (Martyn 1969; Tallon 1978). The formation has been dated using the $^{40}Ar/^{39}Ar$ method (Deino and McBrearty 2002; Dunkley, et al. 1993) and Martyn

(1969) subdivided the formation into 5 members. Members K1, K3, and K5 are largely composed of terrigenous sediments that eroded from the Tugen Hills, and are informally named the Lower, Middle, and Upper Silts and Gravels (Figure 4.2). Pyroclastic members K2 and K4 separate the Silts and Gravels; K2 is informally named the Pumice Tuff Member and is dated to 543 ± 3 ka; K4 is referred to as the Bedded Tuff Member and has several eruptive facies, three of which are dated to 380 ± 7 ka, 284 ± 12 ka, and 235 ± 2 ka. The basal date for K4 was recently refined by through tephrostratigraphic correlation to the Korosi Airfall Pumiceous Tuff (Blegen 2015; Dunkley, et al. 1993), dated using the $^{40}Ar/^{39}Ar$ method. K3 is also subdivided by the Grey Tuff, which is dated to 509 ± 9 ka, and by alluvial facies to the west (K3) and by lacustrine facies to the east (K3'). The sediments of K3 are mainly composed of unstratified silts and pebble beds, massive conglomerates towards the western and southern reaches of the deposits, and occasional soil formation, both below K4 and the Grey Tuff (Tallon 1976). The sediments of K3' are composed of red, black, and green claystones and siltstones; the sedimentary and geochemical structures of these clays and silts indicate deposition in a shallow lake that alternated between freshwater and saline-alkaline (Johnson and McBrearty 2012; Renaut, et al. 1999; Tallon 1978).

The Kapthurin Formation lies unconformably above the Chemeron Formation, which is subdivided and underlain by the Ndau Trachymugearite, dated to 1.57 Ma, using the K-Ar technique (Hill, et al. 1986), providing a maximum age for the Kapthurin Formation (Figure 4.2). However, all of the sediments in the Kapthurin Formation are normally magnetized (Dagley, et al. 1978) and postdate the Matuyana-Brunhes Boundary, dated to 775 ka using the $^{40}Ar/^{39}Ar$ method (Coe, et al. 2004), providing a more accurate maximum age for the Kapthurin Formation.

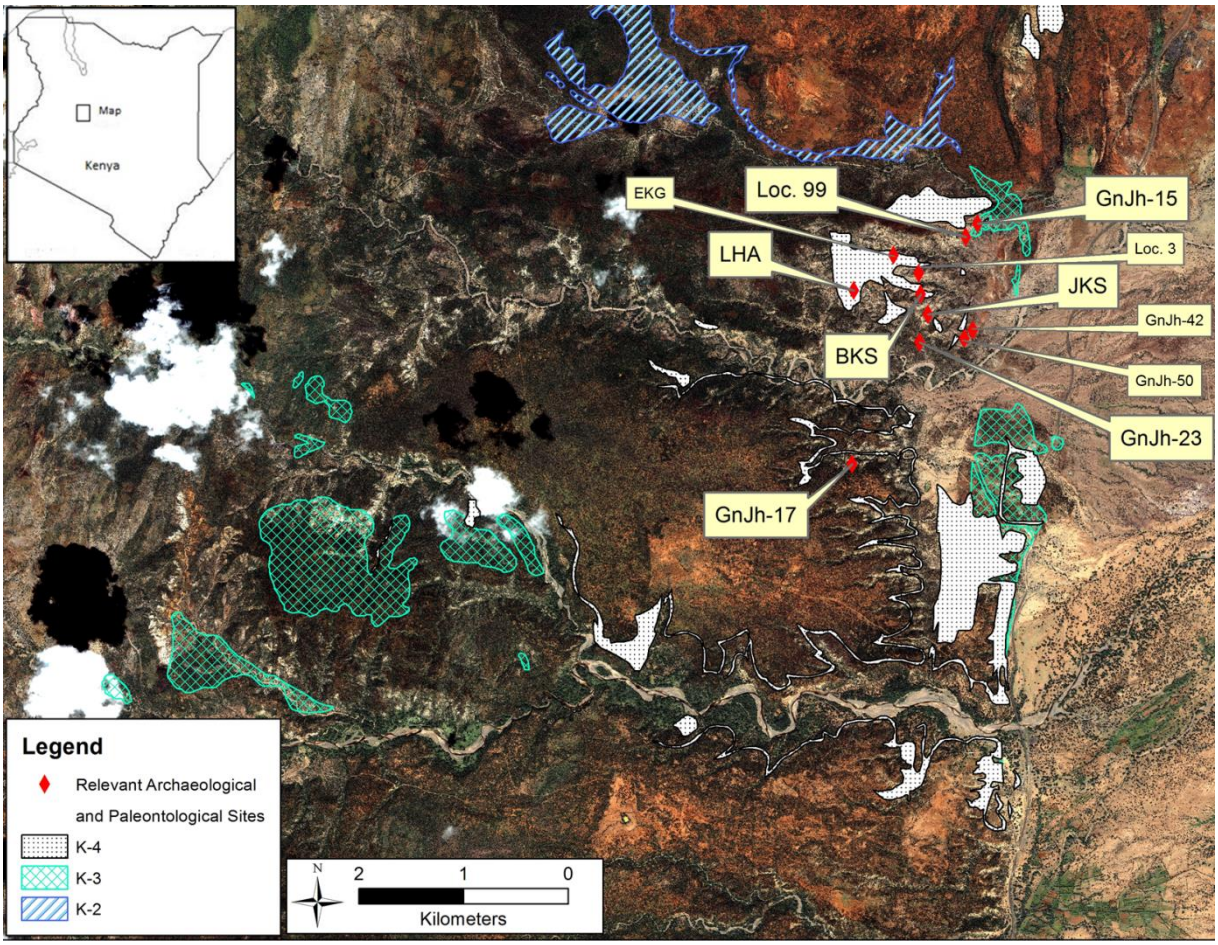

Figure 4.1: Satellite image (IKONOS, 1.8 m resolution) showing relevant geologic exposures and archaeological and paleontological sites of the Kapthurin Formation. Inset not to scale.

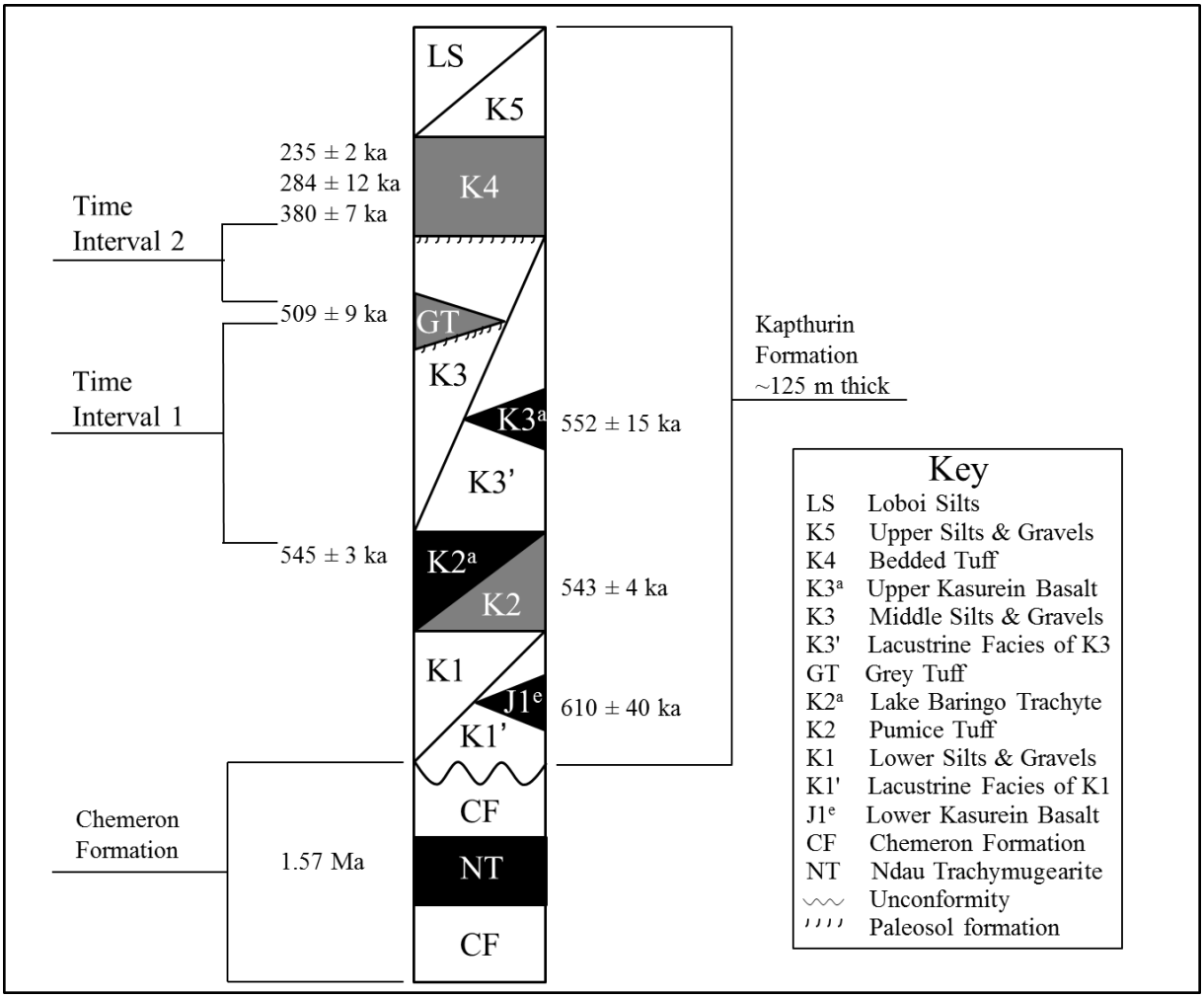

Figure 4.2: Generalized stratigraphic section of the Kapthurin Formation. Section is after Deino and McBrearty (2002) and Tallon (1978). Shaded areas represent pyroclastic sediments while light areas represent fluviolacustrine sediments.

The research presented here focuses on two main time intervals within the Kapthurin Formation, subdividing K3. Time Interval 1 (543 – 509 ka), represents archaeological and paleontological sites within deposits above K2 and below the Grey Tuff (Figure 4.2); Time Interval 2 (509 – 380 ka), represents archaeological and paleontological sites from sediments above the Grey Tuff and below K4. McBrearty (1999) reconstructed the environments of Time Interval 1 from the taxonomic identification of fauna, suggesting that forest and marsh

depositional conditions dominated, in conjunction with a braided river system, with grassland ecosystems farther from rivers. Tallon (1978) also reconstructed braided river systems that dominated both Time Intervals 1 and 2, citing paleochannels above and below the Grey Tuff. Johnson, et al. (2009) described a fossiliferous tufa in the southern exposure of the lacustrine facies, demonstrating the presence of a rich wetland during Time Interval 1. McBrearty and Jablonski (2005) documented the presence of chimpanzee fossils at Locality 99 (Loc.) in fluviolacustrine sediments, and with other fauna recovered from the site (hippopotamus, crocodile, catfish, colobine monkey, and bushpig), indicating a locally wooded habitat with marshy patches near the shores of an alternating freshwater and alkaline lake. Leslie, et al. (2016) also reconstructed environments from Time Interval 1 using stable carbon and oxygen isotope ratios derived from pedogenic carbonates and herbivorous tooth enamel; the results of these analyses suggest the dominance of hyper mesic conditions, driven by an intense monsoonal episode that resulted in woodland areas, perennially active streams, marsh and sumpland environments, and a surrounding grassland ecosystem. Hominin fossils identified to *Homo sp.* and *Homo erectus* (Leakey, et al. 1969; Wood and Van Noten 1986) have also been documented in Time Interval 1 at the site EKG, in the K3 alluvial facies, close to Loc. 99 (<1 km), indicating sympatric evolution of the genus *Homo* and *Pan* in the Lake Baringo Basin (Figure 4.1).

Faunal preservation is poor in Time Interval 2, making it more difficult to reconstruct environments. The deposition of K3 sediments during this time interval was similar to deposition during Time Interval 1; seasonal streams drained the Tugen Hills and resulted in alluvial fan deposition on the margins of a paleo-lake (Tryon 2003). Scott (2005) reconstructed the environment at Rorop Lingop, a footprint site with high vertebrate trace diversity in K4 deposits, and suggested that the site was situated on an alluvial plain near the shores of a

freshwater lake, indicating a species rich environment. Although these deposits post-date this time interval, they provide a framework for the species community that may have interacted with previous iterations of the lake during Time Interval 2. Previous researchers (Cornelissen, et al. 1990; Kingston, et al. 1994) used stable isotope ratios of carbon and oxygen derived from pedogenic carbonates to reconstruct paleoenvironments, although only two sites (GnJh-15 and GnJh-17) were included in these analyses. Cornelissen, et al. (1990) report carbon and oxygen isotope values indicative of an arid grassland environment at GnJh-17, while Kingston, et al. (1994) report carbon isotope values that suggest a mixed grassland and forested environment at GnJh-15.

Researchers have described the variability in Middle Pleistocene toolkits found in the Kapthurin Formation, which include assemblages dominated by handaxes (Leakey Handaxe Area or LHA and GnJh-17), flakes and cores (GnJh-42 and GnJh-50), bifaces produced on cobbles (GnJh-15), the early presence of prepared core technology (LHA and GnJh-17), and the early presence of the systematic production of blades (GnJh-42 and GnJh-50) (Cornelissen 1992; Johnson and McBrearty 2010, 2012; McBrearty 1999; McBrearty, et al. 1996; Tryon 2003) (Figure 4.1). As suggested by Tryon, et al. (2005) regional variability in the production of Acheulean flakes in the Kapthurin Formation, including the Levallois method, demonstrates that variability in artifact manufacturing techniques predates the Middle Stone Age. Moreover, Johnson and McBrearty (2012) have suggested that these innovations in artifact manufacture are related to hominin exploitation of patchy, resource rich environments. In Chapter 2 this hypothesis was tested, modern primary biomass productivity significantly correlates with carbon isotope values measured in modern bulk SOM, and Paleo-NDVI values suggest that hominins exploited environments of low biomass productivity during Time Interval 1 and areas of

intermediate biomass productivity during Time Interval 2. Expanded landscape environmental reconstructions presented here, including pedogenic carbonate data from both time intervals, and combined with previous reconstructions, will provide further data to test the influence of resource rich environments on hominin site choice during both time intervals.

4.3.2 Soil Carbon

Throughout this paper, isotope ratios are reported and discussed using the standard per mil (‰) notation:

Equation 4.1: $\delta^X = \left(\frac{R_{sample}}{R_{standard}} - 1\right) \times 1000 \quad X = {}^{13}C, {}^{18}O; R = {}^{13}C/{}^{12}C, {}^{18}O/{}^{16}O$

The isotope standard ($R_{standard}$) is Vienna Pee Dee Belemnite (VPDB). Paleosols, fossil soils that have experienced minor burial alteration, preserve the SOM and pedogenic carbonates of past soils, and can be used as proxies for past environments (Retallack 1991). Stable carbon isotope values ($\delta^{13}C$) of SOM ($\delta^{13}C_{SOM}$) and pedogenic carbonates ($\delta^{13}C_{PC}$) sampled from paleosols reflect the carbon isotope values of surface vegetation; $\delta^{13}C_{SOM}$ values are directly determined by the fraction of plant litter and soil development process associated with the above ground vegetation (Baisden, et al. 2002; Cerling, et al. 1989); $\delta^{13}C_{PC}$ values are determined by the incorporation of soil CO_2 associated with decaying organic matter derived from surface vegetation during soil development and an associated enrichment factor (Cerling 1984; Cerling and Quade 1993). Paleosols that have undergone minor burial alteration preserve the SOM and pedogenic carbonates of past soils and can be used as reliable indicators of past environments (Retallack 1991). The analysis of $\delta^{13}C$ values derived from paleosols and pedogenic carbonates thus offer paleoanthropologists fine-grained data to reconstruct past environments.

There are three main plant photosynthetic pathways that prevail in East Africa: C_3, C_4, and CAM (Crassulacean Acid Metabolism). C_3 and C_4 plants are more abundant than CAM plants and dominate the landscapes of East Africa. High latitude grasses and wooded plants almost exclusively use the C_3 photosynthetic pathway, while mid-latitude and tropical grasses and flowering plants incorporate CO_2 from the atmosphere using the C_4 photosynthetic pathway (Ehleringer 1978; Ehleringer and Monson 1993). The plants that use the C_3 pathway are diverse; plant types include herbs, trees, aquatic plants, and grasses with $\delta^{13}C$ values ranging from -20 to -37‰, encompassing dense canopy and desert environments (Kohn 2010). In tropical forest ecosystems, the "canopy effect" causes CO_2 to be ^{13}C depleted and produced and recycled during soil respiration, leading to the most negative $\delta^{13}C$ values found in C_3 plants (Ehleringer, et al. 1987; van der Merwe and Medina 1991). This "canopy effect" creates a gradient of negative $\delta^{13}C$ values; the most negative values are measured in the understory at the forest floor and the least negative values are measured in the upper story of the forest (Medina and Minchin 1980). The negative range of $\delta^{13}C$ values associated with C_3 plants is contrasted with the less negative range of $\delta^{13}C$ values derived from C_4 plant matter; C_4 vegetation, generally members of the grasses (*Poaceae*), chenopods (*Chenopodioideae*), and sedges (*Cyperaceae*) plant families, prevail in East Africa in open landscapes with salty soils, extreme deserts, and arid adapted vegetation, and range in $\delta^{13}C$ values from -10 to -14‰ (Farquhar, et al. 1989). Due mainly to these differences in CO_2 discrimination between wooded (C_3) and grassy (C_4) plants in the tropics, analyses of $\delta^{13}C_{SOM}$ and $\delta^{13}C_{PC}$ are useful measures of paleoenvironments.

Pedogenic carbonates are calcitic nodules, clast coverings, and cemented horizons formed in soils that are found in predominantly sub-humid to arid regions of the world (Wright 1986). These carbonates are formed through the dissolution of Calcium-bearing minerals derived from

dust and soil, a process that releases Calcium ions, which are transported downward with soil water and are eventually re-precipitated as pedogenic carbonates, once the saturation point of $CaCO_3$ is crossed, at depth in soils (>40 cm below the surface) (Birkeland 1999). Pedogenic carbonate formation is often inhibited by a few factors, including a seasonal bias in carbonate development; pedogenic carbonates mainly form during warm, dry seasons, and not during the mean growing season of an environment (Breecker, et al. 2009). Densely forested environments also prohibit the formation of pedogenic carbonation; high levels of mean annual precipitation (MAP) and acid leaching actively repress carbonate precipitation, indicating a C_4 bias in environmental reconstructions based on $\delta^{13}C_{PC}$ values (Tucker and Wright 1990). The formation time of pedogenic carbonates can vary, with estimates between 10^2 and 10^5 years required for the formation of individual nodules or horizons (Jenny 1980). Oerter, et al. (2016) used U-Th dating by laser ablation, in conjunction with micro-mill sampling, to illustrate continuously preserved paleoclimate records in pedogenic carbonate ring formation, in some cases over 100 ka.

During the development of soils with high respiration rates, pedogenic carbonates form at depths greater than 30 cm below surface vegetation, incorporating soil CO_2 that is associated with the decaying organic matter derived directly from surface vegetation (Cerling 1984; Cerling and Quade 1993). The main source of variation in $\delta^{13}C_{PC}$ values from the Kapthurin Formation should therefore be local decaying organic matter from surface vegetation during soil formation, assuming minimal fluctuations in atmospheric CO_2 during the Pleistocene (Cerling 1991). Carbon isotope enrichment between soil CO_2 and pedogenic carbonates is determined by both kinetic and temperature dependent equilibrium fractionation processes, which results in a

combined carbon enrichment between plants and pedogenic carbonates of 12-14‰ for soils under high respiration (Cerling, et al. 1991; Levin, et al. 2011; Romanek, et al. 1992).

Carbon isotope ratios of SOM are particularly useful because the values are directly determined by the fraction of litter derived from C_3 and C_4 plants (Wynn and Bird 2007) and the soil development processes that are associated with decomposition of above ground vegetation (Baisden, et al. 2002; Ladd, et al. 2014). This is contrary to pedogenic carbonate formation, although still a useful environmental proxy, can be inhibited by densely forested environments, which are associated with acidic soils and high precipitation (Tucker and Wright 1990). Pedogenic carbonates also have a seasonal bias in formation, and are associated with warm, dry season precipitation conditions, rather than the mean plant growing season (Breecker, et al. 2009). For Middle Pleistocene environmental reconstructions of carbon isotope values, a 2‰ correction is needed to compensate for the differences between pre-industrial and modern atmospheric values of CO_2 (Indermuhle, et al. 1999).

Recently, Cerling et al. (2011) developed a regression equation to calculate the fraction of woody canopy cover (f_{wc}) from $\delta^{13}C_{PC}$ values (and $\delta^{13}C_{SOM}$ values) and used the following isotope values to discriminate difference in vegetation cover: Forests, landscapes with continuous stands of trees at least ten meters tall ($\delta^{13}C_{PC} < -11.5‰$); Woodland/Bushland/Shrubland vegetation cover, where woodlands are an open stand of trees at least eight meters tall and have a field layer dominated by woody cover over 40% of the landscape, bushlands are an open stand of bushes between three and eight meters tall and woody cover dominates over 40% of the landscape, and shrublands are an open or closed stand of bushes up to two meters tall ($-11.5‰<\delta^{13}C_{PC}<-6.5‰$); Wooded Grasslands are landscapes covered with grass and have tree and shrub coverage between 10 and 40% ($-6.5‰<\delta^{13}C_{PC}<-$

2.3‰); Grasslands are landscapes covered with grasses and have less than 10% tree and shrub coverage ($\delta^{13}C_{PC}$ >-2.3‰). Similarly, in Chapter 2 a regression equation was developed to calculate the primary biomass productivity of a past environment, correlating Normalized Differential Vegetation Indices (NDVI), derived from high-resolution mulit-spectral satellite imagery, with modern $\delta^{13}C_{SOM}$ values. NDVI values are derived on a scale from -1 to 1, but values that approximate biomass productivity range from 0 to 1; values that approximate 0 indicates sparse vegetation with a very low carrying capacity and values that approach 1 indicates dense vegetation with a high carrying capacity (Box, et al. 1989; Hunt 1994; Tucker, et al. 1986). NDVI values have also been useful in predicting habitats of modern animal communities, and when applied to the paleontological record may provide information about past animal behavior (Cerling, et al. 2009; Pettorelli, et al. 2006; Pettorelli, et al. 2011). Both the woody cover and NDVI proxies provide complementary information for environmental reconstruction, and importantly are based on SOM values, which are not inhibited in dense forested environments, providing two additional proxies useful for paleoecological reconstructions.

4.3.3 Soil Oxygen

The $\delta^{18}O$ values of pedogenic carbonates ($\delta^{18}O_{PC}$) are determined by the oxygen isotope composition of soil water and soil temperature. The $\delta^{18}O$ value of soil water is controlled by the $\delta^{18}O$ value of meteoric water and the amount of soil water evaporation. Soil water is produced through a mixture of individual rainfall events as soil water is fed through infiltration and surface run-off and the accumulation of rainfall over a season (Breecker, et al. 2009). The $\delta^{18}O$ values of rainfall are dependent on the climate, elevation, and distance from the source of evaporation (Dansgaard 1964); in East Africa, $\delta^{18}O$ values of rainfall are predominantly controlled by rainfall

amounts, elevation, and evaporation source (Levin, et al. 2009; Rozanski, et al. 1996). Values of $\delta^{18}O_{PC}$ derived from near surface samples are often enriched compared to pedogenic carbonates from deeper soil contexts, because surface waters are subject to increased evaporation due to the prolonged amount of time they are available to evaporative processes (Breecker, et al. 2009; Quade, et al. 1989). Values of $\delta^{18}O_{PC}$ are also determined by soil temperatures, because the fractionation between soil water and pedogenic carbonate is temperature dependent (-0.2‰/1°C) (Kim and O'Neil 1997). Passey, et al. (2010) suggested that soil temperatures during the last 4 million years of the Turkana Basin exceeded the Mean Annual Temperature (MAT) ranges for the region today, but more recently, Cerling, Mace, et al. (2015) demonstrated that soil temperatures from samples collected 25 cm below the surface in open environments in East Africa are elevated by 7°C when compared with MAT, while soil temperatures in forest soils approximate MAT estimates. These studies indicate that $\delta^{18}O_{PC}$ values are faithful indicators of the oxygen isotope composition of soil water, and thus may be used to reflect the $\delta^{18}O$ value of meteoric water.

4.4 Methods

4.4.1 Field Methods

During the 2012 and 2011 field seasons, large nodular pedogenic carbonates were collected from 30 locations and paleosol samples were collected from 21 locations, and many of these sampling locations overlap (n=21). Thirty-one samples were collected from Time Interval 1, and 20 samples were collected from Time Interval 2. To reduce issues of time-averaging, samples were collected below dated horizons where possible; samples from Time Interval 1 were probably deposited at approximately 509 ka and samples from Time Interval 2 were probably

deposited at approximately 380 ka. With this procedure, some time averaging among sites that are overlain by the Grey Tuff (509 ± 9 ka) and Bedded Tuff (380 ± 7 ka) must be assumed. The variety of habitats and paleosurfaces may well represent individual short time intervals within the larger time intervals under study. This is likely, due to the sedimentology of the deposit, tectonic and erosional history of the Lake Baringo Basin, and modern geomorphology found in the area today (Martyn 1969; Tallon 1978). However, this method of correlation, following widespread, mappable temporal markers of paleolandscapes is common, and at best provides a paleo-average of a landscape. Archaeological and paleontological sites sampled for pedogenic carbonates and SOM include EKG, Loc. 99, LHA, Loc. 3, JKS, GnJh-23, GnJh-15, GnJh-17, GnJh-47, and GnJh-52. Samples were also taken from well-developed paleosols underlying the Grey Tuff in Time Interval 1 and the Bedded Tuff in Time Interval 2; these sampling locations will be useful for landscape reconstructions and also as controls to provide environmental data about locations lacking evidence of hominin occupation. Paleosols were sampled at least 50 cm below the surface exposure of outcrops in order to minimize any remodeling of pedogenic carbonates or SOM from extant environments (Retallack 1991). All sampling locations were recorded using a differential GPS (Magellan MobileMapper Pro – decimeter accuracy in x and y coordinates) and are stored in a GIS database.

4.4.2 SOM Samples

SOM samples were dried and prepared for isotopic analysis following conventional protocols (Hartman 2011). Paleosol samples were first dried in an oven at 60°C, disaggregated, and sieved through 2 mm screens to remove any large gravels and visible plant remains. Next, samples were immersed in a hyper-saturated sodium chloride (NaCl) solution and agitated to

float and remove any remaining organic detrital materials. Soil samples were subsequently washed with Milli-Q© purified water (EMD Millipore, Billerica MA) and dried. Soil carbonates were then removed by reacting 10 grams of soil samples with 1 M Hyrdochloric Acid (HCl) in open 50 ml tubes and agitated until CO_2 release terminated. Samples were neutralized with Milli-Q© purified water and dried at 60°C.

Bulk $\delta^{13}C_{SOM}$ samples were measured at the Stable Isotope Laboratory, Boston University, after combustion in a Vector Euro elemental analyzer. The combustion gas (CO_2) was separated on a GC column, passed through a GVI diluter (GV Instruments) and reference gas box, and introduced into the GVI IsoPrime isotope ratio mass spectrometer. Water was removed using a magnesium perchlorate water trap. Ratios of $^{13}C/^{12}C$ were expressed as the relative ‰ differences between these samples and the international standard VPDB. Each sample isotope ratio was also compared to a secondary standard with an isotope ratio calibrated to international standard NBS 20 (Solnhofen limestone -1.05 ± 0.02‰). Mass percent C was recorded with continuous flow and were calibrated against known quantities of the peptone and glycine standards (±0.2‰). All international standards were obtained from the National Bureau of standards in Gaithersburg, Maryland, USA. It was assumed that any variation of $\delta^{13}C$ of atmospheric CO_2 from each time interval would be incorporated into the $\delta^{13}C_{SOM}$ at all sites and not affect individual interpretations or results (Tans, et al. 1979).

4.4.3 Soil Carbonate Samples

Pedogenic carbonate nodules were examined macroscopically and microscopically for cracks, infilling, and other diagenetic reworking by detrital carbonate; any soil carbonates with these alterations were discarded from subsequent analyses. Nodules were encased in epoxy-resin

and then cross-sectioned using a precision saw (Buehler Isomet 1000). Cross sections were ground using a Buehler Ecomoet 3, in sequential steps using Milli-Q© purified water and 400, 600, 800, 1200, and 1500 grit paper and polished with fine polishing cloth and alumina powder, producing finely polished cross-sections. Cross-sections were sampled for carbon and oxygen stable isotope values ($\delta^{13}C_{PC}$ and $\delta^{18}O_{PC}$) using a high precision micromill (New Wave) with a 0.5 mm diamond drill bit. 33 Nodules were serially sampled to determine any internal variability during formation (n=326), the serial samples have been averaged and are provided with individual standard deviations. Powdered samples were measured at the *Centre National de la Recherche Scientifique, Museum National d'Histoire Naturelle* (CNRS/MNHN) after combustion using a Thermo-Finnigan Kiel IV carbonate analyzer coupled to a Delta V mass spectrometer. Analytical precision was obtained using internal standards (MarbreLM) which were calibrated against the standard NBS-19. These internal standards were run intermittently with carbonate samples, with standard deviations of 0.03‰ for $\delta^{13}C$ and 0.05‰ for $\delta^{18}O$ values.

Paleosol samples also contained small nodules of carbonate content that were sampled in this analysis for carbon and oxygen stable isotope values ($\delta^{13}C_{SC}$ and $\delta^{18}O_{SC}$). Paleosol samples were dried in an oven at 60°C, then disaggregated and sieved through 2 mm screens to remove any large gravels or visible plant remains. After this, samples were immersed in a hyper-saturated sodium chloride (NaCl) solution and then agitated to float and remove any remaining organic detrital materials. Next, soil samples were washed with Milli-Q© purified water and dried. Bulk organics were then removed from the sample by reacting 10 g of soil with 50 ml of sodium hypochlorite (NaOCl 6.0%) solution and agitated until the reaction terminated. Samples were then neutralized with Milli-Q© purified water and dried at 60°C. Initial soil carbonate samples' carbonate concentration was calculated using the "Karbonat-Bombe" technique (Müller

and Gastner 1971). Soil carbonate samples were processed at the University of Arizona Environmental Isotope Laboratory, using a Thermo Finnigan MAT 252 coupled to a Kiel-III carbonate device. Samples were reacted with dehydrated phosphoric acid under vacuum at 70°C and were run intermittently with standards NBS-19 and NBS-18, providing analytical precision of ± 0.08‰ for $\delta^{13}C$ and ± 0.1‰ for $\delta^{18}O$ values.

4.4.4 Woody Cover and NDVI proxies

To estimate the fraction of woody cover and paleo NDVI values $\delta^{13}C_{PC}$ values must be converted to the isotopic equivalent of $\delta^{13}C_{SOM}$ values by subtracting 14‰; $\delta^{13}C_{SOM}$ values derived from paleosols do not need to be converted to predict f_{wc} or paleo NDVI values. To estimate the fraction of woody cover (f_{wc}) the regression equation developed by Cerling et al. (2011) was applied to $\delta^{13}C_{SOM}$ values and converted $\delta^{13}C_{PC}$ and $\delta^{13}C_{SC}$ values from Time Intervals 1 and 2 using Equation 4.2:

Equation 4.2: $f_{wc} = \{\sin[-1.06688 - 0.08538(\delta^{13}C_{SOM})]\}^2$

To predict paleo NDVI values, the regression equation developed in Chapter 2 was applied to converted $\delta^{13}C_{PC}$ and $\delta^{13}C_{SC}$ values and $\delta^{13}C_{SOM}$ values from Time Intervals 1 and 2 following Equation 4.3 below:

Equation 4.3: $NDVI = e^{\frac{\delta^{13}C_{SOM}+24.014}{-3.946}}$

4.5 Results

4.5.1 Carbon composition of soil carbon

Twenty-five large nodules of pedogenic carbonate sampled for $\delta^{13}C_{PC}$ values from Time Interval 1 (543 – 509 ka) average -3.5 ± 2.3‰, and they range from -9.6 to 0.2‰ (Figure 4.3, Table 4.2). These results indicate that wooded grasslands (number of samples that fall within this vegetation category, n=13) were the most common form of vegetation cover recorded by pedogenic carbonate nodules, the average woody cover (0.19) and paleo-NDVI (0.23) also indicate a grass, shrub, and wooded dominated landscape. The open grassland category is the second most prevalent vegetation cover during this time interval (n=9) and there is some evidence for the woodland/bushland/shrubland category (n=3), while there is no evidence for densely forested environments preserved in the large nodular pedogenic carbonate record. The results of these paleoenvironmental reconstructions are listed below in Table 4.1.

Site	**$\delta^{13}C_{PC}$**	**$\delta^{13}C_{SC}$**	**$\delta^{13}C_{SOM}$**	**PC Paleo-NDVI**	**PC f_{wc}**	**SC Paleo-NDVI**	**SC f_{wc}**	**SOM Paleo-NDVI**	**SOM f_{wc}**
Time Interval 1									
EKG	WG	WG	G	WG	WG	WG	WG	G	G
GnJh-42	G			G	G				
Loc. 99	W	W	W	F	W	F	W	F	W
Time Interval 2									
GnJh-15	WG	WG	W	G	G	G	G	W	W
GnJh-17	WG	W	WG	WG	WG	W	W	G	G
LHA	WG	W	G	WG	G	F	W	G	G

Table 4.1: Vegetation indicated for relevant archaeological and paleontological sites discussed in text, based on measured carbon values from pedogenic carbonates, soil carbonates, and soil organic matter. Paleo-NDVI and *f*wc estimates are listed for each proxy. F = Forested, W = Woodland, WG = Wooded Grassland, and G = Grassland.

Pedogenic carbonate nodules sampled for $\delta^{13}C_{PC}$ values from Time Interval 2 (509 – 380 ka) average -4.7 ± 1.3‰ and they range from -6.2 to -2.6‰ (Figure 4.3 and Table 4.2). All of the pedogenic carbonates sampled average values that are within the range of the wooded grassland vegetation cover category (n=9), and similarly record average woody cover indices of 0.26 and paleo-NDVI estimates of 0.27. There is no evidence for other vegetation covers from the pedogenic carbonate nodule record from Time Interval 2.

Paleosol carbonate sample $\delta^{13}C_{SC}$ values from Time Interval 1 average -7.4 ± 1.8‰ and range from -9.4 to -4.0‰ (Figure 4.4 and Table 4.3). The dominant type of vegetation cover recorded is the woodland/bushland/shrubland category (n=7), the wooded grassland category is also well represented (n=4), there are no other vegetation cover categories recorded from these samples. The f_{wc} estimates for this time interval average 0.48, ranging from 0.21 to 0.64, while the paleo-NDVI estimates average 0.57, ranging from 0.22 to 0.86; these results indicate a landscape dominated by woodland vegetation cover with pockets of grasslands.

Sample	$\bar{x}\ \delta^{13}C$	$\sigma_{\delta 13C}$	$\bar{x}\ \delta^{18}O$	$\sigma_{\delta 18O}$	n	$\bar{x}\ f_{wc}$	$\bar{x}$ NDVI	Site	Time Interval
DL-1-2011	-2.1	0.6	-2.9	0.3	8	0.09	0.14	Below GT	1 (543-509 ka)
DL-2-2011	-2.2	1.4	-4.8	1.0	20	0.11	0.15	Below GT	1 (543-509 ka)
DL-3-2011	-2.1	0.3	-5.7	0.5	16	0.09	0.13	Below GT	1 (543-509 ka)
DL-4-2011	-2.7	0.8	-5.6	0.6	12	0.13	0.16	Below GT	1 (543-509 ka)
DL-5-2011	-2.7	0.3	-6.8	0.6	10	0.12	0.16	Below GT	1 (543-509 ka)
DL-6-2011	-1.1	0.5	-4.5	0.5	10	0.05	0.11	Below GT	1 (543-509 ka)
DL-7-2011	-0.3	0.9	-4.6	0.7	10	0.03	0.09	Below GT	1 (543-509 ka)
DL-7-1-2011	-1.7	1.3	-5.6	2.1	10	0.08	0.13	Below GT	1 (543-509 ka)
DL-8-2011	-3.7	0.9	-3.8	0.4	10	0.19	0.21	Below GT	1 (543-509 ka)
DL-9-2011	-3.1	0.9	-4.5	1.6	10	0.15	0.18	Below GT	1 (543-509 ka)
DL-9-1-2011	-2.6	0.5	-5.2	1.1	10	0.12	0.16	Below GT	1 (543-509 ka)
DL-10-2011	-1.5	0.5	-7.8	0.8	10	0.06	0.12	GnJh-42	1 (543-509 ka)
DL-10-1-2011	-1.6	0.1	-8.6	0.4	10	0.07	0.12	GnJh-42	1 (543-509 ka)
DL-1-2012	-6.5	0.3	-3.7	0.4	10	0.40	0.42	Loc. 3	1 (543-509 ka)
DL-2-2012	0.2	0.4	-0.4	0.9	6	0.01	0.08	Loc. 3	1 (543-509 ka)
DL-3-2012	-4.4	0.9	-3.4	0.4	15	0.24	0.25	Below GT	1 (543-509 ka)
DL-4-2012	-4.8	1.0	-3.5	0.5	15	0.27	0.28	Loc. 3	1 (543-509 ka)
DL-5-2012	-4.8	0.5	-2.5	0.6	10	0.26	0.27	Below GT	1 (543-509 ka)
DL-7-2012	-5.6	0.2	-2.9	1.5	9	0.32	0.32	EKG	1 (543-509 ka)
DL-9-2012	-6.8	0.2	-3.5	0.5	10	0.42	0.44	BKS	1 (543-509 ka)
DL-10-2012	-6.0	0.3	-4.1	0.3	10	0.35	0.36	JKS	1 (543-509 ka)
DL-11-2012	-5.3	0.2	-5.4	0.3	10	0.30	0.30	GnJh-23	1 (543-509 ka)
DL-20-2012	-2.3	1.4	-4.1	0.4	10	0.11	0.15	GnJh-27	1 (543-509 ka)
DL-21-2012	-9.6	0.2	-3.8	0.3	3	0.66	0.90	Loc. 99	1 (543-509 ka)
DL-6-2012	-3.3	0.0	-3.7	0.2	10	0.16	0.18	GnJh-15	2 (509-380 ka)
DL-8-2012	-2.6	0.1	-3.0	0.3	10	0.12	0.15	Loc. 3	2 (509-380 ka)
DL-12-2012	-5.8	NA	-2.3	NA	1	0.34	0.34	Loc. 17	2 (509-380 ka)
DL-13-2012	-5.6	0.3	-3.7	0.7	10	0.32	0.32	Loc. 17	2 (509-380 ka)
DL-14-2012	-6.2	0.3	-4.0	0.2	10	0.37	0.38	GnJh-17	2 (509-380 ka)
DL-16-2012	-5.7	0.3	-3.6	0.5	10	0.30	0.31	Loc. 307	2 (509-380 ka)
DL-17-2012	-3.1	0.4	-3.5	0.3	10	0.15	0.17	Below K4	2 (509-380 ka)
DL-18-2012	-5.8	NA	-3.6	NA	1	0.34	0.35	LHA	2 (509-380 ka)
DL-19-2012	-4.2	0.5	-3.7	0.2	10	0.22	0.23	Below K4	2 (509-380 ka)

Table 4.2: Average stable isotope values and standard deviations of serially sampled pedogenic carbonates (measured in ‰). Fraction Woody Cover (f_{wc}) and paleo-NDVI values are also displayed. Below GT and K4 refers to samples collected from paleosols stratigraphically below the Grey Tuff and Bedded Tuff (K4). $\bar{x}$ = average and σ = standard deviation.

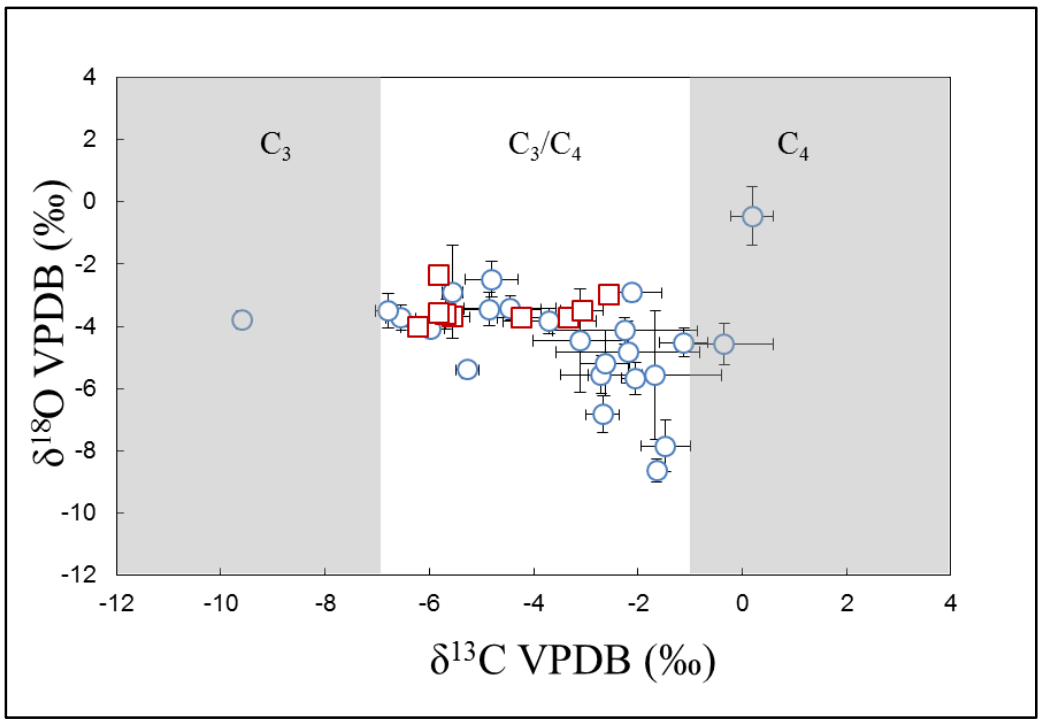

Figure 4.3: Average stable isotope values with one standard deviation of serial pedogenic carbonate nodule samples from Time Interval 1 (blue circles) and Time Interval 2 (red squares), displayed against x-axis ($\delta^{13}C$) and y-axis ($\delta^{18}O$). Samples are displayed with reference to assumed vegetation cover ranges (C_3, C_3/C_4, and C_4) after Cerling, Wynn, et al. (2011).

Paleosol carbonate sample $\delta^{13}C_{SC}$ values from Time Interval 2 average -6.9 ± 2.0‰ and range from -9.4 to -4.4‰ (Figure 4.4 and Table 4.3). The most common vegetation cover represented is the woodland/bushland/shrubland category (n=5), although the wooded grassland category is well represented (n=4). There are no other vegetation cover categories represented by these samples. The f_{wc} estimates for this time interval range from 0.23 to 0.65 and average 0.43. The paleo-NDVI estimates range from 0.25 to 0.86 and average 0.51. These results indicate that wooded vegetation is again the most common form of vegetation, but there are significant grassland components present.

Sample	$\delta^{13}C$	$\delta^{18}O$	f_{wc}	NDVI	Site	Time Interval
DL-1-2012-1	-9.0	-4.9	0.61	0.77	Loc. 3	1 (543-509 ka)
DL-2-2012-1	-4.0	-3.0	0.21	0.22	Loc. 3	1 (543-509 ka)
DL-3-2012-1	-8.7	-4.5	0.58	0.72	Below GT	1 (543-509 ka)
DL-4-2012-1	-7.9	-5.5	0.52	0.59	Loc. 3	1 (543-509 ka)
DL-5-2012-1	-5.7	-3.3	0.33	0.34	Below GT	1 (543-509 ka)
DL-7-2012-1	-5.5	-4.1	0.32	0.32	EKG	1 (543-509 ka)
DL-9-2012-1	-8.4	-5.9	0.56	0.67	BKS	1 (543-509 ka)
DL-10-2012-1	-8.5	-6.2	0.57	0.68	JKS	1 (543-509 ka)
DL-11-2012-1	-5.6	-4.3	0.32	0.32	GnJh-23	1 (543-509 ka)
DL-20-2012-1	-8.9	-5.8	0.60	0.75	GnJh-27	1 (543-509 ka)
DL-21-2012-1	-9.4	-7.7	0.64	0.86	Loc. 99	1 (543-509 ka)
DL-6-2012-1	-4.8	-4.2	0.26	0.27	GnJh-15	2 (509-380 ka)
DL-8-2012-1	-4.4	-2.1	0.23	0.24	Loc. 3	2 (509-380 ka)
DL-12-2012-1	-8.1	-4.6	0.54	0.62	Loc. 17	2 (509-380 ka)
DL-13-2012-1	-8.8	-5.9	0.60	0.74	Loc. 17	2 (509-380 ka)
DL-14-2012-1	-8.0	-4.9	0.53	0.61	GnJh-17	2 (509-380 ka)
DL-16-2012-1	-8.7	-4.4	0.58	0.71	Loc. 307	2 (509-380 ka)
DL-17-2012-1	-4.5	-3.1	0.24	0.25	Below K4	2 (509-380 ka)
DL-18-2012-1	-9.4	-6.3	0.65	0.86	LHA	2 (509-380 ka)
DL-19-2012-1	-5.1	-3.7	0.28	0.28	Below K4	2 (509-380 ka)

Table 4.3: Stable carbon and oxygen isotope values (measured in ‰) from soil carbonates derived from paleosol samples. Fraction Woody Cover (f_{wc}) and paleo-NDVI values are also displayed. Below GT and K4 refers to samples collected from paleosols stratigraphically below the Grey Tuff and Bedded Tuff (K4).

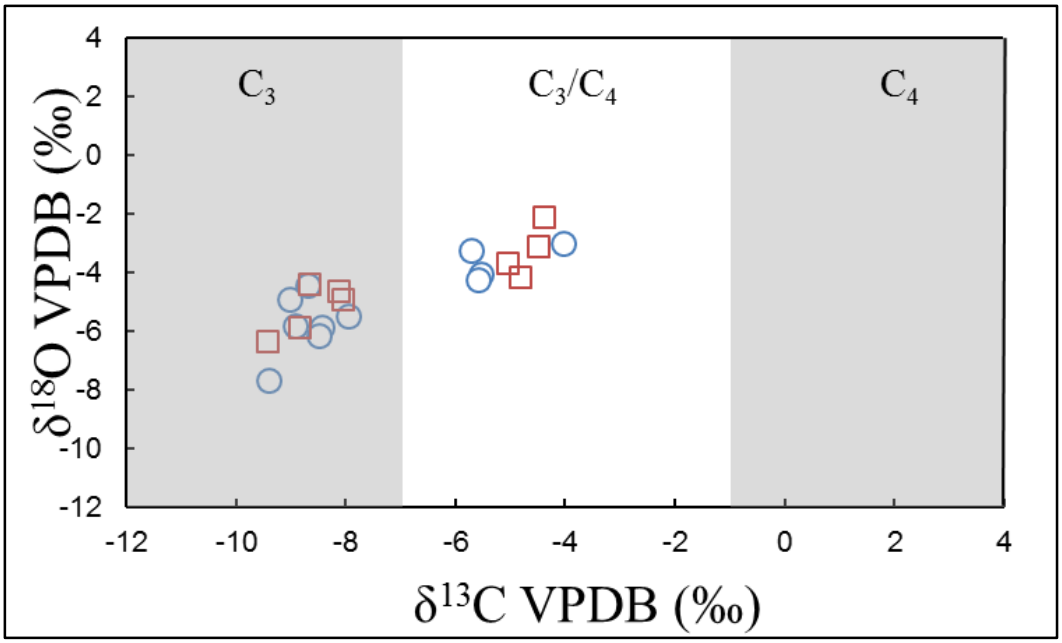

Figure 4.4: Individual paleosol carbonate stable isotope values from Time Interval 1 (blue circles) and Time Interval 2 (red squares), displayed against x-axis ($\delta^{13}C$) and y-axis ($\delta^{18}O$). Samples are displayed with reference to assumed vegetation cover ranges (C_3, C_3/C_4, and C_4) after Cerling, Wynn, et al. (2011).

Paleosols were sampled from Time Interval 1 for $\delta^{13}C_{SOM}$ values; these values average -18.2 ±4.3‰ and range from -23.8 to -7.2‰ (Figure 4.5 and Table 4.4). The woodland/bushland/shrubland category is the most prevalent for $\delta^{13}C_{SOM}$ values (n=6), while the wooded grassland and grassland category are each represented by three samples. There is no evidence for the forested vegetation cover category from these samples. The f_{wc} estimates average 0.31 for this time interval and range from 0.68 to 0.07, while paleo-NDVI estimates average 0.34 and range from 0.96 to 0.12. These results indicate a landscape dominated by woodlands with equal parts wooded grassland and open grassland vegetation cover.

Paleosols sampled for $\delta^{13}C_{SOM}$ values from Time Interval 2 average -18.8 ± 2.6‰ and range from -22.4 to -14.0‰ (Figure 4.5 and Table 4.4). Wooded grassland is the most prevalent vegetation cover category (n=4), followed by woodland/bushland/shrubland (n=3), and the grassland category (n=2). There is no evidence for the forested vegetation cover during this time interval. The f_{wc} estimates average 0.29 and range from 0.56 to 0.02, while paleo-NDVI estimates average 0.32 and range from 0.66 to 0.08. These results indicate that the landscape during this time interval represented a mixture of wooded grasslands, woodlands, and open grasslands.

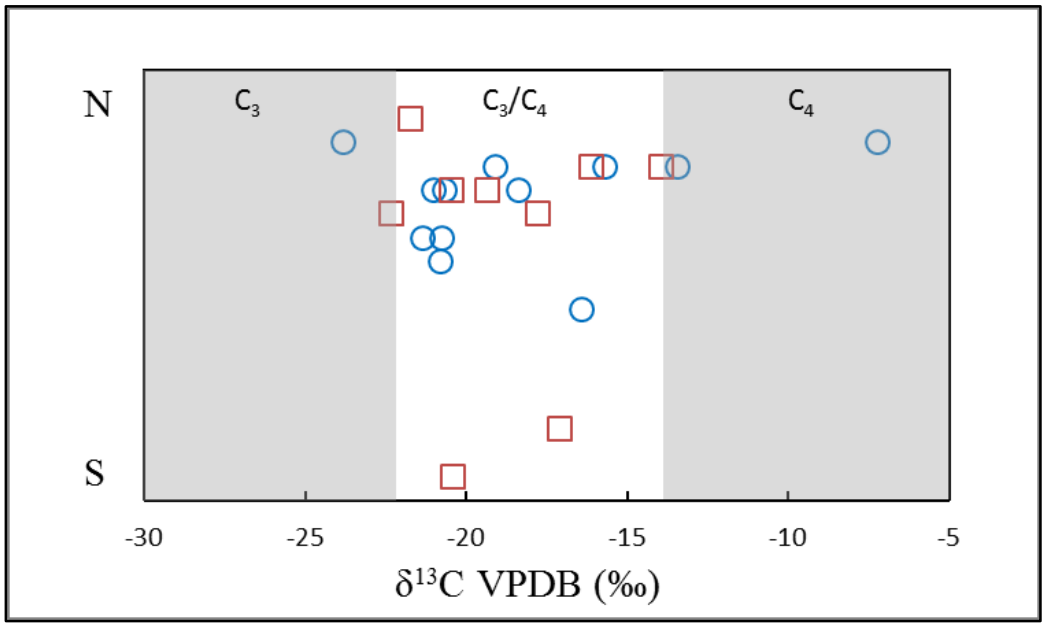

Figure 4.5: Individual $\delta^{13}C_{SOM}$ values from Time Interval 1 (blue circles) and Time Interval 2 (red squares), displayed against x-axis ($\delta^{13}C$ - VPDB‰) and the y-axis (Geographically North to South in the Kapthurin Formation). Samples are displayed with reference to assumed vegetation cover ranges (C_3, C_3/C_4, and C_4) after Cerling, Wynn, et al. (2011).

Sample	$\delta^{13}C_{SOM}$	f_{wc}	NDVI	Site	Time Interval
DL-1-12-2	-21.0	0.44	0.47	Loc. 3	1 (543-509 ka)
DL-2-12-2	-15.7	0.07	0.12	Loc. 3	1 (543-509 ka)
DL-3-12-2	-18.4	0.23	0.24	Below GT	1 (543-509 ka)
DL-4-12-2	-20.7	0.41	0.43	Loc. 3	1 (543-509 ka)
DL-5-12-2	-13.4	0.01	0.07	Below GT	1 (543-509 ka)
DL-7-12-2	-7.2	0.19	0.01	EKG	1 (543-509 ka)
DL-9-12-2	-21.4	0.47	0.51	BKS	1 (543-509 ka)
DL-10-12-2	-20.8	0.42	0.44	JKS	1 (543-509 ka)
DL-11-12-2	-16.4	0.11	0.15	GnJh-23	1 (543-509 ka)
DL-15-12-2	-19.1	0.29	0.29	Below GT	1 (543-509 ka)
DL-20-12-2	-20.8	0.42	0.44	GnJh-27	1 (543-509 ka)
DL-21-12-2	-23.8	0.68	0.96	Loc. 99	1 (543-509 ka)
DL-6-12-2	-21.7	0.50	0.56	GnJh-15	2 (509-380 ka)
DL-8-12-2	-14.0	0.02	0.08	Loc. 3	2 (509-380 ka)
DL-12-12-2	-22.4	0.56	0.66	Loc. 17	2 (509-380 ka)
DL-13-12-2	-17.8	0.19	0.21	Loc. 17	2 (509-380 ka)
DL-14-12-2	-17.1	0.15	0.17	GnJh-17	2 (509-380 ka)
DL-16-12-2	-20.4	0.39	0.40	Loc. 307	2 (509-380 ka)
DL-17-12-2	-19.3	0.30	0.31	Below K4	2 (509-380 ka)
DL-18-12-2	-16.1	0.09	0.14	LHA	2 (509-380 ka)
DL-19-12-2	-20.5	0.40	0.41	Below K4	2 (509-380 ka)

Table 4.4: Stable carbon isotope values from SOM samples derived from paleosols (measured in ‰). Fraction Woody Cover (f_{wc}) and paleo-NDVI values are also displayed. Below GT and K4 refers to samples collected from paleosols stratigraphically below the Grey Tuff and Bedded Tuff (K4).

4.5.2 Oxygen composition of soil oxygen

Large nodule pedogenic carbonate $\delta^{18}O_{PC}$ values from Time Interval 1 average -4.5 ± 1.7‰ and range from -8.6 to -0.4‰, indicating a large range of oxygen values (Figure 4.3 and Table 4.2). The most negative $\delta^{18}O_{PC}$ values are the best estimates of meteoric water $\delta^{18}O$ values because they represent carbonate formation that records the least amount of soil and surface evaporation. Sample DL-10-2011 represents the lowest average oxygen isotope value (-8.6‰);

these samples were taken from a pedogenic carbonate collected from a paleosol adjacent to the Chemichemi Tufa (Johnson, et al. 2009), recording a perennially active stream situated near lake margins and fed by increased ground water inputs, likely due to increased monsoonal activity (Leslie, et al. 2016). Pedogenic carbonate nodules sampled for $\delta^{18}O_{PC}$ values from Time Interval 2 average -3.5 ± 0.5‰ and range from -4.0 to -2.3‰ (Figure 4.3 and Table 4.2). Sample DL-14-2012 represents the most negative average value during this time interval (-4.0‰); these samples were taken from a paleosol preserved at the archaeological site GnJh-17.

Paleosol carbonate samples from both time intervals mirror the results from large nodules sampled; $\delta^{18}O_{SC}$ values from Time Interval 1 average -5.0 ± 1.3‰ and range from -7.7 to -3.0, while $\delta^{18}O_{SC}$ values from Time Interval 2 average -4.4 ± 1.2‰ and range from -6.3 to -2.1‰ (Figure 4.4 and Table 4.3). Sample DL-21-2012-1 represents the most negative $\delta^{18}O_{SC}$ value from Time Interval 1 at -7.7‰ and was derived from a paleosol sampled from Loc. 99, the fossil chimpanzee locality; sample DL-18-2012-1 represents the most negative $\delta^{18}O_{SC}$ value from Target Interval 2 at -6.3‰ and was sampled from a paleosol at the archaeological site LHA.

Given that the large nodules of pedogenic carbonate represent longer periods of carbonate formation, the average oxygen isotope records may better represent general aridity conditions, while the paleosol carbonates represent shorter periods of aridity within these two time intervals. There is clearly a difference in average oxygen isotope values from pedogenic carbonate nodules among Time Interval 1 (-4.5‰), Time Interval 2 (-3.5‰) and the average $\delta^{18}O$ (VSMOW) value of meteoric water in Kenya today (Levin, et al. 2009), and given that pedogenic carbonates form in equilibrium with soil CO_2 and soil water, $\delta^{18}O$ values of soil carbonates can be compared directly to meteoric water (VSMOW) (Breecker, et al. 2009). The minimum $\delta^{18}O_{PC}$ values from Time Intervals 1 (-8.6‰) and 2 (-4.0‰) can also be compared with the average $\delta^{18}O$ (VSMOW)

values of the bodies of water and modern soil carbonate values in the Baringo Basin today; Lake Baringo has an average value of +6.6‰ and the Molo River has an average value of -2.9‰ (Levin, et al. 2009), while modern soil carbonates in the Baringo Basin average -3.3‰. Meteoric water estimates from Time Interval 1 suggest a difference of -5.7‰ from the modern Molo River, while Time Interval 2 estimates for meteoric water have a difference of -1.1‰ from the Molo River. These differences in Time Intervals 1 and 2 may represent lower meteoric water values, which are driven by lower water source values from the Indian Ocean (Niedermeyer, et al. (2014), possible shifts in aridity, or differences in soil temperatures during both time intervals, although carbonate values from Time Interval 2 are within the range of modern soil carbonate oxygen values. The overall $\delta^{18}O_{PC}$ values of large nodules likely suggests that Time Interval 1 was characterized by periods of increased rainfall and decreased soil evaporation, due to an intense monsoonal episode (Leslie, et al. 2016). Comparatively, $\delta^{18}O_{PC}$ values of large nodules from Time Interval 2 are more similar to meteoric water oxygen values in Kenya and from the Baringo Basin today, indicating a period of increased aridity when compared with Time Interval 1, but somewhat milder than arid conditions in the region today.

4.6 Discussion

4.6.1 Paleoenvironmental Implications

Three types of data were used to reconstruct paleoenvironments with each representing different scales of time averaging. Large pedogenic carbonate nodules preserve the longest paleoenvironmental records, forming over 10^2 to 10^5 years (Jenny 1980). Small pedogenic carbonate nodules (less than 0.5 cm in diameter) preserved in paleosols represent an intermediate formation time, they too can form over long periods of time, but given their small size, probably

represent between 10^2 and 10^3 years (Jenny 1980). Bulk soil organic matter from paleosols represents the shortest window of time, capturing approximately the last few decades of active soil formation and organic remodeling before the soils become transformed into geologic records as paleosols (Cerling, et al. 1989). Given these three scales of time averaging, it is best to discuss the implications of each record for landscape reconstructions, as they all capture different paleosurface vegetation and water availability records. It is also important to note that each individual sampling location is likely time averaged within the larger two time intervals under study. This time averaging is unavoidable, given the sedimentology of the deposits, tectonic and erosional history of the Lake Baringo Basin, and modern geomorphology of East Africa (Martyn 1969; Tallon 1976). With such limitations in mind, these paleoenvironmental data will be used to reconstruct the general ecological setting of the Lake Baringo Basin during Time Intervals 1 (543 – 509 ka) and 2 (509 – 380 ka).

4.6.2 Time Interval 1

Paleoenvironmental data from Time Interval 1 indicates that a diverse range of habitats would have been available to hominins, including pockets of woodlands, and more common wooded grasslands and open grasslands. Furthermore, oxygen isotope data from this time interval suggests a water budget influenced by an intense monsoonal episode that provided regular inputs of water in the form of a perennially active stream; previous calculations of the aridity index (Levin, et al. 2006) by Leslie, et al. (2016), based on oxygen isotope values derived from bovid teeth from this time interval, predict a water deficit of 143 mm that is most similar to the water deficit of the modern Ituri Rainforest, -90 mm. This intense monsoonal episode would have provided hominins with hyper mesic environments, ranging from woodlands, wooded

grasslands, open grasslands, and sumplands, and may have acted as an attractor to other important resources, such as large herbivores dependent on water resources. Given this broad range of habitats, hominins appear to prefer open grasslands and wooded grasslands, based on the presence of archaeological and paleontological material at significant sites preserved during Time Interval 1.

At the site of EKG, where a hominin mandible was surface collected, attributed to *Homo erectus*, and associated surface artifacts (one "bifacial core pick tool") (Leakey, et al. 1969), the main vegetation signatures are characterized by open grasslands ($\delta^{13}C_{SOM}$ = -7.2‰) and wooded grasslands ($\delta^{13}C_{PC}$ = -5.6‰ and $\delta^{13}C_{SC}$ = -5.5‰). The oxygen isotope values from pedogenic carbonates at EKG indicate a somewhat mesic environment ($\delta^{18}O_{PC}$ = -4.1‰ and -2.9‰), in line with the overall wetter conditions for this time interval. The occupation of GnJh-42, a site characterized by the early appearance of blade technology (Johnson and McBrearty 2010), coincides with open grassland vegetation cover ($\delta^{13}C_{PC}$ = -1.5‰ and -1.6‰), and very mesic conditions ($\delta^{18}O_{PC}$ = -8.6‰ and -7.7‰) near the margins of a perennially active stream (Johnson, et al. 2009). Both EKG and GnJh-42 are associated with vegetation that have low NDVI (EKG = 0.32 – 0.01, GnJh-42 = 0.12) and f_{wc} estimates (EKG = 0.32 – 0.19, GnJh-42 = 0.07), indicating the exploitation of animals or vegetation associated with open grassland and wooded grassland landscapes. These lower NDVI and f_{wc} environments may have been productive for hominins, given that non-woody vegetation is more readily available as a food source to herbivores (Pettorelli, et al. 2009), and these herbivores, coupled with moderate NDVI and woody cover landscapes and the overall mesic conditions, would have provided hominins with the most resource-rich environments to exploit.

Sites GnJh-42 and EKG can be contrasted with the site of Loc. 99, the fossil chimpanzee locality. Loc. 99 represents the most wooded site sampled from Time Interval 1, displaying the most negative carbon isotope values from large pedogenic carbonates ($\delta^{13}C_{PC}$ = -9.6‰), carbonates from paleosols ($\delta^{13}C_{SC}$ = -9.4‰), and SOM from paleosols ($\delta^{13}C_{SOM}$ = -23.8‰). The oxygen isotope results also indicate a mesic environment, particularly the carbonates from paleosols ($\delta^{18}O_{SC}$ = -7.7‰), this is in keeping with environmental reconstructions by McBrearty and Jablonski (2005) for this site based on faunal assemblages, suggesting a locally wooded habitat with surrounding marshes on the shores of a paleo-Lake Baringo. The NDVI (0.86 – 0.96) and f_{wc} estimates (0.64 – 0.68) for Loc. 99 vary dramatically from the hominin exploitation sites during this time interval, indicating exploitation of landscapes rich in ligneous vegetation, similar to habitat ranges of most chimpanzee populations today.

4.6.3 Time Interval 2

Paleoenvironmental data from Time Interval 2 again indicate that a diverse range of habitats were available to hominins; the wooded grassland category is the most prevalent type of vegetation cover and there are significant grassland and woodland/bushland/shrubland components to this landscape. Oxygen isotope data indicates more xeric conditions when compared with Time Interval 1, although possibly slightly wetter than modern local conditions in the Baringo Basin. Hominins during this time interval appear to have preferred mostly wooded grassland environments, although there is some evidence for open grassland and woodland occupations.

At the site of LHA, where handaxes, blades, and unifacial handaxes made on Levallois flakes have been collected and excavated (Leakey, et al. 1969; McBrearty 1999), the local

vegetation is characterized by a mixture of signatures; large pedogenic carbonates indicate wooded grasslands ($\delta^{13}C_{PC}$ = -5.8‰), carbonates from paleosols indicate woodland/bushland/shrubland vegetation ($\delta^{13}C_{SC}$ = -9.4‰), and SOM from paleosols indicates grassland vegetation ($\delta^{13}C_{SOM}$ = -16.1‰). Similarly, the f_{wc} and paleo-NDVI ranges vary from low values from SOM (f_{wc} = 0.09, NDVI = 0.14), to moderate values from large pedogenic carbonate nodules (f_{wc} = 0.34, NDVI = 0.35), and higher values from paleosol smaller carbonates (f_{wc} = 0.65, NDVI = 0.86). Given the longer record of the large pedogenic carbonate nodules, and the average signal preserved between the SOM and carbonates from paleosols, the wooded grassland vegetation appears to be the best representation of vegetation cover at this site. Oxygen isotope values from large pedogenic carbonates indicate an environment slightly wetter than the region today ($\delta^{18}O_{PC}$ = -3.6‰)

At the site of GnJh-17, where handaxes, picks, and MSA points have been excavated (Cornelissen 1992; McBrearty 1999), the local vegetation is characterized by a mixture of woodland and wooded grassland cover; large pedogenic carbonate nodules indicate a wooded grassland vegetation cover ($\delta^{13}C_{PC}$ = -6.2‰), carbonates from paleosols indicate a woodland vegetation signature ($\delta^{13}C_{SC}$ = -8.0‰), and SOM from paleosols accord with wooded grassland vegetation ($\delta^{13}C_{SOM}$ = -17.1‰). The f_{wc} and paleo-NDVI ranges from GnJh-17 vary from lower values derived from SOM (f_{wc} = 0.15, NDVI = 0.17), to intermediate values derived from large pedogenic carbonate nodules (f_{wc} = 0.37, NDVI = 0.38), to higher values derived from small carbonates in paleosols (f_{wc} = 0.53, NDVI = 0.61). Accounting for the longer period of formation preserved in the large pedogenic carbonate record, and the similarity to the SOM record, the wooded grassland vegetation structure is the most likely vegetation cover at this site. Oxygen isotope values range from -4.0‰ ($\delta^{13}C_{PC}$) to -4.9‰ ($\delta^{13}C_{SC}$), indicating an environment

that was locally wetter than most other sampling locations during Time Interval 2 (Tables 4.2 and 4.3), possibly indicating closer proximity to standing or running water, as predicted by the interstratified alluvial sediments found at the site (Cornelissen 1992).

At the site of GnJh-15, where bifaces made on cobbles, large quantities of red ochre, and grindstones have been excavated (McBrearty 1999; Van Noten, Cornelissen, Gysels, Moeyersons, Nijs, et al. 1987; Van Noten, Cornelissen, Gysels, Moeyersons and Uytterschaut 1987), the local vegetation can be reconstructed as a mixture of woodland and wooded grassland cover types; large carbonate nodule averages indicate wooded grassland vegetation cover ($\delta^{13}C_{PC}$ = -3.3‰), small carbonates from paleosols also indicate wooded grassland vegetation ($\delta^{13}C_{SC}$ = -4.8‰), and SOM from paleosols indicates woodland vegetation cover ($\delta^{13}C_{SOM}$ = -21.7‰). The f_{wc} and paleo-NDVI ranges from GnJh-17 similarly range from lower values derived from the large pedogenic carbonate record (f_{wc} = 0.16, NDVI = 0.18), low values derived from the soil carbonates in paleosol record (f_{wc} = 0.26, NDVI = 0.27), and moderate values derived from the SOM record (f_{wc} = 0.50, NDVI = 0.56). Contrasting these three lines of data, there is more evidence for the wooded grassland vegetation cover at GnJh-15. Oxygen values from GnJh-15 range from -3.7 ‰ ($\delta^{13}C_{PC}$) to -4.0‰ ($\delta^{13}C_{SC}$), indicating an average availability of meteoric water based on oxygen isotope data from this time interval (Tables 4.2 and 4.3).

4.7 Conclusions

Environmental reconstructions from Time Interval 1 (543 – 509 ka) based on pedogenic carbonates, carbonates from paleosols, SOM from paleosols indicate a landscape with a diverse range of local habitats, including woodlands, wooded grasslands, and open grasslands, coupled with a perennially active stream that was likely fed by an intensified monsoonal episode (Leslie,

et al. 2016). Given these ranges of habitats, hominins exploited local environments characterized by grassland and wooded grassland cover, consistent with lower paleo-NDVI and f_{wc} estimates. At the site of GnJh-42, the hominin occupation is also associated with the production of blade technology and very mesic conditions near a perennially active stream (Johnson and McBrearty 2010, 2012). Hominins at the site of EKG also preferred local environments characterized by wooded grassland and grassland traces, while hominins at the site of GnJh-42 preferred open grassland signatures. Given these results, it appears that hominins chose to exploit habitats with open grassland and wooded grassland vegetation, probably due to the associated herbivorous mammals with these low NDVI environments. Comparatively, chimpanzees occupied the habitat with the densest vegetation cover for this time interval at Loc. 99, indicated by the consistent woodland reconstructions from all three lines of data and the associated higher paleo-NDVI and f_{wc} estimates. The local habitat at Loc. 99 represents a similar environment to extant chimpanzee populations, while most populations are restricted to rainforests, smaller populations live within woodland and wooded grassland ecosystems (Kormos, et al. 2003). These different ecological reconstructions indicate that *Homo* and *Pan* were periodically sympatric species during the Middle Pleistocene in the Kapthurin Formation, which has implications for the environmental backdrop of the initial divergences between the hominin and hominid lineages (McBrearty and Jablonski 2005).

Environmental reconstructions from Time Interval 2 (509 – 380 ka) based on three types of data, pedogenic carbonate nodules, smaller pedogenic carbonates from paleosols, and SOM from paleosols, indicate a landscape that was somewhat wetter than the extant Lake Baringo Basin and was dominated by wooded grasslands, with significant grassland and woodland components. With these ranges of environments, hominins exploited sites with significant

wooded grassland components, indicating a preference for this type of vegetation cover during this time interval. At the site of GnJh-17, excavated *in situ* handaxes, picks, and points (Cornelissen 1992; McBrearty 1999) are associated with predominant wooded grassland vegetation cover and slightly wetter conditions than the average for this time interval. Environmental reconstructions from the site of GnJh-15, where bifaces made on cobles, large quantities of red ochre, and grindstones were excavated (McBrearty 1999; Van Noten, Cornelissen, Gysels, Moeyersons, Nijs, et al. 1987; Van Noten, Cornelissen, Gysels, Moeyersons and Uytterschaut 1987)indicate a local environment characterized by wooded grassland vegetation cover, with an average amount of available meteoric water for this time interval. At the site of LHA, where handaxes, unifacial handaxes made on Levallois flakes, and blades have been collected and excavated (Leakey, et al. 1969; McBrearty 1999), the local environment is characterized by wooded grasslands with an average amount of meteoric water available to this site based on oxygen isotope data from this time interval. Given these reconstructions, it does not appear that hominins during Time Interval 2 utilize different types of technology to exploit different environments. Rather, it appears that hominins during Time Interval 2 consistently exploited sites with wooded grassland vegetation cover. This may be expected, given that the wooded grassland environment was the most prevalent vegetation cover for the landscape reconstructed from Time Interval 2, but significant components of open grassland and woodland areas were also reconstructed and do not contain archaeological traces.

A number of possibilities exist for the preference of wooded grassland environments, one is that, like in Time Interval 1, wooded grasslands provide hominins with low to intermediate primary biomass productivity, but are associated with very high amounts of secondary biomass productivity in the form of herbivorous mammals. Wooded grasslands also provide some cover

for hominins to ambush their prey, depending on the type of hunting technology in use (points or wooden implements) (Faith 2008; Wilkins, et al. 2012). Wooded grasslands in East Africa today are excellent sources for water, ligneous vegetation is more expensive to grow than xeric adapted grasses, and are correlated with water availability (Bell 1982). Modern woodland and wooded grassland environments in East Africa are associated with high NDVI values, which are primarily a response to increased rainfall and increased forest vegetation cover (Davenport and Nicholson 1993; Nicholson, et al. 1990). Woodlands also provide fruits and other vegetable food sources that would have been important for hominin diets, and are commonly exploited by modern foragers in East Africa (Marlowe 2010; Vincent 1985). Wooded grasslands also provide modern foragers with a prized resource, honey, which would presumably have been important for Middle Pleistocene hominin's dietary sugar and fat intake (Crittenden 2011; Murray, et al. 2001). Wooded grasslands could have also provided cover from carnivores, this would have been an important feature of the landscape in the Baringo Basin, due to the absence of more traditional shelters such a rock shelters and caves; shelter from carnivores would have been important during the Early to Middle Pleistocene, as indicated by the carnivore damage to hominin remains of *H. erectus* and *H. heidelbergensis* (Dennell 2005; Sala, et al. 2014; Tappen 1987; Treves and Palmqvist 2007). Wooded grasslands also provide hominins with a key resource, wooded vegetation, which can be shaped into other tools, such as spears for hunting or scavenging large mammals, behaviors that have become well established by Time Intervals 1 and 2 (Klein 1988; John J. Shea 1993; Thieme 1997; Wilkins, et al. 2012). Wooded grasslands also provide hominins cover from mid-day solar radiation, open grassland and deserts are associated with increased soil reflectance of solar radiation, this leads to increased temperatures when

compared with woodland environments and is reflected in the clumped isotope paleothermometry of pedogenic carbonates (Cerling, Mace, et al. 2015; Passey, et al. 2010).

Hominins during Time Interval 2 may have chosen to exploit wooded grasslands because these environments offered them a more efficient means of extracting important foraging resources, due to the close proximity of resource to the wooded grassland ecotone, or the cover wooded areas provided hominins for a number of activities. Assuming that these foraging resources follow similar distributions patterns to modern environments and forager choices (Marlowe 2010), the choice of wooded grasslands as sites for exploitation would satisfy several optimal foraging assumptions: minimal energy expenditure, maximum energy returns, and foraging trip distance minimization (Hill, et al. 1987; Marlowe 2005; Winterhalder 1981). Several researchers have suggested that Middle Stone Age foragers began to exploit resources from the wooded grassland ecotone because it provided them with more efficient foraging opportunities than woodland or grassland environments (Ambrose 2001a; Basell 2008; Clark 1988). This research provides the first evidence from high-resolution environmental and landscape data that Middle Pleistocene hominins using Acheulean and Middle Stone Age technology choose to exploit wooded grassland environments, even though other environments were clearly available for exploitation. The early shift to wooded grassland environments during Time Interval 1 is interesting, and bears further consideration. It may be that the shift to wooded grassland environments occurs prior to the shift to Middle Stone Age technology; these resource-rich environments may have provided hominins with a range of resources to exploit, leading to technological innovations (Johnson and McBrearty 2012).

Shifts in environments have been cited as stimuli for technological and biological changes among hominins (Ambrose 1998; Bräuer 2008; deMenocal 2011; Potts 1998; Vrba

1993). Researchers have long noted the general cooling trend during the Pliocene that continues into the Pleistocene, which resulted in an increase in open grassland vegetation coverage and a decrease in meteoric water availability in East Africa (Bobe and Behrensmeyer 2004; Coppens 1975; deMenocal 2004). Isotopic data derived from pedogenic carbonates and SOM from the Kapthurin Formation, indicates that contra to regional expectations, the Lake Baringo Basin records ranges of local vegetative environments and meteoric water availability that may have buffered hominins and chimpanzee populations against larger scale orbital forcing (Behrensmeyer 2006). The presence of an intensified monsoonal system during Time Interval 1 (Leslie, et al. 2016), likely driven by orbital forcing, is clear evidence that this region was not immune to global insolation events, and that indeed these events may have served as attractors for hominins, given the diverse range of habitats produced by the monsoonal episode. The stable isotope results presented here also accord with previous research by Kingston, et al. (1994), who found a range of habitats throughout the Tugen Hills succession, with no clear aridification pattern, contra to the Lake Turkana Basin isotopic record (Cerling, Levin, et al. 2011; Wynn 2004).

Chapter 5: Environmental and Behavioral Variability Traces in the Kapthurin Formation, Kenya

5.1 Introduction

High resolution landscape environmental reconstructions of Middle Pleistocene sediments in East Africa offer valuable information about the diversity of resources that were available to hominins. The Middle Pleistocene is a critical period of human evolution, it marks the transition from Acheulean to Middle Stone Age (MSA) technology and documents the emergence of our own species, *Homo sapiens*, at approximately 195 thousand years ago (ka) (McDougall, et al. 2008). The Kapthurin Formation, Kenya, preserves evidence of Acheulean and Middle Stone Age technology that is interstratified and dated to between 543 and 235 ka (Blegen 2015; Deino and McBrearty 2002; Christian A. Tryon and Sally McBrearty 2002). Global changes to climate, driven by changes in solar insolation, have been hypothesized to affect regional environments, and the evolution and technological choices of hominins (Bräuer 2008; deMenocal 2011; Potts 1996; Potts and Faith 2015; Vrba 1993). Fine-grained environmental reconstructions presented in Chapter 3 indicate that while the regional environments of the Lake Baringo Basin were affected by solar insolation and cycles of monsoon activity (Leslie, et al. 2016), hominin site choice remained fairly consistent in two separate time intervals (Time Interval 1: 543 – 509 ka; Time Interval 2: 509 – 380 ka) and did not differ based on the types of technology preserved at sites; hominin occupation sites mainly preserved evidence of wooded grassland ecosystems, although other environments were available to hominins. Further exploration of these paleolandscapes, the micro-environments preserved in the Kapthurin Formation, and the behavioral plasticity of hominins is warranted.

Theoretical approaches to frame the foraging behaviors of Acheulean and MSA hominins are constrained by the types of data that are recovered from archaeological sites. Foraging behavior during the Middle Pleistocene has been interpreted using multiple lines of evidence, including lithic assemblages, associated faunal remains, raw material transport (mobility), and site choice (Ambrose 2001b; Assefa 2006; J D Clark 2001; Clark, et al. 2003; Marean 1992; McBrearty and Brooks 2000; Tryon and Faith 2013). Optimal foraging theory offers a powerful framework to interpret these varying lines of evidence, with the assumptions that foragers in the past would employ strategies that minimized energy expenditure and foraging trip distance, while maximizing energy returns (Faith 2008; Hill, et al. 1987; Winterhalder 1981). In this paper, I apply a behavioral ecological approach to frame the site choice of hominins associated with Acheulean and MSA technology. Given the preserved evidence of site choice by hominins in two main time intervals of the Kapthurin Formation and associated lithic technology, the main research question of this paper is: is there any noticeable shift toward optimal foraging behavior associated with MSA sites, assessed through site choice?

5.2 Background

5.2.1 Kapthurin Formation

The Kapthurin Formation, located to the west of Lake Baringo, is a part of the Middle Pleistocene sedimentary sequence of the Tugen Hills Succession in the Kenyan Rift Valley (Figure 5.1). The formation consists of interstratified lacustrine, alluvial, and volcanic sediments, is exposed over an area of approximately 150 km^2, and has an observed thickness estimated at 125 meters (Figure 5.2) (Martyn 1969; Tallon 1976; Christian A. Tryon and Sally McBrearty 2002). The formation is subdivided into five members (K1 – K5) (Martyn 1969), and

has been dated using the $^{40}Ar/^{39}Ar$ method (Blegen 2015; Deino and McBrearty 2002; Dunkley, et al. 1993) (Figure 5.2). K1, K3, and K5 are members informally named the Lower, Middle, and Upper Silts and Gravels, and are composed of terrigenous sediments eroded from the Tugen Hills. Pyroclastic members K2 and K4 intercalate the Silts and Gravels members; K2, the Pumice Tuff, is dated to 543 ± 3 ka; K4, the Bedded Tuff, preserves separate eruptive facies dated to 380 ± 7 ka, 284 ± 12 ka, and 235 ± 2 ka. The basal date of K4 was recently refined through tephrostratigraphic correlation to the Korosi Airfall Pumiceous Tuff (Blegen 2015) and dated by Dunkley, et al. (1993) using the $^{40}Ar/^{39}Ar$ method.

K3 sediments preserve the archaeological sites discussed in this text, is subdivided by the Grey Tuff, dated to 509 ± 9 ka, by alluvial facies to the west (referred to as K3), and by lacustrine facies to the east (referred to as K3'). The sediments of K3 consist of unstratified silts and pebble beds, marked by massive conglomerates in the western and southern extents of the formation, and occasional soil formation, mainly below K4 and the Grey Tuff (Tallon 1976). The sediments of K3' are composed of red, black, and green claystones and siltstones; the geochemical and sedimentary structures of these deposits indicate deposition in a shallow lake that alternated between freshwater and saline-alkaline (Johnson and McBrearty 2012; Renaut, et al. 1999; Tallon 1978).

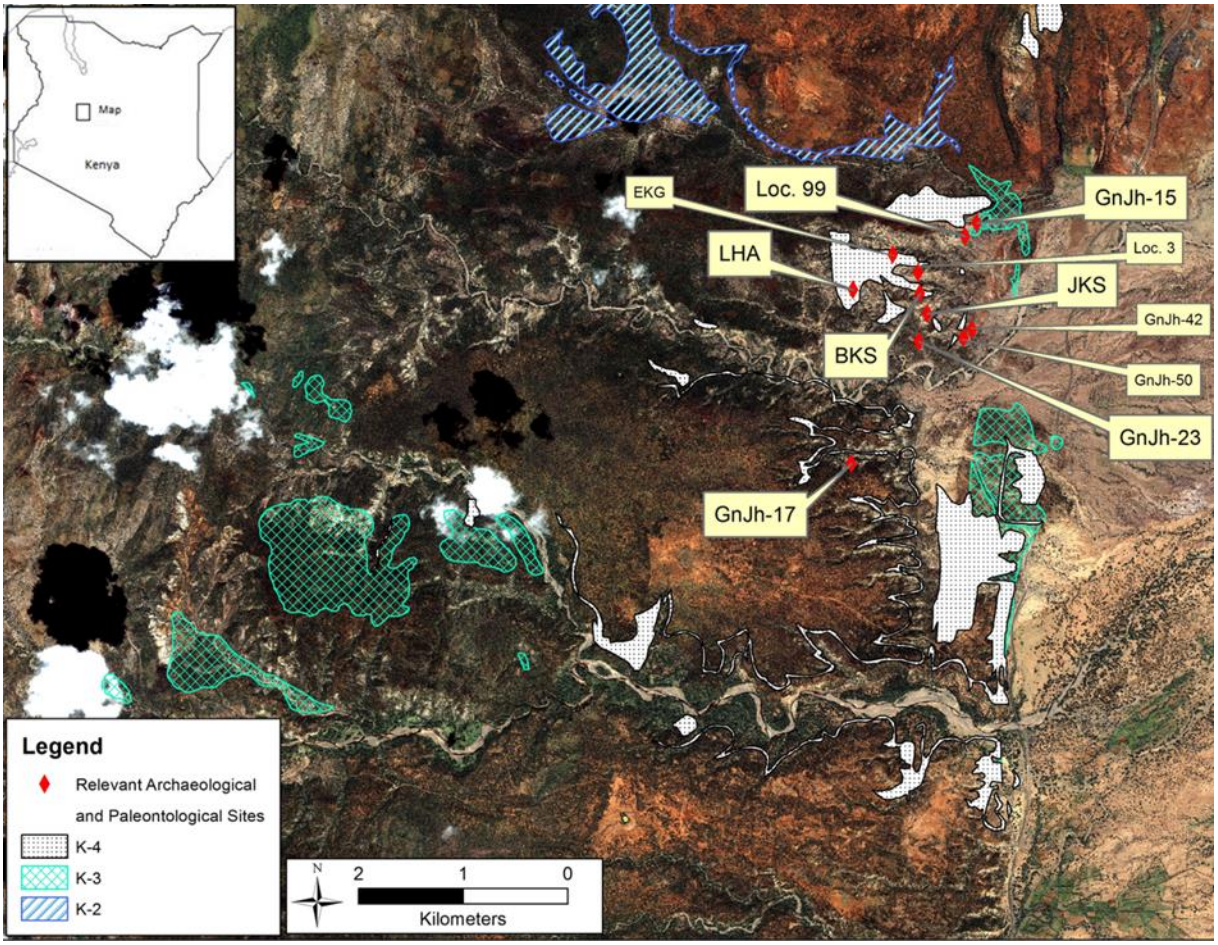

Figure 5.1: Satellite image (IKONOS, 1.8 m resolution) displaying relevant geologic exposures and archaeological and paleontological sites preserved in the Kapthurin Formation. Inset not to scale.

The Kapthurin Formation lies unconformably above the Chemeron Formation, and is underlain by the Ndau Trachymugearite, dated to 1.57 million years ago (Ma), using the K-Ar technique (Hill, et al. 1986), providing a maximum age for the Kapthurin Formation sediments. All of the sediments in the Kapthurin Formation are normally magnetized (Dagley, et al. 1978), postdating the Matuyama-Brunhes Boundary, currently estimated at 775 ka using the $^{40}Ar/^{39}Ar$ method (Coe, et al. 2004). This boundary provides a more accurate estimate for the maximum age of the Kapthurin Formation.

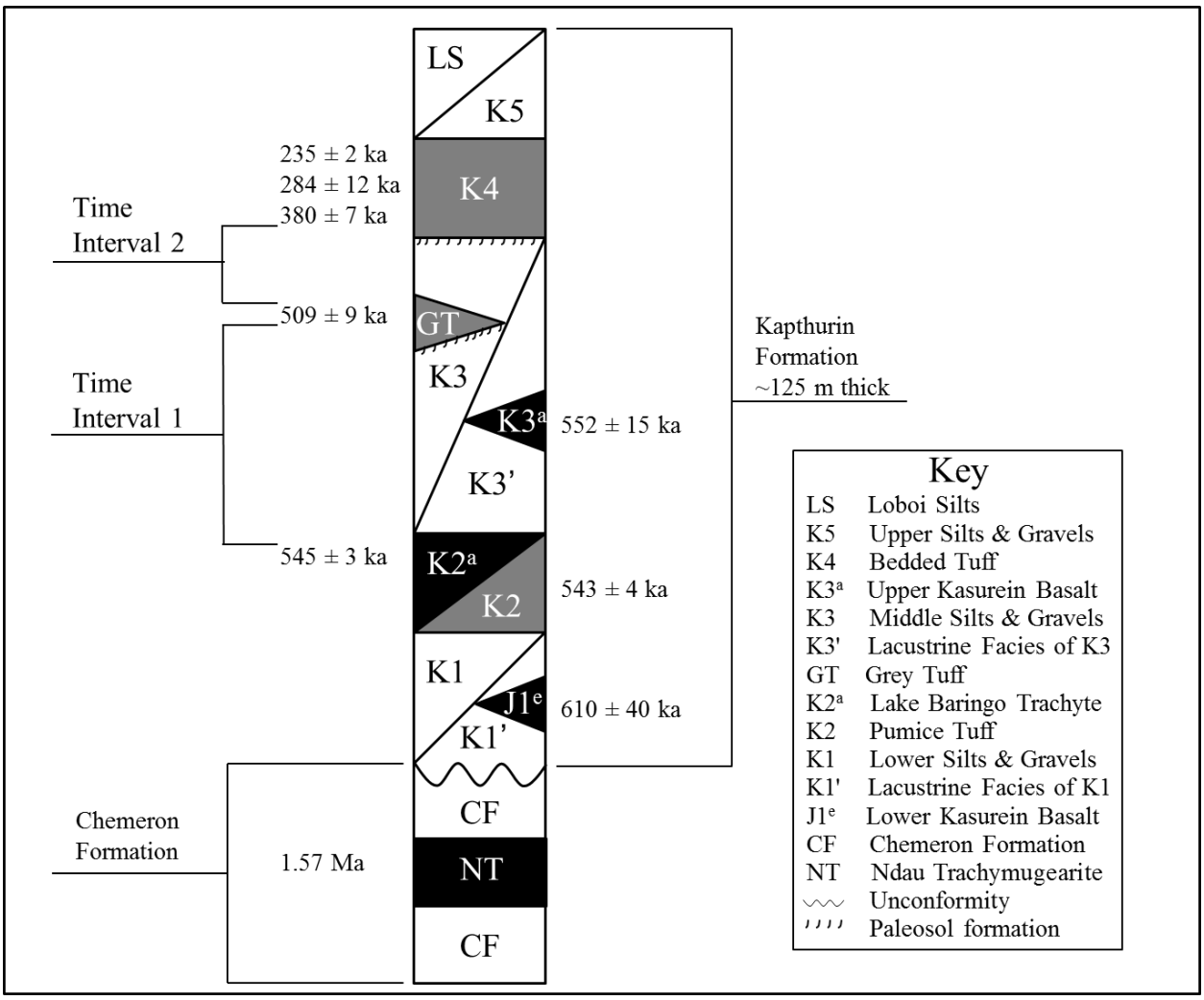

Figure 5.2: Generalized stratigraphic section of the Kapthurin Formation. Section is after Deino and McBrearty (2002) and Tallon (1978). Shaded areas represent pyroclastic sediments while light areas represent fluviolacustrine sediments.

This research is centered on two time intervals preserved within the K3 member of the Kapthurin Formation: Time Interval 1 (543 – 509 ka) represents archaeological and paleontological sites deposited above K2 and below the Grey tuff (Figure 5.2), although most sites and landscape sampling locations are located closer stratigraphically to the Grey Tuff; Time Interval 2 (509 – 380 ka) is marked by archaeological and paleontological sites stratigraphically

located above the Grey Tuff and below the base of K4, although most sites and landscape sampling locations are located below the base of K4.

McBrearty (1999) has reconstructed environments within Time Interval 1, based on taxonomic identifications of fauna, and suggested that forest and marsh depositional conditions were dominate, and were fed by a braided river system that drained the Tugen Hills and supported surrounding grassland ecosystems. Tallon (1978) has also reconstructed braided river systems during Time Intervals 1 and 2, citing paleochannel formation below and above the Grey Tuff. Johnson, et al. (2009) described a semi-continuous tufa in the southern exposures of the lacustrine facies of the Kapthurin Formation, which demonstrate a perennially active stream and associated rich wetland habitat during Time Interval 1. McBrearty and Jablonski (2005) recorded chimpanzee fossils at Locality 99 (Loc. 99) in fluviolacustrine sediments which, when taken with other fauna documented at the site (hippopotamus, crocodile, catfish, colobine monkey, and bushpig) indicate a locally wooded environment with marshes, near the shores of an alternating freshwater and alkaline lake. Hominin fossils have also been documented during Time Interval 1 and identified to *Homo sp.* and *Homo erectus* (Leakey, et al. 1969; Wood and Van Noten 1986) at the sites of EKG and MAS, in the K3 alluvial facies, close to Loc. 99 (<1 km). Leslie, et al. (2016) reconstructed habitats in Time Interval 1 using carbon and oxygen isotope ratios derived from herbivorous mammalian tooth enamel and pedogenic carbonates; the results of this analysis suggest that the Lake Baringo Basin was dominated by hyper mesic conditions, driven by an intense monsoonal episode that resulted in woodland, marsh, and sumpland habitats, perennially active streams, and a surrounding grassland ecosystem. Further landscape reconstructions from Chapters 2 and 3, based on carbon and oxygen stable isotope ratios derived from pedogenic carbonates and bulk soil organic matter, paleo-NDVI values, and

fraction woody cover values (Cerling, Wynn, et al. 2011), corroborate this very wet time interval, and reveal a complicated distribution of microenvironments, that range among woodland, wooded grassland, and open grassland environments, providing hominins with a range of habitats to exploit.

Environmental reconstructions for Time Interval 2 are more difficult, due to poor faunal preservation. The deposition of K3 sediments remained relatively uniform, as seasonal rivers continued to drain the Tugen Hills, which resulted in alluvial fan depositions on the margins of a paleo lake (Tallon 1976). Scott (2005) reconstructed the environment at Rorop Lingop, a footprint site preserved in the Bedded Tuff Member (K4); these footprints preserve a high diversity of vertebrate trace fossils. Scott (2005) suggests that the site was situated on an alluvial plain near the shores of a freshwater lake, indicative of a species rich environment. The deposition of Rorop Lingop postdates Time Interval 2, but provides a framework for the species communities that may have interacted with previous iterations of the paleo Lake Baringo. Kingston, et al. (1994) and Cornelissen, et al. (1990) used stable isotope ratios of carbon and oxygen derived from pedogenic carbonates to reconstruct paleoenvironments during Time Interval 2, although only two sites (GnJh-15 and GnJh-17) were sampled. Kingston, et al. (1994) report carbon values that suggest a locally mixed grassland and forested environment at GnJh-15, while Cornelissen, et al. (1990) suggest an arid grassland environment at GnJh-17 based on measured carbon and oxygen isotope values. In Chapters 2, 3, and 4 landscape reconstructions based on carbon and oxygen isotope values derived from pedogenic carbonates and bulk soil organic matter, as well as paleo-NDVI values and fraction woody cover values (Cerling, Wynn, et al. 2011), indicate that wooded grasslands dominated the vegetation cover during this time

interval, with significant open grassland and woodland components; this time interval was wetter than present conditions in the Lake Baringo Basin, although more xeric than Time Interval 1.

During Time Interval 1, researchers have recorded archaeological sites that lack *fossils directeures*, dominated by flakes and cores, and preserve the early presence of the systematic production of blades (GnJh-42 and GnJh-50) (Johnson and McBrearty 2010, 2012). During Time Interval 1, archaeological sites record handaxe dominated assemblages (Leakey Handaxe Area or LHA and GnJh-17), assemblages with bifaces produced on cobbles (GnJh-15), assemblages with early prepared core technology (LHA and GnJh-17), and assemblages that record MSA point technology (GnJh-17) (Cornelissen 1992; McBrearty 1999; McBrearty, et al. 1996; C. A. Tryon and S. McBrearty 2002). Tryon, et al. (2005) suggested that the regional variability exhibited in the production of Acheulean flakes, including the Levallois method, demonstrates that the variability in artifact manufacturing techniques predates the MSA. Johnson and McBrearty (2012) have suggested that the innovations in artifact manufacture documented in the Kapthurin Formation are related to hominin exploitation of patchy, resource rich environments. Landscape reconstructions presented in Chapters 2 and 3, and site choice by hominins during Time Intervals 1 and 2, will be analyzed from an optimal foraging perspective to further test this hypothesis.

5.2.2 Optimal Foraging Theory

Hunter-gathering societies today do not engage in foraging activities after conference with members of the group about the caloric value of plant and animal resources, the rates at which they encounter prey, the amount of energy they expend with each resource acquisition activity, and the cost-benefit ratio of differing subsistence strategies. However, like other

species' foraging behavior (Dugatkin 2004; Galef and Giraldeau 2001), the numerous foraging activities of hunter-gatherers, such as choosing when, where, and which resources to exploit, which technological choices to make to extract resources, how many individuals to include in a foraging party, and when and where the group should move residential locations, the behavior of foragers is consistent with anthropologists' expectation of minimal energy expenditure, maximum energy returns, and foraging trip distance minimization (Hill, et al. 1987; Marlowe 2005; Winterhalder 1981). These collective adaptive strategies, tailored by natural selective principles, can be described under the umbrella, optimal foraging theory. The central component of optimal foraging theory is that an individual should acquire food at the maximum return rate possible, ensuring that it will be better nourished than other members of its species if food resources are limited, or if other resources are limited it will be able to dedicate more time and energy to reproduction, parenting, or self-defense than other members (Kurland and Beckerman 1985).

One way to estimate optimization behavior is to track both search and handling time of food resources by foragers. Search time will include all time dedicated to finding food, although it is not necessarily tied to any particular food resource; many food items can be searched at the same time. Search time is contrasted by handling time, which includes all the behaviors that are involved in obtaining, subduing, preparing, and ingesting a food resource after it is found (Kurland and Beckerman 1985). Food types are also measured in terms of their energetic yield in calories, and can be contrasted with the calories expended in searching and handling a food item (Winterhalder 2001). These food yields are also weighed against their abundance and distribution in a given environment, or the encounter rate, a probability of how likely a forager is to encounter a given food item based on the speed and type of movement of the forager and

possibly the prey (Kurland and Beckerman 1985). Given these energetic constraints, food types available to foragers should be ranked according to their net yield and foragers should disregard lower ranked foods, due to the low energy yields, and instead search for higher ranked food resources (Hill, et al. 1987).

A wealth of information relating to the optimization behavior of modern foraging societies has been collected by anthropologists, including foragers who live in high, mid, and low latitudes. Well-studied groups of foragers include the !Kung San (Lee 1984; Yellen 1986; Yellen 1991) in southern Africa, the Hadza of eastern Africa (Bunn 2001; Hawkes, et al. 2001; Marlowe 2005; O'Connell, et al. 1999), the Ache of eastern Paraguay (Hill, et al. 1987; Kaplan and Hill 1985), the Inuit of northern North America (Binford 1980; Smith 1985), and many others (Kelly 1995). Ambrose and Lorenz (1990) provide a review of foraging society correlates, namely the relationship between resource structure and territorial and social organization of forager societies, separating foraging societies on the basis of predictable or unpredictable resources, as well as dense or scarce resources. These correlates suggest the following four scenarios: 1.) Foragers with predictable and dense resources should defend their territories, have low information exchange between groups, have low scheduled residential mobility patterns, small group sizes and high population densities, and moderate diet breadths. 2.) Foragers with predictable and scarce resources should have semi-permeable home ranges, intermediate information exchange between groups, intermediate residential mobility patterns that are scheduled, small group sizes and intermediate population densities, and high diet breadths. 3.) Foragers with unpredictable and dense resources should have large, undefended and permeable territories, very high information exchange between groups, high opportunistic residential mobility patterns, large group sizes with intermediate population densities, and very

low diet breadths. 4.) Foragers with unpredictable and scarce resources should have large, undefended and permeable territories, high information exchange between groups, very high opportunistic residential mobility patterns, small group sizes with very low population densities, and very high diet breadths (Ambrose and Lorenz 1990).

What are archaeologists to make of these optimization predictions? Archaeological investigations of behavioral variability during the Middle Pleistocene have focused on several lines of evidence, including lithic technology, prey choice, raw material transport, and site choice. Lithic technology serves as a direct and indirect marker of hominin diet, and shifts in diet should be reflected by shifts in lithic technology. Direct evidence of diet from lithic technology is sparse in the eastern African archaeological record (Tryon and Faith 2013), although the presence of points and scrapers are commonly inferred to correlate with hunting and processing of large mammal prey, as well as aquatic resources (Brooks, et al. 2006; Douze and Delagnes 2016; Milo 1998; Schoville 2010; Shea 2006; Sisk and Shea 2011; Wilkins, et al. 2012). Kelly (1995) predicts that plants would make up the bulk of diet breadth of foragers living near the equator, and Henry, et al. (2014) find evidence for plant remains preserved as micro-residues (starch grains and phytoliths) on MSA stone tools and in the dental calculus of associated hominins.

Prey-choice, indicated by the preservation of faunal remains, provides a direct measure of hominin animal food choices at MSA or Acheulean archaeological sites. Acheulean faunal remains, although scarce, suggest hominins hunted or scavenged large prey such as elephantids and medium sized prey, probably through ambush hunting strategies (Chazan and Horwitz 2006; Isaac and Isaac 1977; Potts 1989; Potts, et al. 1999; Rabinovich, et al. 2012). Faunal remains at associated MSA sites in eastern Africa are relatively rare as Tryon and Faith (2013) note, with

the exception of large faunal assemblages at GvJm 46 at Lukenya Hill (Marean 1992) and Porc Epic (Assefa 2006), and smaller assemblages at Rusinga Island, Kenya (Tryon, et al. 2014; Tryon, et al. 2010), Loiyangalani, Tanzania (Thompson 2005), and the Sibilo School Road Site, in the Kapthurin Formation (Blegen 2015). Tryon and Faith (2013) suggest, based on these faunal assemblages, that by the later Middle Pleistocene MSA hunters regularly hunted large and small ungulates and transported portions of the animal carcasses to central places, similar to behavior documented in the MSA of southern Africa (Faith 2008), a behavior that can be contrasted with the opportunistic hunting or scavenging of large animals during the Early Stone Age (Faith, et al. 2009).

When compared with Acheulean foragers, MSA foragers in East Africa regularly used fine-grained sources of toolstone, such as obsidian, and such materials lend themselves to more accurate geo-chemical sourcing techniques (Ambrose 2012; Merrick, et al. 1994). McBrearty and Brooks (2000) note that raw material transport associated with Acheulan artifacts is generally less than 60 km from site-to-source, while these distances can exceed 300 km with associated MSA assemblages and Blegen (2015) documents site-to-source raw material transport at the Sibilo School Road Site, in the Kapthurin Formation, Kenya that exceeds 100 km.

Site choice also provides a way for archaeologists to assess the foraging behavior of Middle Pleistocene hominins. Overlook locations have been suggested at Porc Epic, Ethiopia and Nasera, Tanzania to provide MSA hominins with higher encounter rates of animal herds (J. Desmond Clark 2001; Mehlman 1989). Clark (1988) and Ambrose (2001a) suggest that MSA hunters began occupying ecological zones between grassland and woodland environments to access resources from both environments. Micro-environments with reliable access to water and tree cover may have been important sites for MSA hominins to hunt large ungulate prey

(Johnson, et al. 2009; Johnson and McBrearty 2012). Basell (2008) also suggests that MSA sites were concentrated at the margins of woodland, grassland, and water resources due to climate variability and increasing resource fragmentation and refugia. Environmental reconstructions presented in Chapters 2 and 3 provide high resolution landscape reconstructions for a relatively small resource area (<150 km^2) to test the site choices of hominins associated with Acheulean and MSA technology in Time Intervals 1 and 2. Although this study area is certainly smaller than the larger resource areas Middle Pleistocene foragers would have exploited, given the large territories exploited through long distance site-to source raw material transfer (McBrearty and Brooks 2000), this study provides the first test of site choice on a regional scale against the backdrop of fine-grained micro-habitat reconstructions of associated archaeological and paleontological site, but see Blome, et al. (2012) and Basell (2008) for a continent wide analysis of site choice.

5.3 Discussion

5.3.1 Hominin Site Choice in the Kapthurin Formation

Landscape environmental reconstructions from Time Interval 1 (543 – 509 ka), presented in Chapter 3, are based on pedogenic carbonate nodules, paleosol carbonate, and soil organic matter (SOM) from paleosols. The carbon and oxygen stable isotope values of these proxies, as well as associated paleo-NDVI and fraction woody cover values, indicate a landscape with a diverse range of local habitats, which included woodlands, wooded grasslands, and open grasslands. These local environments were coupled with a perennially active stream and seasonal river systems that were likely fed by an intensified monsoonal episode (Leslie, et al. 2016). Given this range of habitats, archaeological traces from this time interval indicate that

hominins exploited open grassland and wooded grassland environments. A modern wooded grassland is displayed below in Figure 5.3.

Figure 5.3: A modern wooded grassland in the Baringo Basin, Kenya.

Hominins at the site of EKG, where a hominin mandible has been surface collected and attributed to *Homo erectus* and associated surface artifacts (one "bifacial core pick tool") (Leakey, et al. 1969), exploited local environments characterized by wooded grassland and grassland traces. This exploitation can be juxtaposed with the lithic technology recovered at GnJh-42, a site with early evidence of blade technology, characterized by open grassland signatures and close access to a perennially active stream (Johnson and McBrearty 2012). Both of these sites are associated with medium to low paleo-NDVI and fraction woody cover values

(all values produced are less than 0.33; see Chapter 3), indicating that hominins exploited vegetative areas with low primary biomass productivity, vegetative areas that are often correlated with high secondary (animal) biomass productivity (Pettorelli, et al. 2009; Pettorelli, et al. 2011). The ecotone between grassland and woodland environments has been noted before as an attractive location for MSA hominins to exploit large mammal game (Ambrose 2001a; Clark 1988), and it appears that hominins associated with Acheulean technology and innovations that appear later in the MSA, had begun to exploit this productive ecotone as well.

Landscape environmental reconstructions from Time Interval 2 (509 – 380 ka), presented in Chapter 3, are based on based on carbon and oxygen isotope values derived from pedogenic carbonate nodules, paleosol carbonate, and bulk SOM from paleosols. The isotope values of these proxies, as well as the associated paleo-NDVI and fraction woody cover estimates, indicate a landscape that was dominated by wooded grassland ecosystems, with significant open grassland and woodland components. The oxygen values of pedogenic carbonate nodules and paleosol carbonates indicate a landscape that was slightly wetter than the modern Lake Baringo Basin, but significantly more arid when compared with Time Interval 1. Within these ranges of local habitats, archaeological traces of hominin site choice indicate that hominins exploited sites that record significant wooded grassland components. At the site of GnJh-17, where handaxes, picks, and points were recovered *in situ* through excavations (Cornelissen 1992; McBrearty 1999), hominin activity is associated with predominantly wooded grassland vegetation cover and slightly wetter conditions than are average for this time interval. At the site of GnJh-15, where bifaces made on cobbles, large quantities of red ochre, and associated grindstones were discovered *in situ* through excavations (McBrearty 1999; Van Noten, Cornelissen, Gysels, Moeyersons, Nijs, et al. 1987; Van Noten, Cornelissen, Gysels, Moeyersons and Uytterschaut

1987), the local habitat is characterized by wooded grasslands and average oxygen isotope values for this time interval, indicating a slightly wetter environment than the modern Baringo Basin. At the site of LHA (GnJh-03), where handaxes, unifacial handaxes made on Levallois flakes, and blades have been surface collected and recovered *in situ* through excavations, the immediate environment is characterized by wooded grassland signatures and an average amount of water available, indicating slightly wetter conditions than at present in the Baringo Basin. Given these three archaeological sites, there is clear evidence for the exploitation of the ecotone between woodland and grassland ecosystems, as predicted by Clark (1988) and Ambrose (2001a).

5.3.2 Optimal Foraging Implications

Hominins in both Time Intervals 1 and 2 are associated with significant wooded grassland vegetative environments. There does not appear to be a shift towards this ecotone associated with MSA sites in the Kapthurin Formation, instead, it appears that this particular ecotone had begun to be exploited by hominins associated with Terminal Acheulean technology. Wooded grasslands would have provided hominins with a range of resources important to their survival. These resources include access to water, as ligneous vegetation is more expensive to grow than xeric adapted grasses, and is correlated with water availability. Woodlands also provide fruits and other food sources that would have been important for hominin diets. Wooded grasslands could provide cover from carnivores, a particularly important feature of the landscape in the Baringo Basin, given the absence of more traditional shelters such a rock shelters and caves. Wooded vegetation is critically important for the production of tools, such as spears for hunting or scavenging large mammals, behaviors that are well established by Time Intervals 1 and 2 (Klein 1988; J. J. Shea 1993; Thieme 1997, 2000; Wilkins, et al. 2012); wooded grasslands

would have provided hominins with easy access to this key resource. Wooded grasslands also provide hominins ample tree coverage to hide from animal herds, allowing them to ambush their prey, probably in groups (Ambrose 2001a; Clark 1988). Cover from ambient solar radiation is also important for hominins; open air sites have increased soil reflectance of solar radiation, which leads to increased temperatures when compared with woodland environments and is reflected in the clumped isotope paleothermometry of pedogenic carbonates (Cerling, Mace, et al. 2015; Passey, et al. 2010). Wooded grasslands would have provided hominins access to shade while still in close proximity to open grassland resources. The exploitation of wooded grassland habitats in both time intervals provides a range of implications for discussion.

Woodland environments in East Africa are associated with increased water availability (Bell 1982). This prediction is borne out by lower oxygen isotope values derived from pedogenic carbonate nodules and paleosol carbonates presented in Chapter 3. Modern ecosystems in East Africa provide evidence for increased NDVI values associated with increased meteoric water availability, primarily as a response to increased rainfall, and increased forest vegetation cover (Davenport and Nicholson 1993; Nicholson, et al. 1990). Increased meteoric water availability would have provided hominins with a reliable source of water, an important resource for group survival. Basell (2008) has also suggested that the meteoric water available to hominins in wooded environments would have been instrumental for MSA hominins during periods of dramatic climate fluctuations, resulting in environmental refugia and possible concentrations of large herbivorous mammals at the ecotone between woodlands and grasslands as well.

Wooded grasslands provide easy access and foraging opportunities for fruits and other vegetables important for hominin diets. Plant food sources probably made up the bulk of the

diets of Middle Pleistocene hominins living near the equator (Kelly 1995). Important plant resources for modern foraging societies in central and eastern Africa today include numerous species of berries, other fruits, tubers, and grasses (Marlowe 2005; Marlowe and Berbesque 2009; Murray, et al. 2001; Schoeninger, et al. 2001; Tadashi 1981; Terashima 2003; Terashima and Ichikawa 2003; Vincent 1985). These plant resources can be found across a range of ecological zones, but many are concentrated in woodland, wooded grassland, and aquatic environments (Marlowe 2010). Woodland environments also provide access to another important resource for modern foraging societies in East and Central Africa, honey (Marlowe 2010; Murray, et al. 2001). Honey is an incredibly valued resource among modern East African foragers, they rank it as their most valued food resource, and it provides them with high levels of dietary sugar and fat derived from bee larvae (Marlowe 2010; Murray, et al. 2001). Other researchers have suggested the antiquity of honey foraging could date to the Oldowan, and use evidence of chimpanzee populations foraging for honey as possible evidence, indicating that honey extraction from wooded grassland environments may predate Acheulean tools (Crittenden 2011; Stanford, et al. 2000). Acheulean and MSA hominins might have chosen wooded grasslands for extraction sites because of their easy access to numerous plant resources and honey.

Protection from large carnivores is also an important factor to consider for any hominin, including recent *Homo sapiens* (Treves and Naughton-Treves 1999; Treves and Palmqvist 2007). Carnivore damage to hominin remains is well documented during the Middle and Early Pleistocene, on *H. erectus* and *H. heidelbergensis* remains found in Africa and Eurasia (Dennell 2005; Sala, et al. 2014; Tappen 1987). By the Middle Pleistocene, hominins had begun to use hafted points and wooden spears to hunt or scavenge large mammal prey (John J. Shea 1993;

Thieme 1997, 2000; Wilkins, et al. 2012), but this new technology would not have prevented direct confrontations with large carnivores (Antón, et al. 2005). Many of the extant large carnivores in East Africa inhabit the grassland ecosystem, except for the leopard, which can generally be found in wooded grassland environments (Kingdon 1988). Wooded grassland environments may have provided Acheulean and MSA hominins with some protection from large social carnivores, especially given the absence of rock shelters or caves in close proximity to the open grasslands and paleo-lake Baringo, a source of large mammal prey.

Wooded grasslands would also provide Middle Pleistocene hominins with a key resource for foragers, wood for the production of tools. Residue and phytolith analysis of Acheulean tools indicates that tools were commonly used to shape and fashion wood into tools (Dominguez-Rodrigo, et al. 2001; Hardy and Garufi 1998; Rots and Van Peer 2006). Wood also provides hominins with another key resource, fuel for fire. Although the traces of fire are ephemeral at open air sites that predominate in Sub-Saharan Africa, there have been varying degrees of evidence for fire preserved at several sites dating to the Middle and Early Pleistocene (Berna, et al. 2012; Clark and Harris 1985; James, et al. 1989). There is also good evidence that by the MSA, ochre and *Acacia* resin was used as an adhesive for hafting stone points, and heat is a necessary component of this hafting procedure (Wadley 2005; Zipkin, et al. 2014). In any case, wooded grasslands would have clearly provided Middle Pleistocene hominins with wood, a key resource with numerous uses.

The ecotone boundary between woodlands and open grasslands would provide Middle Pleistocene hominins with hunting blinds, areas to hide from large mammal prey. Modern foragers today commonly use this ecotone to hide from their prey, simultaneously using complex projectile technology to take down game, although some use projectile weapons without regard

to terrain features (Churchill 1993; Lee 1984; Marlowe 2010). Several researchers have suggested that Middle Pleistocene hominins, armed with stone tipped spears for hunting large mammal prey, would have exploited this boundary between woodland and grassland ecosystems, because it provided the best cover from prey, and the closest proximity to large mammal prey (Ambrose 2001a; Basell 2008; Clark 1988). Wooded grasslands would also provide hominins with a shady area to process the remains of a kill, possibly for transport to residential locations, a common activity of modern foragers (Binford 1980; Steward 1938). Wooded grasslands would clearly have provided Middle Pleistocene hominins with coverage to ambush and process prey.

The effects of solar radiation on foraging groups are not insignificant. Prolonged exposure to solar radiation increases the body temperature of hominins, particularly near the equator, as well as the need for increased water consumption. Given these constraints, humans have a number of cultural and biological adaptations that protect their bodies from direct exposure to sunlight, such as skin pigmentation and clothing, but modern foraging populations near the equator also avoid direct sunlight when possible (Luxwolda, et al. 2012; Luxwolda, et al. 2013; Marlowe 2010; Yuen and Jablonski 2010). Paleosol carbonate studies in the Turkana Basin, based on the "clumped" isotope paleothermometry (Δ_{47}), reveal soil temperatures over the last 4 million years were typically above 30-35°C, and are elevated by approximately 7°C when compared with air temperatures; soil temperatures of forested environments approximate Mean Annual Temperatures (MAT) because the soils are not directly exposed to solar radiation (Cerling, Mace, et al. 2015; Passey, et al. 2010). These studies indicate that high MAT may have been relatively constant throughout the hominin occupation of East Africa, indicating similar conditions to those that modern foragers face. Broad-leaved woodland environments also provide increased humidity, which would help effectively cool hominins and other animals in

otherwise arid environments, due to the evapotranspiration process associated with leaf water (Nicholson, et al. 1990; Ruff 1994; Veenendaal, et al. 2004). This may have been of greater concern to hominins during Time Interval 2, when conditions were considerably more arid than Time Interval 1 (Leslie, et al. 2016). Wooded grasslands would also provide Middle Pleistocene hominins with shelter from rain storms, particularly during the wet season.

There are several reasons why Middle Pleistocene hominins may have chosen wooded grasslands for site exploitation. However, many of these reasons revolve directly around foraging activities (vegetables, fruits, animals, and water extraction), other processing activities (wood, animal or plant processing), and temporary shelter from solar radiation or carnivores. There are many other activities of foragers that would not be conducive to the wooded grassland ecotone, including extraction of toolstones from lithic sources, direct hunting of large herbivorous mammals associated with grasslands, and efficient travel between resource patches.

A feature of the Middle Stone Age is longer distances of transport (site-to-source) of high quality obsidian for stone tool production, distances over 100 km and upwards of 300 km (Ambrose 2012; Blegen 2015; McBrearty and Brooks 2000; Mehlman 1989). Using Brantingham's (2003) neutral model of stone tool procurement, these long distances associated with raw material transport deviate from the neutral model of random walk foraging. Exotic obsidian often makes up significant percentages of East African MSA assemblages (Blegen 2015; Brooks, et al. 2014), and transported significant distances (Ambrose 2012; McBrearty and Brooks 2000), indicating a depth of planning for foraging activities. This depth of planning can be compared with Binford's (1980) models of foragers and collectors; increased instances of logistical mobility correlate with collector strategies in areas where resources are sparsely

populated. In either the case of collector or forager mobility patterns, there are a number of sites modern foragers create that would not occur in wooded grassland environments (Binford 1980).

Ambrose and Lorenz (1990) outline four scenarios and cultural correlates for modern foragers based on the predictability and density of resources; when these are contrasted with modern ecological data about wooded grasslands and the distribution of resource patches relevant to modern foragers (Bell 1982; Marlowe 2010), as well as the environmental reconstructions highlighted in this paper, there are significant implications for the foraging behavior of hominins during Time Intervals 1 and 2. Hominins during Time Interval 1 are best characterized by Ambrose and Lorenz's (1990) scenario 1, given the increased productivity of primary biomass associated with the monsoonal episode (Leslie, et al. 2016), and the decreased distance of raw material transport, when compared with MSA hominins; foragers with predictable and dense resources should defend their territories, have low information exchange between groups, have low scheduled residential mobility patterns, small group sizes and high population densities, and moderate diet breadths. Based on the increased long-distance transport of raw materials associated with MSA behavior (McBrearty and Brooks 2000), and the constant association of sites with wooded grasslands, hominins during Time Interval 2 are best characterized by Ambrose and Lorenz's (1990) scenario 2; foragers with predictable and scarce resources should have semi-permeable home ranges, intermediate information exchange between groups, intermediate residential mobility patterns that are scheduled, small group sizes and intermediate population densities, and high diet breadths. Further archaeological investigation in both Time Intervals 1 and 2 is necessary to verify these assumptions about Middle Pleistocene foraging activities.

5.4 Conclusions

High-resolution, landscape reconstructions from Time Intervals 1 and 2 that were presented in Chapters 2 and 3 indicate that hominins associated with Terminal Acheulean and MSA technology regularly occupied and extracted resources from wooded grasslands. Wooded grasslands offer numerous advantages to Middle Pleistocene hominins, including greater access to water resources, which is important not only for hominin consumption, but because fruit bearing plants and tubers require access to water, and are found within the wooded grassland ecosystem. Wooded grasslands would have also provided Middle Pleistocene hominins access to another important foraging resource, honey, which provides high levels of dietary sugar and fat to modern foragers in East Africa. The occupation, at least periodically, of wooded grasslands would also have provided cover from large social carnivores, especially with the absence of other more traditional shelters such as rock shelters and caves. Wooded grasslands also provide access to an important resource for tool production, wood, as well as access for resources important for the production of fire. Perhaps most importantly, wooded grasslands would also provide Middle Pleistocene hominins with cover to use as hunting blinds, and close proximity to grassland ecosystems, so they could ambush large mammal prey. Finally, wooded grasslands would provide hominins shelter from the high levels of solar radiation, particularly at mid-day, a behavior that is common among foragers that live near the equator today.

Wooded grasslands appear to represent an optimal site for the extraction of resources and other activities; the archaeological signatures in the Kapthurin Formation are consistently associated with wooded grasslands, evidence for other environments is preserved but without significant archaeological traces (see Chapters 2 and 3), and there are many optimal reasons for these occupations, as outlined above. The occupation of the wooded grassland by MSA

hominins has been assumed by several researchers (Ambrose 2001a; Basell 2008; Clark 1988), but this research represents the first time that fine-grained landscape reconstructions verify this assumption. It is also clear, that the occupation of the wooded grassland ecotone predates MSA technology and occurs with Terminal Acheulean technology, at least in the Kapthurin Formation during Time Interval 1. This early occupation of the wooded grassland ecosystem by Terminal Acheulean hominins may be tied to the striking ecological diversity preserved in the Kapthurin Formation's Time Interval 1, due to the intense monsoonal episode (Leslie, et al. 2016), and could have provided hominins with a laboratory to test new behaviors, and technologies, such as blades (Johnson and McBrearty 2010, 2012). The high resolution landscape reconstructions presented in Chapters 2 and 3, and explored here, provide the first evidence for hominin site choice in a well-documented landscape, indicating that both Terminal Acheulean and MSA foragers regularly occupied wooded grassland ecosystems. It also appears, at least in the Baringo Basin, that Middle Pleistocene hominins persistently occupy wooded grasslands, despite shifts in climate conditions, or prevalent material culture used and deposited at a site.

Chapter 6: Conclusions

Shifts in global, regional, and local environments, driven by solar insolation, during the Pleistocene epoch, are thought to have shaped much of the evolution and adaptive behavioral responses of the genus *Homo* (Ambrose 1998; Bräuer 2008; deMenocal 2011; Kingston, et al. 2007; Potts 1998; Potts and Faith 2015; Vrba 1993). These hypotheses are supported by continental and global environmental proxies (deMenocal, et al. 2000; Lüthi, et al. 2008; Petit, et al. 1999; Schmieder, et al. 2000), and lack high-resolution, regional environmental data, although recent work by Cohen, et al. (2016), who is leading a large research team drilling east African rift lakes, and will hopefully provide a wealth of information about regional environments during the Plio-Pleistocene of East Africa. In this dissertation, I have provided a novel method for producing biomass productivity environmental reconstructions, several high-resolution environmental proxies based on stable isotope analyses from the Kapthurin Formation, Kenya; I reconstructed landscapes relevant to two main time intervals (Time Interval 1: 543 – 509 ka; Time Interval 2: 509 – 380 ka) during the Middle Pleistocene, to determine the differences or similarities between Acheulean and Middle Stone Age hominin site choice and landscape use during these time intervals in the Lake Baringo Basin.

6.1 Bovid Teeth and Pedogenic Carbonates from Time Interval 1

Isotopic analyses of bovid fossil teeth and pedogenic carbonates from the Kapthurin Formation, collected from localities within the Middle Silts and Gravels (K3) member of the Kapthurin Formation, stratigraphically from Time Interval 1, above the Pumice Tuff (K2) (543 ± 3 ka) and below the Grey Tuff (509 ± 9 ka), were useful in reconstructing vegetative habitats of hominins and general aridity. The teeth were represented by taxa from six tribes and were

sampled serially to reconstruct dietary vegetation and ancient habitats. The fauna sampled represents the full range of dietary adaptations, ranging from pure C_3 to pure C_4, although there is little evidence for mixed (C_3/C_4) diets. The stable oxygen isotope data, compared with criteria set forth in Levin, et al. (2006), suggests that most bovid taxa were evaporative insensitive (EI), tracking meteoric water faithfully, while a few were evaporative sensitive (ES), their values tracking the oxygen isotope composition of the C_3 vegetation they consumed. Applying the modified aridity index of Levin, et al. (2006), the oxygen enrichment was estimated between these two groups as $\varepsilon_{ES\text{-}EI} = -1.77$, approximating a paleowater deficit of 143 mm. The $\delta^{13}C_{pc}$ values suggest a landscape that was dominated by wooded grassland vegetation, with open grassland and woodland components; the $\delta^{18}O_{pc}$ values suggest a wetter environment than the modern basin, and confirm the presence of a perennially active stream during Time Interval 1 (Johnson, et al. 2009). These values suggest a paleohabitat that was perforated with very mesic and mildly xeric components, with riparian woodland, sumpland, and fringe open grassland ecosystems.

These general paleoenvironmental indicators suggest a region rich in biodiversity, and accord well with faunal identifications that have portrayed the regional environment as closed, wet, and marshy habitats near an alternating alkaline and freshwater lake with arid components farther afield (McBrearty 1999). A Middle Pleistocene African monsoonal system that dominated Time Interval 1 is the most likely explanation for the rapid sedimentation rates, numerous paleochannels, good fossil preservation and burial, and modified paleoaridity index of -1.77. This dissertation and the publication of Leslie, et al. (2016) represents the first confirmation of this Middle Pleistocene African monsoonal event with African paleoecological data (Clark, et al. 2003; Rossignol-Strick, et al. 1998). The general paleolandscape of Time

Interval 1 preserves exceptional ecological diversity, and could have provided hominins with a number of different local habitats and a broad range of resources for exploitation. From the archaeological evidence, hominins exploited both wet and dry locales with wooded, marshy, and grassland vegetation.

Isotope data from the Kapthurin Formation suggests, contrary to regional expectations (deMenocal 1995), that during Time Interval 1 the Lake Baringo region provided hominins and chimpanzees with hyper mesic, wooded refugium, in addition to nearby grasslands, both sources of valuable resources. Increased monsoonal activity at the onset of MIS 13 (~533 ka) probably drove the appearance of this hyper mesic environment, stimulating the production and use of new technologies (Johnson and McBrearty 2010), although further exploration and additional examples are necessary to test this hypothesis. This correlation allows for more precision when dating K3 and K3' sediments of the Kapthurin Formation, suggesting a more precise time interval of ~533 – 509 ka. This reconstruction accords with other researchers (Kingston, et al. 1994) who noted that the Tugen Hills succession does not provide evidence for a shift to C_4 dominated environments throughout the Neogene and Pliocene, and that a range of local habitats existed throughout this time period. The results of this research highlight the need to ground global and regional paleoclimate data with local paleoecological data from individual archaeological and paleontological sites.

6.2 Biomass Productivity and Bulk Soil Organic Matter

Remote sensing techniques, such as Normalized Differential Vegetation Indices (NDVI), provide landscape ecologists with an accurate means of predicting the modern primary biomass productivity of above-ground plants and the distribution of modern animal communities (Oindo

and Skidmore 2002; Pettorelli, et al. 2009; Pettorelli, et al. 2011). NDVI values were extracted from high resolution satellite imagery that was captured in February of 2012 from the Lake Baringo Basin; these values are well correlated with modern $\delta^{13}C_{SOM}$ values (R^2=0.79) collected in January of 2012 from the same geographic locations. NDVI values were chosen from the spectrum of relevant biomass productivity values (0.01 – 1.00) representing a range of different environments from the Lake Baringo Basin, an area with relatively little modern agricultural disturbance. Using this correlation, it was possible to devise an equation to estimate the paleo-NDVI values, if fossil $\delta^{13}C_{SOM}$ or $\delta^{13}C_{PC}$ values are known (Equation 2.2 in Chapter 2).

Paleo-NDVI calculations provide paleoanthropologists with a new method for reconstructing past primary biomass productivity, an exciting new avenue for paleoenvironmental reconstructions. As Cerling, Andanje, et al. (2015) illustrated, many animals in East Africa between 1 and 4 million years ago had diets that differed substantially from their modern counterparts, which they assessed through $\delta^{13}C$ values derived from tooth enamel, suggesting differences in habitat preference in the past. With this caveat in mind, and the understanding that large fauna in East Africa was modern by the Middle Pleistocene (Faith, et al. 2012; Potts and Deino 1995), I reconstructed paleo-NDVI values from Time Intervals 1 and 2 in the Kapthurin Formation (543 – 509 ka) and (509 – 380 ka), using fossil $\delta^{13}C_{SOM}$ values, and compared these results with fraction woody cover values, after Cerling et al. (2011). A range of different habitats are available to hominins in both time intervals, yet there is archaeological evidence of hominin exploitation in areas with moderate to low NDVI values. The paleolandscape of Time Interval 1 was exceptionally diverse ecologically and non-continuous, yet chimpanzee fossils were found in a fragmented woody habitat, while hominin fossils were found in an open grassland habitat (McBrearty and Jablonski 2005). Hominins extracted

resources mainly from wooded grassland environments with moderate NDVI values during Time Interval 2, although other environments were present. Widespread application of this novel method, using a landscape perspective, to a variety of time intervals and geographic locations, in conjunction with the application of the woody cover index developed by Cerling, Wynn, et al. (2011), will revolutionize our understanding of hominin evolution in Africa and finally allow the direct testing of environment-based hypotheses. Paleo-NDVI values provide another ecological proxy that will be useful to paleoanthropologists for reconstructing the paleohabitats of hominins and other fauna.

6.3 Contrasting Environmental Reconstructions based on Pedogenic Carbonate and Soil Organic Matter

Environmental reconstructions from Time Interval 1 (543 – 509 ka) based on pedogenic carbonates, carbonates from paleosols, and SOM from paleosols indicate a paleolandscape with a diverse range of local habitats. These habitats included significant woodland, wooded grassland, and open grassland components, and were coupled with a perennially active stream, which was likely fed by an intensified monsoonal episode (Leslie, et al. 2016). With this broad range of habitats, archaeological evidence of hominin exploitation is characterized by grassland and wooded grassland cover, and is consistent with lower paleo-NDVI and f_{wc} estimates. The hominin occupation at the site of GnJh-42 is associated with the production of blade technology and very mesic conditions near a perennially active stream with open grassland signatures (Johnson and McBrearty 2010, 2012). Hominins at the site of EKG appear to have preferred local environments characterized by wooded grassland and grassland vegetation coverage. Based on these results, it appears that hominins chose to exploit habitats with open grassland and

wooded grassland vegetation cover, probably due to the associated herbivorous mammals with low to moderate NDVI environments (Pettorelli, et al. 2009). This preference for open and wooded grassland environments can be contrasted with chimpanzees, who occupied the densest vegetation cover reconstructed for this time interval at Loc. 99, indicated by the consistent woodland reconstructions from all three lines of data and the associated higher paleo-NDVI and f_{wc} estimates. The local habitat at Loc. 99 represents a similar environment to extant chimpanzee populations; most populations are restricted to rainforests today, but smaller populations live within woodland and wooded grassland ecosystems (Kormos, et al. 2003).

Environmental reconstructions from Time Interval 2 (509 – 380 ka) indicate a landscape that was somewhat wetter than then extant Lake Baringo Basin and was dominated by wooded grasslands, with significant open grassland and woodland components; these environmental reconstructions are based on three lines of data: pedogenic carbonate nodules, smaller pedogenic carbonates from paleosols, and SOM from paleosols. Based on the range of environments during Time Interval 2, and contrasting these environments with archaeological evidence of hominin activity, hominins chose to exploit sites with significant wooded grassland components, indicating a preference for this type of vegetation cover. At the site of GnJh-17, excavated *in situ* handaxes, picks, and points (Cornelissen 1992; McBrearty 1999) are associated with wooded grassland vegetation and slightly wetter conditions than the average aridity conditions for this time interval. Environmental reconstructions from the site of GnJh-15, where bifaces made on cobles, large quantities of red ochre, and grindstones were excavated (McBrearty 1999; Van Noten, Cornelissen, Gysels, Moeyersons, Nijs, et al. 1987; Van Noten, Cornelissen, Gysels, Moeyersons and Uytterschaut 1987) indicate a local environment characterized by wooded grassland vegetation cover, with average aridity for this time interval. At the site of LHA, where

handaxes, unifacial handaxes made on Levallois flakes, and blades have been collected and excavated (Leakey, et al. 1969; McBrearty 1999), the local environment is characterized by wooded grasslands with an average amount of meteoric water available to this site based on oxygen isotope data from this time interval. Based on these environmental reconstructions, hominins apparently did not utilize different types of technology to exploit different environments during Time Interval 2, or the data is too coarse-grained to test this hypothesis. Instead, it appears that hominins consistently exploited sites with wooded grassland vegetation cover during Time Interval 2.

6.4 Behavioral Variability Traces in the Kapthurin Formation

High-resolution, landscape reconstructions from Time Intervals 1 and 2 presented in this dissertation indicate that hominins associated with Terminal Acheulean and MSA technology regularly occupied and extracted resources from wooded grasslands. Wooded grasslands offer numerous advantages to Middle Pleistocene hominins, including easier access to water resources, which is important not only for hominin consumption, but because fruit bearing plants and tubers require access to water, and are found within the wooded grassland ecotone. Wooded grasslands also provide access to another important foraging resource, honey, which provides high levels of dietary sugar and fat to modern foragers in East Africa (Murray, et al. 2001). The occupation, at least periodically, of wooded grasslands would also provide cover from large social carnivores, especially with the absence of other more traditional shelters such as rock shelters and caves. Wooded grasslands provide access to an important resource for tool production, wood, as well as access for resources important for the production of fire. Perhaps most importantly, wooded grasslands also provide cover to use as hunting blinds, and close

proximity to grassland ecosystems, to practice ambush-style hunting of large mammal prey. Finally, wooded grasslands provide shelter from the high levels of solar radiation, particularly at mid-day, a behavior that is common among foragers that live near the equator today (Marlowe 2010).

Wooded grasslands represent an optimal site for the extraction of resources and other activities by hominins; the archaeological signatures in the Kapthurin Formation are consistently associated with wooded grasslands, evidence for other environments is preserved but without significant archaeological traces (see Chapters 2 and 3), and there are many optimal reasons for these occupations, outlined in Chapter 4. The occupation of the wooded grassland by MSA hominins has long been assumed by several researchers (Ambrose 2001a; Basell 2008; Clark 1988), but this research represents the first time that fine-grained landscape reconstructions verify this assumption in a landscape setting. The occupation of the wooded grassland ecotone apparently predates MSA technology and occurs with Terminal Acheulean technology, at least in the Kapthurin Formation during Time Interval 1. This early occupation of the wooded grassland ecosystem by Terminal Acheulean hominins could be related to the striking ecological diversity reconstructed from Time Interval 1, due to the intense monsoonal episode (Leslie, et al. 2016); this ecological diversity could have provided hominins with a laboratory to test new behaviors, and technologies, such as blades (Johnson and McBrearty 2010, 2012). The high resolution landscape reconstructions presented in this dissertation provide the first evidence for hominin site choice in two well-documented landscapes, indicating that both Terminal Acheulean and MSA foragers regularly occupied wooded grassland ecosystems.

Appendix 1: Modern Soil Sampling Locations and associated NDVI values

Sample ID	Location	Easting	Northing	NDVI	%C	CO_2 Ht.	$\delta^{13}C_{SOM}$
DL-1	Kapth R1	62631.4	161093.7	0.914	4.32	12.70	-26.4
DL-2	Kapth R2	62631.4	161093.7	0.914	1.32	3.99	-24.2
DL-3	Kapth R3	62631.4	161093.7	0.914	1.45	4.40	-24.0
DL-4	Kapth R4	62458.8	161496.0	0.685	2.42	3.70	-22.0
DL-5	Kapth R5	62458.8	161496.0	0.685	2.54	8.59	-21.2
DL-6	Kapth R6	62458.8	161496.0	0.685	3.10	5.34	-22.0
DL-7	Kapth R7	62330.7	162597.7	0.217	0.06	0.20	-20.0
DL-8	Kapth R8	62330.7	162597.7	0.217	0.08	0.26	-21.9
DL-9	Kapth R9	62330.7	162597.7	0.217	0.15	0.50	-22.2
DL-10	Kapth R10	62398.7	162559.6	0.266	1.16	2.15	-22.0
DL-11	Kapth R11	62398.7	162559.6	0.266	0.91	1.54	-21.0
DL-12	Kapth R12	62398.7	162559.6	0.266	1.18	3.12	-21.7
DL-13	Kapth R13	62318.2	162902.5	0.729	3.06	7.63	-23.5
DL-14	Kapth R14	62318.2	162902.5	0.729	1.24	2.36	-21.1
DL-15	Kapth R15	62318.2	162902.5	0.729	3.30	7.10	-22.9
DL-16	Kapth R19	61852.6	162375.5	0.218	3.02	4.93	-21.8
DL-17	Kapth R20	61852.6	162375.5	0.218	3.31	5.79	-21.8
DL-18	Kapth R21	61852.6	162375.5	0.218	2.37	5.05	-21.1
DL-19	Kapth R22	61923.1	162913.3	0.755	1.49	4.08	-26.3
DL-20	Kapth R23	61923.1	162913.3	0.755	0.47	1.43	-25.2
DL-21	Kapth R24	61923.1	162913.3	0.755	1.03	2.17	-26.5
DL-22	Kapth R25	61835.2	163173.5	0.271	0.77	2.32	-18.3
DL-23	Kapth R27	61835.2	163173.5	0.271	0.54	1.10	-18.5
DL-24	Kapth R28	61973.2	163472.5	0.437	0.74	2.25	-19.9
DL-25	Kapth R29	61973.2	163472.5	0.437	1.22	2.09	-21.1
DL-26	Kapth R30	61973.2	163472.5	0.437	1.13	2.49	-20.6
DL-27	Kapth R31	62095.9	163388.2	0.357	1.98	3.10	-20.8
DL-28	Kapth R32	62095.9	163388.2	0.357	1.15	1.35	-19.9
DL-29	Kapth R33	62095.9	163388.2	0.357	1.56	2.46	-19.9
DL-30	Barte R5	63376.9	163880.2	0.111	0.12	0.35	-18.7
DL-31	Barte R7	63316.0	164036.0	0.310	0.78	1.16	-20.1
DL-32	Barte R8	63316.0	164036.0	0.310	0.63	0.82	-19.8
DL-33	Barte R9	63316.0	164036.0	0.310	0.72	1.31	-20.5
DL-34	Barte R10	63243.7	164060.8	0.478	0.09	0.24	-21.0
DL-35	Barte R11	63243.7	164060.8	0.478	0.57	1.56	-21.9
DL-36	Barte R12	63243.7	164060.8	0.478	0.29	0.94	-21.1
DL-37	Barte R13	62885.2	163909.1	0.127	0.10	0.30	-18.6
DL-38	Barte R14	62885.2	163909.1	0.127	0.10	0.28	-19.0
DL-39	Barte R15	62885.2	163909.1	0.127	0.07	0.22	-19.9
DL-40	Barte R16	63343.7	164444.3	0.012	0.07	0.21	-6.2
DL-41	Barte R17	63343.7	164444.3	0.012	0.20	0.60	-7.6
DL-42	Barte R18	63343.7	164444.3	0.012	0.09	0.29	-7.1
DL-43	Barte R19	62947.7	164575.2	0.203	0.80	1.29	-22.7
DL-44	Barte R21	62947.7	164575.2	0.203	0.54	0.87	-22.7

Table A1.1: Easting and Northing Coordinates (UTM Zone 36N) for modern soil sample locations, NDVI values for individual sampling locations, and $\delta^{13}C_{SOM}$ values for sample locations. Modern $\delta^{13}C_{SOM}$ (VPDB ‰) values are listed in parts per thousand. %C based on mass% and CO_2 Ht measured in nanoamperes (*nA*).

Sample ID	Location	Easting	Northing	NDVI	%C	CO_2 Ht.	$\delta^{13}C_{SOM}$
DL-45	Barte R22	62939.5	164705.5	0.252	0.30	0.89	-20.4
DL-46	Barte R23	62939.5	164705.5	0.252	0.34	1.09	-19.5
DL-47	Barte R24	62939.5	164705.5	0.252	0.48	1.52	-20.6
DL-48	Kaseurin R1	64376.4	162036.3	0.480	2.54	7.47	-23.6
DL-49	Kaseurin R2	64376.4	162036.3	0.480	0.62	0.96	-20.2
DL-50	Kaseurin R3	64376.4	162036.3	0.480	0.42	1.26	-19.3
DL-51	Kaseurin R4	64588.8	161728.9	0.212	0.78	1.22	-20.3
DL-52	Kaseurin R5	64588.8	161728.9	0.212	1.51	4.50	-23.0
DL-53	Kaseurin R6	64588.8	161728.9	0.212	0.80	1.61	-19.6
DL-54	Kaseurin R7	64377.6	161032.6	0.064	1.69	5.07	-11.4
DL-55	Kaseurin R8	64377.6	161032.6	0.064	1.06	3.20	-13.0
DL-56	Kaseurin R9	64377.6	161032.6	0.064	0.79	1.61	-14.0
DL-57	Kaseurin R10	64360.4	161571.9	0.328	0.85	2.49	-18.8
DL-58	Kaseurin R11	64360.4	161571.9	0.328	0.98	2.84	-20.0
DL-59	Kaseurin R12	64360.4	161571.9	0.328	0.84	1.29	-17.7
DL-60	Kaseurin R13	64167.6	162857.6	0.449	2.11	5.29	-24.3
DL-61	Kaseurin R14	64167.6	162857.6	0.449	1.08	3.21	-23.4
DL-62	Kaseurin R15	64167.6	162857.6	0.449	1.62	4.83	-23.3
DL-63	Kaseurin R16	63747.0	164500.8	0.325	0.50	0.75	-17.6
DL-64	Kaseurin R17	63747.0	164500.8	0.325	0.41	1.24	-20.1
DL-65	Kaseurin R18	63747.0	164500.8	0.325	1.13	1.48	-21.0
DL-66	Ngenyin1	70762.0	169182.6	0.507	0.50	1.53	-23.9
DL-67	Ngenyin2	70762.0	169182.6	0.507	0.76	3.68	-23.9
DL-68	Ngenyin3	70762.0	169182.6	0.507	0.97	1.28	-23.6
DL-69	Ngenyin4	70850.6	169223.1	0.692	0.25	0.76	-24.9
DL-70	Ngenyin5	70850.6	169223.1	0.692	0.25	0.76	-25.4
DL-71	Ngenyin6	70850.6	169223.1	0.692	0.19	0.56	-25.2
DL-72	Ngenyin7	70864.5	169239.3	0.854	1.48	2.42	-24.2
DL-73	Ngenyin8	70864.5	169239.3	0.854	1.26	3.20	-24.2
DL-74	Ngenyin9	70864.5	169239.3	0.854	1.73	3.09	-25.4
DL-75	Kipchere1	63997.9	158729.4	0.513	0.99	2.97	-23.5
DL-76	Kipchere2	63997.9	158729.4	0.513	2.27	3.68	-23.5
DL-77	Kipchere3	63997.9	158729.4	0.513	1.50	2.22	-23.8
DL-78	Ndau R1	58798.1	162301.4	1.000	1.78		-27.2
DL-79	Ndau R2	58798.1	162301.4	1.000	1.51		-26.7
DL-80	Ndau R3	58798.1	162301.4	1.000	1.59		-26.5
DL-81	Ndau R4	58884.4	162317.9	0.237	0.40		-17.7
DL-82	Ndau R5	58884.4	162317.9	0.237	0.39		-17.1
DL-83	Ndau R6	58884.4	162317.9	0.237	0.39		-18.5
DL-84	Ndau R7	59123.0	162854.7	0.241	0.26		-21.0
DL-85	Ndau R8	59123.0	162854.7	0.241	0.23		-23.0
DL-86	Ndau R9	59123.0	162854.7	0.241	0.32		-21.1
DL-87	Ndau R16	59048.3	164146.2	0.214	0.53		-20.5
DL-88	Ndau R17	59048.3	164146.2	0.214	0.46		-20.0
DL-89	Ndau R18	59048.3	164146.2	0.214	0.65		-20.9

Table A1.1 (cont): Easting and Northing Coordinates (UTM Zone 36N) for modern soil sample locations, NDVI values for individual sampling locations, and $\delta^{13}C_{SOM}$ values for sample locations. Modern $\delta^{13}C_{SOM}$ (VPDB ‰) values are listed in parts per thousand. %C based on mass% and CO_2 Ht measured in nanoamperes (*nA*).

Appendix 2: Paleosol $\delta^{13}C_{SOM}$ and paleo-NDVI values from Time Intervals 1 and 2

Sample	Site	CO_2 Ht.	%C	$\delta^{13}C_{SOM}$	Paleo-NDVI	Woody Cover
DL-1-12	Below GT	0.20	0.07	-21.02	0.47	0.44
DL-2-12	Loc. 3	0.25	0.08	-15.68	0.12	0.07
DL-3-12	Below GT	0.15	0.05	-18.37	0.24	0.23
DL-4-12	Below GT	0.13	0.04	-20.67	0.43	0.41
DL-5-12	Loc. 3	0.34	0.11	-13.43	0.07	0.01
DL-7-12	EKG	0.90	0.30	-7.21	0.01	0.19
DL-9-12	BKS	0.11	0.07	-21.37	0.51	0.47
DL-10-12	JKS	0.17	0.06	-20.81	0.44	0.42
DL-11-12	Lion Site	0.38	0.12	-16.43	0.15	0.11
DL-15-12	Loc. 3	0.36	0.09	-19.11	0.29	0.29
DL-20-12	Loc. 12	0.12	0.04	-20.75	0.44	0.42
DL-21-12	Loc. 99	0.24	0.14	-23.84	0.96	0.68

Table A2.1 (above): Paleosol $\delta^{13}C_{SOM}$ values from Time Interval 1 (543 – 509 ka). Modern $\delta^{13}C_{SOM}$ (VPDB ‰) values are listed in parts per thousand. %C based on mass% and CO_2 Ht measured in nanoamperes (*nA*). GT = Grey Tuff

Sample	Site	CO_2 Ht.	%C	$\delta^{13}C_{SOM}$	Paleo-NDVI	Woody Cover
DL-6-12	GnJh-15	0.19	0.06	-21.73	0.56	0.384
DL-8-12	Loc. 3	0.21	0.07	-13.97	0.08	0.016
DL-12-12	Loc. 17	0.19	0.05	-22.36	0.66	0.652
DL-13-12	Loc. 17	0.15	0.05	-17.78	0.21	0.190
DL-14-12	GnJh-17	0.20	0.06	-17.10	0.17	0.147
DL-16-12	Loc. 307	0.20	0.07	-20.40	0.40	0.391
DL-17-12	Below K4	0.33	0.11	-19.34	0.31	0.304
DL-18-12	LHA	0.18	0.06	-16.11	0.14	0.092
DL-19-12	Below K4	0.20	0.07	-20.47	0.41	0.396

Table A2.2 (above): Paleosol $\delta^{13}C_{SOM}$ values from Time Interval 2 (509 – 380 ka). Modern $\delta^{13}C_{SOM}$ (VPDB ‰) values are listed in parts per thousand. %C based on mass% and CO_2 Ht measured in nanoamperes (*nA*).

Appendix 3: Serial Pedogenic Carbonate Data

Sample Number	$\delta^{13}C$	$\delta^{13}C$ σ	$\delta^{18}O$	$\delta^{18}O$ σ		Sample Number	$\delta^{13}C$	$\delta^{13}C$ σ	$\delta^{18}O$	$\delta^{18}O$ σ
DL 1-2011-1	-2.3	0.03	-2.8	0.03		DL 3 2011 8	-2.1	0.03	-5.9	0.02
DL 1-2011-2	-2.2	0.01	-2.6	0.03		DL 3 2011 9	-1.9	0.02	-5.8	0.03
DL 1-2011-3	-3.0	0.01	-2.9	0.02		DL 3 2011 10	-1.9	0.01	-5.1	0.03
DL 1-2011-4	-2.2	0.02	-2.6	0.01		DL 3 2011 11	-1.8	0.03	-6.2	0.04
DL 1-2011-5	-2.0	0.02	-2.9	0.02		DL 3 2011 12	-1.8	0.02	-6.3	0.03
DL 1-2011-6	-2.0	0.02	-3.3	0.04		DL 3 2011 13	-2.1	0.02	-5.4	0.04
DL 1-2011-7	-0.8	0.02	-2.9	0.03		DL 3 2011 14	-1.8	0.02	-6.4	0.05
DL 1-2011-8	-2.3	0.02	-3.4	0.01		DL 3 2011 16	-2.4	0.02	-6.0	0.02
DL 2-2011-1	-6.5	0.02	-2.8	0.03		DL 4 2011 1	-4.9	0.01	-4.4	0.01
DL 2-2011-2	-3.5	0.01	-4.0	0.03		DL 4 2011 2	-3.0	0.01	-5.9	0.04
DL 2-2011-3	-4.9	0.01	-4.6	0.03		DL 4 2011 3	-2.8	0.03	-6.1	0.02
DL 2-2011-4	-2.5	0.02	-3.9	0.01		DL 4 2011 4	-2.6	0.01	-6.4	0.02
DL 2-2011-5	-2.1	0.03	-5.3	0.03		DL 4 2011 5	-2.4	0.02	-5.7	0.05
DL 2-2011-6	-2.0	0.02	-6.1	0.02		DL 4 2011 6	-3.3	0.02	-4.8	0.02
DL 2 2011 7	-1.8	0.02	-5.0	0.03		DL 4 2011 7	-2.9	0.03	-5.2	0.03
DL 2 2011 8	-1.8	0.03	-6.1	0.03		DL 4 2011 8	-2.6	0.02	-4.9	0.03
DL 2 2011 9	-1.8	0.01	-5.3	0.03		DL 4 2011 9	-1.8	0.01	-6.0	0.02
DL 2 2011 10	-1.9	0.01	-4.6	0.03		DL 4 2011 10	-2.1	0.02	-5.5	0.02
DL 2 2011 11	-2.0	0.01	-5.9	0.04		DL 4 2011 11	-2.0	0.03	-6.1	0.03
DL 2 2011 12	-1.2	0.02	-5.6	0.03		DL 4 2011 12	-2.1	0.02	-5.5	0.02
DL 2 2011 13	-1.0	0.01	-5.5	0.06		DL 5 2011 1	-2.1	0.03	-5.7	0.03
DL 2 2011 14	-1.3	0.01	-5.2	0.03		DL 5 2011 2	-2.3	0.03	-6.4	0.03
DL 2 2011 15	-1.1	0.01	-4.5	0.03		DL 5 2011 3	-3.0	0.01	-6.6	0.01
DL 2 2011 16	-1.3	0.01	-4.4	0.03		DL 5 2011 4	-2.9	0.02	-6.4	0.04
DL 2 2011 17	-1.4	0.02	-5.3	0.03		DL 5 2011 5	-2.9	0.02	-6.7	0.04
DL 2 2011 18	-1.1	0.02	-5.1	0.03		DL 5 2011 6	-3.0	0.01	-6.8	0.02
DL 2 2011 19	-1.3	0.03	-5.1	0.04		DL 5 2011 7	-3.0	0.03	-7.1	0.04
DL 2 2011 20	-3.4	0.02	-2.3	0.03		DL 5 2011 8	-2.8	0.02	-7.4	0.02
DL 3 2011 1	-2.8	0.04	-5.4	0.02		DL 5 2011 9	-2.5	0.03	-7.9	0.03
DL 3 2011 2	-2.3	0.01	-5.1	0.03		DL 5 2011 10	-2.3	0.01	-7.3	0.03
DL 3 2011 3	-2.1	0.01	-5.1	0.05		DL 6 2011 1	-1.1	0.01	-5.1	0.04
DL 3 2011 4	-2.0	0.02	-4.8	0.02		DL 6 2011 2	-1.1	0.02	-4.0	0.02
DL 3 2011 5	-2.0	0.02	-6.1	0.04		DL 6 2011 3	0.0	0.01	-5.4	0.04
DL 3 2011 6	-1.8	0.03	-6.3	0.06		DL 6 2011 4	-0.9	0.01	-4.6	0.03
DL 3 2011 7	-2.0	0.02	-5.3	0.03		DL 6 2011 5	-1.4	0.02	-4.7	0.03

A3.1 Serial Carbon and Oxygen values derived from pedogenic carbonate nodules. Standard deviations of individual measurements are also displayed.

Sample Number	$\delta^{13}C$	$\delta^{13}C$ σ	$\delta^{18}O$	$\delta^{18}O$ σ		Sample Number	$\delta^{13}C$	$\delta^{13}C$ σ	$\delta^{18}O$	$\delta^{18}O$ σ
DL 6 2011 6	-1.9	0.02	-4.2	0.03		DL10 2011-1	-1.8	0.03	-6.4	0.05
DL 6 2011 7	-1.0	0.01	-4.2	0.04		DL10 2011-2	-1.9	0.01	-8.5	0.01
DL 6 2011 8	-1.0	0.01	-3.9	0.02		DL10 2011-3	-2.2	0.02	-9.2	0.01
DL 6 2011 9	-1.2	0.02	-4.4	0.04		DL10 2011-4	-1.7	0.04	-7.0	0.04
DL 6 2011 10	-1.5	0.01	-4.7	0.03		DL10 2011-5	-1.4	0.02	-7.4	0.04
DL 7 2011 1	-1.0	0.04	-5.4	0.09		DL10 2011-6	-1.2	0.02	-7.7	0.03
DL 7 2011 2	-0.2	0.02	-3.8	0.05		DL10 2011-7	-1.1	0.01	-7.4	0.01
DL 7 2011 3	-0.6	0.02	-4.5	0.02		DL10 2011-8	-1.4	0.02	-7.6	0.03
DL 7 2011 4	-1.5	0.01	-3.8	0.02		DL10 2011-9	-1.4	0.02	-8.8	0.01
DL 7 2011 5	-0.8	0.02	-5.5	0.03		DL10 2011-10	-0.4	0.02	-8.5	0.03
DL 7 2011 6	0.2	0.02	-5.5	0.03		DL1 2012-1	-5.7	0.03	-4.6	0.03
DL 7 2011 7	1.9	0.02	-4.1	0.04		DL1 2012-2	-6.5	0.01	-4.0	0.02
DL 7 2011 8	0.4	0.01	-4.6	0.03		DL1 2012-3	-6.8	0.02	-3.5	0.04
DL 7 2011 9	-1.2	0.01	-4.0	0.04		DL1 2012-4	-6.8	0.01	-3.7	0.02
DL 7 2011 10	-0.7	0.02	-4.6	0.03		DL1 2012-5	-6.7	0.02	-3.4	0.03
DL 8 2011 1	-4.1	0.02	-4.1	0.03		DL1 2012-6	-6.5	0.02	-2.9	0.03
DL 8 2011 2	-4.7	0.03	-3.3	0.03		DL1 2012-7	-6.6	0.02	-3.9	0.02
DL 8 2011 3	-4.6	0.02	-3.7	0.03		DL1 2012-8	-6.7	0.01	-3.9	0.02
DL 8 2011 4	-4.2	0.02	-3.9	0.06		DL1 2012-9	-6.5	0.02	-3.8	0.02
DL 8 2011 5	-3.9	0.01	-3.6	0.04		DL1 2012-10	-6.5	0.02	-3.6	0.03
DL 8 2011 6	-4.0	0.01	-4.3	0.01		DL2 2012-1	0.0	0.02	-1.3	0.04
DL 8 2011 7	-3.7	0.02	-3.5	0.02		DL2 2012-2	0.4	0.01	-1.3	0.03
DL 8 2011 8	-3.4	0.03	-3.3	0.03		DL2 2012-3	0.4	0.01	-0.8	0.02
DL 8 2011 9	-2.8	0.01	-4.5	0.01		DL2 2012-4	0.2	0.04	0.2	0.03
DL 8 2011 10	-1.5	0.02	-4.0	0.02		DL2 2012-5	0.3	0.04	-1.3	0.05
DL9 2011-1	-3.2	0.01	-8.2	0.02		DL2 2012-6	-0.9	0.07	-0.8	0.11
DL9 2011-2	-2.8	0.03	-7.0	0.03		DL2 2012-7	0.1	0.02	-1.3	0.09
DL9 2011-3	-1.9	0.02	-4.8	0.04		DL2 2012-8	0.6	0.02	1.5	0.01
DL9 2011-4	-1.8	0.03	-4.0	0.02		DL 2 2012-9	0.5	0.03	0.2	0.02
DL9 2011-5	-2.6	0.01	-3.3	0.03		DL 2 2012-10	0.4	0.02	0.4	0.03
DL9 2011-6	-3.9	0.03	-3.0	0.04		DL 3 2012-1	-3.7	0.01	-3.5	0.03
DL9 2011-7	-4.2	0.01	-3.7	0.02		DL 3 2012-2	-3.9	0.02	-3.6	0.03
DL9 2011-8	-4.3	0.01	-3.5	0.03		DL 3 2012-3	-4.1	0.02	-3.3	0.02
DL9 2011-9	-4.1	0.01	-3.5	0.03		DL 3 2012-4	-3.7	0.03	-4.0	0.04
DL9 2011-10	-2.4	0.02	-3.6	0.02		DL 3 2012-5	-5.0	0.01	-4.2	0.04

A3.1 (cont.) Serial Carbon and Oxygen values derived from pedogenic carbonate nodules. Standard deviations of individual measurements are also displayed.

Sample Number	$\delta^{13}C$	$\delta^{13}C$ σ	$\delta^{18}O$	$\delta^{18}O$ σ		Sample Number	$\delta^{13}C$	$\delta^{13}C$ σ	$\delta^{18}O$	$\delta^{18}O$ σ
DL 3 2012-6	-6.2	0.03	-3.3	0.04		DL 6 2012 1	-3.3	0.02	-3.6	0.03
DL 3 2012-7	-6.3	0.02	-3.2	0.03		DL 6 2012 2	-3.2	0.01	-4.0	0.02
DL 3 2012-8	-5.6	0.02	-3.5	0.02		DL 6 2012 3	-3.3	0.01	-3.8	0.01
DL 3 2012-9	-4.3	0.01	-3.2	0.02		DL 6 2012 4	-3.4	0.02	-3.8	0.03
DL 3 2012-10	-4.3	0.02	-3.6	0.04		DL 6 2012 5	-3.3	0.02	-3.9	0.03
DL 3 2012-11	-3.7	0.02	-3.0	0.05		DL 6 2012 6	-3.4	0.02	-3.6	0.01
DL 3 2012-12	-4.3	0.02	-3.8	0.04		DL 6 2012 7	-3.3	0.03	-3.5	0.02
DL 3 2012-13	-4.3	0.02	-3.5	0.02		DL 6 2012 8	-3.4	0.01	-3.2	0.03
DL 3 2012-14	-3.8	0.03	-2.6	0.03		DL 6 2012 9	-3.3	0.02	-3.8	0.02
DL 3 2012-15	-3.5	0.02	-3.1	0.05		DL 6 2012 10	-3.3	0.02	-4.0	0.03
DL 4 2012 1	-6.2	0.03	-2.3	0.04		DL 7 2012-1	-5.6	0.02	-3.5	0.04
DL 4 2012 2	-6.6	0.02	-2.7	0.04		DL 7 2012-2	-5.8	0.03	-3.5	0.04
DL 4 2012 3	-6.8	0.03	-3.3	0.05		DL 7 2012-3	-5.2	0.01	-3.1	0.03
DL 4 2012 4	-6.2	0.02	-2.7	0.04		DL 7 2012-4	-5.3	0.03	-3.7	0.02
DL 4 2012 5	-4.6	0.01	-3.4	0.03		DL 7 2012-5	-5.5	0.02	-3.5	0.02
DL 4 2012 6	-4.4	0.02	-4.3	0.03		DL 7 2012-6	-5.5	0.01	1.2	0.02
DL 4 2012 7	-3.8	0.02	-3.8	0.01		DL 7 2012-7	-5.7	0.01	-2.9	0.03
DL 4 2012 8	-4.3	0.03	-3.9	0.02		DL 7 2012-8	-5.9	0.01	-3.2	0.02
DL 4 2012 9	-4.3	0.03	-3.4	0.04		DL 7 2012-9	-5.5	0.02	-3.9	0.05
DL 4 2012 10	-4.3	0.01	-4.0	0.03		DL 8 2012-1	-2.7	0.03	-3.1	0.03
DL 4 2012 11	-4.3	0.02	-3.8	0.02		DL 8 2012-2	-2.3	0.02	-3.0	0.03
DL 4 2012 12	-4.1	0.01	-4.0	0.02		DL 8 2012-3	-2.6	0.01	-3.1	0.03
DL 4 2012 13	-4.1	0.02	-3.5	0.03		DL 8 2012-4	-2.6	0.02	-2.8	0.04
DL 4 2012 14	-4.4	0.03	-3.2	0.03		DL 8 2012-5	-2.5	0.02	-3.2	0.02
DL 4 2012 15	-4.2	0.02	-3.6	0.02		DL 8 2012-6	-2.4	0.01	-2.8	0.02
DL 5 2012 1	-4.8	0.03	-1.3	0.05		DL 8 2012-7	-2.6	0.01	-2.5	0.02
DL 5 2012 2	-5.2	0.03	-2.6	0.07		DL 8 2012-8	-2.7	0.02	-2.7	0.02
DL 5 2012 3	-5.3	0.01	-1.9	0.03		DL 8 2012-9	-2.7	0.02	-3.4	0.03
DL 5 2012 4	-5.2	0.03	-1.8	0.05		DL 8 2012-10	-2.7	0.02	-3.3	0.02
DL 5 2012 5	-5.5	0.01	-2.8	0.04		DL 9 2012-1	-7.3	0.02	-3.9	0.04
DL 5 2012 6	-4.5	0.02	-2.9	0.02		DL 9 2012-2	-7.0	0.02	-4.2	0.02
DL 5 2012 7	-4.9	0.01	-3.2	0.05		DL 9 2012-3	-6.7	0.01	-4.0	0.02
DL 5 2012 8	-4.6	0.01	-2.9	0.05		DL 9 2012-4	-6.7	0.02	-4.6	0.01
DL 5 2012 9	-3.9	0.02	-2.8	0.04		DL 9 2012-5	-6.6	0.01	-3.6	0.02
DL 5 2012 10	-4.2	0.02	-2.7	0.03		DL 9 2012-6	-6.7	0.01	-4.2	0.01

A3.1 (cont.) Serial Carbon and Oxygen values derived from pedogenic carbonate nodules. Standard deviations of individual measurements are also displayed.

Sample Number	$\delta^{13}C$	$\delta^{13}C$ σ	$\delta^{18}O$	$\delta^{18}O$ σ		Sample Number	$\delta^{13}C$	$\delta^{13}C$ σ	$\delta^{18}O$	$\delta^{18}O$ σ
DL 9 2012-7	-6.5	0.02	-3.9	0.03		DL 13 2012-9	-6.0	0.03	-4.5	0.03
DL 9 2012-8	-6.5	0.03	-2.8	0.05		DL 13 2012-10	-5.6	0.01	-3.1	0.05
DL 9 2012-9	-6.8	0.06	-3.0	0.11		DL 14 2012-1	-5.6	0.02	-4.0	0.02
DL 9 2012-10	-7.1	0.02	-3.2	0.05		DL 14 2012-2	-6.0	0.02	-4.0	0.02
DL 10 2012-1	-6.6	0.01	-3.9	0.02		DL 14 2012-3	-6.4	0.02	-4.3	0.02
DL 10 2012-2	-5.7	0.02	-4.2	0.02		DL 14 2012-4	-6.8	0.01	-3.9	0.04
DL 10 2012-3	-5.5	0.01	-4.5	0.03		DL 14 2012-5	-6.5	0.02	-3.9	0.02
DL 10 2012-4	-5.9	0.02	-4.3	0.03		DL 14 2012-6	-6.6	0.01	-3.9	0.02
DL 10 2012-5	-6.1	0.02	-3.8	0.02		DL 14 2012-7	-5.9	0.02	-4.0	0.03
DL 10 2012-6	-5.9	0.02	-4.0	0.03		DL 14 2012-8	-6.0	0.02	-3.8	0.01
DL 10 2012-7	-6.0	0.02	-3.5	0.02		DL 14 2012-9	-6.2	0.02	-4.1	0.02
DL 10 2012-8	-6.0	0.01	-4.2	0.01		DL 14 2012-10	-6.2	0.01	-4.4	0.03
DL 10 2012-9	-6.1	0.01	-4.2	0.04		DL 15 2012-1	-9.7	0.03	-4.2	0.03
DL 10 2012-10	-6.1	0.02	-4.0	0.04		DL 15 2012-2	-9.4	0.01	-3.6	0.02
DL 11 2012-1	-5.6	0.01	-5.2	0.02		DL 15 2012-3	-9.7	0.01	-3.6	0.01
DL 11 2012-2	-5.4	0.01	-5.2	0.01		DL 16 2012-1	-5.9	0.02	-3.9	0.04
DL 11 2012-3	-5.6	0.02	-5.2	0.02		DL 16 2012-2	-5.9	0.01	-2.7	0.04
DL 11 2012-4	-5.0	0.02	-5.5	0.02		DL 16 2012-4	-4.9	0.03	-3.0	0.02
DL 11 2012-5	-5.3	0.01	-5.1	0.03		DL 16 2012-5	-5.6	0.02	-3.6	0.02
DL 11 2012-6	-5.3	0.01	-5.7	0.04		DL 16 2012-6	-5.9	0.02	-4.0	0.03
DL 11 2012-7	-5.3	0.02	-5.9	0.03		DL 16 2012-7	-5.6	0.02	-3.9	0.03
DL 11 2012-8	-5.2	0.01	-5.0	0.01		DL 16 2012-8	-5.3	0.02	-3.6	0.03
DL 11 2012-9	-5.0	0.01	-5.5	0.02		DL 16 2012-9	-5.9	0.01	-4.4	0.05
DL 11 2012-10	-5.0	0.01	-5.7	0.02		DL 16 2012-10	-6.0	0.02	-3.5	0.04
DL 12 2012-1	-5.8	0.03	-1.6	0.04		DL 17 2012-1	-3.2	0.01	-3.4	0.01
DL 12 2012-2	-5.8	0.08	1.7	0.09		DL 17 2012-2	-2.4	0.01	-3.6	0.02
DL 12 2012-3	-5.8	0.02	-2.4	0.02		DL 17 2012-3	-2.8	0.02	-3.8	0.02
DL 13 2012-1	-4.9	0.03	-3.8	0.05		DL 17 2012-4	-3.1	0.02	-3.2	0.02
DL 13 2012-2	-5.2	0.02	-2.0	0.05		DL 17 2012-5	-3.7	0.02	-3.1	0.04
DL 13 2012-3	-5.4	0.03	-3.9	0.02		DL 17 2012-6	-3.7	0.02	-3.7	0.02
DL 13 2012-4	-5.3	0.02	-3.8	0.06		DL 17 2012-7	-2.8	0.01	-4.1	0.03
DL 13 2012-5	-5.5	0.02	-4.2	0.03		DL 17 2012-8	-2.8	0.01	-3.5	0.02
DL 13 2012-6	-5.8	0.02	-4.2	0.02		DL 17 2012-9	-2.9	0.02	-3.5	0.02
DL 13 2012-7	-5.9	0.02	-3.4	0.03		DL 17 2012-10	-3.4	0.01	-3.2	0.03
DL 13 2012-8	-6.1	0.02	-4.0	0.04		DL 18 2012-3	-5.8	0.02	-3.6	0.06

A3.1 (cont.) Serial Carbon and Oxygen values derived from pedogenic carbonate nodules. Standard deviations of individual measurements are also displayed.

Sample Number	$\delta^{13}C$	$\delta^{13}C$ σ	$\delta^{18}O$	$\delta^{18}O$ σ		Sample Number	$\delta^{13}C$	$\delta^{13}C$ σ	$\delta^{18}O$	$\delta^{18}O$ σ
DL 19 2012-1	-4.6	0.03	-3.8	0.03		DL 7 1 2011 - 6	-1.2	0.02	-4.2	0.03
DL 19 2012-2	-4.6	0.01	-3.8	0.02		DL 7 1 2011 - 7	-0.9	0.02	-2.8	0.04
DL 19 2012-3	-4.6	0.02	-3.8	0.03		DL 7 1 2011 - 8	-0.9	0.04	-3.8	0.04
DL 19 2012-4	-4.6	0.02	-3.9	0.02		DL 7 1 2011 - 9	-0.7	0.02	-6.5	0.04
DL 19 2012-5	-4.7	0.01	-3.5	0.02		DL 7 1 2011 - 10	-1.4	0.03	-8.5	0.09
DL 19 2012-6	-4.4	0.01	-3.6	0.03		DL 9 1 2011 - 1	-2.8	0.02	-7.6	0.04
DL 19 2012-7	-4.0	0.01	-3.7	0.03		DL 9 1 2011 - 2	-2.0	0.02	-6.6	0.03
DL 19 2012-8	-3.8	0.03	-3.9	0.03		DL 9 1 2011 - 3	-2.5	0.02	-5.0	0.02
DL 19 2012-9	-3.4	0.03	-3.4	0.01		DL 9 1 2011 - 4	-3.0	0.03	-4.5	0.04
DL 19 2012-10	-3.5	0.01	-3.7	0.02		DL 9 1 2011 - 5	-1.8	0.01	-4.3	0.02
DL 20 2012 - 1	-5.4	0.02	-4.1	0.02		DL 9 1 2011 - 6	-2.7	0.02	-5.7	0.03
DL 20 2012 - 2	-4.0	0.01	-3.7	0.01		DL 9 1 2011 - 7	-2.3	0.01	-4.7	0.03
DL 20 2012 - 3	-2.6	0.01	-4.6	0.02		DL 9 1 2011 - 8	-3.3	0.02	-4.4	0.02
DL 20 2012 - 4	-2.5	0.02	-4.6	0.02		DL 9 1 2011 - 9	-2.8	0.02	-4.3	0.01
DL 20 2012 - 5	-2.0	0.02	-4.2	0.04		DL 9 1 2011 - 10	-3.2	0.02	-4.6	0.03
DL 20 2012 - 6	-1.3	0.01	-4.5	0.02		DL 10 1 2011 - 1	-1.7	0.03	-8.1	0.02
DL 20 2012 - 7	-1.2	0.01	-3.6	0.01		DL 10 1 2011 - 2	-1.7	0.02	-8.8	0.02
DL 20 2012 - 8	-0.8	0.02	-3.9	0.02		DL 10 1 2011 - 3	-1.5	0.02	-8.3	0.02
DL 20 2012 - 9	-1.3	0.02	-4.7	0.05		DL 10 1 2011 - 4	-1.9	0.02	-8.2	0.02
DL 20 2012 - 10	-1.4	0.02	-3.6	0.03		DL 10 1 2011 - 5	-1.6	0.01	-8.5	0.02
DL 7 1 2011 - 1	-5.2	0.01	-7.5	0.03		DL 10 1 2011 - 6	-1.7	0.02	-9.1	0.02
DL 7 1 2011 - 2	-1.4	0.02	-7.8	0.02		DL 10 1 2011 - 7	-1.7	0.01	-9.2	0.02
DL 7 1 2011 - 3	-1.1	0.01	-6.9	0.02		DL 10 1 2011 - 8	-1.6	0.03	-9.0	0.04
DL 7 1 2011 - 4	-2.6	0.02	-5.4	0.02		DL 10 1 2011 9	-1.5	0.01	-8.9	0.03
DL 7 1 2011 - 5	-1.3	0.02	-2.3	0.02		DL 10 1 2011 10	-1.5	0.01	-8.5	0.01

A3.1 (cont.) Serial Carbon and Oxygen values derived from pedogenic carbonate nodules. Standard deviations of individual measurements are also displayed.

References Cited

Adler, D., K. Wilkinson, S. Blockley, D. Mark, R. Pinhasi, B. Schmidt-Magee, S. Nahapetyan, C. Mallol, F. Berna and P. Glauberman

2014 Early Levallois technology and the Lower to Middle Paleolithic transition in the Southern Caucasus. *Science* 345(6204):1609-1613.

Aiello, L. C. and P. Wheeler

1995 The expensive-tissue hypothesis: the brain and the digestive system in human and primate evolution. *Current Anthropology* 36(2):199-221.

Ambrose, S. H.

1998 Late Pleistocene human population bottlenecks, volcanic winter, and differentiation of modern humans. *Journal of Human Evolution* 34(6):623-651.

2001a Middle and Later Stone Age settlement patterns in the Central Rift Valley, Kenya. In *Settlement dynamics in the Middle Paleolithic and Middle Stone Age*, edited by N. J. Conard, pp. 21-44. Kerns, Tübingen.

2001b Paleolithic technology and human evolution. *Science* 291:1748-1753.

2012 Obsidian Dating and Source Exploitation Studies in Africa. *Obsidian and Ancient Manufactured Glasses*.

Ambrose, S. H. and M. J. DeNiro

1986 The isotopic ecology of East African mammals. *Oecologia* 69(3):395-406.

Ambrose, S. H. and K. G. Lorenz

1990 Social and ecological models for the Middle Stone Age in southern Africa. *The emergence of modern humans: An archaeological perspective*:3-33.

Antón, M., A. Galobart and A. Turner

2005 Co-existence of scimitar-toothed cats, lions and hominins in the European Pleistocene. Implications of the post-cranial anatomy of Homotherium latidens (Owen) for comparative palaeoecology. *Quaternary Science Reviews* 24(10):1287-1301.

Ashley, G. M., D. Barboni, M. Dominguez-Rodrigo, H. T. Bunn, A. Z. P. Mabulla, F. Diez-Martin, R. Barba and E. Baquedano

2010 A spring and wooded habitat at FLK Zinj and their relevance to origins of human behavior. *Quaternary Research* 74(3):304-314.

Assefa, Z.

2006 Faunal remains from Porc-Epic: paleoecological and zooarchaeological investigations from a Middle Stone Age site in southeastern Ethiopia. *Journal of Human Evolution* 51(1):50-75.

Assefa, Z., S. Yirga and K. E. Reed

2008 The large-mammal fauna from the Kibish Formation. *Journal of Human Evolution* 55(3):501-512.

Ayliffe, L. K. and A. R. Chivas

1990 Oxygen isotope composition of the bone phosphate of Australian kangaroos: potential as a paleoenvironmental recorder. *Geochimica et Cosmochimica Acta* 54:2603-2609.

Baisden, W., R. Amundson, A. Cook and D. Brenner

2002 Turnover and storage of C and N in five density fractions from California annual grassland surface soils. *Global Biogeochemical Cycles* 16(4):64-61-64-16.

Balasse, M.

2002 Reconstructing dietary and environmental history from enamel isotopic analysis: time resolution of intra-tooth sequential sampling. *International Journal of Osteoarchaeology* 12:155-165.

2003 Potential biases in sampling design and interpretation of intra-tooth isotope analysis. *International Journal of Osteoarchaeology* 13(1-2):3-10.

Balasse, M., A. B. Smith, S. H. Ambrose and S. R. Leigh

2003 Determining Sheep Birth Seasonality by Analysis of Tooth Enamel Oxygen Isotope Ratios: The Late Stone Age Site of Kasteelberg (South Africa). *Journal of Archaeological Science* 30(2):205-215.

Basell, L. S.

2008 Middle Stone Age (MSA) site distributions in eastern Africa and their relationship to Quaternary environmental change, refugia and the evolution of Homo sapiens. *Quaternary Science Reviews* 27(27):2484-2498.

Bedaso, Z. K., J. G. Wynn, Z. Alemseged and D. Geraads

2010 Paleoenvironmental reconstruction of the Asbole fauna (Busidima Formation, Afar, Ethiopia) using stable isotopes. *Géobios* 43(2):165-177.

2013 Dietary and paleoenvironmental reconstruction using stable isotopes of herbivore tooth enamel from middle Pliocene Dikika, Ethiopia: Implication for Australopithecus afarensis habitat and food resources. *Journal of Human Evolution* 64(1):21-38.

Behrensmeyer, A. K.

2006 Climate change and human evolution. *Science(Washington)* 311(5760):476-478.

Behrensmeyer, A. K., R. Bobe and Z. Alemseged

2007 Approaches to the analysis of faunal change during the East African Pliocene. In *Hominin environments in the East African Pliocene: An assessment of the faunal evidence*, pp. 1-24. Springer.

Behrensmeyer, A. K. and A. P. Hill

1988 *Fossils in the making: vertebrate taphonomy and paleoecology*. University of Chicago Press.

Bell, R. H.

1982 The effect of soil nutrient availability on community structure in African ecosystems. In *Ecology of tropical savannas*, pp. 193-216. Springer.

Bender, M. M.

1971 Variations in the 13C/ 12C ratios of plants in relation to the pathway of photosynthetic carbon dioxide fixation. *Phytochemistry* 10(6):1239-1244.

Berna, F., P. Goldberg, L. K. Horwitz, J. Brink, S. Holt, M. Bamford and M. Chazan

2012 Microstratigraphic evidence of in situ fire in the Acheulean strata of Wonderwerk Cave, Northern Cape province, South Africa. *Proceedings of the National Academy of Sciences of the United States of America* 109(20):E1215-E1220.

Bibi, F.

2013 A multi-calibrated mitochondrial phylogeny of extant Bovidae (Artiodactyla, Ruminantia) and the importance of the fossil record to systematics. *BMC evolutionary biology* 13(1):166.

Bibi, F., M. Bukhsianidze, A. W. Gentry, D. Geraads, D. S. Kostopoulos and E. S. Vrba

2009 The fossil record and evolution of bovidae: State of the field. *Palaeontologia Electronica* 12(3).

Binford, L. R.

1980 Willow smoke and dogs' tails: hunter-gatherer settlement systems and archaeological site formation. *American antiquity*:4-20.

Birkeland, P.

1999 Soils and Geomorphology. Oxford University Press, New York.

Blegen, N. T.

2015 The Middle Stone Age on the Margins: Chronological and Archaeological Contexts for Hominin Behavioral Evolution in the Middle and Late Pleistocene of East Africa. Doctoral Dissertation, Anthropology, University of Connecticut, Storrs, CT.

Blome, M. W., A. S. Cohen, C. A. Tryon, A. S. Brooks and J. Russell

2012 The environmental context for the origins of modern human diversity: a synthesis of regional variability in African climate 150,000–30,000 years ago. *Journal of Human Evolution* 62(5):563-592.

Blumenschine, R. J., F. T. Masao, H. Stollhofen, I. G. Stanistreet, M. K. Bamford, R. M. Albert, J. K. Njau and K. A. Prassack

2012 Landscape distribution of Oldowan stone artifact assemblages across the fault compartments of the eastern Olduvai Lake Basin during early lowermost Bed II times. *Journal of human evolution* 63(2):384-394.

Blumenschine, R. J., C. R. Peters, S. D. Capaldo, P. Andrews, J. K. Njau and B. L. Pobiner

2007 Vertebrate taphonomic perspectives on Oldowan hominin land use in the Plio-Pleistocene Olduvai Basin, Tanzania. *Breathing Life into Fossils: Taphonomic Studies in Honor of CK (Bob) Brain. Stone Age Institute Press, Gosport, Indiana*:161-179.

Bobe, R. and A. K. Behrensmeyer

2004 The expansion of grassland ecosystems in Africa in relation to mammalian evolution and the origin of the genus Homo. *Palaeogeography, Palaeoclimatology, Palaeoecology* 207(3):399-420.

Boone, R. B., S. J. Thirgood and J. G. C. Hopcraft

2006 Serengeti wildebeest migratory patterns modeled from rainfall and new vegetation growth. *Ecology* 87(8):1987-1994.

Box, E. O., B. N. Holben and V. Kalb

1989 Accuracy of the AVHRR vegetation index as a predictor of biomass, primary productivity and net CO2 flux. *Vegetatio* 80(2):71-89.

Brantingham, P. J.

2003 A neutral model of stone raw material procurement. *American Antiquity*:487-509.

Bräuer, G.

2008 The origin of modern anatomy: By speciation or intraspecific evolution? *Evolutionary Anthropology: Issues, News, and Reviews* 17(1):22-37.

Braun, D. R., M. J. Rogers, J. W. Harris and S. J. Walker

2008 Landscape-scale variation in hominin tool use: evidence from the developed Oldowan. *Journal of Human Evolution* 55(6):1053-1063.

Breecker, D. O., Z. D. Sharp and L. D. McFadden

2009 Seasonal bias in the formation and stable isotopic composition of pedogenic carbonate in modern soils from central New Mexico, USA. *GSA Bulletin* 121(3-4):630-640.

Brooks, A. S., D. M. Helgren, J. S. Cramer, A. Franklin, W. Hornyak, J. M. Keating, R. G. Klein, W. J. Rink, H. P. Schwarcz, J. N. L. Smith, K. M. Stewart, N. E. Todd, J. Verniers and J. E. Yellen

1995 Dating and context of three Middle Stone Age sites with bone points in the Upper Semliki Valley, Zaire. *Science* 268:548-553.

Brooks, A. S., R. Potts and J. E. Yellen

2014 Early Levallois tEchnology and Its Implications: New Data from Olorgesailie, Kenya. Paper presented at the Society for American Archaeology, Austin, Texas.

Brooks, A. S., J. E. Yellen, L. Nevell and G. Hartman

2006 Projectile technologies of the African MSA: implications for modern human origins. In *Transitions before the transition*, edited by E. Hovers and S. L. Kuhn, pp. 233-256. Interdisciplinary contributions to archaeology, M. Joachim, general editor, New-York.

Brovkin, V., A. Cherkinsky and S. Goryachkin

2008 Estimating soil carbon turnover using radiocarbon data: A case-study for European Russia. *Ecological modelling* 216(2):178-187.

Brown, F. H., I. McDougall and J. G. Fleagle

2012 Correlation of the KHS Tuff of the Kibish Formation to volcanic ash layers at other sites, and the age of early Homo sapiens (Omo I and Omo II). *Journal of human evolution* 63(4):577-585.

Bryant, J. D. and P. N. Froelich

1995 A model of oxygen isotope fractination in body water of large mammals. *Geochimica et Cosmochimica Acta* 59(21):4523-4537.

Bunn, H. T.

2001 *Hunting, power scavenging, and butchering by Hadza foragers and by Plio-Pleistocene Homo*. Meat-Eating and Human Evolution. Oxford University Press, Oxford.

Cerling, T. E.

1984 The stable isotopic composition of modern soil carbonate and its relationship to climate. *Earth and Planetary Science Letters* 71(2):229-240.

1991 Carbon dioxide in the atmosphere: evidence from Cenozoic and Mesozoic paleosols. *American Journal of Science;(United States)* 291(4).

Cerling, T. E., S. A. Andanje, S. A. Blumenthal, F. H. Brown, K. L. Chritz, J. M. Harris, J. A. Hart, F. M. Kirera, P. Kaleme and L. N. Leakey

2015 Dietary changes of large herbivores in the Turkana Basin, Kenya from 4 to 1 Ma. *Proceedings of the National Academy of Sciences* 112(37):11467-11472.

Cerling, T. E. and J. M. Harris

1999 Carbon isotope fractionation between diet and bioapatite in ungulate mammals and implications for ecological and paleecological studies. *Oecologia* 120:347-363.

Cerling, T. E., J. M. Harris and B. H. Passey

2003 Diets of East African Bovidae based on Stable Isotope Analysis. *Journal of mammalogy* 84(2):456-470.

Cerling, T. E., N. E. Levin and B. H. Passey

2011 Stable Isotope Ecology in the Omo-Turkana Basin. *Evolutionary Anthropology: Issues, News, and Reviews* 20(6):228-237.

Cerling, T. E., W. D. Mace, M. Davis and C. Remien

2015 How hot is it anyway? Daily skin-surface soil temperature in East Africa. Paper presented at the Geological Society of America, Baltimore, MD.

Cerling, T. E. and J. Quade

1993 Stable carbon and oxygen isotopes in soil carbonates. *Climate change in continental isotopic records*:217-231.

Cerling, T. E., J. Quade, Y. Wang and J. R. Bowman

1989 Carbon isotopes in soils and paleosols as ecology and paleoecology indicators. *Nature* 341(6238):138-139.

Cerling, T. E., D. K. Solomon, J. Quade and J. R. Bowman

1991 On the isotopic composition of carbon in soil carbon dioxide. *Geochimica et Cosmochimica Acta* 55(11):3403-3405.

Cerling, T. E., G. Wittemyer, J. R. Ehleringer, C. H. Remien and I. Douglas-Hamilton

2009 History of animals using isotope records (HAIR): a 6-year dietary history of one family of African elephants. *Proceedings of the National Academy of Sciences* 106(20):8093-8100.

Cerling, T. E., J. G. Wynn, S. A. Andanje, M. I. Bird, D. K. Korir, N. E. Levin, W. MacE, A. N. MacHaria, J. Quade and C. H. Remien

2011 Woody cover and hominin environments in the past 6-million years. *Nature* 476(7358):51-56.

Chazan, M. and L. K. Horwitz

2006 Finding the message in intricacy: the association of lithics and fauna on Lower Paleolithic multiple carcass sites. *Journal of Anthropological Archaeology* 25(4):436-447.

Chenery, C. A., V. Pashley, A. L. Lamb, H. J. Sloane and J. A. Evans

2012 The oxygen isotope relationship between the phosphate and structural carbonate fractions of human bioapatite. *Rapid Communications in Mass Spectrometry* 26(3):309-319.

Churchill, S. E.

1993 Weapon technology, prey size selection, and hunting methods in modern hunter-gatherers: Implications for hunting in the Palaeolithic and Mesolithic. *Archeological Papers of the American Anthropological Association* 4(1):11-24.

Clark, A. M.

1999 Late Pleistocene technology at Rose Cottage Cave: A search for modern behavior in an MSA context. *African Archaeological Review* 16(2):93-119.

Clark, G.

1977 *World prehistory: in new perspective*. Cambridge University Press.

Clark, J. D.

1988 The Middle Stone Age of East Africa and the beginnings of regional identity. *Journal of World Prehistory* 2(3):235-305.

Clark, J. D.

1994 The Acheulian industrial complex in Africa and elsewhere. *Integrative Paths to the Past: Paleoanthropological Advances in Honor of F. Clark Howell. Prentice-Hall, Englewood Cliffs, NJ*:451-469.

Clark, J. D.

2001 Ecological and behavioral implications of the siting of Middle Stone Age rockshelter and cave settlements in Africa. In *Settlement dynamics of the Middle Paleolithic and Middle Stone Age*, edited by N. J. Conard, pp. 91-98. Kerngs, Tübingen.

Clark, J. D.

2001 Variability in primary and secondary technologies of the Later Acheulian in Africa. *A very remote period indeed: papers on the palaeolithic presented to Derek Roe. Oxbow Books, Oxford*:1-18.

Clark, J. D., Y. Beyene, G. WoldeGabriel, W. K. Hart, P. R. Renne, H. Gilbert, A. Defleur, G. Suwa, S. Katoh, K. R. Ludwig, J. R. Boisserie, B. Asfaw and T. D. White

2003 Stratigraphic, chronological and behavioural contexts of Pleistocene Homo sapiens from Middle Awash, Ethiopia. *Nature* 423(6941):747-752.

Clark, J. D. and J. W. Harris

1985 Fire and its roles in early hominid lifeways. *African Archaeological Review* 3(1):3-27.

Clark, J. D. and M. R. Kleindienst

1974 The Stone Age cultural sequence: terminology, typology and raw material. *Kalambo falls prehistoric Site* 2:71-106.

Clark, P. U., D. Archer, D. Pollard, J. D. Blum, J. A. Rial, V. Brovkin, A. C. Mix, N. G. Pisias and M. Roy

2006 The middle Pleistocene transition: characteristics. mechanisms, and implications for long-term changes in atmospheric PCO2. *Quaternary Science Reviews* 25(23-24):3150-3184.

Coe, R. S., B. S. Singer, M. S. Pringle and X. Zhao

2004 Matuyama–Brunhes reversal and Kamikatsura event on Maui: paleomagnetic directions, 40 Ar/39 Ar ages and implications. *Earth and Planetary Science Letters* 222(2):667-684.

Cohen, A., C. Campisano, R. Arrowsmith, A. Asrat, A. Behrensmeyer, A. Deino, C. Feibel, A. Hill, R. Johnson and J. Kingston

2016 The Hominin Sites and Paleolakes Drilling Project: inferring the environmental context of human evolution from eastern African rift lake deposits. *Scientific Drilling* 21:1.

Coppens, Y.

1975 Évolution des hominidés et de leur environnement au cours du plio-pleistocene dans la basse vallée de l'Omo en Éthiopie. *Comptes Rendus de l'Académie des Sciences* 281:1693-1696.

Cornelissen, E.

1992 *Site GNJH-17 and its implications for the Archaeology of the Middle Kapthurin Formation, Baringo, Kenya* 133. Koninklijk Museum voor Midden Afrika.

Cornelissen, E., A. Boven, A. Dabi, J. Hus, K. J. Yong, E. Keppens, R. Langohr, J. Moeyersons, P. Pasteels and M. Pieters

1990 The Kapthurin formation revisited. *African Archaeological Review* 8(1):23-75.

Crittenden, A. N.

2011 The importance of honey consumption in human evolution. *Food and Foodways* 19(4):257-273.

Curnoe, D., A. Herries, J. Brink, P. Hopley, K. van Reyneveld, Z. Henderson and D. Morris

2006 Discovery of Middle Pleistocene fossil and stone tool-bearing deposits at Groot Kloof, Ghaap escarpment, Northern Cape province. *South African journal of science* 102(5/6):180.

Dagley, P., A. E. Mussett and H. Palmer

1978 Preliminary observations on the palaeomagnetic stratigraphy of the area west of Lake Baringo, Kenya. *Geological Society, London, Special Publications* 6(1):225-235.

Dansgaard, W.

1964 Stable isotope in precipitation. *Tellus* 16:436-468.

Darwin, C.

1871 *The descent of man: and selection in relation to sex*. Murray, London.

Daux, V., C. Lécuyer, M.-A. Héran, R. Amiot, L. Simon, F. Fourel, F. Martineau, N. Lynnerup, H. Reychler and G. Escarguel

2008 Oxygen isotope fractionation between human phosphate and water revisited. *Journal of human evolution* 55(6):1138-1147.

Davenport, M. and S. Nicholson

1993 On the relation between rainfall and the Normalized Difference Vegetation Index for diverse vegetation types in East Africa. *International Journal of Remote Sensing* 14(12):2369-2389.

Deino, A. L., J. D. Kingston, J. M. Glen, R. K. Edgar and A. Hill

2006 Precessional forcing of lacustrine sedimentation in the late Cenozoic Chemeron Basin, Central Kenya Rift, and calibration of the Gauss/Matuyama boundary. *Earth and Planetary Science Letters* 247(1):41-60.

Deino, A. L. and S. McBrearty

2002 40Ar/ 39Ar dating of the Kapthurin Formation, Baringo, Kenya. *Journal of Human Evolution* 42(1):185-210.

Deino, A. L., L. Tauxe, M. Monaghan and A. Hill

2002 Ar-40/Ar-30 geochronology and paleomagnetic stratigraphy of the Lukeino and lower Chemeron Formations at Tabarin and Kapcheberek, Tugen Hills, Kenya. *Journal of human evolution* 42(1-2):117-140.

deMenocal, P. B.

1995 Plio-Pleistocene African Climate. *Science* 270(5233):53-59.

2004 African climate change and faunal evolution during the Pliocene–Pleistocene. *Earth and Planetary Science Letters* 220(1):3-24.

2011 Climate and human evolution. *Science* 331(6017):540-542.

deMenocal, P. B., J. Ortiz, T. Guilderson, J. Adkins, M. Sarnthein, L. Baker and M. Yarusinsky

2000 Abrupt onset and termination of the African Humid Period: rapid climate responses to gradual insolation forcing. *Quaternary Science Reviews* 19(1-5):347-361.

DeNiro, M. J. and S. Epstein

1978a Carbon isotopic evidences for different feeding patterns in two hyrax species occupying the same habitat. *Science* 201:906-908.

1978b Influence of diet on distribution of carbon isotopes in animals. *Geochimica et Cosmochimica Acta* 42(5):495-506.

Dennell, R.

2005 The Solo (Ngandong) Homo erectus assemblage: a taphonomic assessment. *Archaeology in Oceania* 40(3):81-90.

Domínguez-Rodrigo, M., H. Bunn, A. Mabulla, E. Baquedano, D. Uribelarrea, A. Pérez-González, A. Gidna, J. Yravedra, F. Diez-Martin and C. Egeland

2014 On meat eating and human evolution: A taphonomic analysis of BK4b (Upper Bed II, Olduvai Gorge, Tanzania), and its bearing on hominin megafaunal consumption. *Quaternary International* 322:129-152.

Dominguez-Rodrigo, M., J. Serrallonga, J. Juan-Tresserras, L. Alcala and L. Luque

2001 Woodworking activities by early humans: a plant residue analysis on Acheulian stone tools from Peninj (Tanzania). *Journal of Human Evolution* 40(4):289-299.

Dongmann, G., H. Nürnberg, H. Förstel and K. Wagener

1974 On the enrichment of H2 18O in the leaves of transpiring plants. *Radiation and environmental biophysics* 11(1):41-52.

Douze, K. and A. Delagnes

2016 The pattern of emergence of a Middle Stone Age tradition at Gademotta and Kulkuletti (Ethiopia) through convergent tool and point technologies. *Journal of Human Evolution* 91:93-121.

Dugatkin, L. A.

2004 *Principles of animal behavior*. WW Norton New York, New York, USA.

Dunkley, P., M. Smith, D. Allen and W. Darling

1993 The geothermal activity and geology of the northern sector of the Kenya Rift Valley.

Dunnell, R. C. and W. S. Dancey

1983 The siteless survey: a regional scale data collection strategy. *Advances in archaeological method and theory* 6:267-287.

Ebert, J. I.

1992 *Distributional archaeology*. University of Utah Press.

Ehleringer, J. R.

1978 Implications of quantum yield differences on distributions of C_3 and C_4 grasses. *Oecologia* 31(3):255-267.

Ehleringer, J. R., T. E. Cerling and B. R. Helliker

1997 C_4 photosynthesis, atmospheric CO_2 and climate. *Oecologia* 112(3):285-299.

Ehleringer, J. R. and T. E. Dawson

1992 Water uptake by plants: perspectives from stable isotope composition. *Plant, Cell & Environment* 15(9):1073-1082.

Ehleringer, J. R., Z. F. Lin, C. B. Field, G. C. Sun and C. Y. Kuo

1987 Leaf carbon isotope ratios of plants from a subtropical monsoon forest. *Oecologia* 72(1):109-114.

Ehleringer, J. R. and R. K. Monson

1993 Evolutionary and ecological aspects of photosynthetic pathway variation. *Annual Review of Ecology and Systematics* 24:411-439.

Faith, J. T.

2008 Eland, buffalo, and wild pigs: were Middle Stone Age humans ineffective hunters? *Journal of Human Evolution* 55(1):24-36.

Faith, J. T., M. Domínguez-Rodrigo and A. D. Gordon

2009 Long-distance carcass transport at Olduvai Gorge? A quantitative examination of Bed I skeletal element abundances. *Journal of Human Evolution* 56(3):247-256.

Faith, J. T., R. Potts, T. W. Plummer, L. C. Bishop, C. W. Marean and C. A. Tryon

2012 New perspectives on middle Pleistocene change in the large mammal faunas of East Africa: Damaliscus hypsodon sp. nov.(Mammalia, Artiodactyla) from Lainyamok, Kenya. *Palaeogeography, Palaeoclimatology, Palaeoecology* 361:84-93.

Farquhar, G. D., J. R. Ehleringer and K. T. Hubick

1989 Carbon Isotope Discrimination and Photosynthesis. *Annual Review of Plant Physiology and Plant Molecular Biology* 40:503-537.

Foley, R.

1981 Off-site archaeology and human adaption in East Africa. BAR Int Ser.

Fricke, H. C., W. C. Clyde, J. R. O'Neil and P. D. Gingerich

1998 Evidence for rapid climate change in North America during the latest Paleocene thermal maximum: oxygen isotope compositions of biogenic phosphate from the Bighorn Basin (Wyoming). *Earth and Planetary Science Letters* 160(1):193-208.

Fricke, H. C. and J. R. O'Neil

1996 Inter-and intra-tooth variation in the oxygen isotope composition of mammalian tooth enamel phosphate: implications for palaeoclimatological and palaeobiological research. *Palaeogeography, Palaeoclimatology, Palaeoecology* 126(1):91-99.

Friedman, I. and J. R. O'Neil

1977 *Data of geochemistry: Compilation of stable isotope fractionation factors of geochemical interest* 440. US Government Printing Office.

Galef, B. G. and L.-A. Giraldeau

2001 Social influences on foraging in vertebrates: causal mechanisms and adaptive functions. *Animal behaviour* 61(1):3-15.

Gentry, A. W.

1978 Bovidae. In *Evolution of African Mammals*, edited by V. J. Maglio and H. B. S. Cooke, pp. 540-572. Harvard University Press, Cambridge, MA.

Gentry, A. W., L. Werdelin and W. J. Sanders

2010 Bovidae. In *Cenozoic Mammals of Africa*. University of California Press, Berkeley.

Gifford, D. P. and A. K. Behrensmeyer

1977 Observed formation and burial of a recent human occupation site in Kenya. *Quaternary Research* 8(3):245-266.

Hardy, B. L. and G. T. Garufi

1998 Identification of woodworking on stone tools through residue and use-wear analyses: experimental results. *Journal of Archaeological Science* 25(2):177-184.

Hartman, G.

2011 Reconstructing Mid-Pleistocene paleovegetation and paleoclimate in the Golan Heights using the $\delta^{13}C$ values of modern vegetation and soil organic carbon of paleosols. *Journal of Human Evolution* 60:452-463.

Hawkes, K., J. F. O'Connell and N. G. B. Jones

2001 Hadza meat sharing. *Evolution and Human Behavior* 22(2):113-142.

Henry, A. G., A. S. Brooks and D. R. Piperno

2014 Plant foods and the dietary ecology of Neanderthals and early modern humans. *Journal of human evolution* 69:44-54.

Henshilwood, C., F. d'Errico, R. Yates, Z. Jacobs, C. Tribolo, G. A. T. Duller, N. Mercier, J. C. Sealy, H. Valladas, I. Watts and A. G. Wintle

2002 Emergance of modern human behavior: Middle Stone Age engravings from South Africa. *Science* 295:1278-1280.

Henshilwood, Christopher S. and Curtis W. Marean

2003 The Origin of Modern Human Behavior: Critique of the Models and Their Test Implications. *Current Anthropology* 44(5):627-651.

Henshilwood, C. S. and C. W. Marean

2003 The origins of modern human behavior. Critique of the models and their test implications. *Current Anthropology* 44(5):627-651.

Higgins, J. A., A. V. Kurbatov, N. E. Spaulding, E. Brook, D. S. Introne, L. M. Chimiak, Y. Yan, P. A. Mayewski and M. L. Bender

2015 Atmospheric composition 1 million years ago from blue ice in the Allan Hills, Antarctica. *Proceedings of the National Academy of Sciences*:201420232.

Higgins, J. A., A. V. Kurbatov, N. E. Spaulding, E. Brook, D. S. Introne, L. M. Chimiak, Y. Yan, P. A. Mayewski and M. L. Bender

2015 Atmospheric composition 1 million years ago from blue ice in the Allan Hills, Antarctica. *Proceedings of the National Academy of Sciences* 112(22):6887-6891.

Hilgen, F.

1991 Astronomical calibration of Gauss to Matuyama sapropels in the Mediterranean and implication for the geomagnetic polarity time scale. *Earth and planetary science letters* 104(2):226-244.

Hill, A.

1979 Disarticulation and scattering of mammal skeletons. *Paleobiology* 5(3):261-274.

Hill, A., G. Curtis and R. Drake

1986 Sedimentary stratigraphy of the Tugen Hills, Baringo, Kenya. *Geological Society Special Publication* 25:285-295.

Hill, K., H. Kaplan, K. Hawkes and A. M. Hurtado

1987 Foraging decisions among Ache hunter-gatherers: new data and implications for optimal foraging models. *Ethology and Sociobiology* 8(1):1-36.

Hillenbrand, C. D., G. Kuhn and T. Frederichs

2009 Record of a Mid-Pleistocene depositional anomaly in West Antarctic continental margin sediments: an indicator for ice-sheet collapse? *Quaternary Science Reviews* 28(13):1147-1159.

Hoppe, K. A., S. M. Stover, J. R. Pascoe and R. Amundson

2004 Tooth enamel biomineralization in extant horses: implications for isotopic microsampling. *Palaeogeography, Palaeoclimatology, Palaeoecology* 206(3):355-365.

Hunt, E. R., Jr.

1994 Relationship between woody biomass and PAR conversion efficiency for estimating net primary production from NDVI. *International Journal of Remote Sensing* 15(8):1725-1729.

Indermuhle, A., T. F. Stocker, F. Joos, H. Fischer, H. J. Smith, M. Wahlen, B. Deck, D. Mastroianni, J. Tschumi, T. Blunier, R. Meyer and B. Stauffer

1999 Holocene carbon-cycle dynamics based on CO2 trapped in ice at Taylor Dome, Antarctica. *Nature* 398(6723):121-126.

Isaac, G. L.

1972 Identification of cultural entities in the Middle Pleistocene. In *Actes de 6° Session, Congrès Panafricain de Préhistoire Dakar*, pp. 556-562. Les Imprimeries Réunies de Chambéry Chambéry.

Isaac, G. L. and B. Isaac

1977 *Olorgesailie: archeological studies of a Middle Pleistocene lake basin in Kenya*. University of Chicago Press, Chicago.

James, S. R., R. Dennell, A. S. Gilbert, H. T. Lewis, J. Gowlett, T. F. Lynch, W. McGrew, C. R. Peters, G. G. Pope and A. B. Stahl

1989 Hominid use of fire in the Lower and Middle Pleistocene: A review of the evidence [and comments and replies]. *Current Anthropology* 30(1):1-26.

Jarman, M. R., C. Vita-Finzi and E. S. Higgs

1972 Site catchment analysis in archaeology. *Man, settlement and urbanism*:61-66.

Jenny, H.

1980 *The soil resource: origin and behavior*. Springer New York.

Johnson, C. R., G. M. Ashley, C. B. De Wet, R. Dvoretsky, L. Park, V. C. Hover, R. B. Owen and S. McBrearty

2009 Tufa as a record of perennial fresh water in a semi-arid rift basin, Kapthurin Formation, Kenya. *Sedimentology* 56(4):1115-1137.

Johnson, C. R. and S. McBrearty

2010 500,000 year old blades from the Kapthurin Formation, Kenya. *Journal of Human Evolution* 58(2):193-200.

2012 Archaeology of middle Pleistocene lacustrine and spring paleoenvironments in the Kapthurin Formation, Kenya. *Journal of Anthropological Archaeology* 31(4):485-499.

Johnston, C. A.

1998 *Geographic information systems in ecology*. Blackwell Science.

Kaplan, H. and K. Hill

1985 Hunting ability and reproductive success among male Ache foragers: Preliminary results. *Current anthropology* 26(1):131-133.

Kelly, R. L.

1995 The foraging spectrum. Washington, DC: Smithsonian Institution Press.

Kim, S.-T. and J. R. O'Neil

1997 Equilibrium and nonequilibrium oxygen isotope effects in synthetic carbonates. *Geochimica et Cosmochimica Acta* 61(16):3461-3475.

Kingdon, J.

1988 *East African mammals: An Atlas of Evolution in Africa*. University of Chicago Press, Chicago.

Kingston, J. D.

2007 Shifting adaptive landscapes: Progress and challenges in reconstructing early hominid environments. *Yearbook of Physical Anthropology* 50(S45):20-58.

Kingston, J. D., A. L. Deino, R. K. Edgar and A. Hill

2007 Astronomically forced climate change in the Kenyan Rift Valley 2.7–2.55 Ma: implications for the evolution of early hominin ecosystems. *Journal of Human Evolution* 53(5):487-503.

Kingston, J. D. and T. Harrison

2007 Isotopic dietary reconstructions of Pliocene herbivores at Laetoli: Implications for early hominin paleoecology. *Palaeogeography, Palaeoclimatology, Palaeoecology* 243(3):272-306.

Kingston, J. D., A. Hill and B. D. Marino

1994 Isotopic evidence for Neogene hominid paleoenvironments in the Kenya Rift Valley. *Science* 264(5161):955-959.

Kipkorir, E.

2002 Analysis of rainfall climate on the Njemps flats, Baringo District, Kenya. *Journal of arid environments* 50(3):445-458.

Klein, R. G.

1982 Age (mortality) profiles as a means of distinguishing hunted species from scavenged ones in Stone Age archaeological sites. *Paleobiology* 8(2):151-158.

1988 The archaeological significance of animal bones from Acheulean sites in southern Africa. *African Archaeological Review* 6(1):3-25.

2009 *The human career: human biological and cultural origins*. University of Chicago Press.

Koch, P. L.

1998 Isotopic reconstruction of past continental environments. *Annual Review of Earth and Planetary Sciences* 26:573-613.

Koch, P. L., D. C. Fisher and D. Dettman

1989 Oxygen isotope variation in the tusks of extinct proboscideans: A measure of season of death and seasonality. *Geology* 17(6):515-519.

Koch, P. L., N. Tuross and M. L. Fogel

1997 The effects of sample treatment and diagenesis on the isotopic integrity of carbonate in biogenic hydroxylapatite. *Journal of Archaeological Science* 24(5):417-429.

Kohn, M. J.

1996 Predicting animal $\delta^{18}O$: accounting for diet and physiological adaptation. *Geochimica et Cosmochimica Acta* 60(23):4811-4829.

Kohn, M. J.

2010 Carbon isotope compositions of terrestrial C3 plants as indicators of (paleo) ecology and (paleo) climate. *Proceedings of the National Academy of Sciences* 107(46):19691-19695.

Kohn, M. J., M. J. Schoeninger and J. W. Valley

1996 Herbivore tooth oxygen isotope compositions: Effects of diet and physiology. *Geochimica Et Cosmochimica Acta* 60(20):3889-3896.

1998 Variability in oxygen isotope compositions of herbivore teeth: reflections of seasonality or developmental physiology. *Chemical Geology* 152:97-112.

Kormos, R., C. Boesch, M. I. Bakarr and T. M. Butynski

2003 *West African chimpanzees: Status survey and conservation action plan*. International Union for Conservation of Nature and Natural Resources.

Kukla, G. and V. Cílek

1996 Plio-Pleistocene megacycles: record of climate and tectonics. *Palaeogeography, Palaeoclimatology, Palaeoecology* 120(1):171-194.

Kurland, J. A. and S. J. Beckerman

1985 Optimal foraging and hominid evolution: labor and reciprocity. *American Anthropologist* 87(1):73-93.

Ladd, B., P. L. Peri, D. A. Pepper, L. C. R. Silva, D. Sheil, S. P. Bonser, S. W. Laffan, W. Amelung, A. Ekblad, P. Eliasson, H. Bahamonde, S. Duarte-Guardia, M. Bird and H. Cornelissen

2014 Carbon isotopic signatures of soil organic matter correlate with leaf area index across woody biomes. *Journal of Ecology* 102(6):1606-1611.

Leakey, M., P. V. Tobias, J. E. Martyn and R. E. Leakey

1969 An Acheulean Industry with Prepared Core Technique and the Discovery of a Contemporary Hominid Mandible at Lake Baringo, Kenya. *Proceedings of the Prehistoric Society (New Series)* 35:48-76.

Leakey, M. D.

1971 *Olduvai Gorge: Volume 3, Excavations in Beds I and II, 1960-1963*. University Press.

Lee, R. B.

1984 *The Dobe! Kung*. Holt Rinehart & Winston.

Lepre, C. J., H. Roche, D. V. Kent, S. Harmand, R. L. Quinn, J.-P. Brugal, P.-J. Texier, A. Lenoble and C. S. Feibel

2011 An earlier origin for the Acheulian. *Nature* 477(7362):82-85.

Leslie, D. E., S. McBrearty and G. Hartman

2014 Stable Isotopic Evidence for Landscape Environmental Reconstructions, Kapthurin Formation, Kenya. Paper presented at the Society for American Archaeology, Austin, Texas.

2016 A Middle Pleistocene intense monsoonal episode from the Kapthurin Formation, Kenya: Stable isotopic evidence from bovid teeth and pedogenic carbonates. *Palaeogeography, Palaeoclimatology, Palaeoecology* 449:27-40.

Leuenberger, M., U. Siegenthaler and C. C. Langway

1992 Carbon isotope composition of atmospheric CO_2 During the last ice-age from an Antarctic ice core. *Nature* 357(6378):488-490.

Levin, N. E., F. H. Brown, A. K. Behrensmeyer, R. Bobe and T. E. Cerling

2011 Paleosol carbonates from the Omo Group: Isotopic records of local and regional environmental change in East Africa. *Palaeogeography, Palaeoclimatology, Palaeoecology* 307(1):75-89.

Levin, N. E., T. E. Cerling, B. H. Passey, J. M. Harris and J. R. Ehleringer

2006 A stable isotope aridity index for terrestrial environments. *Proceedings of the National Academy of Sciences of the United States of America* 103:11201-11205.

Levin, N. E., J. Quade, S. W. Simpson, S. Semaw and M. Rogers

2004 Isotopic evidence for Plio–Pleistocene environmental change at Gona, Ethiopia. *Earth and Planetary Science Letters* 219(1):93-110.

Levin, N. E., E. J. Zipser and T. E. Cerling

2009 Isotopic composition of waters from Ethiopia and Kenya: insights into moisture sources for eastern Africa. *Journal of Geophysical Research: Atmospheres (1984–2012)* 114(D23).

Lisiecki, L. E. and M. E. Raymo

2005 A Pliocene-Pleistocene stack of 57 globally distributed benthic $\delta^{18}O$ records. *Paleoceanography* 20(1):1-17.

Loftus, E., P. Roberts and J. A. Lee-Thorp

2016 An isotopic generation: four decades of stable isotope analysis in African archaeology. *Azania: Archaeological Research in Africa* 51(1):88-114.

Lüthi, D., M. Le Floch, B. Bereiter, T. Blunier, J. M. Barnola, U. Siegenthaler, D. Raynaud, J. Jouzel, H. Fischer, K. Kawamura and T. F. Stocker

2008 High-resolution carbon dioxide concentration record 650,000-800,000 years before present. *Nature* 453(7193):379-382.

Luxwolda, M. F., R. S. Kuipers, I. P. Kema, D. J. Dijck-Brouwer and F. A. Muskiet

2012 Traditionally living populations in East Africa have a mean serum 25-hydroxyvitamin D concentration of 115 nmol/l. *British Journal of Nutrition* 108(09):1557-1561.

Luxwolda, M. F., R. S. Kuipers, I. P. Kema, E. van der Veer, D. J. Dijck-Brouwer and F. A. Muskiet

2013 Vitamin D status indicators in indigenous populations in East Africa. *European journal of nutrition* 52(3):1115-1125.

Marean, C. W.

1992 Implications of late Quaternary mammalian fauna from Lukenya Hill (south-central Kenya) for paleoenvironmental change and faunal extinctions. *Quaternary Research* 37(2):239-255.

1997 Hunter–gatherer foraging strategies in tropical grasslands: model building and testing in the East African Middle and Later Stone Age. *Journal of Anthropological Archaeology* 16(3):189-225.

Marlowe, F. W.

2005 Hunter-gatherers and human evolution. *Evolutionary Anthropology: Issues, News, and Reviews* 14(2):54-67.

2010 *The Hadza: hunter-gatherers of Tanzania* 3. Univ of California Press.

Marlowe, F. W. and J. C. Berbesque

2009 Tubers as fallback foods and their impact on Hadza hunter-gatherers. *American Journal of Physical Anthropology* 140(4):751-758.

Martyn, J.

1969 Geological history of the country between Lake Baringo and the Kerio river, Baringo district, Kenya, Royal Holloway, University of London.

McBrearty, S.

1999 Archaeology of the Kapthurin formation. In *Late Cenozoic environments and hominid evolution: a tribute to Bill Bishop*, edited by P. Andrews and P. Banham, pp. 143-156. Geological Society of London & Scottish Academic Press, London.

2001 The Middle Pleistocene of East Africa. In *Human Roots: Africa and Asia in the Middle Pleistocene*, edited by L. H. Barham and K. Robson-Brown, pp. 81-97. Western Academic & Specialist Press, Bristol, U.K.

McBrearty, S., L. Bishop and J. Kingston

1996 Variability in traces of Middle Pleistocene hominid behavior in the Kapthurin Formation, Baringo, Kenya. *Journal of Human Evolution* 30(6):563-580.

McBrearty, S. and A. S. Brooks

2000 The revolution that wasn't: a new interpretation of the origion of modern human behavior. *Journal of Human Evolution* 39 (5):453-563.

McBrearty, S., A. Deino and C. Tryon

2001 Chronology of Middle Pleistocene events in the Kapthurin Formation, Baringo, Kenya. *Journal of Human Evolution* 40(3):A14-A14.

McBrearty, S. and N. G. Jablonski

2005 First fossil chimpanzee. *Nature* 437(7055):105-108.

McCarthy, T., W. Ellery, L. Backwell, P. Marren, B. De Klerk, S. Tooth, D. Brandt and S. Woodborne

2010 The character, origin and palaeoenvironmental significance of the Wonderkrater spring mound, South Africa. *Journal of African Earth Sciences* 58(1):115-126.

McDougall, I., F. H. Brown and J. G. Fleagle

2008 Sapropels and the age of hominins Omo I and II, Kibish, Ethiopia. *Journal of Human Evolution* 55(3):409-420.

Medina, E. and P. Minchin

1980 Stratification of δ13C values of leaves in Amazonian rain forests. *Oecologia* 45(3):377-378.

Mehlman, M. J.

1989 Later Quaternary archaeological sequences in northern Tanzania, University of Illinois at Urbana-Champaign.

Mehrer, M. W. and K. L. Wescott

2005 *GIS and archaeological site location modeling*. crc Press.

Merrick, H. V., F. H. Brown and W. P. Nash

1994 Use and movement of obsidian in the Early and Middle Stone Ages of Kenya and northern Tanzania. *Society, culture, and technology in Africa* 11(6):29-44.

Mikkelsen, N.

1977 On the origin ofEthmodiscus ooze. *Marine Micropaleontology* 2:35-46.

Milo, R. G.

1998 Evidence for Hominid Predation at Klasies River Mouth, South Africa, and its Implications for the Behaviour of Early Modern Humans. *Journal of Archaeological Science* 25(2):99-133.

Morgan, L. E. and P. R. Renne

2008 Diachronous dawn of Africa's Middle Stone Age: new 40Ar/39Ar ages from the Ethiopian Rift. *Geology* 36(12):967-970.

Müller, G. and M. Gastner

1971 The'Karbonat-Bombe', a simple device for the determination of carbonate content in sediment, soils, and other materials. *Neues Jahrbuch für Mineralogie-Monatshefte* 10:466-469.

Murray, S. S., M. J. Schoeninger, H. T. Bunn, T. R. Pickering and J. A. Marlett

2001 Nutritional composition of some wild plant foods and honey used by Hadza foragers of Tanzania. *Journal of food composition and analysis* 14(1):3-13.

Ngugi, M. K. and R. T. Conant

2008 Ecological and social characterization of key resource areas in Kenyan rangelands. *Journal of Arid Environments* 72(5):820-835.

Nicholson, S. E., M. L. Davenport and A. R. Malo

1990 A comparison of the vegetation response to rainfall in the Sahel and East Africa, using normalized difference vegetation index from NOAA AVHRR. *Climatic change* 17(2-3):209-241.

Niedermeyer, E. M., A. L. Sessions, S. J. Feakins and M. Mohtadi

2014 Hydroclimate of the western Indo-Pacific Warm Pool during the past 24,000 years. *Proceedings of the National Academy of Sciences* 111(26):9402-9406.

O'Connell, J. F., K. Hawkes and N. G. Blurton Jones

1999 Grandmothering and the evolution of *Homo erectus*. *Journal of Human Evolution* 36:461-485.

Oerter, E. J., W. D. Sharp, J. L. Oster, A. Ebeling, J. W. Valley, R. Kozdon, I. J. Orland, J. Hellstrom, J. D. Woodhead and J. M. Hergt

2016 Pedothem carbonates reveal anomalous North American atmospheric circulation 70,000–55,000 years ago. *Proceedings of the National Academy of Sciences*:201515478.

Oindo, B. O. and A. K. Skidmore

2002 Interannual variability of NDVI and species richness in Kenya. *International journal of remote sensing* 23(2):285-298.

Osmond, C., K. Winter and H. Ziegler

1982 Functional significance of different pathways of CO2 fixation in photosynthesis. In *Physiological plant ecology II*, pp. 479-547. Springer.

Passey, B. H., T. E. Cerling, G. T. Schuster, T. F. Robinson, B. L. Roeder and S. K. e. Krueger

2005 Inverse methods for estimating primary input signals from time-averaged isotope profiles. *Geochimica et Cosmochimica Acta* 69(16):4101-4116.

Passey, B. H., N. E. Levin, T. E. Cerling, F. H. Brown and J. M. Eiler

2010 High-temperature environments of human evolution in East Africa based on bond ordering in paleosol carbonates. *Proceedings of the National Academy of Sciences* 107(25):11245-11249.

Passey, B. H., T. F. Robinson, L. K. Ayliffe, T. E. Cerling, M. Sphonheimer, M. D. Dearing, B. L. Roeder and J. R. Ehleringer

2005 Carbon isotope fractionation between diet, breath CO2, and bioapatite in different mammals. *Journal of Archaeological Science* 32(10):1459-1470.

Peters, C. R. and R. J. Blumenschine

1995 Landscape perspectives on possible land use patterns for Early Pleistocene hominids in the Olduvai Basin, Tanzania. *Journal of human evolution* 29(4):321-362.

Petit, J. R., J. Jouzel, D. Raynaud, N. I. Barkov, J. M. Barnola, I. Basile, M. Bender, J. Chappellaz, M. Davis, G. Delaygue, M. Delmotte, V. M. Kotlyakov, M. Legrand, V. Y. Lipenkov, C. Lorius, L. Pepin, C. Ritz, E. Saltzman and M. Stievenard

1999 Climate and atmospheric history of the past 420,000 years from the Vostok ice core, Antarctica. *Nature* 399(6735):429-436.

Pettorelli, N., J. Bro-Jørgensen, S. M. Durant, T. Blackburn and C. Carbone

2009 Energy availability and density estimates in African ungulates. *The American Naturalist* 173(5):698-704.

Pettorelli, N., J. M. Gaillard, A. Mysterud, P. Duncan, D. Delorme, G. Van Laere, C. Toïgo and F. Klein

2006 Using a proxy of plant productivity (NDVI) to find key periods for animal performance: the case of roe deer. *Oikos* 112(3):565-572.

Pettorelli, N., S. J. Ryan, T. Mueller, N. Bunnefeld, B. Jedrzejewsk, M. Lima and K. Kausrud

2011 The Normalized Difference Vegetation Index (NDVI): unforeseen successes in animal ecology. *Climate Research* (46):15-27.

Pettorelli, N., J. O. Vik, A. Mysterud, J.-M. Gaillard, C. J. Tucker and N. C. Stenseth

2005 Using the satellite-derived NDVI to assess ecological responses to environmental change. *Trends in ecology & evolution* 20(9):503-510.

Pollard, A., M. Pellegrini and J. Lee-Thorp

2011 Technical note: Some observations on the conversion of dental enamel δ18op values to δ18ow to determine human mobility. *American journal of physical anthropology* 145(3):499-504.

Potts, R.

1989 Olorgesailie: new excavations and findings in Early and Middle Pleistocene contexts, southern Kenya rift valley. *Journal of Human Evolution* 18(5):477-484.

1991 Why the Oldowan? Plio-Pleistocene toolmaking and the transport of resources. *Journal of Anthropological Research*:153-176.

1996 Evolution and Climate Variability. *Science* 273(5277):922-923.

Potts, R.

1998 Variability selection in hominid evolution. *evolutionary Anthropology* 7:81-96.

Potts, R., A. K. Behrensmeyer and P. Ditchfield

1999 Paleolandscape variation and Early Pleistocene hominid activities: Members 1 and 7, Olorgesailie Formation, Kenya. *Journal of human evolution* 37(5):747-788.

Potts, R. and A. Deino

1995 Mid-Pleistocene change in large mammal faunas of East Africa. *Quaternary Research* 43(1):106-113.

Potts, R. and J. T. Faith

2015 Alternating high and low climate variability: The context of natural selection and speciation in Plio-Pleistocene hominin evolution. *Journal of Human Evolution* 87:5-20.

Quade, J., T. E. Cerling, J. C. Barry, M. E. Morgan, D. R. Pilbeam, A. R. Chivas, J. A. Leethorp and N. J. Vandermerwe

1992 A 16-Ma Record of Paleodiet using Carbon and Oxygen Isotopes in Fossil Teeth from Pakistan. *Chemical Geology* 94(3):183-192.

Quade, J., T. E. Cerling and J. R. Bowman

1989 Systematic variations in the carbon and oxygen isotopic composition of pedogenic carbonate along elevation transects in the southern Great Basin, United States. *Geological Society of America Bulletin* 101(4):464-475.

Quinn, R. L., C. J. Lepre, C. S. Feibel, J. D. Wright, R. A. Mortlock, S. Harmand, J. P. Brugal and H. Roche

2013 Pedogenic carbonate stable isotopic evidence for wooded habitat preference of early Pleistocene tool makers in the Turkana Basin. *Journal of human evolution* 65(1):65-78.

Rabinovich, R., O. Ackermann, E. Aladjem, R. Barkai, R. Biton, I. Milevski, N. Solodenko and O. Marder

2012 Elephants at the middle Pleistocene Acheulian open-air site of Revadim Quarry, Israel. *Quaternary International* 276:183-197.

Reed, K. E.

1997 Early hominid evolution and ecological change through the African Plio-Pleistocene. *Journal of human evolution* 32(2):289-322.

Renaut, R. W., J. Ego, J.-J. Tiercelin, C. Le Turdu and R. B. Owen

1999 Saline, alkaline palaeolakes of the Tugen Hills-Kerio Valley region, Kenya Rift Valley. *Late Cenozoic Environments and Hominid Evolution: A Tribute to Bill Bishop. Geological Society, London*:41-58.

Renaut, R. W., J.-J. Tiercelin and R. B. Owen

2000 Lake Baringo, Kenya Rift Valley, and its Pleistocene precursors. In *Lake Basins Through Space and Time*, edited by K. R. K. E. H. Gierlowski-Kordesch, pp. 561-568. vol. 46. AAPG Studies in Geology, Tulsa OK.

Retallack, G. J.

1991 Untangling the effects of burial alteration and ancient soil formation. *Annual Review of Earth and Planetary Sciences* 19:183-206.

Robinson, J. R., J. Rowan, J. T. Faith and J. G. Fleagle

2016 Paleoenvironmental change in the late middle Pleistocene–Holocene kibish formation, Southern Ethiopia: Evidence from ungulate isotopic ecology. *Palaeogeography, Palaeoclimatology, Palaeoecology*.

Rogers, M. J., J. W. Harris and C. S. Feibel

1994 Changing patterns of land use by Plio-Pleistocene hominids in the Lake Turkana Basin. *Journal of Human Evolution* 27(1):139-158.

Romanek, C. S., E. L. Grossman and J. W. Morse

1992 Carbon isotopic fractionation in synthetic aragonite and calcite: effects of temperature and precipitation rate. *Geochimica et Cosmochimica Acta* 56(1):419-430.

Rossignol-Strick, M.

1983 African monsoons, an immediate climate response to orbital insolation. *Nature* 304(5921):46-49.

Rossignol-Strick, M., W. Nesteroff, P. Olive and C. Vergnaud-Grazzini

1982 After the deluge: Mediterranean stagnation and sapropel formation.

Rossignol-Strick, M. and M. Paterne

1999 A synthetic pollen record of the eastern Mediterranean sapropels of the last 1 Ma: implications for the time-scale and formation of sapropels. *Marine Geology* 153(1-4):221-237.

Rossignol-Strick, M., M. Paterne, F. C. Bassinot, K. C. Emeis and G. J. De Lange

1998 An unusual mid-pleistocene monsoon period over Africa and Asia. *Nature* 392(6673):269-272.

Rots, V. and P. Van Peer

2006 Early evidence of complexity in lithic economy: core-axe production, hafting and use at Late Middle Pleistocene site 8-B-11, Sai Island (Sudan). *Journal of Archaeological Science* 33(3):360-371.

Rozanski, K., L. Araguas-Araguas and R. Gonfiantini

1996 Isotope patterns of precipitation in the East African region. *The Limnology, climatology and paleoclimatology of the East African Lakes*:79-94.

Ruff, C.

1994 Morphological adaptation to climate in modern and fossil humans. *Yearbook of Physical Anthropology* 37:65-107.

Ryan, S. J., C. U. Knechtel and W. M. Getz

2006 Range and habitat selection of African buffalo in South Africa. *Journal of Wildlife Management* 70(3):764-776.

Sahle, Y., W. K. Hutchings, D. R. Braun, J. C. Sealy, L. E. Morgan, A. Negash and B. Atnafu

2013 Earliest stone-tipped projectiles from the Ethiopian Rift date to> 279,000 years ago. *PloS one* 8(11):e78092.

Sala, N., J. L. Arsuaga, I. Martínez and A. Gracia-Téllez

2014 Carnivore activity in the Sima de los Huesos (Atapuerca, Spain) hominin sample. *Quaternary Science Reviews* 97:71-83.

Schefuß, E., S. Schouten, J. F. Jansen and J. S. S. Damsté

2003 African vegetation controlled by tropical sea surface temperatures in the mid-Pleistocene period. *Nature* 422(6930):418-421.

Schick, K. D.

1997 Experimental studies of site-formation processes. *Koobi Fora Research Project* 5:244-256.

Schmieder, F., T. von Dobeneck and U. Bleil

2000 The Mid-Pleistocene climate transition as documented in the deep South Atlantic Ocean: initiation, interim state and terminal event. *Earth and Planetary Science Letters* 179(3):539-549.

Schoeninger, M. J., H. T. Bunn, S. S. Murray and J. A. Marlett

2001 Composition of tubers used by Hadza foragers of Tanzania. *Journal of Food Composition and Analysis* 14(1):15-25.

Schoville, B. J.

2010 Frequency and distribution of edge damage on Middle Stone Age lithic points, Pinnacle Point 13B, South Africa. *Journal of human evolution* 59(3):378-391.

Scott, J. J.

2005 Taphonomy of modern and ancient vertebrate traces in the marginal sediments of saline, alkaline and freshwater lakes, Baringo-Bogoria basin, Kenya Rift Valley, Geological Sciences, University of Saskatchewan.

Shea, J. J.

1993 Lithic Use-Wear Evidence for Hunting by Neandertals and Early Modern Humans from the Levantine Mousterian. In *Hunting and Animal Exploitation in the Later Palaeolithic and Mesolithic of Eurasia*, edited by G. L. Peterkin, H. B. Bricker and P. Mellars, pp. 189-197. Archaeological Papers of the American Anthropological Association. vol. 4, G. A. Clark, general editor. 6 vols, Washington DC.

Shea, J. J.

1993 Lithic Use-Wear Evidence for Hunting by Neandertals and Early Modern Humans from the Levantine Mousterian. *Archeological Papers of the American Anthropological Association* 4(1):189-197.

Shea, J. J.

2006 The origins of lithic projectile point technology: evidence from Africa, the Levant, and Europe. *Journal of Archaeological Science* 33(6):823-846.

Sisk, M. L. and J. J. Shea

2011 The African origin of complex projectile technology: an analysis using tip cross-sectional area and perimeter. *International journal of evolutionary biology* 2011.

Smith, B. N. and S. Epstein

1971 Two categories of 13C/12C ratios for higher plants. *Plant physiology* 47(3):380-384.

Smith, E. A.

1985 Inuit foraging groups: some simple models incorporating conflicts of interest, relatedness, and central-place sharing. *Ethology and Sociobiology* 6(1):27-47.

Sponheimer, M. and J. A. Lee-Thorp

2003 Using carbon isotope data of fossil bovid communities for palaeoenvironmental reconstruction. *South African Journal of Science* 99(5-6):273-275.

Sponheimer, M., J. A. Lee-Thorp, D. J. DeRuiter, J. M. Smith, N. J. van der Merwe, K. Reed, C. C. Grant, L. K. Ayliffe, T. F. Robinson, C. Heidelberger and W. Marcus

2003 Diets of Southern African Bovidae: Stable Isotope Evidence. *Journal of Mammalogy* 84(2):471-479.

Stanford, C. B., C. Gambaneza, J. B. Nkurunungi and M. L. Goldsmith

2000 Chimpanzees in Bwindi-Impenetrable National Park, Uganda, use different tools to obtain different types of honey. *Primates* 41(3):337-341.

Sternberg, L. d. S. L.

1989 Oxygen and hydrogen isotope ratios in plant cellulose: mechanisms and applications. In *Stable isotopes in ecological research*, pp. 124-141. Springer.

Stevens, R. E., M. Balasse and T. C. O'Connell

2011 Intra-tooth oxygen isotope variation in a known population of red deer: implications for past climate and seasonality reconstructions. *Palaeogeography, Palaeoclimatology, Palaeoecology* 301(1):64-74.

Steward, J. H.

1938 *Basin-plateau aboriginal sociopolitical groups* 120. US Government Printing Office Washington, DC.

Stratigraphy, I. C. o.

2014 International Chronostratigraphic Chart.

Tadashi, T. A.

1981 Plant utilization of the Mbuti Pygmies-with special reference to their material culture and use of wild vegetable foods.

Tallon, P. W. J.

1976 The Stratigraphy, Palaeoenvironments and Geomorphology of the Pleistocene Kapthurin Formation, Kenya, Queen Mary, University of London.

Tallon, P. W. J.

1978 Geological setting of the hominid fossils and Acheulian artifacts from the Kapthurin Formation, Baringo District, Kenya. *Geological Society Special Publication* 6:361-373.

Tan, K. C., H. San Lim, M. Z. MatJafri and K. Abdullah

2012 A comparison of radiometric correction techniques in the evaluation of the relationship between LST and NDVI in Landsat imagery. *Environmental monitoring and assessment* 184(6):3813-3829.

Tans, P., A. De Jong and W. Mook

1979 Natural atmospheric 14C variation and the Suess effect.

Tappen, N. G.

1987 Circum-mortem damage to some ancient African hominid crania: a taphonomic and evolutionary essay. *African Archaeological Review* 5(1):39-47.

Terashima, H.

2003 Names, use and attributes of plants and animals among the Ituri forest foragers: a comparative ethnobotanical and ethnozoological study.

Terashima, H. and M. Ichikawa

2003 A comparative ethnobotany of the Mbuti and Efe hunter-gatherers in the Ituri forest, Democratic Republic of Congo.

Thieme, H.

1997 Lower Palaeolithic hunting spears from Germany. *Nature* 385(6619):807-810.

2000 Lower Paleolithic hunting weapons from Schöningen, Germany—the oldest spears in the world. *Acta Anthropol Sin* 19:140-147.

Thom, D. J. and N. L. Martin

1983 Ecology and Production in Baringo-Kerio Valley, Kenya. *Geographical Review* 73(1):15-29.

Thompson, J. C.

2005 The impact of post-depositional processes on bone surface modification frequencies: a corrective strategy and its application to the Loiyangalani site, Serengeti Plain, Tanzania. *Journal of Taphonomy* 3(2-3):67-89.

Treves, A. and L. Naughton-Treves

1999 Risk and opportunity for humans coexisting with large carnivores. *Journal of Human Evolution* 36(3):275-282.

Treves, A. and P. Palmqvist

2007 Reconstructing hominin interactions with mammalian carnivores (6.0–1.8 Ma). In *Primate anti-predator strategies*, pp. 355-381. Springer.

Tryon, C. A.

2003 The Acheulian to Middle Stone Age Transition: tephrostratigraphic context for archaeological change in the Kapthurin Formation, Kenya, Anthropology, University of Connecticut, Storrs, CT.

Tryon, C. A.

2006 "Early" Middle Stone Age Lithic Technology of the Kapthurin Formation (Kenya). *Current Anthropology* 47(2):367-375.

Tryon, C. A., J. Faith, D. Peppe, W. Keegan, K. Keegan, K. Jenkins, S. Nightingale, D. Patterson, A. Van Plantinga and S. Driese

2014 Sites on the landscape: Paleoenvironmental context of late Pleistocene archaeological sites from the Lake Victoria basin, equatorial East Africa. *Quaternary International* 331:20-30.

Tryon, C. A. and J. T. Faith

2013 Variability in the Middle Stone Age of Eastern Africa. *Current Anthropology* 54(S8):S234-S254.

Tryon, C. A., J. T. Faith, D. J. Peppe, D. L. Fox, K. P. McNulty, K. Jenkins, H. Dunsworth and W. Harcourt-Smith

2010 The Pleistocene archaeology and environments of the Wasiriya Beds, Rusinga Island, Kenya. *Journal of Human Evolution* 59(6):657-671.

Tryon, C. A. and S. McBrearty

2002 The Middle Stone Age of the southern Kapthurin Formation, Baringo, Kenya. *Journal of Human Evolution* 42(3):A37-A37.

Tryon, C. A. and S. McBrearty

2002 Tephrostratigraphy and the Acheulian to Middle Stone Age transition in the Kapthurin Formation, Kenya. *Journal of human evolution* 42(1):211-235.

2006 Tephrostratigraphy of the Bedded Tuff Member (Kapthurin Formation, Kenya) and the nature of archaeological change in the later middle Pleistocene. *Quaternary Research* 65(3):492-507.

Tryon, C. A., S. McBrearty and P.-J. Texier

2005 Levallois Lithic Technology from the Kapthurin Formation, Kenya: Acheulian Origin and Middle Stone Age Diversity. *African Archaeological Review* 22(4):199-229.

Tucker, C., I. Fung, C. Keeling and R. Gammon

1986 Relationship between atmospheric CO2 variations and a satellite-derived vegetation index. *Nature* 319:195-199.

Tucker, M. E. and V. P. Wright

1990 *Carbonate sedimentology*. Blackwell Scientific Publications, Boston; Oxford [England]; Brookline Village, Mass.

Ungar, P. S., F. E. Grine, M. F. Teaford and S. El Zaatari

2006 Dental microwear and diets of African early Homo. *Journal of Human Evolution* 50(1):78-95.

Ungar, P. S. and M. Sponheimer

2011 The Diets of Early Hominins. *Science* 334(6053):190-193.

van der Merwe, N. J. and E. Medina

1991 The Canopy Effect, Carbon Isotope Ratios and Foodwebs in Amazonia. *Journal of Archaeological Science* 18(3):249-259.

Van Noten, F., E. Cornelissen, J. Gysels, J. Moeyersons, K. Nijs and H. Uytterschaut

1987 The Kapthurin project, Baringo: the 1984 season. *Nyame akuma* (28):20-27.

Van Noten, F., E. Cornelissen, J. Gysels, J. Moeyersons and H. Uytterschaut

1987 The Kapthurin Project Baringo: the 1985 Season. *Nyame akuma* (29):36-42.

Veenendaal, E. M., O. Kolle and J. Lloyd

2004 Seasonal variation in energy fluxes and carbon dioxide exchange for a broad-leaved semi-arid savanna (Mopane woodland) in Southern Africa. *Global Change Biology* 10(3):318-328.

Vetter, S.

2005 Rangelands at equilibrium and non-equilibrium: recent developments in the debate. *Journal of Arid Environments* 62(2):321-341.

Villmoare, B., W. H. Kimbel, C. Seyoum, C. J. Campisano, E. N. DiMaggio, J. Rowan, D. R. Braun, J. R. Arrowsmith and K. E. Reed

2015 Early Homo at 2.8 Ma from Ledi-Geraru, Afar, Ethiopia. *Science* 347(6228):1352-1355.

Vincent, A. S.

1985 Plant foods in savanna environments: a preliminary report of tubers eaten by the Hadza of northern Tanzania. *World Archaeology* 17(2):131-148.

Vrba, E. S.

1985 Environment and evolution: alternative causes of the temporal distribution of evolutionary events. *South African Journal of Science* 81(5):229-236.

Vrba, E. S.

1993 Turnover-pulses, the Red Queen, and related topics. *American Journal of Science* 293(A):418-452.

Wadley, L.

2005 Putting ochre to the test: replication studies of adhesives that may have been used for hafting tools in the Middle Stone Age. *Journal of Human Evolution* 49(5):587-601.

Wang, Y. and T. E. Cerling

1994 A model of fossil tooth and bone diagenesis: implications for paleodiet reconstruction from stable isotopes. *Palaeogeography, Palaeoclimatology, Palaeoecology* 107(3-4):281-289.

Wasonga, V. O., D. M. Nyariki and R. K. Ngugi

2011 Assessing socioecological change dynamics using local knowledge in the semi-arid lowlands of Baringo district, Kenya. *Environmental Research Journal* 5(1):11-17.

Waters, M. R. and D. D. Kuehn

1996 The Geoarchaeology of Place: The Effect of Geological Processes on the Preservation and Interpretation of the Archaeological Record. *American Antiquity* 61(3):483-497.

Wescott, K. L. and R. J. Brandon

2003 *Practical applications of GIS for archaeologists: A predictive modelling toolkit*. CRC Press.

Western, D. and A. K. Behrensmeyer

2009 Bone assemblages track animal community structure over 40 years in an African savanna ecosystem. *Science* 324(5930):1061-1064.

Wilkins, J. and M. Chazan

2012 Blade production ~500 thousand years ago at Kathu Pan 1, South Africa: Support for a multiple origins hypothesis for early Middle Pleistocene blade technologies. *Journal of Archaeological Science* 39(6):1883-1900.

Wilkins, J., B. J. Schoville, K. S. Brown and M. Chazan

2012 Evidence for early hafted hunting technology. *Science* 338(6109):942-946.

Winterhalder, B.

1981 Optimal foraging strategies and hunter-gatherer research in anthropology: theory and models. *Huntergatherer foraging strategies* 38065:13-35.

Winterhalder, B.

2001 The behavioural ecology of hunter-gatherers. *Hunter-gatherers: an interdisciplinary perspective* 13:12.

Wittemyer, G., T. E. Cerling and I. Douglas-Hamilton

2009 Establishing chronologies from isotopic profiles in serially collected animal tissues: An example using tail hairs from African elephants. *Chemical Geology* 267(1):3-11.

Wood, B. A. and F. L. Van Noten

1986 Preliminary observations on the BK 8518 mandible from Baringo, Kenya. *American Journal of Physical Anthropology* 69(1):117-127.

Wright, V. P.

1986 *Paleosols: their recognition and interpretation*. Blackwell Scientific Publications Oxford.

Wynn, J. G.

2004 Influence of Plio-Pleistocene Aridification on Human Evolution: Evidence from Paleosols of the Turkana Basin, Kenya. *American Journal of Physical Anthropology* 123(2):106-118.

Wynn, J. G. and M. I. Bird

2007 C_4-derived soil organic carbon decomposes faster than its C_3 counterpart in mixed C_3/C_4 soils. *Global Change Biology* 13(10):2206-2217.

Yellen, J. E.

1986 Optimization and risk in human foraging strategies. *Journal of Human Evolution* 15(8):733-750.

Yellen, J. E.

1991 Small mammals: !Kung San utilization and the production of faunal assemblages. *Journal of Anthropological Archaeology* 10:1-26.

Yellen, J. E., A. Brooks, D. Helgren, M. Tappen, S. Ambrose, R. Bonnefille, J. Feathers, G. Goodfriend, K. Ludwig and P. Renne

2005 The archaeology of Aduma Middle Stone Age sites in the Awash Valley, Ethiopia. *PaleoAnthropology* 10(2).

Yellen, J. E., A. S. Brooks, E. Cornelissen, M. J. Mehlman and K. Stewart

1995 A Middle Stone Age worked bone industry from Katanda, Upper Semliki Valley, Zaire. *Science* 268:553-556.

Yuen, A. and N. Jablonski

2010 Vitamin D: in the evolution of human skin colour. *Medical hypotheses* 74(1):39-44.

Zazzo, A., M. Balasse and W. P. Patterson

2005 High-resolution δ 13 C intratooth profiles in bovine enamel: Implications for mineralization pattern and isotopic attenuation. *Geochimica et Cosmochimica Acta* 69(14):3631-3642.

Zazzo, A., A. Mariotti, C. Lécuyer and E. Heintz

2002 Intra-tooth isotope variations in late Miocene bovid enamel from Afghanistan: paleobiological, taphonomic, and climatic implications. *Palaeogeography, Palaeoclimatology, Palaeoecology* 186(1):145-161.

Zipkin, A. M., M. Wagner, K. McGrath, A. S. Brooks and P. W. Lucas

2014 An experimental study of hafting adhesives and the implications for compound tool technology. *PloS one* 9(11):e112560.